MATHEMATICAL MODELING AND EXPERIMENTAL STUDIES OF THERMAL REACTIONS OF COAL

Thesis by

Ravi Jain

In Partial Fulfillment of the Requirements

for the Degree of

Doctor of Philosophy

California Institute of Technology
Pasadena, California

1980

(Submitted June 1, 1979)

Dedicated to my parents
who have always encouraged
me to strive for newer horizons, and...

... to Jo Ellen for
her love, support and care.

Acknowledgments

I am thankful to Professor George R. Gavalas for his guidance during the course of this work. I am also thankful to the California Institute of Technology for financial support through assistantships.

I would like to acknowledge the help rendered by Dr. Karl A. Wilks who was an equal partner in the experimental work. Thanks are also due to Dr. Paul H. Cheong and Dr. M. Oka for their contributions to this research.

Mr. George Griffith built the experimental apparatus and provided other technical assistance. Mr. Henry Smith helped in many different ways, including in the use of the apparatus.

Ms. Kathy Lewis deserves credit for her skillful typing and other assistance in the preparation of this dissertation.

Ravi Jain

Abstract

This dissertation discusses theoretical and experimental research on coal pyrolysis.

In the theoretical part, a mathematical model based on coal's chemical structure and its reactions is developed for computer simulation of pyrolysis. Firstly, the important organic functional groups of carbon, hydrogen and oxygen in medium and high rank coals are organized into a conceptual model for coal's chemical structure. Using the principles of thermochemistry of free radicals as guidelines, the important categories of chemical reactions in coal pyrolysis are postulated. A set of 41 series-parallel reactions represents the chemical change. It is concluded that there is no à priori distinction between volatiles and non-volatiles in a coal. They are both formed from the same chemical structure, and are basically an inevitable consequence of each other's formation.

For the purpose of mathematical modeling, coal is considered to be a population of randomly distributed functional groups on a matrix. A scheme based on statistical transformations is devised to compute concentrations of reacting configurations before and during pyrolysis. The rates of reactions are expressed in terms of these concentrations. Differential equations governing the rate of change of state variables with pyrolysis time are formulated and numerically integrated on the computer. Pyrolysis results are predicted in terms of the state variables.

The dependence of the yield and composition of volatiles on (a) transport parameters like particle size and pressure, and (b) kinetic parameters like time, temperature and time-temperature history, is

investigated experimentally. Gaseous products are analyzed using chromatography, while tar is characterized by GPC, NMR and elemental analysis.

Basic research on coal helps in developing a general "theory" about its structure and chemical behavior. It enhances our ability to meet process, economic and environmental goals in coal's industrial utilization.

Table of Contents

Page

Chapter I

INTRODUCTION

1. Importance of coal.

The 1970's have witnessed a world-wide focus on research and development in the area of energy resources. Governments and industries alike are seeking ways to utilize traditional fuels more efficiently, while developing new sources of energy with due concern for environmental side-effects.

There has always been an interest in developing coal as a major source of energy. Different ways of utilizing it have been proposed and it has been widely researched from various viewpoints. However, the intensity of interest in coal has fluctuated depending on the availability and relative economics of other fuels. Accordingly, ever since the oil crisis of the early 70's, countries like the United States, which have abundant supply of coal, have put extra emphasis on its utilization. The U.S. policy makers now envisage an increasingly important role for coal in the coming years.

Coal can be used directly as a fuel as in some power plants, or indirectly as a raw material for synthetic fuels. An example of the latter case is the production of Substitute Natural Gas (SNG) from coal. SNG is a clean-burning fuel gas which can be used as a partial or total replacement for natural gas which is at a premium. Another advantage of the SNG conversion is that its plant design can provide ample flexibility for utilizing coals of various quality, including coals of high sulfur content which are unsuitable for direct combustion.

Apart from its large scale potential use as a fuel directly or indirectly, coal is also a very attractive raw material for producing

industrially important hydrocarbons. In fact, considering the variety of organic compounds that can be recovered from coal, its use as an industrial raw material may well exceed that as a fuel.

2. Need for basic research on coal.

In many industrial chemical reactions, reactants are well characterized and reaction mechanism and kinetics are well understood. Such understanding helps in attaining economic, environmental, and process goals. Accordingly, in order to meet these goals in coal conversion processes, it is desirable to understand coal's structure and reactivity in great detail. Basic research in these two areas will enhance our ability to overcome problems associated with coal's industrial use For example, coal utilization schemes devised in the past cannot meet modern standards of pollution control for oxides of nitrogen and sulfur. To modify these schemes or to devise better schemes in the future, it will be very helpful to acquire knowledge about the nature of nitrogen and sulfur groups in coal and mechanism of their conversion into pollutants.

Direction of fundamental research in coal is further discussed in the rest of this section. A summary of the aims and contents of the research presented in this thesis appears in the next section.

Coal is a product of decomposition of plant material. Different coals have different compositions based on the plant materials they were derived from and the degree of coalification. Over the years, a substantial amount of research has been done on the origin of coal in terms of characterization of the parent material and the factors affecting the

coalification process. Such research, although very important, has had little utilitarian value. Its findings could not be used to predict the chemical behavior of coal under various process conditions.

Coal can be considered a mixture of hydrocarbons containing hetero-atoms like nitrogen and sulfur, distributed in a heterogeneous mass of mineral matter. Its principal elements are carbon, hydrogen, oxygen, nitrogen, and sulfur. Investigators have tried to describe reactions of coal in terms of reactions of these elements. For example, combustion of coal was described as reactions of carbon (graphite) with oxygen (Tingey and Morrey, 1972).

It has now been recognized that as with other organic compounds, reactivity of coal is due to its functional groups. These groups are formed by combinations of atoms, and have different chemical characteristics depending on the nature of bonding, etc. Thus, one of the fundamental tasks in coal research is to develop methods for identifying the various functional groups present in a given coal, and to determine how these groups will react with each other and with an externally provided reactant under various experimental conditions. This is not an easy task considering the great complexity of coal, the fact that it is a solid, and the diversity of various coals.

Appreciable amount of effort has been made and is being made in applying the modern techniques of analytical chemistry to investigate coal and coal-derived compounds. The urgent need now is to correlate various pieces of information and to develop unifying concepts about structure and reactivity of coal. A general model of chemically relevant aspects of coal needs to be developed and tested for its ability to simulate experimental

results. One of course cannot hope to develop 'the model'. Different models of different complexities may be required to describe behavior of the entire spectrum of coals. Nevertheless, a loose conceptual structure can be built to capture the essence of the various findings by coal researchers. This conceptual picture might turn out to be a very satisfactory representation of some coals, while being applicable in broad terms to all coals.

3. Aim and scope of this work.

The basic aim of this work was to understand coal by understanding the physical and chemical changes associated with rapid pyrolysis of coal particles at temperatures up to 700°C. Pyrolysis involves heating coal in the absence of oxygen — in vacuum or in an inert atmosphere. Pyrolysis was chosen over other processes (e.g. extraction, gasification, etc.) for several reasons:

[a] It yields a lot of valuable information about structure and reactivity of coal though it is a relatively simple process. For example, by analyzing the volatile products of pyrolysis we can infer the important functional groups present in coal. Low temperatures and absence of externally provided reactants results in a one-to-one correspondence between the products and the various components of coal's chemical structure.

[b] Pyrolytic changes occur in many coal-conversion processes. For example, it is believed that in hydrogasification hydrogen reacts separately with the volatiles and the char produced during the first few seconds of heating. Table 1.3.1 gives examples

Table 1.3.1

ROLE OF PYROLYSIS IN COAL CONVERSION PROCESSES

TYPE OF PROCESS	EXAMPLES	ROLE OF PYROLYSIS
Low BTU Gas	Koppers-Totzek F.W., C.E.	Negligible
High BTU Gas (SNG)	Hygas, Synthane	Moderate: Reactivity of Char
Solvent Extraction	SRC	Large: Free Radical Reactions Determine M.W.
Liquid Phase Catalytic Conversion to Fuel Oil	H-Coal, Synthoil	Large (Thermal Reactions in Initial Phase)
Gas Phase Hydrogenation (Noncatalytic)	C.U.N.Y., Co-Gas	Large
Flash Pyrolysis	Occidental Research	Large

of the importance of pyrolysis in various processes. Thus, elucidation of pyrolysis will help the research on other coal-conversion processes.

[c] Pyrolysis has been studied as an independent industrial process for recovering lighter hydrocarbons from coal. A good example is the Flash Pyrolysis process developed by the Occidental Research Corporation. Although it is doubtful that pyrolysis itself will become an economically attractive process (yields are less than 50%), it might be incorporated as the first step in an integrated scheme involving several processes.

The theoretical work in this thesis consists of the following steps:

[1] Development of a conceptual model for chemical structure of medium and high rank (subbituminous and higher) coals. The effort involved meshing together the various well-accepted facts and ideas regarding coal's chemical structure, and developing a conceptual picture representing the important chemical characteristics of most coals.

[2] Formulation of a mathematical scheme to calculate the concentrations of reacting configurations in terms of easily obtainable information on coal. This was necessary because coal does not have a 'molecule' as such but has a mixture of several functional groups.

[3] Identification of important chemical reactions in pyrolysis (up to 700^{o}C), and consequently elucidation of mechanism of product formation. Use was made of the theory of thermochemistry of free radicals which was originally developed to explain

pyrolysis of simple aliphatic and aromatic compounds.

[4] Formulation of rate expressions for chemical reactions and physical processes (e.g. transport) within a coal particle undergoing pyrolysis.

[5] Selection of State Variables to characterize the chemical system, and formulation of a set of differential equations governing the rate of change of the State Variables with time during pyrolysis.

[6] Implementation of the mathematical scheme on computer (IBM 370). The differential equations were integrated to predict pyrolysis results.

The experimental work presented in this thesis involved pyrolysis experiments on several different coals under different conditions of temperature, pressure, particle size, etc. The steps involved were:

[1] Selection of a pyrolysis technique, and design, construction, and assembly of pyrolysis reactors and associated accessory systems, e.g., instrumentation for measurement and control of temperature.

[2] Development of techniques for efficient collection of gaseous and liquid products.

[3] Selection, set-up, and calibration of analytical techniques for characterizing the gaseous and liquid products.

[4] Execution of experimental program involving tar collection, transport, and kinetic experiments.

The concepts used and the conclusions reached in this work were both limited by several factors, among them the temperature range of interest. Both theoretical and experimental work was limited to temperatures up to

700°C. Hence, direct applicability of results of this work is questionable in high temperature situations such as devolatilization that preceeds coal combustion. At high temperatures, pyrolysis may lead to a rather drastic change in coal's chemical structure such that very little useful information about the coal can be derived by analyzing the products. These situations can be tackled later, after a reasonable level of confidence is achieved in predicting coal's chemical behavior by working at low temperatures.

The most important purpose served by the research presented in this thesis is that it demonstrates both qualitatively and quantitatively our ability to develop a general, comprehensive 'theory' about coal's chemical behavior. We need such a theory in order to facilitate large scale industrial use of coal.

Chapter II

CHEMICAL AND PHYSICAL STRUCTURE OF COAL

1. General

In this chapter a model is developed for chemical structure of coal, using information available in literature and observations from pyrolysis experiments. There is no attempt to discuss the merits and demerits of various conflicting opinions about aspects of coal's structure. Instead, the vast body of literature in this field has been sieved, retaining the most widely accepted and well-established concepts. These concepts provided the building blocks for a general framework, which is expected to provide the basis for modeling chemical structures of most medium and high rank coals. The physical structure of coal is also discussed.

The rest of this section points out the important questions to be answered regarding structure and reactivity.

A fundamental task in coal research is to identify the important functional groups present in coal. The concept of a functional group is well established in organic chemistry, and it postulates that reactivity of organic compounds is due to the reactivity of their functional groups. Coal contains a variety of functional groups formed by various combinations of its principal constituent elements. It is natural to ask: do different coals have the same functional groups in different amounts, or do they have entirely different groups? How do these groups react with each other and with external reactants under various conditions?

In general, the answers have been difficult to come by despite a world-wide interest and activity in coal research over several decades. Even today the progress is slow and at times confusing. There is a vast reservoir of available information, but it does not readily lend itself to

basic understanding. There are several reasons for this difficulty in characterization of coal. Firstly, there is no 'molecule' of coal in the usually understood sense. Coal is more like a polymer, with the additional complication that there is no single monomer which makes the polymer. It is a population of different monomers and the make-up of such a population is different for different coals. The heterogeneity and complexity of the wide range of plants which formed the starting material for coal, together with the abstruse coalification process, result in a diversified and intractable structure.

Secondly, the various physical and chemical techniques in analytical chemistry are relatively recent and not sufficiently advanced to deal with the complexity of coal. The picture is further complicated because coal, being a solid, is not easily amenable to analysis using these techniques. To circumvent this difficulty, investigators have tried to work with coal-derived compounds instead of coal itself. Various methods have been used, but the perennial question in this approach is: to what degree can findings on the products of a coal-conversion process be applied to the parent coal?

From a practical standpoint, coal's chemical structure alone will not suffice to predict its chemical behavior. Knowledge about physical structure is also important. Coal is a porous solid, and therefore, the reactants and products have to be transported in and out of a particle. Although there are well-established techniques for elucidating the physical structure of porous solids, the difficulty with coal is that the picture changes during reaction. Medium and high rank coals go through a plastic

state at high temperatures, which results in a complete collapse of the original structure. The question then is: how can one account for the effect that the physical processes of heat and mass transfer within a coal particle have on the chemical behavior of coal?

Discussion about reactivity of coal would be a much simpler task if its structure were known. Even then it would require a high level of expertise in organic chemistry to postulate the important reactions of the various functional groups. A simple organic compound like propane subjected to high temperatures in an inert atmosphere reacts with a rather complex mechanism. To tabulate the possible reactions of coal would be a monumental task indeed. What is more, reactivity of coal is used to deduce the structure of coal and vice-versa. One has to speculate about both the structure and the reactions simultaneously, based on the experimentally observable products and the constraints placed by thermodynamics, chemistry, etc. Reactivity of coal, whether it be in oxidation, hydrogenation, pyrolysis, or solvent extraction, can be best understood in terms of the reactivity of its functional groups.

The above discussion establishes in a general sense the tremendous need and opportunity that exists in investigating the physical and chemical structure of coal and its reactions. This thesis is basically an effort in this direction.

2. Chemical structure of coal.

A model for chemical structure of medium and high rank coals is presented in this section. Traditional ways of classifying coals are discussed in brief first. Then we go on to identify the important organic

structures formed in coal by its constituent elements: carbon, hydrogen, oxygen, nitrogen, and sulfur. This is followed by a brief discussion on mineral matter.

Coal is a predominantly organic substance with a small but in some ways important inorganic part. It is the organic portion which is of utilitarian interest whether coal is to be used as a fuel or as a source of industrial chemicals. The inorganic part, generally termed mineral matter, is important in that it is believed to affect the chemical behavior of the organic part.

Coal petrography and rank classification are two traditional ways in which investigators and coal industry have tried to understand the complexity of coal. Petrography is concerned with characterization of coal in terms of 'minerals' known as macerals. The fossil origins of some of the maceral fractions are very distinct. Petrographic classification is mostly based on reflection of light, a property only obliquely related to chemical reactivity. Coals have also been classified into various ranks which roughly indicate the extent to which coalification process has altered the original plant matter. Carbon content, calorific value, volatile matter, etc., are some of the criteria for such a classification scheme. Some relationships between rank and chemistry can be drawn (Tingey and Morrey, 1972, and Suuberg, 1977). However, coals of the same rank may exhibit markedly different chemical characteristics. Hence, although rank classification is widely used (for example by coking industry) and it provides a gross chemical classification, it will not be sufficient to meet the needs of an advanced coal technology.

Various physical (e.g. X-ray diffraction, IR, UV, NMR, ESR, etc.) and

chemical (e.g. pyrolysis, solvent extraction, oxidation, etc.) methods have been used for elucidation of chemical structure of coal. The information that can be obtained from these techniques is enormous. Suuberg (1977) has presented a table listing the type of structural information that can be derived from each technique. Discussion on these techniques can also be found in Lowry (1963). Basically, the information desired is about the types of functional groups and their concentration.

The Carbon-Hydrogen Structure in Coal:

A salient feature of the medium and high rank coals is their aromaticity. It is generally accepted that a significant portion of the carbon in coal is contained in multi-ring aromatic clusters. Napthalene and pyrene are examples of such multi-ring clusters.

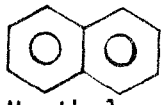

Napthalene

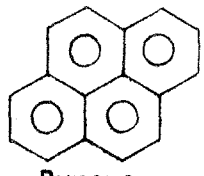

Pyrene

The size of these ring systems has not been fully established but is believed to range from between two and four rings in lower rank coals up to bituminous, to more than twelve in anthracite (Cheong, 1976). A coal may contain more than one size rings. The occurrence of these rings in coal makes aromaticity — fraction of carbon that is aromatic — a very important parameter for coal characterization. Coals with high carbon content have high aromaticity. In general, aromaticity is related to the rank of a coal. Figure 2.2.1 (from Suuberg, 1977) shows the aromaticity as a function of carbon content of the coal. It is obvious that most coals have a significant

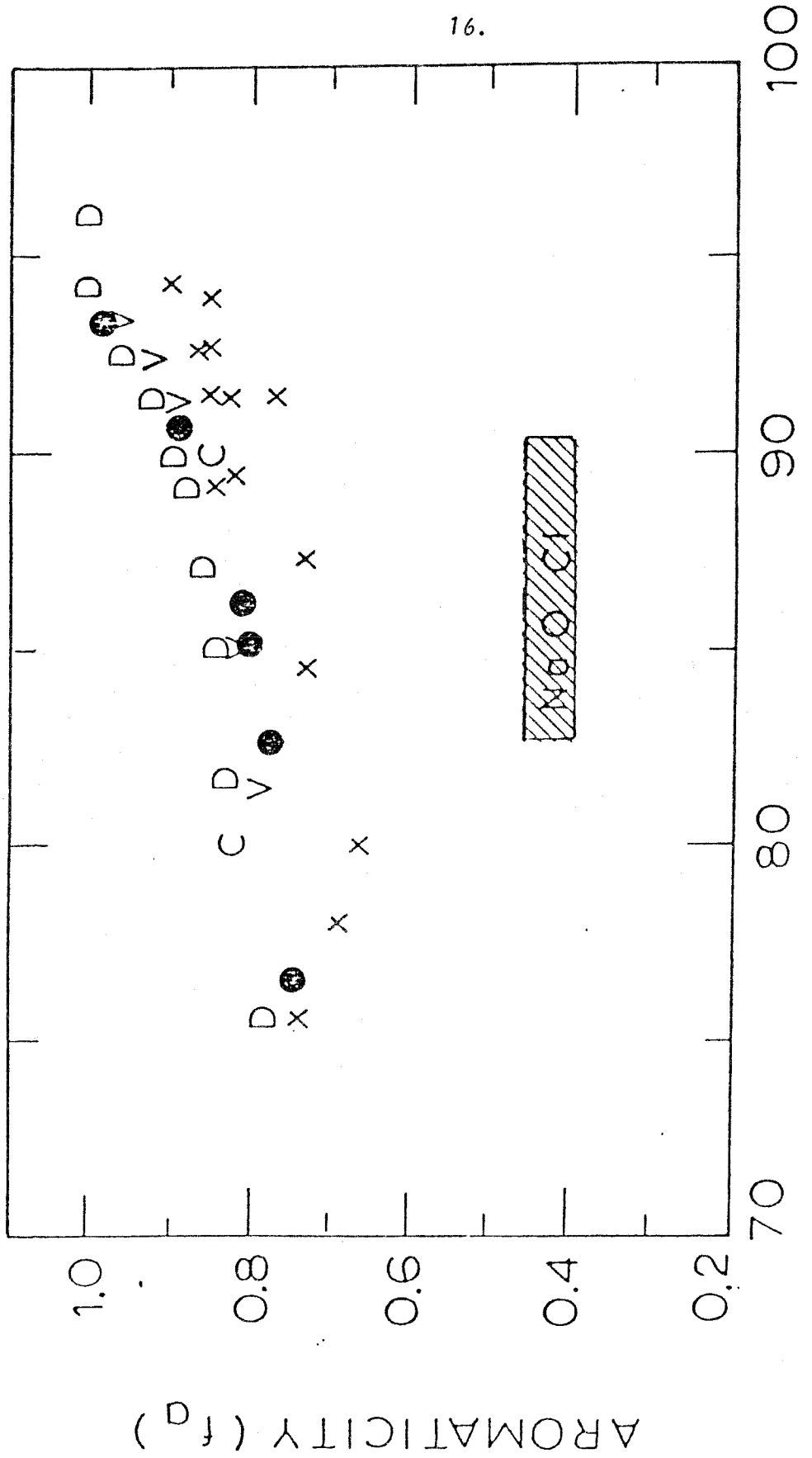

Figure 2.2.1: Aromaticity as a Function of Carbon Content (from Suuberg, 1977).

portion of their carbon in condensed multi-ring aromatic clusters. Suuberg (1977) has presented and discussed literature data pertaining to aromaticity. One point of importance is that characteristics such as aromaticity are overall averages for the different macerals contained in the coal. In reality, for a particular carbon content, different maceral fractions may have quite different characteristics.

Several concepts for characterizing a multi-ring aromatic cluster have been proposed. Van Krevelen (1961) chose to represent coal as a 'polymer' made up of monomers containing one 'average' condensed aromatic structure. This viewpoint will be further discussed later in this thesis as it constitutes one of the basic ideas in the modeling of coal structure. Calculations for determining the initial conditions of the various functional groups in coal will be later shown to be directly related to the size of an 'average' cluster.

It should be noted that not all researchers agree with the magnitude of aromaticity in coals as presented in Fig. 2.2.1. Chakrabartty and co-workers (1972, 1974, 1974) attempted controlled oxidation of coals and model compounds with sodium hypochlorite to infer that contrary to the generally accepted view, "skeletal carbon arrangements appear to be largely made up of nonaromatic clusters". They have suggested that these structures are modified bridged tricycloalkane systems or poly-amantanes. Many workers, however, have questioned these conclusions pointing out that hypochlorite oxidation is not specific enough and that products of coal liquefaction do not support the existence of poly-amantanes (Suuberg, 1977).

Recently, application of carbon-13 NMR to solid coal structure determinations was made possible by development of ^{13}C-^{1}H cross-polarization

technique. Such NMR, in principle, provides the percentage of aromatic carbon in coal. Further developments in this area would help clear up the controversy regarding aromaticity.

The nonaromatic portion of carbon in coal is believed to be present in one of the following forms:

[a] Side chains attached to the aromatic ring systems. A ($-CH_3$) or a ($-C_2H_5$), or in general ($-C_xH_y$) attached to an aromatic carbon are examples of aliphatic sidechains:

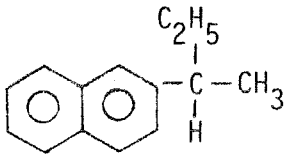

[b] Bridges that connect the aromatic clusters with each other. Most aromatic clusters are connected to their neighboring clusters through different types of bridges, thus giving rise to a matrix of clusters. It is conceivable that two- or three-cluster fragments exist in isolation from the rest of the matrix, but unconnected single clusters are unlikely. Such clusters would have volatilized during the process of coalification, unless of course they were trapped because of transport limitations.

A substantial amount of carbon can be present in the aliphatic bridges connecting the aromatic clusters. A bridge might consist of just one aliphatic carbon between two clusters, e.g.:

$$\Phi - CH_2 - \Phi'$$

where Φ and Φ' represent peripheral aromatic carbons on any two clusters; or two or more aliphatic carbons, e.g.:

$$\Phi - CH_2 - CH_2 - \phi',$$

$$\Phi - \underset{\displaystyle CH_3}{\overset{\displaystyle H}{\overset{|}{\underset{|}{C}}}} - CH_2 - \Phi',$$

$$\Phi - CH_2 - R - CH_2 - \Phi'$$

where R is an alkyl group.

[c] Alicyclic and hydroaromatic compounds. An example of alicyclic compounds is:

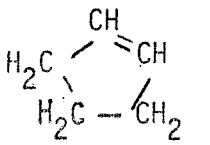

Cyclopentene

Hydroaromatic compounds contain the carbon skeleton of an aromatic system but too many hydrogen atoms for aromaticity (Morrison and Boyd, 1966). Tetralin is such a compound:

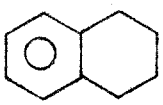

Tetralin

It is interesting to note that since such structures can undergo aromatization by losing hydrogen atoms, they could be the precursors of the multi-ring aromatic clusters. Their presence will explain why some coals which have a lot of beta hydrogen (hydrogen atoms attached to the carbon which is in beta position with respect to an aromatic carbon) do not produce substantial amounts of hydrocarbon gases when pyrolyzed.

From a modeling viewpoint, it is interesting to note that all the above

functional groups occur as substituents on the aromatic rings of the clusters. In other words, some of the peripheral aromatic carbons carry aliphatic carbons instead of hydrogen atoms. These aliphatic carbons, which are in the alpha position, in turn carry other atoms or groups of atoms. Therefore, these groups can be considered as substituents on alpha carbons rather than as substituents on aromatic rings. For example, a ($-CH_3$) can be considered as an alpha carbon carrying three alpha hydrogens. A ($-C_2H_5$) can be thought of as an alpha carbon carrying two alpha hydrogens and one ($-CH_3$) group. This concept makes the alpha carbon position very important in coal chemistry, and as we shall see later, in mathematical modeling.

Unlike carbon, hydrogen is concentrated in the nonaromatic structures in coal. Most of the hydrogen is used to satisfy the valence requirements of aliphatic carbons. This is particularly so because of the absence of double bonds in the aliphatic portion of coal. Infrared analysis on solid coal (Brown, 1955) shows that olefinic double bonds and acetylenic triple bonds are both absent.

^1H NMR on coal extracts and pyrolysates have been performed by the author's research group and results reported (Gavalas and Oka, 1978). They clearly show that most of the hydrogen in these coal-derived liquids is present in the aliphatic portion. This conclusion can also be applied to the original coal because these liquids are considered to be random samples of the coal and presumably have very similar structural characteristics. These results will be presented later in this thesis.

The concepts presented above are based on numerous findings of various

investigators. Efforts have been made previously to synthesize a consistent theory about coal structure (for example: Van Krevelen, 1961; Dryden, 1963). Suuberg (1977) and Tingey and Morrey (1972) have presented fairly comprehensive reviews of literature and bring out essentially the same features as mentioned above. The interested reader can refer to their work for relevant references.

The aforementioned aspects of carbon-hydrogen skeleton can now be synthesized into a model of the chemical structure of coal. Fig. 2.2.2 is an example.

Oxygen in Coal:

The concentration and distribution of oxygen varies among coals of different ranks. Reactivity of some coals, specifically those of low rank, is greatly affected by the presence of oxygen groups.

The prevailing view on oxygen functional groups is that most of the oxygen is in the form of phenolic, carboxylic, and carbonyl groups (Dryden, 1963). Coal contains negligible amounts of alcoholic hydroxyl groups. Therefore, phenolic groups are the only hydroxyl functional groups of importance. Etheric linkages are also probably present in the lower rank coals which generally contain more oxygen than the higher rank coals. As will become clear during the discussion on pyrolysis mechanism (Chapter III), if one postulates production of water during pyrolysis by phenolic condensation, ether bridges that are consequently formed lead to a decrease in tar production. Thus, coals which have high phenolic concentration generally have lower tar yields. This is confirmed experimentally and theoretically as shown later. Accordingly, accurate determination of

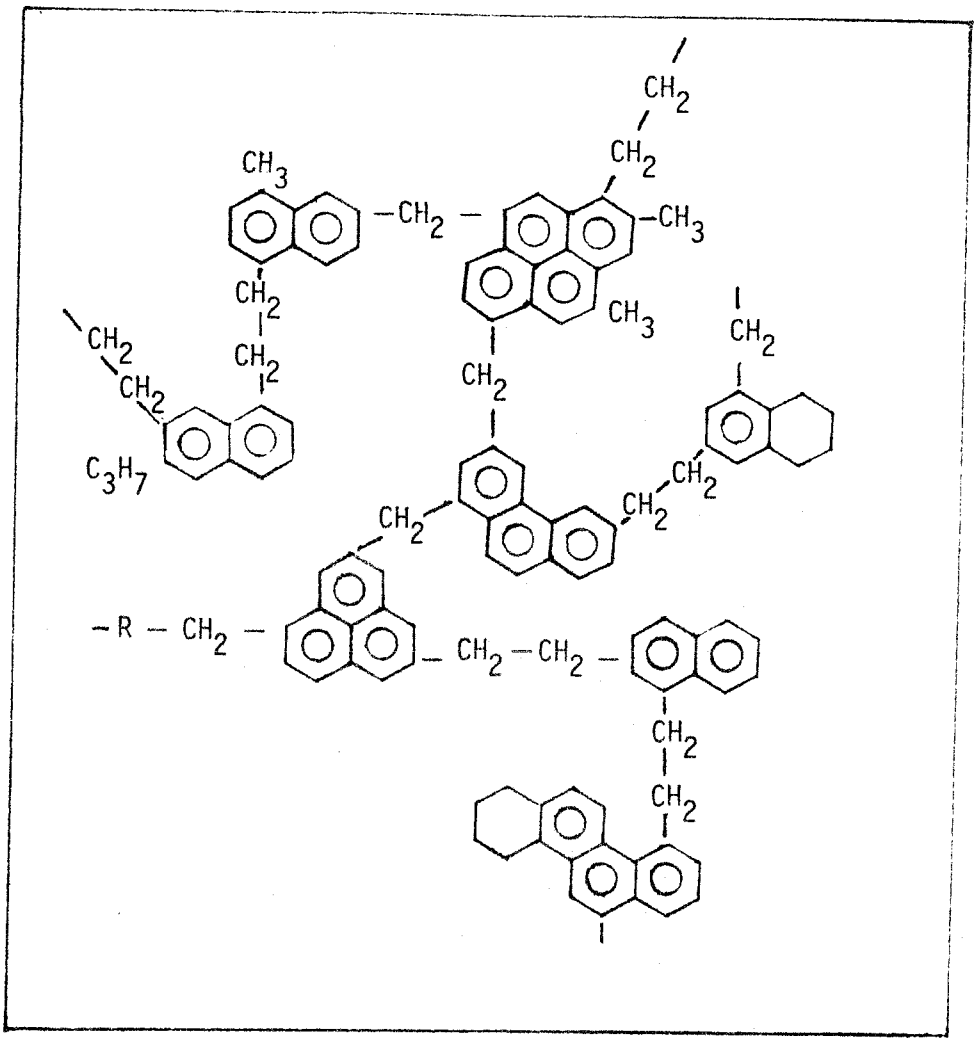

Figure 2.2.2: A Conceptual Model of the Carbon-Hydrogen Skeleton in Coals.

concentration of phenolic groups in coal becomes very important. Unfortunately, phenolic hydrogen cannot be distinguished from aromatic hydrogen by using physical methods. One has to rely on chemical,or a combination of chemical and physical,techniques for such distinction.

Carboxylic groups have a high concentration in low rank coals and lignites, but become almost negligible in many bituminous and upper rank coals (Blom, 1960). Carbonyl groups are generally believed to be present in quinone-like structures:

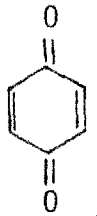

P - Benzoquinone

Nitrogen and Sulfur in Coal:

It is generally believed that nitrogen in coal exists primarily in tightly bound rings (for background literature refer to Solomon, 1977), although there is some evidence for small amounts in sidechains. Solomon concluded from his investigations that coal nitrogen is contained almost entirely in the rings. The conclusion was based on the observation that the nitrogen concentration in the tar obtained by low temperature pyrolysis is the same as in the parent coal, and that little nitrogen appears in the gas. Then the conclusion follows because tar in pyrolysis is formed by clusters escaping from coal, while gases are formed by dissociation of sidechains. Pohl (Suuberg, 1977) proposed that most of the nitrogen is present in pyridine-like aromatic structures:

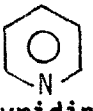

Pyridine

Considerable research is being conducted on sulfur forms in coal. Broadly speaking, approximately half of the sulfur in coal is part of the organic structure, the other half being in the mineral matter — principally as pyritic iron sulfide. Previous researchers (refer to Solomon, 1977) have classified organic sulfur into various forms using such distinctions as 'loosely bound' and 'tightly bound'. The prevailing view is that in the lower rank coals, sulfur is present mostly as thioethers (R-S-R), while in higher rank coals thiophenic structures predominate.

Thioether

Thiophene

Dibenzothiophene

Attar and Corcoran (1977) have provided a review of the sulfur functional groups and have estimated the relative amounts of thiophenic, aromatic (Ar—S—), and aliphatic (R—S—) sulfide forms.

Solomon and Manzione (1977) have developed a new method for determining the organic sulfur concentration and the stoichiometry of iron sulfide compounds in coals and chars. Presently, the organic sulfur content is determined indirectly by subtracting the sulfate and sulfide contents from the total sulfur.

The modeling work presented in this thesis does not account for reactions of nitrogen and sulfur during coal pyrolysis. Inclusion of nitrogen in the model does not appear to be a formidable task considering that its presence in substituent groups on aromatic rings can be neglected. Modeling of reactions of sulfur forms, however, must await further insight into their complex reaction mechanism; for example, better understanding of

reactions of inorganic sulfur (FeS_2) with organic material is needed (Attar, 1978). Both nitrogen and sulfur are very important from the point of view of the impact of coal utilization on the environment. Solomon's work (1977) was primarily directed towards studying the evolution of pollutants during rapid devolatilization and by extension during any coal-conversion process.

Figure 2.2.2 can now be modified to include the hetero-atoms O, N, and S. The modified model is presented in the Fig. 2.2.3, which was originally proposed by Given (1960) and subsequently modified by Wiser (1973) and others. It should be pointed out that the picture presented is not meant to be 'the' structure of any coal, but merely an educated guess based on literature on medium and high rank coals. As we shall see later, such a structure comes very close to being able to predict the products of pyrolysis and presumably other conversion processes. In the structures presented in this thesis, the actual three-dimensional packing of the material in coal is not a consideration. Hence, aspects like lamellar structure of coal (i.e. interatomic distances in one direction are much greater than in the other two directions) are not part of the model.

Mineral Matter in Coal:

Suuberg (1977) and Ode (in Lowry, 1963) provide good reviews of pertinent information on mineral matter in coal. Important points regarding the mineral matter are:

[a] It is different (generally more) from ash because during a coal-conversion process, it gives off some gases and vapors which are not accounted for in the ash left behind. Examples are CO_2 from carbonates, H_2O from water of hydration, sulfur dioxide by burning

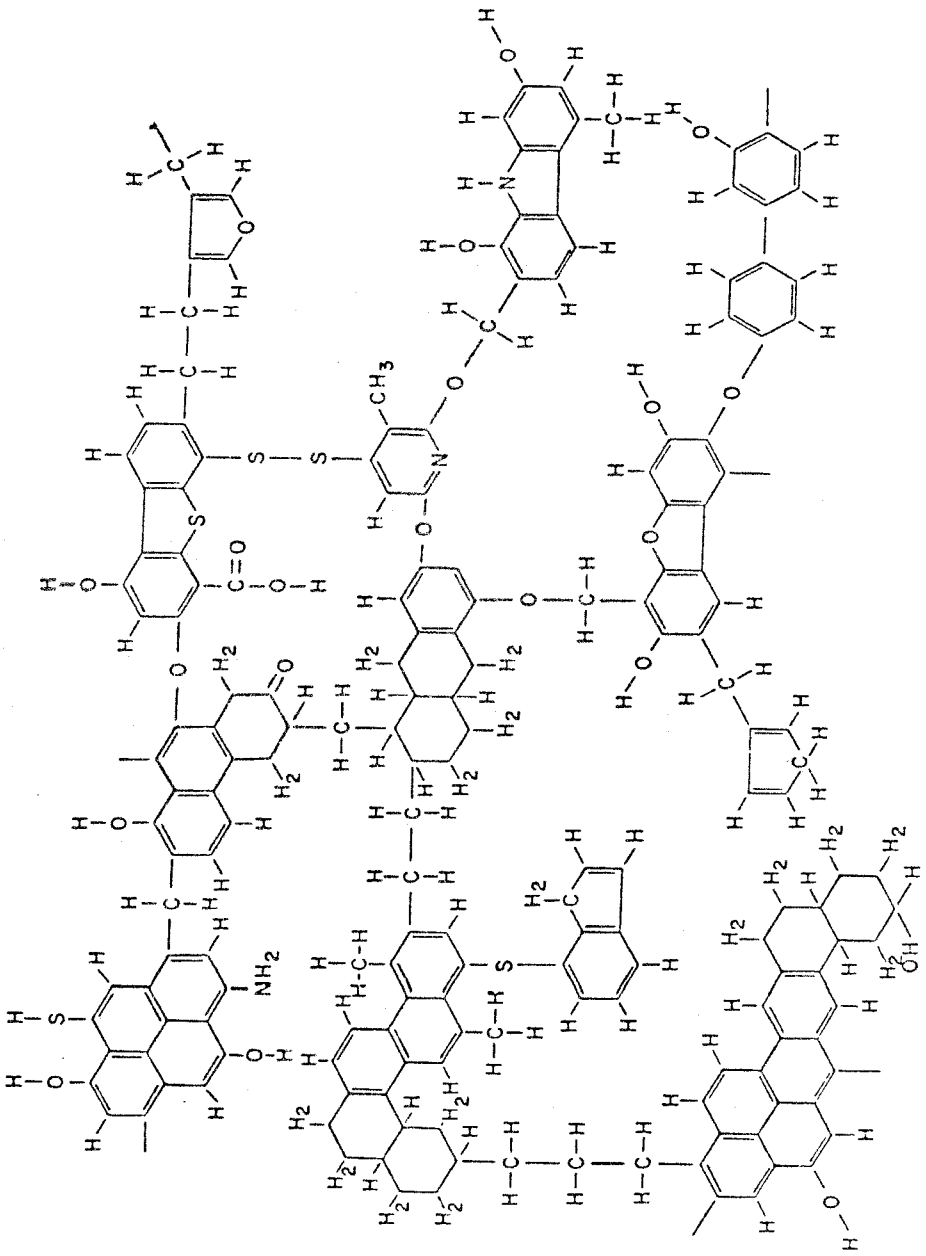

Figure 2.2.3: A Model for Chemical Structure of Bituminous Coals (after Given, 1960; and, Wiser, 1973).

of pyrites to give iron oxides, etc.

[b] Relations are available which do a fairly good job of relating the ash, which can be determined easily, to mineral matter which is difficult to determine.

[c] Mineral matter, as mentioned earlier, is believed to be important in coal reactivity because of its possible catalytic effects. A discussion on these effects and the relevant literature can be found in Suuberg (1977). While this may be a very important area for research in coal chemistry, it is beyond the scope of this thesis.

3. Physical Structure of Coal

Coal is a porous solid. This section discusses the pore structure in coals and points out the associated heat and mass transfer problems within coal particles.

The relevant questions regarding the physical structure of coal are: how are the aromatic clusters arranged in the coal matrix? Are they continuously dispersed or grouped together in small subunits separated by vacant spaces? We are interested in the physical layout and porosity of coal which plays a pivotal role in mass transport within coal particles. Poresize distribution and other related porosity measurements on coal have been made (Gan et al., 1972a) by nitrogen adsorption, helium and mercury displacement, and mercury porosimetry techniques. The results indicate that most coals have a significant pore volume with porosity ranging from 4% to 23%. Three size-dependent categories of pores were found: micropores

between 4 to 12 Å, transitional pores between 12 and 300 Å, and macropores above 300 Å and up to possibly 10,000 Å. Pores between 4 to 12 Å account for a substantial fraction of the open pore volume in many medium and high rank coals. In the low rank coals on the other hand, macropores (> 300 Å) make the greatest contribution to porosity. Transitional pores are important in the low rank bituminous coals. This trend is consistent with the coalification process because the coal structure becomes more compact with increasing rank.

The transitional pores and the macropores can be collectively thought of as spaces partitioning coal into smaller units containing the micropores. Then a coal particle can be modeled as consisting of two phases: a bulk phase, and a pore phase. If a coal does not undergo drastic changes in its physical structure during reactions, such models help in analyzing the effect of porosity on the reaction. Subbituminous coals are believed to conform to these models. On the other hand, bituminous coals exhibit thermoplastic behavior. Upon heating,these coals soften and become deformable, altering their original structure. They resolidify on cooling. In such coals the original pore structure may not have much relevance to the situation during reaction.

The physical structure of coal may have an important effect on its reactivity in terms of heat and mass transfer limitations within coal particles. For example, if a coal particle is heated rapidly and undergoes an endothermic reaction, its center and surface temperature may differ significantly at any given moment. Such lack of uniformity of temperature within the particle will result in different parts of it reacting at different temperatures leading to different product compositions. Similarly, if mass transfer resistance within a particle is high, both the

reactants (externally supplied, e.g., hydrogen) diffusing inwards and the products diffusing outwards will be slowed down. Hindrance in inward diffusion of reactants will reduce the reaction rate, while slower outward diffusion of products increases the probability of their participation in secondary reactions.

Considering the diversity of physical changes undergone by coals during conversion processes and the wide range of experimental conditions encountered, a general analysis resulting in predictive capability regarding the effect of heat and mass transfer limitations on coals' chemical behavior remains a challenging problem. Some attempts made in this direction will be discussed in the next chapter.

Chapter III

PYROLYSIS OF COAL:
MECHANISM OF CHAR, TAR AND GAS FORMATION

1. General

In this chapter we discuss the chemical and physical processes involved in coal pyrolysis. Firstly, the portions of coal's chemical structure likely to participate in chemical reactions are identified, and the types of reactions are postulated. Then, the mechanism of volatile product formation is discussed in the context of the overall change. It is concluded that there is no à priori distinction between volatiles and non-volatiles in a coal and they are both formed from the same chemical structure. Finally, we discuss the heat and mass transfer limitations within coal particles and how these limitations can be modeled.

In the rest of this section we answer two pertinent questions: what is pyrolysis in practical terms, and what are the parameters affecting its outcome ? The answers identify in a general sense the avenues of investigation open for research on pyrolysis.

Removal of gases and liquids from coal by heating it in a vacuum or an inert environment is generally referred to as devolatilization or pyrolysis. This process is basically a laboratory equivalent of the natural process of carbonization in which the decomposing organic matter slowly acquires a graphite-like structure. The natural process is very slow, taking perhaps millions of years to go from plant matter to the final graphite structure, while in the laboratory the change is artificially accelerated. The laboratory process starts with a material — coal — which is well on its way to complete carbonization, and results in a residue which although not very close to the graphite structure, is less reactive than the original coal. In both the processes, the chemical change basically

involves rupture and loss of the weakly bound portions of the organic matrix in the material. The mechanism of this change during the natural carbonization process has been investigated for several decades. The mechanism in the laboratory process is discussed in section 3 of this chapter.

In a typical pyrolysis process, a sample of coal particles is heated to a high temperature inside a reactor in which a vacuum or an inert atmosphere is maintained. Three types of products are formed (refer to figure 3.1.1):

(i) the relatively lighter inorganic and lower hydrocarbon gases which are usually swept away from the reaction zone by a stream of inert gas,

(ii) the medium and heavy molecular weight organic compounds which escape from coal in vapor form and are generally found deposited as liquids on the surfaces in the vicinity of the reaction zone; the liquids are called tar, and

(iii) the solid residue left behind in place of the original coal sample; the residue is termed char.

Collection and analysis of these classes of products has become an essential feature of the research on pyrolysis. Substantial progress has been made in using modern techniques of analytical chemistry for characterization of these products. The information obtained can be used to formulate basic concepts about the chemical structure of coal and the mechanism of its reactions.

The parameters affecting the relative yields of the three kinds of products can be divided into two groups: those related to the coal; and

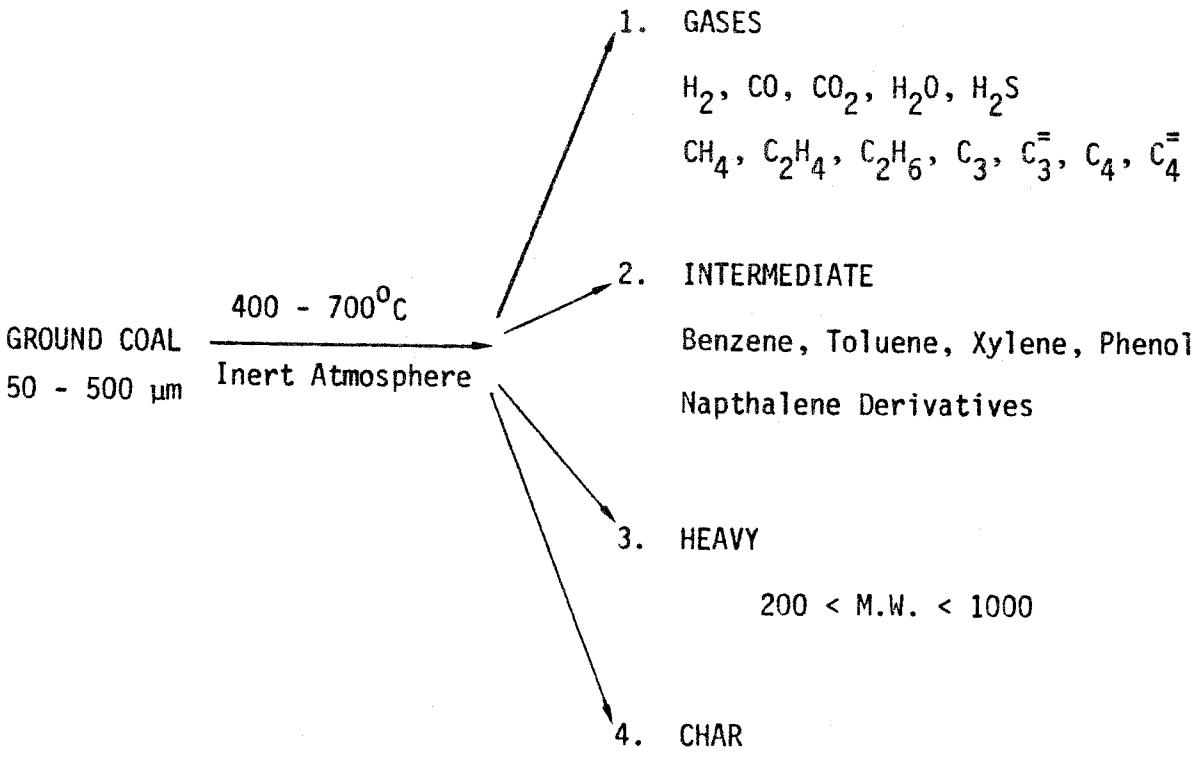

Figure 3.1.1: Products of Pyrolysis of Coal

those representing the experimental conditions. Such characteristics of coal as its chemical composition and functionality and physical structure and thermoplasticity, fall in the first group. The diversity among different coals provides a wide range for these characteristics, and makes it a challenging task to identify the features common to all coals.

Temperature is the parameter of foremost importance in the second group. So much so that appreciable amounts of products are formed only above a certain decomposition temperature, which although rank dependent is generally around 400^{o}C. As the temperature is increased, the chemical structure of coal begins to break down more drastically and the total yield of volatile products and the relative yield of gases increases. It is believed that beyond 700^{o}C or so, the bonds in the aromatic clusters in coal (refer to section 2 of chapter 2) are destabilized, and at very high temperatures the products formed yield little information about the original structure. This work is limited to temperatures between 400^{o}C and 700^{o}C at which the change is less drastic.

In the past few decades it has been recognized that not only the highest temperature but also the time-temperature history is an important variable. For example, earlier work on pyrolysis mostly used low heating rates which resulted in low yields. The present trend is to rapidly elevate the coal sample to the final temperature and maintain it there for the desired duration of time. The rate of production of volatiles is highest at the beginning, and it steadily goes down until a point is

crease the yield beyond this asymptotic value, one has to raise the

temperature. This observation was used to devise some novel heating schemes in which the sample was deliberately maintained at intermediate temperatures before reaching the highest temperature. The aim was to compare the yield and composition of products with the case in which the highest temperature was attained directly. Definitive conclusions have not yet been reached about the extent to which time-temperature history affects the pyrolysis results.

Besides temperature, the other parameters that belong to the second group include:

(i) those affecting the physical processes of heat and mass transfer within coal particles, e.g., size of the particles, pressure in the reactor, etc., and

(ii) those affecting the chemical processes directly, e.g., nature of the environment — inert, hydrogen-rich, etc. — around the sample, foreign material in contact with the sample, etc.

The effects of some of these parameters will be discussed in Chapter 6.

The important questions that need to be answered about pyrolysis can now be enumerated as follows:

- What portions of the coal's structure are weakly bound and are susceptible to thermal rupture?
- What reactions follow this rupture of the weaker bonds?
- How do these reactions account for the various products?
- What is the effect of the various experimental variables on: the total yield, the relative yields of the three kinds of products, composition of the products?

We attempt to answer the first three questions in this chapter. The effect of the physical structure of coal on the pyrolysis results is also discussed.

2. Chemical Reactions of Pyrolysis

In this section we postulate the type of chemical reactions that are likely to take place during pyrolysis at temperatures between 400^{o} and $700^{o}C$.

The discussion presented here is limited to the reactions of carbon, hydrogen and oxygen structures in coal as described in the last chapter. Reactions of nitrogen and sulfur functional groups and of the inorganic portion of coal are not considered here and are not included in the mathematical model developed in the next chapter. Most coals investigated in this work had low nitrogen and sulfur concentrations (less than 2% and 4% by weight, respectively) and hence nitrogen and sulfur reactions could not have had a significant effect on the overall results. They should be incorporated in general coal models because of the concern about the impact of coal utilization on the environment. Similarly, the inorganic portion of coal may be important because of its possible interaction with the organic reactions. It is believed that this interaction will be more important in gasification and oxidation reactions than in pyrolysis.

Pyrolysis of hydrocarbons has been studied for a long time. Most of these studies were done on aliphatic compounds, although some investigated reactions of aromatic compounds and their associated aliphatic groups. It is well established now that pyrolysis involves free-radical chain reactions

initiated by thermal rupture of weaker bonds. The chemistry of such reactions holds a prominent place in organic chemistry, and a fair amount of generalized concepts and information is available in literature. We will use these concepts to formulate reactions of coal pyrolysis. The problem in coal is more complicated than those in literature, firstly because unlike hydrocarbons coal does not have a representative molecule, and secondly because of lack of knowledge about kinetics of condensed phase reactions. The first difficulty arises because of the complexity of coal's chemical structure which consists of several different types of functional groups. Reactions of any one functional group will be affected by the presence of other groups in its vicinity. The second difficulty is a result of the past focus on gas phase pyrolysis. Not withstanding these difficulties, the basic ideas developed in the literature are still expected to apply to coal pyrolysis.

It was concluded in Chapter 2 that the carbon, hydrogen and oxygen structures in coal consist of a population of aromatic clusters connected together by aliphatic and etheric bridges, and carrying aliphatic, phenolic, carboxylic and carbonyl groups. Based on the results of pyrolysis of alkyl aromatic compounds, it has been established that aromatic bonds do not rupture below about 700^{o}C and the aromatic rings are stable and maintain their integrity. Thus, the individual carbon and hydrogen atoms involved in the rings are unable to participate in separate reactions. This is a conclusion of great significance when applied to coal pyrolysis in the temperature range of interest, i.e., up to 700^{o}C. It implies that the multi-ring aromatic clusters in coal retain their structure during thermal

treatment. Hence, although a cluster as a whole might take part in a reaction by virtue of some reactive functional groups on its peripheral aromatic carbons, the atoms involved in the ring system are unavailable for reaction. Of course, some rings might destabilize because of the complicated reaction mechanism some of their substituent functional groups may have to undergo. But, by and large, most of the clusters will remain intact.

Obviously then, such individual characteristics of the clusters as their size (number of rings involved) cannot be of crucial significance to the outcome of pyrolysis reactions. It is possible that the kinetics of the reactions are altered by such characteristics, but in general one can neglect any qualitative effects on the chemistry. The importance of their size on the physical process of mass transfer within coal particles will be discussed later.

Consider another feature of the population of clusters. Although different clusters in a coal would contain different number of rings, the spread in their size would be small. Most clusters would be at the most one or two rings smaller or larger than each other. The mean of the population will depend on the rank of the coal, with higher rank corresponding to larger number of rings.

Given the above two features, namely:

[a] unlikelyhood of rupture of clusters makes it possible to treat them as whole units, and

[b] most clusters in a coal would not be too different from each other,

we can simplify the coal structure, for our purposes, by visualizing it in terms of 'average' clusters. We replace the real situation of a population of multi-size clusters with a model consisting of a population of 'average' clusters. The size and other characteristics of this 'average' cluster will depend on the overall properties of the coal — the total concentrations of aromatic carbons, clusters, etc. Section 4 of the next chapter discusses the relationship between the initial values of the state variables and the representative characteristic parameters of an average cluster.

Unbreakability of the ring system leaves the non-aromatic portion of coal as the prime agent of reactivity in pyrolysis. Since most of this portion occurs as substituent groups on the aromatic rings, the peripheral aromatic carbons in each cluster become the focus of attention in the chemical structure of coal. These are those aromatic carbons which are connected to only two other aromatic carbons, and thus must bear either an hydrogen atom or a substituent group.

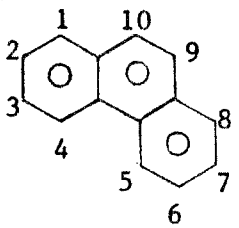

In the above figure, the cluster has a total of 14 aromatic carbons, but only 10 of them are peripheral.

The substituent on a peripheral carbon can be either a carbon-hydrogen aliphatic group, like ($-CH_3$), ($-C_2H_5$), etc., or an heteroatom group, like (-OH), (-O-), (-COOH). More specifically, in light of our discussion on

structure in Chapter 2, the following are the substituent groups of interest:

(1) $-CH_3$, $-C_2H_5$, in general -R, and $-CH_2-CH_2\cdots$

(2) $-CH_2-$, $-C_2H_4-$, in general $-CH_2-R-CH_2-$

(3) -OH, -O-, -COOH, =O

In the above depiction, solid lines at ends of the groups represent bonds with peripheral aromatic carbons in clusters. However, when there are lines at both ends, e.g. $(-C_2H_4-)$, the peripheral aromatic carbons at the two ends belong to different clusters, thus representing bridges. A dotted line represents a hydroaromatic structure on two neighboring peripheral carbons of the same cluster.

Although we have eliminated the aromatic rings from consideration of reactivity, we are still left with the problem of dealing with the peripheral aromatic carbons because they carry the substituent groups. It will now be shown that by comparing the strengths of the various bonds, we can go one step further in our simplification such that we have to concern ourselves only with the non-aromatic portion of a coal.

There are only two types of carbon-carbon bonds which are of interest to us from the point of view of reactivity:

(1) $C_{aromatic}-C_{aliphatic}$ bonds.

An example is:

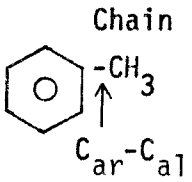

All members of the first two categories of the substituent groups

mentioned before have at least one such bond. Those groups which constitute bridges between the clusters have two such bonds, one at either end.

(2) $C_{aliphatic}$-$C_{aliphatic}$ bonds.

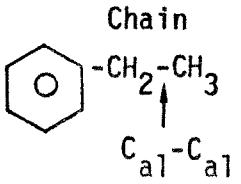

Such bonds are present only in those groups which consist of at least two carbons.

In the above figures, benzene rings are intended to represent aromatic clusters. However, while comparing the strengths of these two types of bonds, we will neglect the effect of the size of the clusters. Benson (1976) has listed the bond-dissociation energy for the first type to be about 100 kcal/mole, and for the second type to be about 72 kcal/mole. Therefore, at 600°C the dissociation of second kind is approximately seven orders of magnitude faster than that of the first kind. Obviously, we can neglect the dissociation of C_{ar}-C_{al} bonds that connect the substitutent groups to the peripheral aromatic carbons on clusters. There is one exception to this, namely, the bonds involved in the methylene bridge group:

Methylene Bridge

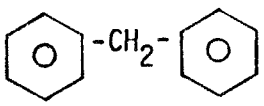

The strength of the two C_{ar}-C_{al} bonds in this case is approximated by Benson to be about 77 kcal/mole which is comparable to the C_{al}-C_{al} bond

strength. Rupture at either of the two places is then as fast as Cal-Cal rupture.

Since we are going to neglect C_{ar}-C_{al} bond rupture (except in the case noted above), the first aliphatic carbon next to a peripheral aromatic carbon, i.e., an alpha carbon, becomes the atom of pivotal importance in the carbon-hydrogen skeleton of a coal. By moving one carbon atom away from a ring system, we can consider substituent groups on aromatic carbons as substituent groups on alpha carbons. For example, in Φ-CH_3 (where Φ as before represents a peripheral aromatic carbon on a cluster) ($-CH_3$) which is a substituent group on the ring can be looked upon as an alpha carbon carrying three alpha hydrogens. We will then have to consider only the rupture of C_α-H_α bonds, and subsequent reactions of the products of such rupture.

Similarly, a Φ-C_2H_5 can be considered to be an aromatic carbon connected to an alpha carbon, which in turn carries two alpha hydrogens and one ($-CH_3$) group. The carbon in such a ($-CH_3$) group is in beta position with respect to the aromatic ring. A Φ-CH_2-CH_2-Φ' can be interpreted as two hydrogen-carrying alpha carbons connected to each other, and each connected to a different cluster. Instead of carrying two hydrogens, the two alpha carbons could have carried (-H) and (-R) in any combination. What is significant is that for each of the alpha carbons one valence is satisfied by bonding with the other, thus giving rise to a bridge between two clusters.

Hence, side chains like ($-CH_3$), ($-C_2H_5$), etc. and bridges like ($-CH_2$-CH_2-), etc. can be considered as substituents on alpha carbons. This

feature is used in the mathematical model presented in the next chapter for calculating concentrations of combinations of substituent groups. These combinations constitute the reacting configurations in coal.

As mentioned before, pyrolysis of hydrocarbons consists of a set of chain reactions initiated by formation of free radicals due to dissociation of weak bonds in the chemical structure. Once the free radicals are generated, they take part in a variety of reactions ranging from abstraction of hydrogen to formation of double bonds, etc. Generally, such chain reactions are divided into several classes and only the most important reactions (based on their contribution to product formation) in each class are considered. The primary reactions of the carbon-hydrogen structure in coal pyrolysis can be categorized as follows:

[A] Bond Dissociation: Since we have discounted the rupture of C_{ar}-C_{ar} and C_{ar}-C_{al} bonds, the bonds which rupture belong to the non-aromatic portion of coal, and are listed below:

(i) C_{α}-C_{α}

(ii) C_{α}-C_{β}

(iii) C_{β}-C_{β}

(iv) C_{α}-H_{α}

(v) C_{α}-C_{arm}, in the case of methylene bridge.

In all except the third case, dissociation occurs at the alpha carbon position. Chains or bridges attached to alpha carbons would break away, generating what are called alpha radicals and other small radicals. Examples are:

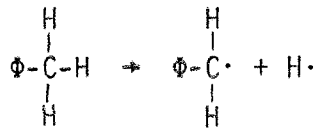

Hydrogen Dissociation

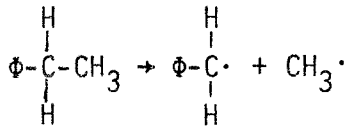

Chain Dissociation

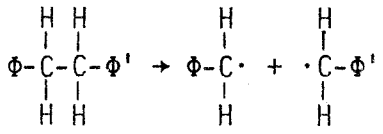

Ethylene Bridge Dissociation

And, as mentioned before, dissociation of C_{ar}-C_{al} bonds in methylene bridges will also be considered:

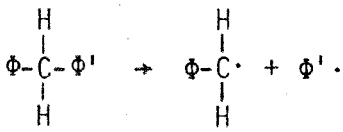

Methylene Bridge Dissociation

The alpha radicals produced are considered very stable (Benson, 1976), resonance being responsible for their stability. Although the above illustrations show alpha radicals having two alpha hydrogens, those two bonds can in general be occupied by any two substituents. However, if an alpha carbon already had a radical or a double bond on it, such dissociation reactions would be unlikely because of the unstable nature of the resulting structure. This structure would be so reactive that the dissociating bond would be reinstalled immediately. This means that in our chemical system we will not encounter an alpha

carbon carrying two radicals, or one radical and one double bond. This convenience is fully exploited in random mathematical distribution of the substituent groups as will be seen in the next chapter. The small radicals produced (e.g. $CH_3\cdot$) will take part in hydrogen abstraction reactions, thus propagating the chain. The kinetics of such decomposition reactions would obviously depend on the strengths of the bonds being ruptured.

(B) Hydrogen Abstraction: Alkyl radicals such as $CH_3\cdot$, phenyl radicals like $\Phi\cdot$, beta radicals like $\Phi\text{-}CH_2CH_2\cdot$, and protons $H\cdot$, rapidly participate in a series of hydrogen abstraction reactions. The hydrogen atom abstracted can be either an alpha hydrogen or a beta hydrogen (in beta hydrogens are included hydrogens on beta-plus carbons). These reactions lead to formation of alpha and beta radicals. Examples are:

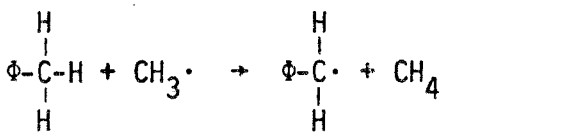

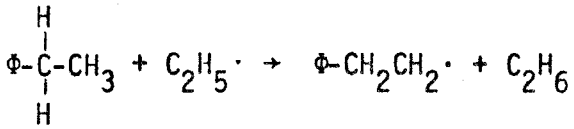

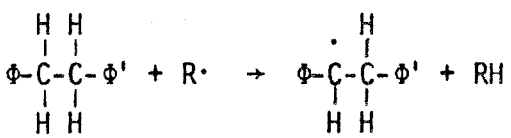

It is interesting to note that these will be vapor-solid reactions because the alkyl and other radicals will be in the vapor form while donors of hydrogen atoms will be a part of the solid organic structure.

In other words, we are discounting those reactions in which both the reactants are in the vapor phase. This is because such homogeneous reactions will actually constitute a set of secondary reactions in pyrolysis, while we are interested here only in the primary reactions. Reactions which in some way alter the solid chemical structure of coal will qualify for primary reactions. This point will be applicable to all reactions postulated in this thesis, unless otherwise mentioned. At the same time it should be clarified that although these are vapor-solid reactions, we will not be concerned with adsorption, desorption and such other aspects of gas-solid reactions.

Alpha radicals do not abstract hydrogen atoms from their surroundings (in significant quantities) because of their resonance stabilization.

[C] Double Bond Formation: As mentioned before, spectroscopic techniques applied towards determination of coal's structure have indicated among other things that olefinic double bonds are absent. However, both alpha and beta radicals generated during pyrolysis can lead to the formation of double bonds in the aliphatic portion of the carbon-hydrogen structure. The three possible configurations are:

(i) $C_\alpha = C_\beta$

(ii) $C_\alpha = C_\alpha$

(iii) $C_\beta = C_\beta$

Examples are:

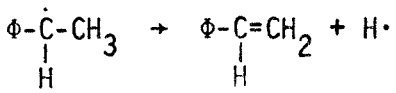

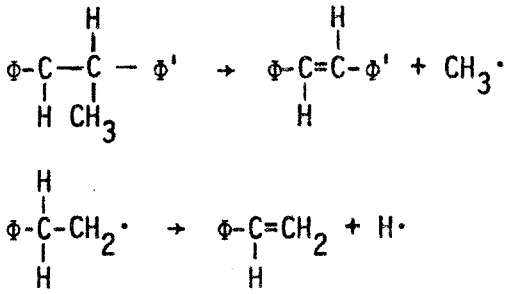

The strength of double bonds is in the vicinity of 180 kcal/mole. Therefore, in the temperature range of interest in this study (up to 700°C), these bonds can be considered unbreakable. This, in addition to the earlier mentioned unlikelihood of the co-existence of double bonds and radicals on the same carbon, removes the carbons involved in double bonds and their substituents from active participation in the reaction mechanism. Thus as pyrolysis progresses and more double bonds are formed, the carbon-hydrogen structure loses its reactivity. Finally, it leads to a complete halt in volatile product formation as will be discussed in detail later in this chapter.

In principle, double bonds are open to addition reactions in which they are attacked by protons or small alkyl radicals — essentially reverse of the above reactions. However, it can be postulated that hydrogen abstraction will be faster due to higher hydrogen concentrations, and small radicals will leave as stable gas molecules rather than reattach to the double bonds. From the overall viewpoint, addition to the double bonds is equivalent to a reduction in the availability of alkyl radicals and hence production of hydrocarbon gases. Therefore, one can reduce the rate of the forward reaction in order to account for the reverse reaction of addition.

One interesting point to note here in brief is about the self-deactivating characteristic of the chemical system in pyrolysis. Consider the fact that double-bond formation is accompanied by generation of small radicals, which by abstracting hydrogen give rise to alpha and beta radicals, which in turn lead to formation of more double bonds, thereby further deactivating the structure. Hence, as more and more of these reactions take place, coal becomes less and less reactive. Such a behavior agrees well with experimental observations. It will be further discussed later in this chapter.

[D] Addition-Displacement: It was mentioned earlier that since C_{ar}-C_{al} bonds have high bond energies, their thermal decomposition is not of much consequence in this work, except in the case of the methylene bridges. However, these bonds can still undergo scission if attacked by hydrogen or small alkyl radicals. It is believed that the mechanism of such reactions involves an intermediate stage in which the aromatic ring is temporarily disturbed to make an additional valence of the aromatic carbon free for the attacking radical. Subsequently, the original substituent on the aromatic carbon is lost, while the attacking radical stays and becomes the new substituent. Examples are:

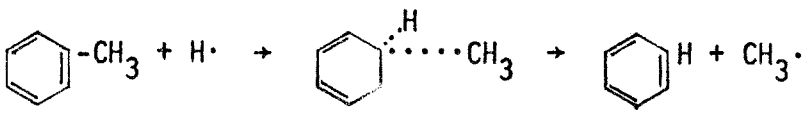

Similarly for a bridge:

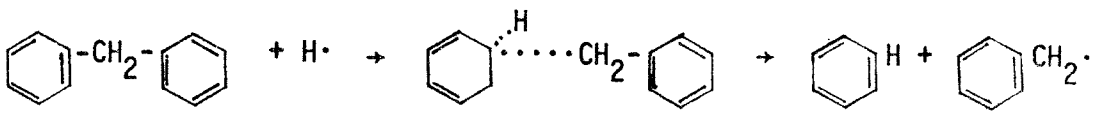

Strong support for the addition-displacement mechanism is provided by the work of Sharkey et al. (1966) and Levy et al. (1954).

There are at least two important consequences of these reactions. For the sidechains, they result in an enhancement of generation of ($CH_3\cdot$) radical, and hence methane gas. This is because (as will be clear from actual numerical values in the chapter on computer simulation) most bituminous coals have a substantially higher concentration of alpha hydrogens compared to the concentrations of alkyl substituents on alpha carbons. Accordingly, there is a high probability that an alpha carbon will have three alpha hydrogens on it, and consequently high probability that when a C_{ar}-C_{al} bond ruptures a ($CH_3\cdot$) radical is produced. Therefore, even in the absence of high concentrations of ($-CH_3$) substituents on alpha carbons, a high concentration of alpha hydrogen assures production of substantial amounts of methane.

Similarly, even if we limit the size of the general alkyl substituent (-R) on alpha carbons to at the most two carbons (i.e. a $-C_2H_5$), then addition-displacement reactions will explain the production of higher alkanes and alkenes — those containing more than two carbons. This is very important because in most coals alkyl substituents containing more than two carbons are not present in substantial amounts:

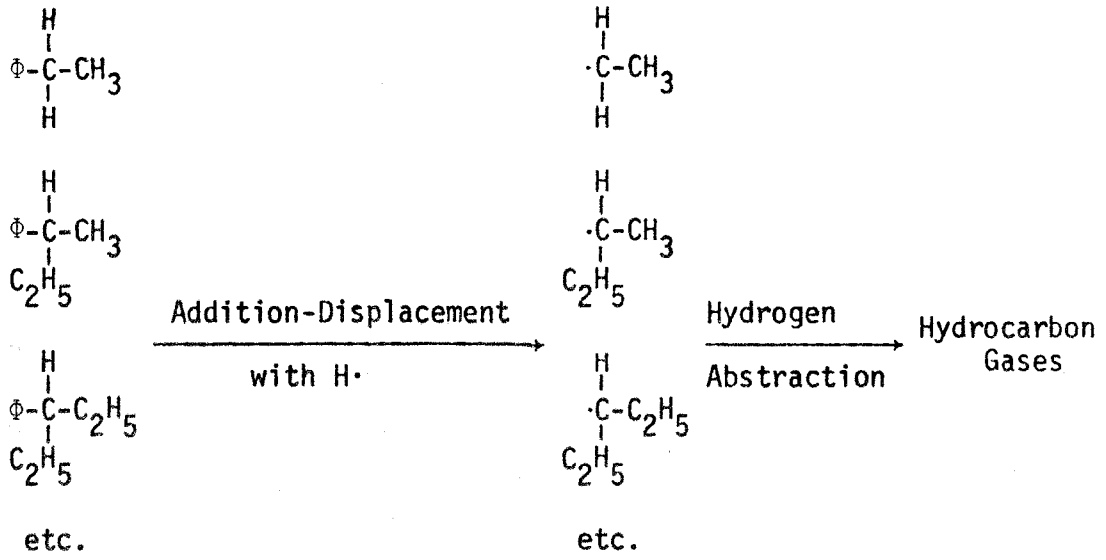

Secondly, such reactions help the process of bridge rupture. As was discussed before, the C_{ar}-C_{al} bond strength in a methylene bridge Φ-CH_2-Φ is about 77 kcal/mole, while the strength of a C_α-C_α bond in an ethylene bridge Φ-CH_2-$CH_2\Phi'$ is about 50 kcal/mole. Therefore, if most connections between aromatic clusters involve the latter kind of bridges, elevating the temperature to 600^oC or so would ensure a substantial rate of rupture of these connections. However, if methylene bridges are more abundant in a given coal, thermal decomposition alone will not suffice to explain the tar formation (which is a result of bridge rupture). In such cases addition-displacement reactions would be of great significance because their energy requirements are lower.

[E] Recombination: Although, in principle, one should be concerned about various kinds of recombination reactions, the one discussed here will be between alpha radicals leading to the formation of a bridge. Such a reaction is of great significance from point of view of tar formation:

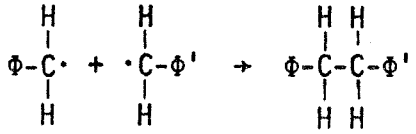

It results in an increase in the number of connections that a cluster has with its neighboring clusters in the coal matrix. This leads to a more compact structure, which slows down production of tar. The recombination reaction above is not merely a reverse of a bridge rupture reaction. Alpha radicals generated by dissociation of sidechains are also going to take part in such recombination reactions. At the same time, both the reactants here are meant to be in the solid phase, and hence only alpha radicals very close to each other would be eligible for recombination. That too would be hindered by such constraints as orientation, etc. Reactions in which one of the two units is in the vapor form, i.e. secondary recombinations of free clusters, are very important because of the possible transport limitations. In this thesis they are accounted for by a parameter x, which is a fraction by which the rate of bridge rupture is reduced. This idea will be expanded later on.

Recombinations in which both the units are in the vapor phase are not considered here because they do not affect the chemical structure of coal. They would be more significant in predicting the molecular weight distribution in tar, something which has not been attempted in this thesis.

This concludes the discussion on the major types of reactions of the carbon-hydrogen structures. The mechanism of product formation based on these reactions will be discussed in the next section.

Reactions of the oxygen functional groups, namely, phenolic, carboxylic, and carbonyl, have not yet been discussed. Although these groups also occur as substituents on the aromatic clusters, we assume that their reactions can be considered separately from those of the aliphatic substituents. Each of them is allowed to participate in one characteristic reaction, producing water, or carbon dioxide, or carbon monoxide, respectively.

Separation of oxygen reactions from the general reaction mechanism simplifies modeling. We assume that the coal structure does not contain combinations of oxygen and aliphatic groups, e.g., (Φ-O-CH_2-Φ'), and that they do not interfere with each other's reactions. However, as we will see in the next section, concentration of ether linkages has a direct bearing on the amount of tar produced.

Experimentally, volatile products of pyrolysis are found to include carbon monoxide, carbon dioxide, and water vapor among other gases. Although part of the carbon dioxide could be evolved from carbonates in the mineral matter, a substantial portion of it must be produced from carboxylic functional groups. The reaction is generally represented as follows:

$$Ph - COOH \xrightarrow{heat} Ph\overset{COO}{\cdots\cdots}H \longrightarrow Ph\text{-}H + CO_2$$

where Ph is an aryl group. If one postulates that presence of (-COOH) groups does not interfere with carbon-hydrogen reactions, then the only other effect of these groups on the structure is that they take up some of the peripheral aromatic carbon sites on the clusters in coal. Also, one should subtract the concentration of carbon involved in these groups

(and in carbonyl groups) from the total aliphatic carbon while determining the concentration of carbon in bridges and sidechains.

Carbonyl groups are believed to be the source of carbon monoxide in pyrolysis. Some investigators (Depp et al., 1956, and Factor, 1969) have reported CO from pyrolysis of (-OH) bearing aromatic compounds. However, in these cases the amount of CO formed as a percentage of the initial sample was so small that it can be explained as a result of the very slow process of ring-rupture. The reaction of the carbonyl groups is generally represented as:

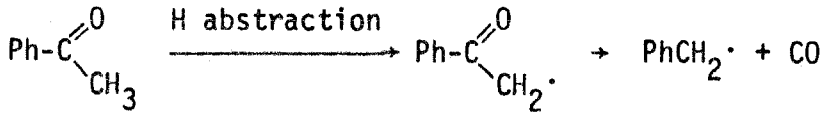

Since this reaction produces an alpha radical, it would contribute to the reactions of the C-H skeleton. However, the amounts of carbon monoxide produced by pyrolyzing medium and high rank coals is so low that this complication can be overlooked. Thus CO production, like CO_2 production, leaves the C-H structure unaffected.

A portion of the water-vapor detected in the gaseous products of pyrolysis can be accounted for by the physically adsorbed water on coal surfaces, which was left behind due to incomplete desorption during coal sample preparation. The rest of the water must be produced chemically, and hence is termed chemical water.

Reactions involving phenolic groups (-OH) are the prime candidates for production of water. Two neighboring phenolic groups will react to give a molecule of water and an ether bond :

$$\Phi\text{-OH} + \text{HO-}\Phi' \rightarrow \Phi\text{-O-}\Phi' + H_2O$$

Each of the two clusters involved in the reaction gets an additional bridge (in addition to the already existing aliphatic bridges) in the form of ether linkages. Therefore, production of substantial amounts of water during pyrolysis would be indicative of increased etheric cross-linking between the aromatic clusters. This would also mean a reduction in the probability that a cluster would become 'free' of any connections with the coal matrix merely by the dissociation of aliphatic bridges. Therefore, this reaction has to be taken into account while computing the rate at which clusters become free. The pyrolysis behavior of subbituminous and other coals which have high oxygen contents are significantly affected by phenolic condensation reactions.

Some literature relevant to this section is listed separately in the references. It consists of papers on subjects ranging from pyrolysis of model compounds to mechanism of thermochemical reactions. These papers are meant primarily as a starting point for the reader interested in gaining an insight into coal pyrolysis by understanding the pyrolytic reactions of hydrocarbons.

3. Mechanism of Char, Tar, and Gas Formation

Although, in the last section the mechanism of formation of some of the products is obvious, a coherent discussion on volatile generation and char deactivation would be of great help in laying the foundations of mathematical modeling. The model as described in the later chapters is

basically a representation of the rates of the various mechanistic steps postulated in this section.

To recapitulate in brief, in pyrolysis one starts with a sample of coal particles which when heated in vacuum or in an inert atmosphere generate two kinds of volatiles, gaseous and liquid (called tar), while a solid residue called char is left behind. The amounts of volatiles formed are characteristic of the coal, the temperature of pyrolysis, etc. The following is a list of some of the salient features of pyrolysis which we would like to explain with the help of the theoretical concepts developed so far in this thesis:

[a] Production of the volatiles.

[b] Formation of char — a deactivated solid residue.

[c] Limited amount of volatile yield.

[d] Composition of the gaseous products — hydrocarbon gases, oxides of carbon, water, some hydrogen.

[e] Molecular weight distribution of tar.

[f] Higher the oxygen content of a coal, lesser the amount of tar formed.

[g] In general, an inverse relationship between the amount of gases formed and the amount of tar formed.

[h] Dominance of tar production during the earlier part of pyrolysis.

[i] Dominance of gas production during the later part of pyrolysis.

[j] Presence of double bonds and alpha radicals in the char.

[k] Similarity of elemental analysis and other characteristics between tar and the original coal sample.

These and similar other characteristics need to be explained within the framework of chemical structure and reactions already postulated.

Firstly, dissociation of sidechains leads to the formation of small alkyl radicals and hydrogen atoms, which by abstracting either an alpha or a beta hydrogen form lower alkanes and hydrogen gas. The alkenes are formed by the transfer of radical sites from beta carbons (actually beta-plus carbons) to alpha carbons. Addition-displacement reactions release complex radicals which later form higher hydrocarbon gases. As mentioned in the last section, this mechanism provides a way for production of heavier hydrocarbon gases despite the fact that in most coals the alkyl groups on alpha carbons contain at the most two or three carbons.

Alpha and beta radicals are the most important functional groups generated in coal as a consequence of the reactions producing hydrocarbon gases. In the case of the dissociation of an hydroaromatic structure at an alpha carbon, a beta radical would be produced at the other alpha carbon involved in the structure. An ethylene molecule can be subsequently eliminated from such a beta radical.

Oxides of carbon in pyrolysis products originate from carbonyl and carboxylic groups. Water is produced as a result of phenolic condensation reactions. Traces of hydrogen sulfide and sulfur dioxide can also be detected in gases produced in pyrolysis of high sulfur coals.

Production of tar can be explained with the help of an experimental observation. Tar produced by low temperature vacuum pyrolysis is found to resemble the parent coal in chemical composition (Solomon, 1977), infrared spectra (Solomon, 1977, Orning and Greifer, 1956, Brown et al.

1958), and NMR spectra (Solomon, 1977). The similarity of the infrared spectra is illustrated in Fig. 3.3.1 for four coals (taken from Solomon, 1979). This close resemblance suggests that the chemical structure of tar is very similar to that of the parent coal. In fact, the prevalent view is that basically tar consists of a random sample of the original coal,i.e., a mixture of aromatic clusters carrying substituent groups. There may be some minor differences between a coal and its tar due to either primary or secondary reactions as discussed later. The two would be less similar if pyrolysis was carried out at high temperatures and/or pressures.

Consider now the chemical structure of coal. Although there would be some 'free' clusters with no connections to the coal matrix, their amounts would be negligible in the coals of interest in this work. Most clusters would be connected to some of their neighboring clusters and so on, giving rise to a matrix of interlinked units. In reality each of these units is different — clusters may have different number of rings and so on — but we had earlier discussed the possibility of modeling them in terms of an 'average' unit. Similarly, in the absence of any information on how exactly these clusters are connected to each other, they can be considered randomly connected. The only constraint is that each one of them should have <u>at least</u> one bridge on it. The maximum number of aliphatic bridges on a cluster would obviously equal 3 x No. of alpha carbons on that cluster, for each of the three possible substituents on each of the alpha carbons. The number of bridges on most clusters would be somewhere in between the two extremes. A greater insight into the coalification process

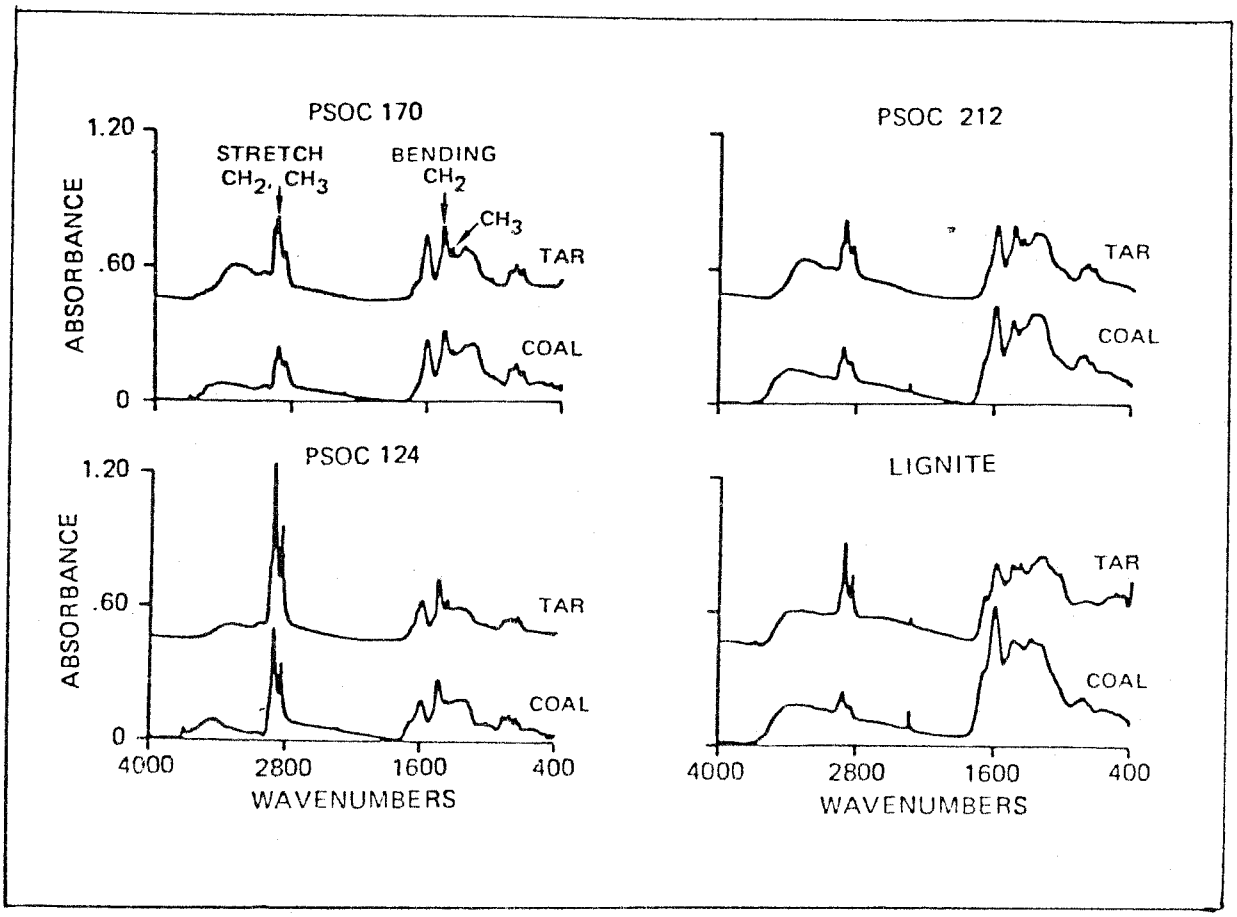

Figure 3.3.1: Comparison of Infrared Spectra of Parent Coal and its Tar for Four Coals (from Solomon, 1979).

would answer the question whether there is a naturally preferred arrangement of bridges. Distribution of bridges and other functional groups will be taken up in more detail in the next chapter. For now it will suffice to note that there is no à priori system of connections among clusters.

During pyrolysis some of these bridges will dissociate. The rate of such dissociation will be a function of the temperature, bond strength, and concentration of bridges. The strength of (C_α-C_α) bond in an ethylene bridge (Φ-$\overset{|}{\underset{|}{C}}$-$\overset{|}{\underset{|}{C}}$-$\Phi'$) is about 50 kcal/mole. This value is lower than the bond strengths of sidechains (approximately 65 kcal/mole), and hence bridges will break faster than sidechains.

Let us consider the rupture of ethylene bridges

$$\Phi\text{-}\overset{|}{\underset{|}{C}}\text{-}\overset{|}{\underset{|}{C}}\text{-}\Phi' \rightarrow \Phi\text{-}\overset{|}{C}\cdot + \cdot\overset{|}{C}\text{-}\Phi'$$

Three possible situations may arise as a consequence of such a rupture:

(1) Both the clusters involved have several other bridges connecting them to several other clusters.

(2) One of the two clusters either has no other bridge on it, or is connected to just one other cluster which in turn is not connected to any other cluster.

(3) Instead of just one, both the clusters involved in the reaction have the same characteristics as described in (2) above.

In the first case, bridge dissociation will not result in either of the clusters breaking loose from the coal matrix. Both of them may take part in a recombination reaction re-establishing the bridge.

In the second case, one of the clusters will again remain trapped.

However, the other one will be free of connections with the network; either all by itself, or in conjunction with another cluster. In other words, it will give rise to either a single-cluster free fragment or a double-cluster free fragment. Such free fragments may volatilize at the temperature of pyrolysis (whether or not they would have appreciable vapor pressure would depend on their molecular weight), and start diffusing out of the coal particle. In fact, in low-rank coals in which clusters consist of fewer aromatic rings, even a three or four cluster free fragment may become volatile. So there is no theoretical requirement to limit oneself to two cluster fragments. We choose to do so for the following three reasons:

(a) The primary interest of this work is in the intermediate and higher rank coals. The three and four cluster fragments in such coals would be too heavy to have appreciable vapor pressure at temperatures of interest here (up to 700^{o}C).

(b) Transport limitations are more severe for bulkier fragments. Their mobility thus curtailed, these large fragments would be of little consequence in tar production, as will be clear shortly.

(c) For sake of simplicity in modeling; neglecting them does not affect the process significantly.

These comments also apply to the third case in which both the clusters would be part of free fragments. We again discount the possibility that both the clusters would form single unit fragments, for it will imply that initially a two cluster fragment may be present in coal.

Figure 3.3.2 illustrates the process of generation of free fragments

Before Rupture

After Rupture

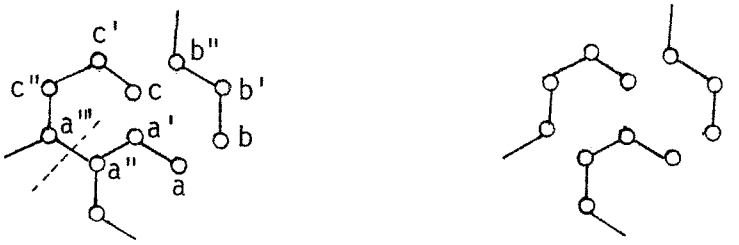

(a): No Volatile Fragments

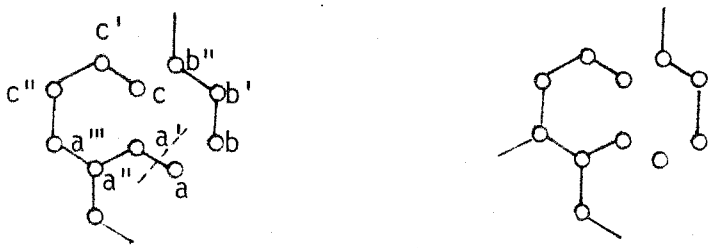

(b): Single Cluster Free Fragment

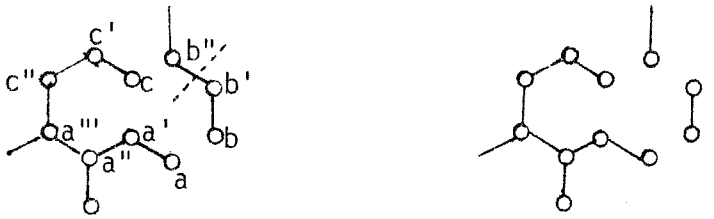

(c): Two Cluster Free Fragment

Figure 3.3.2: Generation of Free Fragments by Bridge Dissociation. See text for explanation.

schematically. Circles represent aromatic clusters and solid lines represent aliphatic bridges. They have been arranged in a honeycomb structure simply for the sake of this illustration. It is not meant to imply that such arrangements occur in coal. Bridge rupture is depicted by broken lines intersecting with the solid lines. In case (a), dissociation of the bridge a"-a"' does not lead to formation of one- or two- cluster fragments. The structure has been disturbed but still no cluster or group of clusters can volatilize. In case (b), dissociation of the bridge a-a', or b-b', or c-c' will each lead to a one-cluster free fragment. Such a fragment would become mobile as a vapor molecule, and start its journey out of the coal particle. It may or may not come out of the particle depending on whether it recombines with a radical site on the coal matrix along the path of diffusion. This would be further discussed under mass transfer limitations in the next section.

In case (c), dissociation of the bridge a'-a", or b'-b", or c'-c" will each lead to a two cluster free fragment. Such a fragment will also volatilize under our assumptions. It should be noted that although not all bridge-breaking reactions generate free clusters, they indirectly contribute by loosening the structure. Since we are dealing with a random process in a large population, the rates of bridge dissociation and volatile generation can be related through the probability that a cluster is free.

Rupture of ethylene bridges leads to formation of two alpha radicals. Longer bridges like (Φ-$\dot{C}$-R-$\dot{C}$-Φ') lead to an alpha radical and a beta radical. Methylene bridges (Φ-$\dot{C}$-Φ') rupture via additions more easily than by simple dissociation, and produce just one alpha radical.

Tar consists of the free fragments of clusters which are successful in escaping the coal particle. Not all free fragments are able to escape because of recombination with radical sites which they encounter on their way out. Alternatively, the free fragments themselves may combine resulting in a bulky molecule which condenses. Both these processes return some of the free fragments to the coal matrix, and therefore should be taken into account while formulating rate expressions. However, if the free fragments combine with each other in moderation without resulting in heavy molecules, or if the recombination occurs outside the particle, tar will be a mixture of one, two, three, etc. cluster molecules. This implies a molecular weight distribution in tar. Such a distribution has been observed experimentally as presented in Chapter 6. The recombination occurs because of the alpha and beta radicals on the clusters at those locations where they broke from the coal structure. These radical sites could otherwise be satisfied by hydrogen or other small radicals.

Substituent groups on a cluster leave with it when it becomes free and escapes the coal particle. Therefore, production of tar depletes not only the clusters but also the substituent groups like aliphatic sidechains and oxygen groups. Since these groups are the source of hydrocarbon and other gases, production of tar suppresses production of gases. The lower bond strength for ethylene bridges as compared to side chains, assures a faster rate of production of tar compared to gases. Therefore, in the earlier part of pyrolysis, more sidechains are being lost with the outgoing clusters than by simple dissociation. This situation prevails so long as the rate of free cluster production remains high. Later, when production

of tar slows down (for reasons we will discuss shortly), more sidechains are available for gas formation reactions. It is thus clear that there is an inverse relationship, in both rate and total amount formed, between tar and gases. In low temperature pyrolysis, most of the clusters in tar can be expected to bear their original substituents in coal, and therefore tar will closely resemble the parent coal in its structural characteristics. This conclusion substantiates the earlier statement that tar is basically a random sample taken from coal, the degree of similarity depending on the severity of pyrolysis conditions. The randomness feature is an essential consequence of treating the distribution of bridges and sidechains among clusters as random.

In light of the above discussion on mechanism of tar production, any reaction that increases connectivity among clusters is bound to reduce production of tar by reducing the probability that a cluster becomes free by dissociation of a bridge. One such reaction is phenolic condensation, which leads to ether linkages among clusters. Since phenols are a

$$\Phi\text{-OH} + \text{HO-}\Phi' \rightarrow \Phi\text{-O-}\Phi' + H_2O$$

prominent functional groups in high oxygen coals, this reaction cannot be neglected. Solomon (1979) has presented infrared spectra on a coal and its chars at several temperatures. They clearly show a rapid disappearance of hydroxyl peaks and an increase in the intensity of ether peaks with pyrolysis. He has explained this result in terms of the above reaction.

The increased cross-linking among clusters due to ether bonds necessitates two changes in the modeling of pyrolysis mechanism discussed so far. Firstly, we cannot make a complete distinction between reactions

of oxygen groups and those of the carbon-hydrogen skeleton. Especially, the phenolic groups have to be included in the random distribution of substituents on clusters. It should be noted however that alpha carbons have nothing to do with the distribution of phenolic groups, except that they together should equal the concentration of substituted peripheral sites on clusters. Secondly, the rate of generation of tar will be modified by the probability that clusters are unable to become free because of ether linkages. This will have an adverse effect on tar production. The amount of gases produced may increase. Many of the sidechain functional groups which would have been otherwise lost with the departing free clusters will now be available for forming alkyl radicals and eventually gas molecules. Such an effect was observed for the subbituminous coal studied in this work.

So far, our discussion has been limited to the production of volatiles during pyrolysis. No mention has been made of char — the solid residue left behind after pyrolysis. At temperatures of interest in this work, char will range between 70 and 90% of the original sample, depending on coal and other experimental conditions (Chapter 6). It is typical of pyrolysis experiments that volatile generation (especially tar) progressively slows down with time, with negligible weight loss beyond a point. It is obvious that this deactivation phenomenon is responsible for the solid char, which one would expect to have a modified version of the original structure of coal. Reactivity of chars is generally much less than that of coals. This is a result of a qualitative as well as a quantitative change in the chemical bonds in the structure, as will become clear shortly.

Therefore, it is not as if there is an à priori distinction between volatiles and non-volatiles in a coal. They are both formed from the same chemical structure, and are basically an inevitable consequence of each other's production.

Two chemical processes occuring during pyrolysis can account for the the progressive loss of reactivity. They are:

(a) Formation of double bonds, and

(b) Formation of new bridges by radical recombination.

The first one brings about a qualitative change, in the sense that double bonds are not initially present in the coal sample but are formed during pyrolysis. As discussed in the previous section, double bonds are formed via alpha and beta radicals. Bonds involved in sidechains as well as bridges are susceptible to such transformations.

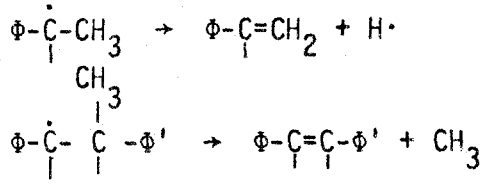

It was mentioned earlier that double bonds can be considered unbreakable at temperatures of interest in this work. Consequently, a double bond on a bridge can be referred to as unbreakable. Similarly, there would be unbreakable chains. Even dissociation of the other substituent on an alpha carbon carrying a double bond will be affected. Such a dissociation will result in the simultaneous occurrence of a radical and a double bond on the same carbon, a situation which is unstable and unlikely. In effect then, substituent groups and clusters associated with alpha carbons carrying double bonds will no longer contribute to volatile product

formation. As the concentration of double bonds increases, the rate of weight loss from coal will plummet.

It is interesting to note that we are dealing with a self-deactivating process, i.e., its own characteristics force it to halt after some time. Tar and gas production necessitates rupture of bonds. But bond rupture also produces alpha and beta radicals. These radicals subsequently lead to formation of double bonds, which render their neighboring bonds unbreakable. This way every single bond that breaks can contribute to the unbreakability of some other bonds in the system. Naturally, volatile generation will be rapidly driven to a complete halt.

The second process involving formation of new bridges has quantitative rather that qualitative importance. It does not produce any new kind of bond. Recombination among radicals on different clusters will increase the number of bridges per cluster beyond its original level. This increased crosslinking between clusters will reduce the probability that a single cluster fragment or a double cluster fragment becomes free whan a bridge breaks. Therefore, although rate of bridge rupture may be appreciable, rate of free cluster formation may be negligible. In such a case, rupturing bridges will be re-established because the clusters involved are so heavily tied down that they cannot separate.

Of the two processes, only the second will allow continued production of gases beyond the point at which production of tar becomes negligible. In the first process, double bonds will deactivate not only the bridges but also the sidechains. In the second process, although clusters cannot

leave because of increased connectivity with other clusters, sidechains can still rupture leading to formation of gas. It has been experimentally observed that gas production continues for a longer time than tar production. In the presence of a hydrogen donor reactant, both deactivating phenomena will be suppressed because the alpha radicals could be satisfied by hydrogen. This explains why yields obtained in hydropyrolysis are much larger than in pyrolysis under vacuum or an inert atmosphere.

In light of the above discussion, pyrolysis char will be found to carry radicals and double bonds on its aliphatic carbons. In addition, it will contain the ash formed by depletion of inorganic gases from the mineral matter.

In Fig. 3.3.3, the pyrolytic chemical system as discussed so far is presented schematically. The broken lines represent the deactivating influence of alpha radicals and double bonds on further dissociation of sidechains and bridges. The rest of the figure is self-explanatory. Two features of the system are prominent in this schematic diagram. They are:

(a) importance of alpha radicals, and

(b) presence of feedback loops.

All mechanisms in the system are shown to be either leading to or emanating from alpha radicals. They are also responsible for the feedback loops. These radicals are an inevitable consequence of volatiles generation. The feedback occurs because they inhibit the subsequent dissociation of some of the sidechains and bridges either directly or via double bonds. The latter also produce more small radicals which by hydrogen abstraction lead to more alpha and beta radicals. Tar molecules are shown to be formed

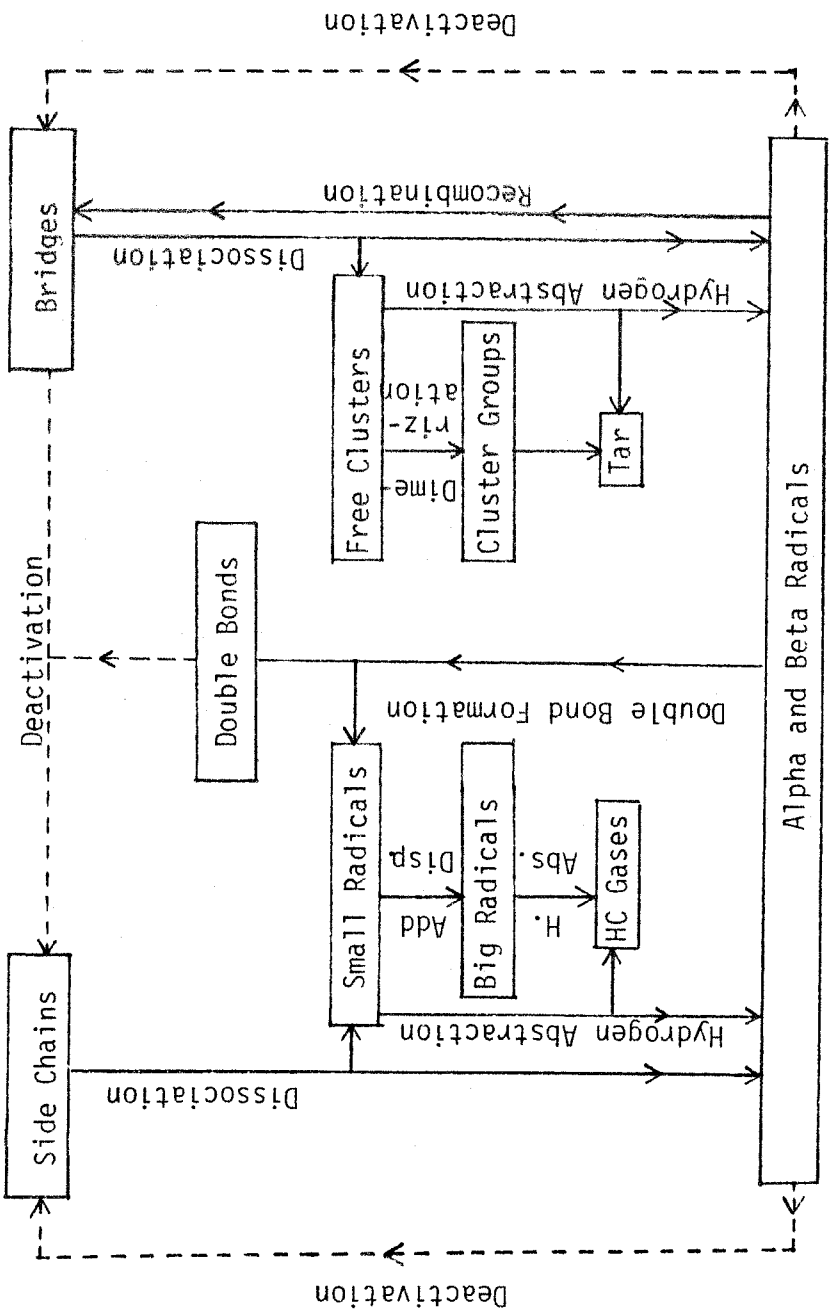

Fig. 3.3.3: Schematic of the system of chemical reactions in pyrolysis.

either by single free clusters whose radical sites have been satisfied by picking up hydrogen, or by groups of free clusters formed by combination of free individual clusters. Recombination of radicals in the system (right side) leads to more bridges which reduces the probability of free cluster generation and hence tar production falls.

4. Heat and Mass Transfer in Coal Particles During Pyrolysis

The earlier sections of this chapter discussed the chemical processes occurring inpyrolysis. However, coal samples used for pyrolysis generally consist of particles. The physical process of intra-particle heat and mass transfer could have an important bearing on the outcome of pyrolysis. This section discusses these effects and some of the attempts that have been made to account for them.

There was an implicit assumption of isothermal conditions in our earlier discussions of pyrolysis reactions. In reality, a coal sample will take some time in attaining the final temperature of pyrolysis. There would be three contributions to this heat-up time:

(a) Time required by the heating medium to reach the final temperature.

(b) Additional time required for the surfaces of the particles.

(c) Additional time required for the interior of the particles.

In some experimental systems in which coal particles are dispersed in a preheated medium, the first two contributions will be negligible. In the captive-sample technique used for experiments in this work, the particle surface temperature was found to follow an exponential profile with a time constant between one and two seconds. Magnitude of the third contribution

will determine the severity of heat transfer problem in coal.

Rates of pyrolysis reactions become appreciable after about 400^{o}C. If the interior of a particle takes a long time in rising from 400^{o}C to the final temperature, considerable conversion may take place at the intermediate temperatures. Thus, experimental results may not be characteristic of the final temperature. As discussed in the previous section, various reactions in pyrolysis compete with each other and often a product is formed at the expense of other products. Any factor which affects the rates of different reactions to different degrees would change the amount and distribution of products. Because of the differences in the activation energies of the reactions, temperature is one such factor which has a profound impact on the outcome of pyrolysis.

Endothermicity of the pyrolysis reactions will add to the heat transfer problem. The intra-particle temperature profile will be particularly steep if both the rate of reaction and the heat of reaction are high. When this occurs, different parts of the coal matrix will undergo chemical changes which are qualitatively or quantitatively different. Such effects can be experimentally examined by comparing results of pyrolyzing finely powdered coal at the same final temperature but using different heating schemes.

In Chapter 2, a brief description of the physical structure of coal was presented. Compared to porous catalysts, coal has low porosity and broad pore size distribution. Product generation in pyrolysis appears to be a volumetric process and hence surface area distribution is not as critical as in catalytic reactions. Subbituminous coals and lignites retain a relatively stable pore structure during pyrolysis. High Volatile

Bituminous and higher rank coals pass through a plastic stage during heating and suffer a drastic change.

Mass transfer limitations within coal particles are particularly important because of their relation to secondary reactions. If a product molecule spends more time within a coal particle, it is more likely to undergo secondary reactions. Such reactions reduce yields of products and defy understanding of the primary processes.

Light hydrocarbon gases like methane, ethane, etc., and inorganic gases like oxides of carbon and water vapor, can be considered fairly unreactive during their passage out of the particle. They will face minimal mass transfer resistance because their molecules are small. In effect, once a molecule of any of these gases is produced by a reaction, it can be considered a "product" of pyrolysis.

Unfortunately this is not the case with the clusters which constitute tar. A fragment of clusters (one or two) becomes 'free' if it is devoid of any aliphatic or etheric linkages with other clusters. It becomes volatile and starts its journey out of the coal particle. However, because of its radical sites, it could be reattached to the coal matrix on its way out. There are several radicals distributed all over the cluster network which would serve as the likely sites for reattachment.

Likelihood of reattachment would depend on the concentration of radicals in the structure and residence time in the particle. The first factor depends on rates of dissociation reactions and the overall chemistry. The second is determined by the mechanism of transport — diffusive, convective, bubble — and consequently by such parameters as diffusivity, particle size, pressure, etc. There are difficulties associated with

quantitative treatments of each of these two factors. The chemistry of pyrolysis is not well understood, and a mathematical description of the kinetic rates is quite complicated, as will be seen in the next two chapters. Consideration of spatial variation in the concentration of radicals in a coal particle undergoing pyrolysis will add significantly to the complexity of the mathematics. Similarly, analysis of transport mechanisms in a collapsing structure is a difficult problem.

Difficulties with residence time determination are both qualitative and quantitative. Depending on whether a coal melts, the physical mechanism of transport would be different. In case of coals whose pore structure is only slightly altered by heat treatment, volatile species generated in the interior of a particle will escape by way of a series of pores that lead to the outside. It was mentioned earlier that pores in coal can be divided into three categories: micropores, transitional pores, and macropores. The macropores (> 300 Å) and the transitional pores (> 12 Å), hereafter referred to collectively as macropores, can be thought of as partitioning the coal particle into two phases: the bulk phase and the pore phase. The bulk phase containing the micropores is a condensed phase where the volatiles are generated. Transport in ultrafine micropores takes place by means of activated diffusion (Walker et al., 1966). Rate of such transport is very slow compared to Knudsen or bulk diffusion, and depends critically on the size of the diffusing molecule. The micropores empty into the pore phase consisting of macropores. To escape outwards, the volatiles then travel along this macropore system by bulk diffusion or hydrodynamic flow.

Clearly, there are two processes in series involved in the volatile transport: in the micropores in the bulk phases, in the macropores in the pore phase. Two characteristic path lengths would be of significance (Cheong, 1977). The first one is the average distance between two neighboring macropores, the other is the particle radius. Nandi and Walker (1970) used the former to partition coal into smaller units. The average separation between macropores was postulated to be the characteristic dimension of these smaller units or 'subunits'.

Cheong (1977, see also Cheong et al., 1975) has used the idea of subunits in setting up his mathematical model for pyrolysis. The size of a subunit was estimated to be about ten times the average diameter of transitional pores ($\sim$ 30 - 50 Å). This simple estimate is supported by some electron microsocopy work (McCartney et al., 1966). For fragments larger than about 10 Å, transport limitations in the micropore system were considered very severe. The high residence time in these pores made recombination very likely. It was postulated that only when a free fragment is generated near the surface of the subunit (Fig. 3.4.1), i.e. near the pore phase, can it escape recombination. Accordingly, each subunit was divided into regions: surface region, and internal region. Free cluster fragments were produced throughout the subunit by dissociation of bridges. They escaped as products only if they were generated in the surface region. In the interior, they underwent instant recombination. However, every cluster that escaped from the surface region into the gas phase in the macropores was replaced by a cluster from the interior. The volume of the surface region was taken to be about 15% of the subunit volume. In the macropore system, although recombination

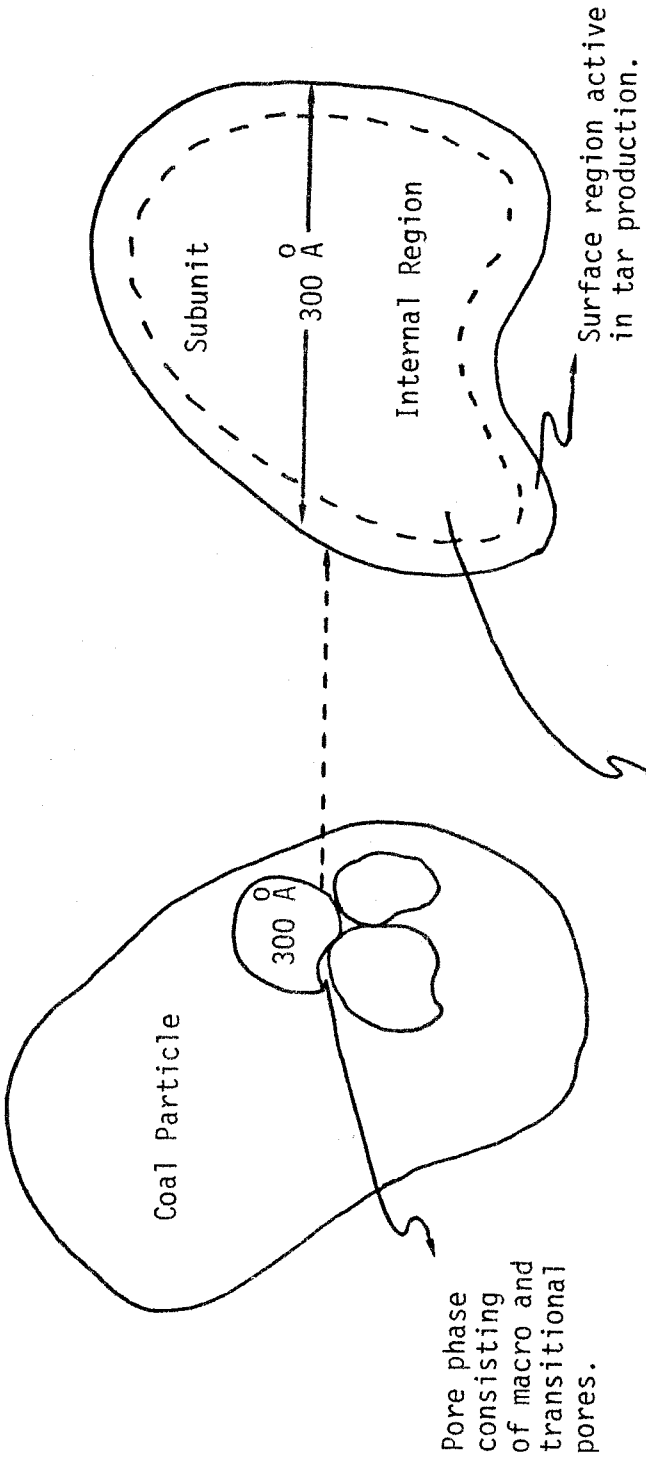

Fig. 3.4.1: Physical Model of a Porous Coal Particle; Subunits and the Surface Region.

was possible, it was considered negligible because of very low residence time of the product molecules for the particle size of interest.

Recently, Gavalas and Wilks (1978) have presented a model for predicting the product yield as a function of pressure and particle size. Its applicability is again limited to subbituminous coals which "undergo some pore enlargement but otherwise maintain a stable pore structure during pyrolysis". The detailed chemistry of pyrolysis was bypassed by treating the net production of tar and gases as known quantities. A simple pore model was developed by representing the pore size distribution curve with pores of five different diameters: micropores, 80 Å, 1000 Å, 1 μm, and 3 μm. Pores of 1000 Å were considered most important in mass transfer. Accordingly, the pore model consisted of uniform pores of this diameter. However, pores of 80 Å were postulated to be important in production and recombination of free fragments. The gaseous species were lumped into three generalized components: tar, gases (CO, CO_2, CH_4, C_2H_6, etc.), and inert carrier (e.g. He). Flux relationships were obtained using the dusty gas model. The resulting system of three ordinary differential equations was solved numerically. The main conclusions were:

(i) At low pressures, the average tar concentration in a particle is independent of pressure but increases with the particle size.

(ii) At high pressures, the average tar concentration increases with both pressure and particle size.

Large tar concentration implied extensive recombination to the free radical sites on the coal matrix. Experimental results with a subbituminous coal were in qualitative agreement with the model predictions.

The model presented in this thesis is based primarily on the kinetics

of the chemical processes occurring in coal. Detailed treatment of transport limitations is not included in this work. However, it was felt that recombination reactions have a very pronounced effect on the rate of weight loss as well as the relative yields of tar and gases. Hence, they were accounted for by modifying the rates of bridge-dissociation reactions by a parameter $x(x \leq 1)$. This reduced the rate of generation of free clusters below that postulated by kinetic parameters alone. This parameter will be further discussed in the chapter on simulation.

Some experimental results from transport experiments on coal are also presented in Chapter 6. Coal particles of four different sizes, ranging from about 100 to 500 μm, were pyrolyzed for 30 secs. under vacuum ($\sim$ 70 mm Hg) and under one atm of helium. The results confirm that product yields are affected by both pressure and particle size. Under vacuum conditions the free fragments generated spend less time within the particle and they have a higher likelihood of escaping recombination. Correspondingly more sidechains would be lost and less gases would be produced. A similar but less pronounced effect (probably because size-range used was small) is observed by decreasing the particle size.

In coals which exhibit thermoplastic behavior, like several bituminous coals, the growth and escape of gas-filled bubbles constitutes an important mode of volatiles transport. Hydrodynamic and diffusional flows become greatly impeded during the period of plasticity, thus giving rise to regions of high pressure due to the volatiles. These regions, or bubbles, expand against the viscous and other forces, and eventually burst through the particle surface as small jets.

The earlier discussed concepts of transport modeling using coal's pore structure will not be applicable to the 'plastic coals' (coals which become fluid like during heat treatment). The occurrence of the plastic state is associated with and kinetically similar in many ways to pyrolysis (Anthony and Howard, 1976). It typically starts at 420^{o}C and depending on the heating rate may extend up to 500^{o}C (at 0.05 ^{o}C/s) or up to 2000^{o}C or higher (at 10^{4} ^{o}C/s). As mentioned earlier, kinetic processes in pyrolysis also become significant beyond about 400^{o}C. Hence, volatiles would be generated at the same time as the coal is passing through the plastic state and the pore structure is collapsing. Lewellen (1975) has developed a bubble transport model for volatiles escaping from coal particles in such coals. The 'fluidity' of the coal passing through the plastic state was related to the pyrolysis rate. Secondary reactions were postulated to occur at the bubble surfaces. The predicted trends of the model are in good agreement with experimental results on effects of particle size, pressure, and heating rate on volatiles yield and particle swelling.

Chapter 4

MATHEMATICAL MODELING OF PYROLYSIS

1. General

This chapter contains the proposed mathematical simulation of coal pyrolysis. Some general comments about the scope and utility of mathematical representation of pyrolysis process are presented in this section.

As in the case of pyrolysis of simple gaseous hydrocarbons (Allara and Edelson, 1975), mathematical modeling of coal pyrolysis basically involves computation of the rates of generation of products of interest. In case of hydrocarbons, the chemistry and kinetics of thermochemical reactions provide the basis for modeling. The number of reactions involved increases with increasing molecular weight of the hydrocarbon and numerical computation becomes difficult. Some simplifications can be made by neglecting the reactions that do not contribute much to product formation. A similar approach in the case of coal pyrolysis modeling runs into two additional problems:

(a) There is no 'molecule' of coal and the chemical structure and the concentration of its reactive groups is difficult to determine.

(b) Physical processes of heat and mass transfer within coal particles can be of significance in determining the yield and distribution of products.

Research on the chemical and the physical structure of coal is required to tackle these two problems. Substantial progress has been made in this regard as was discussed in the last two chapters. In the meantime, several phenomenological models have been developed which circumvent the need for knowledge of coal chemistry by modeling the overall product generation

processes. Basically, such models attempt to develop mathematical functions which fit the experimentally obtained product formation curves. These will be discussed in the next section.

Hence, two extremes exist in mathematical modeling of coal pyrolysis: the phenomenological models, and the chemical models. The latter could not be attempted before modern techniques of analytical chemistry were applied to elucidate coal's chemical structure. In that sense, the former were justified even though they did not lead to a basic understanding of the process. Today however, much more information exists on coal chemistry and, therefore, an attempt has been made to formulate a chemical model in this thesis. The philosophy is similar to that adopted for modeling hydrocarbon pyrolysis (e.g. Allara and Edelson, 1975) with the additional complications of modeling the chemical structure of coal and the mass transfer processes.

Any kind of model for coal pyrolysis implies a bold assertion, viz., pyrolysis is a unique mechanism affecting all coals in a similar manner. This also entails an implication about a fundamental similarity of structure among various coals. This similarity would be one of the basic tenets of a chemical model. Actually, there would not be much theoretical incentive for modeling if different coals required totally different mathematical treatment. One of the objectives of modeling is to develop unifying concepts about structure and reactivity of coals. A successful model would be expected to provide a generalized theory about their chemical behavior. Such a theory could then be used in devising improved coal-conversion processes for industrial use.

An example of the applicability of a chemical model in coal-conversion

processes can be found in the problem of analyzing NO_x formation during combustion. It is believed that the first step in coal combustion involves devolatilization. Oxygen subsequently reacts with both the volatiles and the char. Obviously, one would expect reaction with volatiles to be faster than with char (rate of reaction with char would most likely be transport controlled). Therefore, in an oxygen lean atmosphere, nitrogen in the volatiles would be the primary source for NO_x. Accordingly, knowledge about the composition of the volatiles would be very desirable. A chemical model can provide the ability to predict volatile composition for different coals.

The scope of a chemical model is not strictly limited to pyrolysis. For example, it can be adapted to hydropyrolysis as well. Additional reactions accounting for the interaction of hydrogen with the reacting species and the volatiles produced would be required. Higher yields compared to simple pyrolysis would be explained by the interference by hydrogen in char-forming reactions. Relative importance of homogeneous and heterogeneous reactions of hydrogen can also be determined using the model.

In brief then, mathematical modeling of coal pyrolysis involves rates of physical and chemical processes taking place within a coal particle, and such modeling serves to formulate general concepts about structure and reactivity of coals, and also helps in beneficial modification of coal-utilization processes.

2. Previous Models

This section discusses in brief some of the models presented in the

literature and compares their philosophy with that of the model formulated in the subsequent sections of this chapter.

Most of the models in coal pyrolysis have followed a phenomenological approach. Anthony and Howard (1976) have recently reviewed such models. These models attempt to describe the kinetics of pyrolysis in terms of the overall rates of generation of products, either each product individually or all the volatile products collectively. They do not take into account the chemical structure of coal and the thermochemistry of pyrolysis. Therefore, they do not represent any fundamental chemical reactions but simply observable rates of a phenomena, by means of mathematical expressions whose parameters are calculated by curve-fitting. Such an approach was necessitated because of lack of cohesive information on the nature of the reactive species in coal and the mechanism and kinetics of heat-initiated reactions. With the application of modern techniques of analytical chemistry towards elucidation of the functional groups in coal and an increased understanding of the thermochemical reactions, chemistry based pyrolysis modeling has become a reasonable alternative. This thesis is an effort in this direction. Both advances in knowledge about coal chemistry and necessity to gain a basic understanding of coal devolatilization make the future of such models promising.

Examples of phenomenological and chemical models are listed in the Tables 4.2.1 and 4.2.2, respectively, and discussed in the following text. The lists are not intended to be exhaustive.

The equation most basic to phenomenological modeling is the expression

$$\frac{dV}{dt} = k(V^* - V) \qquad \ldots(4.2.1)$$

Table 4.2.1. Phenomenological Models for Coal Pyrolysis

	Authors	Salient Features
[1]	Several Authors	Simple First Order: $dV/dt = k(V^* - V)$. V^*: ultimate weight loss, $k = k_o \exp(-E/RT)$.
[2]	Chermin & Van Krevelen(1957)	Three consecutive reactions, with evolution of primary gas during the second step and of secondary gas during the third step.
[3]	Stone et al. (1954) Shapatina et al. (1960)	Pyrolysis divided into several intervals, each modeled by a single first-order process.
[4]	Wiser et al. (1967) Skylar et al. (1969)	$dV/dt = k(V^* - V)^n$ $n = 2 - 8$
[5]	Pitt (1962)	Simple first-order for each product i: $dV_i/dt = k_i(V_i^* - V)$
[6]	Kobayashi (1972)	Two Competing First-Order Processes.
[7]	Anthony et al. (1975)	Similar to [5] but assumption of Gaussian Distribution of Activation Energies E_i, parametrized by mean and variance.
[8]	Reidelbach & Summerfield (1975)	Ten step model representing the reactions of "thermally activated" coal.
[9]	Suuberg (1977)	Similar to [3] but for each product i.

Table 4.2.2. Chemical Models for Coal Pyrolysis

Authors	Salient Features
[1] Cheong (1976)	Reactive portions of chemical structure of coal represented by aliphatic sidechains and bridges. Pyrolysis involved free radical reactions of these aliphatic groups.
[2] Solomon (1979)	Kinetics of volatilization (into gas or tar) of seven functional groups in coal represented by simple first-order rates.
[3] Present Study	Similar to [1] but rigorous mathematical schemes devised for computing concentrations and rates in terms of probabilities of various configurations in a randomly distributed system. Hydroaromatic structures, phenolic groups, and ether linkages considered. Effect of mass transfer taken into account in a simple way by reducing the rates of forward reactions.

where V(t) is the amount of volatiles formed up to time t, and V^* is the value of V as $t \to \infty$. It implies that the rate of volatile generation at any time is proportional to the amount of unreleased volatiles in coal at that time. The constant k is generally taken to be an Arrhenius type rate constant:

$$k = k_o e^{-E/RT} \qquad ...(4.2.2)$$

The parameters k_o and E do not have any fundamental significance.

Two points regarding V^* should be noted. Firstly, it is not necessarily equal to volatile matter VM determined by proximate analysis. As Anthony and Howard (1976) have pointed out, depending on the experimental technique employed, V^* can be greater or lesser than VM. Secondly, it is a function of coal type and temperature. If the initial heating rate in pyrolysis is slow, different values of V^* would be applicable at different times during the heat up, affecting the rates and raising questions about integration of eq. 4.2.1 over the entire pyrolysis period. Accordingly, attempts have been made to describe pyrolysis as a series of several first-order processes occurring in different time intervals.

Pitt (1962) formulated a model consisting of a number of independent, parallel processes, each (i) represented by the expression

$$\frac{dV_i}{dt} = k_i(V_i^* - V_i) \qquad ...(4.2.3)$$

where

$$k_i = k_{oi}\, e^{-E_i/RT} \qquad ...(4.2.4)$$

He further assumed that the k_i's differed only in activation energy (i.e., $k_{oi} = k_o$ for all i) and that the number of reactions was large enough to

permit E_i's to be expressed as a continuous distribution function f(E). Then f(E)dE represented the function of the potential volatile loss V^* which had an activation energy between E and E + dE. In other words, V_i^* became a differential part of the total V^*:

$$\frac{dV_i^*}{dE} = V^* f(E) \qquad \ldots(4.2.5)$$

and

$$\int_0^\infty f(E)dE = 1 \qquad \ldots(4.2.6)$$

This formulation allowed complete elimination of V_i^* from the equations. The activation energy distribution f(E) was determined on the basis of weight loss data.

Anthony et al. (1975) assumed a Gaussian distribution of f(E) with mean activation energy E_o and standard deviation σ. Thus,

$$f(E) = \frac{1}{\sqrt{2\pi\sigma^2}} \exp[-(E - E_o)^2/2\sigma^2] \qquad \ldots(4.2.7)$$

This permitted correlation of devolatilization data by using four parameters, viz., V^*, k_o, E_o and σ. which is only one more than required in the simple single step model of eq. 4.2.1, viz., V^*, k_o and E. Again, all parameters were determined using experimental results.

Suuberg (1977) recently used a distributed activation energies model for each product of pyrolysis of a bituminous coal. Results for lignite pyrolysis on the other hand were modeled using a multi-first-order-step scheme for each product.

In brief, phenomenological modeling has progressed along the path of developing more and more complex mathematical functions to duplicate the

experimentally observed phenomena as closely as possible. In contrast, chemical models are based on the rates of processes bringing about a transformation in the chemical structure of coal during pyrolysis. Formation of observable products is considered to be just a part of the overall transformation.

Solomon (1979) recently studied thermal decomposition of two coals, a lignite and a bituminous coal, in terms of rates of reaction of seven functional groups. The initial coal composition was described by the fraction Y_i^o of each functional group i and the fraction of coal x^o which was considered to be potentially tar forming. A volatile component evolved either as gas or as tar. The evolution of a component into tar was described by the diminishing of the x dimension and into the gas by the diminishing of the Y_i dimensions according to

$$x = x^o e^{-k_x t} \qquad \ldots(4.2.8)$$

$$Y_i = Y_i^o e^{-k_i t} \qquad \ldots(4.2.9)$$

The rate constants k_i and k_x were computed using the experimental data. They are shown in Table 4.2.3. For some functional groups like carboxyl and hydroxyl, the rate parameters can be associated with their typical reactions,

$$\text{Carboxyl} \rightarrow CO_2$$

$$\text{Hydroxyl} \rightarrow H_2O$$

However, groups like aliphatic would be involved in many competing reactions, making it difficult to associate their parameters with specific reactions.

The model implied that the tar contains a mix of functional groups

Table 4.2.3. Kinetic Constants for Lignite and Bituminous Coals (from Solomon, 1979)

Functional Group		Kinetic Constant
[1]	Carboxyl	$k_1 = 6 \exp(-4000/T)\ sec^{-1}$
[2]	Hydroxyl	$k_2 = 15 \exp(-4950/T)$
[3]	Ether	$k_3 = 890 \exp(-12000/T)$
[4]	Aliphatic	$k_4 = 4200 \exp(-9000/T)$
[5]	Aromatic H	$k_5 = 3600 \exp(-12700/T)$
[6]	Aromatic C	$k_6 = 0$
[7]	Tar	$k_x = 750 \exp(-8000/T)$

similar to that in the parent coal. The major difference observed between the infrared spectra of tar and the parent coal was the higher quantity of aliphatic CH_2 and CH_3 in tar. This was postulated to be because of hydrogen abstraction by the molecules to stabilize their free radical sites.

Solomon's model, although based on important reactive groups constituting the chemical structure of coal, did not express the rates in terms of kinetics of thermochemical reactions. Cheong's (1976) recognition of the importance of thermochemistry in pyrolysis modeling led him to postulate a set of 56 chemical reactions describing the pyrolytic changes. He formulated an elaborate mathematical model to compute the rate of generation of products in terms of the rates of chemical reactions.

Cheong modeled the carbon-hydrogen structure in coal in terms of concentrations of six functional groups representing sidechains and bridges. The concentrations were determined using elemental analysis of coal, NMR spectra of pyrolysates, and some assumptions regarding relative importance of each functional group in a given coal. A computer program was developed to implement the scheme for calculating the initial concentrations. During pyrolysis, chemical reactions produced several new functional groups, and 17 such groups were included in the state variables along with the six original ones.

The set of 56 primary reactions of coal pyrolysis was classified into six categories:

(1) Bond Dissociation

(2) Hydrogen Abstraction

(3) Beta Scission of Long Chain and Bridge Radicals

(4) Hydrogen Elimination

(5) Addition

(6) Recombination

The rates were expressed in terms of the concentrations of the functional groups appropriately modified to take into consideration the presence of radicals and double bonds in the system. The kinetic parameters were obtained from literature on similar reactions of other organic compounds.

Production of alkanes and alkenes was postulated to be a result of dissociation of alkyl sidechains. Water vapor, CO and CO_2 were produced from phenolic, carbonyl and carboxylic groups, respectively. Their reactions were assumed to have no effect on the reactions of the carbon-hydrogen structure. Production of tar involved release of free cluster fragments following rupture of bridges among clusters. To relate the rate of tar production to the rate of bridge dissociation, coal was modeled as a honeycomb structure of interconnected clusters, with a maximum of three connections per cluster and two bridges per connection. Probabilities of generation of single cluster and double cluster free fragments were calculated on the basis of random distribution of bridges among clusters. Generation of tar was postulated to be possible only in the surface region of a subunit (refer to section 4 of the previous chapter). In the interior region, bridge dissociation did not lead to free clusters. However, gaseous products were generated throughout the subunit.

Eventually, differential equations governing the rate of change of the state variables with time were formulated independently for each region. The set of simultaneous equations was integrated using a special code based on Gear's method (1971) for stiff differential equations. Results of interest in pyrolysis, e.g. weight loss, were expressed in terms of the

differences in values of the state variables before and after pyrolysis.

This modeling effort by Cheong was an important step towards a basic understanding and description of the pyrolysis process. The greatest accomplishment of the model was in laying down the infrastructure of concepts and methodology for chemistry-based modeling of coal devolatilization. Alternatives are sure to be proposed in the future, but his work contains one and probably the first comprehensive approach.

The model presented in this thesis is similar to that of Cheong in most basic concepts, but differs in details and mathematics. Some changes in the state variables (functional groups) and reactions have been introduced. The effect of phenolic condensation on the carbon-hydrogen structure has been incorporated. The mechanics of tar formation have been changed completely so as to allow for simpler and more general quantitative representations. Wherever possible, random distributions have been assumed so as to avoid à priori biases. The mathematics is more rigorous and subject to fewer constraining assumptions.

Phenomenological models cannot serve the needs of an advanced coal-conversion industry. Chemical models are likely to be more widely adopted in the future.

3. The State Variables

In this section we begin to develop mathematical schemes for modeling the chemical sysetm discussed in Chapter 3.

The basic assumptions of the model are discussed below. Other assumptions will be presented as the model develops.

(1) The system being modeled consists of a sample of coal particles heated in vacuum or in an inert atmosphere, e.g. of helium. However, the approach is also applicable to other processes like combustion and hydrogasification in which pyrolysis occurs as the first step.

(2) The chemical model for which mathematics is being developed is valid approximately up to 700°C. Most calculations will be made for temperatures between 450°C and 600°C.

(3) While the kinetics of the chemical processes are modeled in detail, the effect of intra-particle transport limitations is accounted for in an overall sense. An elaborate modeling of the transport processes is not attempted. Consequently, size of the coal particles, pressure, etc. are not included in the input data. They would affect the results indirectly through a parameter x.

(4) Isothermal kinetics are assumed for calculations. However, the model is also applicable to non-isothermal situations.

(5) All secondary effects like those of the heating medium, reactor geometry, etc., are neglected.

Recalling the concepts developed in the previous two chapters, the physical system described under the first assumption can be translated into a chemical system. It consists of a number of functional groups representing the sidechains and bridges in the coal structure, undergoing various kinds of chemical reactions. Gases produced by these reactions are assumed to escape the coal particle without secondary reactions. Dis-

sociation of bridges leads to formation of 'free' fragments of clusters which become volatile depending on their molecular weight. Some of these free fragments can get reattached to the coal matrix on their way out of the coal particle. Those which successfully escape constitute tar. They carry all their substituent groups which are thus lost from the system. Formation of double bonds and increase in the number of bridges per cluster progressively deactivate the chemical structure. A point is reached beyond which very little product formation takes place.

The overall mathematical strategy is presented in Fig. 4.3.1. State variables are postulated to represent concentrations of functional groups — the ones initially present as well as those generated during reactions — and gaseous products and other relevant variables. Probability functions are calculated based on random distribution schemes to compute the concentrations of various reacting configurations representing combinations of functional groups. Rates of reactions are expressed in terms of these concentrations of configurations. The kinetic parameters are either estimated or taken from the literature. Rates of generation of free clusters and rates of loss of functional groups with free clusters are related to the rate of bridge dissociation. Differential equation governing the rate of change of concentration of each functional group (i.e. a state variable) with time is formulated. The change occurs because of the reactions and the loss with the departing clusters. The initial conditions for the differential equations are the initial values of the functional groups which are calculated as shown in the next section. The set of differential equations is integrated numerically in the next chapter.

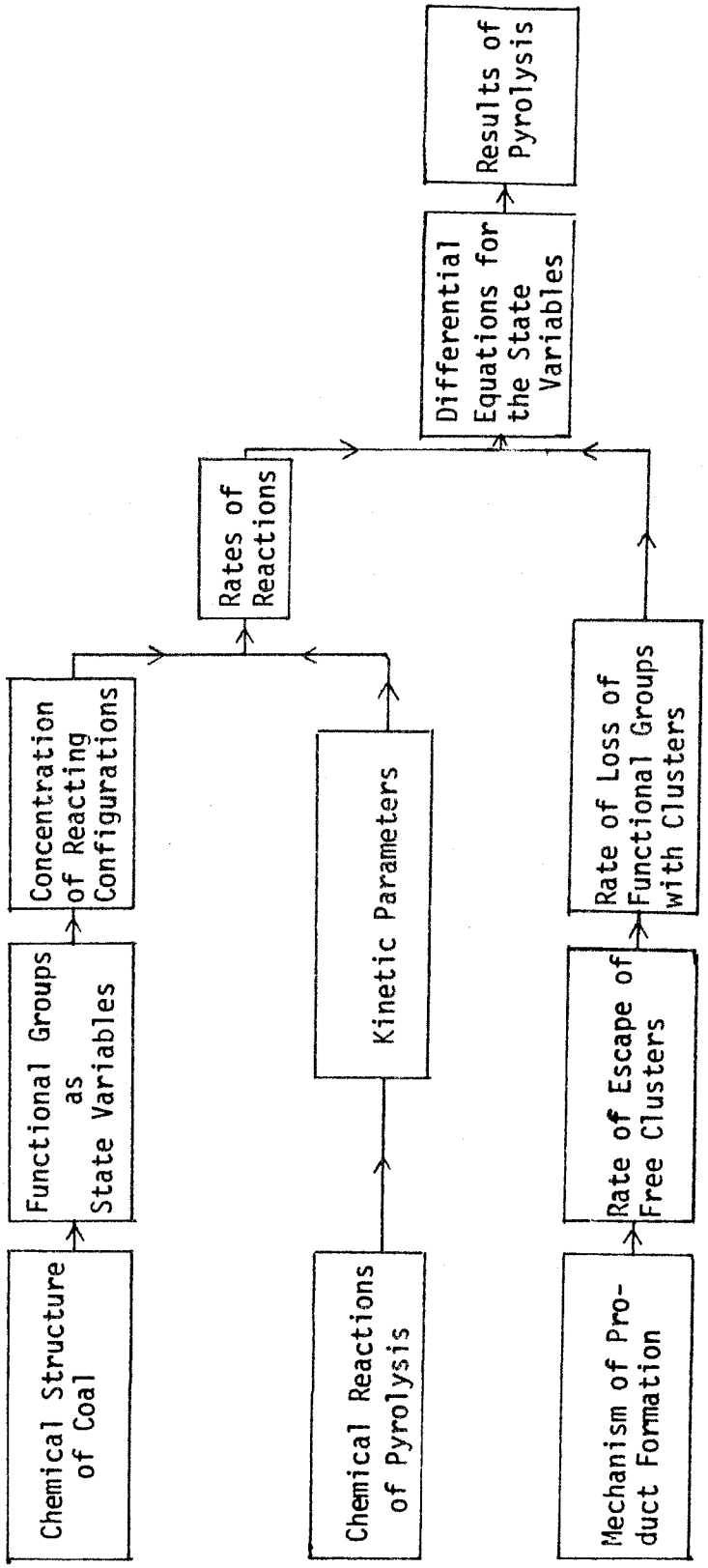

Figure 4.3.1: Strategy for Mathematical Modeling of Coal Pyrolysis.

Choice of State Variables

State variables to characterize the system are chosen on the basis of two criteria:

(a) They should adequately represent the system; should be easily calculable from available information on coal and in turn lend themselves to computations of quantities of interest.

(b) Either they should represent concentrations of reacting configurations in the rate expressions, or should lend themselves to calculations of such concentrations.

It was concluded in Chapter 3 that the reactions of the carbon-hydrogen structure occur in terms of substituent side-chains and bridges on alpha carbons attached to peripheral aromatic carbons. Then, two choices for selecting state variables that would approximately satisfy at least one of the above two criteria are: total concentration of each substituent group; concentration of each combination of substituent groups on alpha carbons (it should be remembered that each alpha carbon can carry three substituents). Since reactions of a substituent group are affected by the presence of a radical or a double bond on the same alpha carbon, total concentrations of substituents cannot be used in rate expressions, and therefore their choice fails to satisfy the second criterion. Similarly, concentration of each combination of substituents cannot be calculated on the basis of information on coal such as proximate and elemental analysis, density, pyrolysis results, and NMR spectra of pyrolysates and extracts. No theoretical or experimental method is presently available for a direct determination of their values. Consequently, the second choice for state

variables is also not satisfactory.

There seems to be no alternative but to select one of the above two or similar types of state variables. Subsequently, efforts will be made to make the selection satisfy both the criteria.

We choose the total concentrations as the state variables for two reasons:

(i) The number of differential equations is smaller compared to that of the other choice; integration is consequently easier. The number of substituent groups is much smaller than the number of their various possible combinations.

(ii) A scheme can be devised to calculate their initial values in coal using the information mentioned in the preceding paragraph.

This choice also seems more appealing intuitively because it relates to the concept of characterization of organic structures in terms of their functional groups.

There will be two kinds of state variables: those corresponding to the functional groups initially present in coal and those corresponding to the functional groups generated during reaction. The following are included in the first kind:

(1) Alpha Hydrogens: $\Phi\text{-}\overset{|}{\underset{|\alpha}{C}}\cdots H$: Y_1 (moles/liter)

(2) Methyl Sidechains: $\Phi\text{-}\overset{|}{\underset{|\alpha}{C}}\cdots CH_3$: Y_2' (moles/liter)

(3) Ethyl Sidechains: $\Phi\text{-}\overset{|}{\underset{|\alpha}{C}}\cdots C_2H_5$: Y_3' (moles/liter)

(4) Ethylene Bridges: $\Phi\text{-}\overset{|}{\underset{|\alpha}{C}}\cdots\overset{|}{\underset{|\alpha}{C}}\text{-}\Phi'$: $Y_4/2$ (moles/liter)

Hence, Y_4 corresponds to the number of alpha carbons involved in such bridges.

(5) Hydroaromatic Structures: 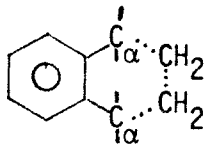 $:Y_5'/2$ moles/liter

A hydroaromatic structure can be visualized to be divided into two halves, and Y_5' corresponds to the concentration of such imaginary half structures.

(6) Alpha Carbon Bonds: $\Phi\cdots C_{\alpha}-$ $:Y_8$ moles/liter

(7) Alpha Carbons: $\Phi-C_{\alpha}-$ $:Y_{18}$ moles/liter

(8) Phenolic Groups: $\Phi\cdots OH:Y_{10}$ moles/liter

(9) Aromatic Clusters: $N_c:Y_{24}$ moles/liter

(10) Volume of the coal particles: $V:Y_{19}$ liters

Here, Φ, as before, represents a peripheral aromatic carbon on a cluster, and the benzene ring shown is intended to be a part of a cluster. Bonds of interest are denoted by broken lines. The difference between the alpha carbon bonds, Y_8, and alpha carbons, Y_{18}, will equal the concentration of methylene bridges in the system. Hence, implicitly there is one more variable:

Methylene Bridges: $\Phi-C_{\alpha}-\Phi':Y_8-Y_{18}$ moles/liter

The concentration of aromatic clusters, Y_{24}, should be considered in light of the concept of 'average' cluster discussed in Chapter 3 and again in the next section. The volume, Y_{19}, is intended to be the true volume, i.e. excluding porosity. Thus:

Y_{19} = weight of particles/true density

The functional groups generated during reaction include:

(11) Double Bond Bridges: $\Phi\text{-}\dot{C}=\dot{C}_{\alpha}\text{-}\Phi' : Y_6/2$ moles liter

Y_6 corresponds to the number of alpha carbons involved in such bridges.

(12) Double Bond Sidechains: $\Phi\text{-}\dot{C}_{\alpha}=CH_2$, $\Phi\text{-}\dot{C}_{\alpha}=C_2H_4$, Half hydroaromatic structure with a double bond, i.e.: Y_7 moles/liter

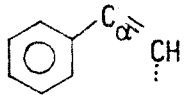

(13) Alpha Radicals: $\Phi\text{-}\dot{C}_{\alpha}\cdot$: Y_9 moles/liter

(14) Ether Linkages: $\Phi\text{-}O\text{-}\Phi'$: $Y_{11}/2$ moles/liter

Hence, Y_{11} equals the number of clusters involved in ether linkages.

(15) Beta Radicals: $\Phi\text{-}\dot{C}_{\alpha}\text{-}\dot{C}H_2$, $\Phi\text{-}\dot{C}_{\alpha}\text{-}CH_2\dot{C}H_2$, Half hydroaromatic structure with a beta radical, i.e. : Y_{12} moles/liter

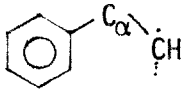

(16) Hydrogen Radicals: $H\cdot$: Y_{21} moles/liter

(17) Methyl Radicals: $CH_3\cdot$: Y_{22} moles/liter

(18) Ethyl Radicals: $C_2H_5\cdot$: Y_{23} moles liter

(19) Hydrogen Gas: H_2 : Y_{13} moles

(20) Methane Gas: CH_4 : Y_{14} moles

(21) Ethylene Gas: C_2H_4 : Y_{15} moles

(22) Ethane Gas: C_2H_6 : Y_{16} moles

(23) Higher (C_2+) Gas: C_nH_m : Y_{17} moles

(24) Water Vapor: H_2O : Y_{20} moles

Each of the two variables, Y_7 and Y_{12}, corresponding to double bond

sidechains and beta radicals, respectively, includes contributions originating from functional groups represented by Y_2', Y_3' and Y_5'. To separate the contributions one can define three new variables to replace Y_2', Y_3' and Y_5' as follows:

Methyl Groups: $\Phi\text{-}\dot{C}_{\alpha}\text{-}CH_3$, $\Phi\text{-}\dot{C}_{\alpha}\text{=}CH_2$, $\Phi\text{-}\dot{C}_{\alpha}\text{-}\dot{C}H_2$: Y_2 moles/liter

Ethyl Groups: $\Phi\text{-}\dot{C}_{\alpha}\text{-}C_2H_5$, $\Phi\text{-}\dot{C}_{\alpha}\text{=}CHCH_3$, $\Phi\text{-}\dot{C}_{\alpha}\text{-}CH_2\dot{C}H_2$: Y_3 moles/liter

Hydroaromatic Groups: As before, only half-structures are used:

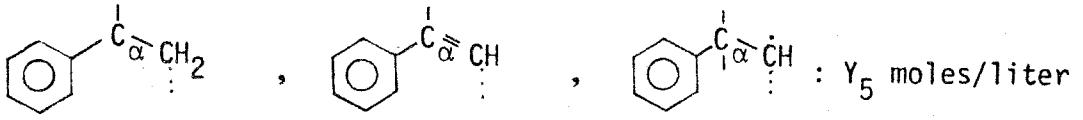

: Y_5 moles/liter

Then, using simple proportionality assumptions (as shown in section 5) each contribution can be computed.

The small radicals, H·, CH_3· and C_2H_5· will occur in vapor phase and the volume relevant to their concentrations is the same as the volume of the particles. Of course, this volume will change with time during pyrolysis as free clusters leave the system. The state variables for gases are expressed as cumulative moles produced rather than as concentrations, because a gas molecule once produced is assumed to avoid any secondary reactions. Hence, these state variables do not appear in any rate expressions. All hydrocarbon gases containing more than two carbons have been lumped together in the variable Y_{17} for the purpose of reducing the number of state variables.

The state variables are listed in Appendix I for quick reference.

The choice of functional groups has been determined by the chemical structure of coal and the chemistry of pyrolysis as discussed in the previous two chapters. Basically, two types of bridges and four types of

sidechains have been included. By dissociation and addition-displacement reactions, these sidechains can lead to hydrocarbons containing up to seven carbons (a seven-carbon radical will be produced by addition-displacement reaction of an alpha carbon carrying three $-C_2H_5$ groups). Generally, experimental studies on pyrolysis have reported quantitative measurements of hydrocarbons up to C_6. Literature (Chakrabartty and Kretschmer, 1972; Given, 1959; Gaines, 1962) supports the inclusion of methylene-type bridges (Y_8 - Y_{18}) in the model. These bridges dissociate (activation energy about 70 kcal/mole) at a slower rate compared to the ethylene-type bridges (activation energy about 50 kcal/mole) and thus lead to less tar formation.

Although the concentrations of carboxylic and carbonyl groups are not included in the state variables, they are estimated using the amount of carbon dioxide and carbon monoxide formed experimentally. They can be assumed to undergo first-order reactions which are unaffected by the reactions in the carbon-hydrogen structure. If methods are developed for their independent determination, they can be included in the main stream of the model.

The next two sections demonstrate how the two criteria for state variables are satisfied by the choice made in this section.

4. Initial Conditions for the State Variables; Pyrolysis Results in Terms of the State Variables

This section consists of two parts. In the first part, a scheme is devised to calculate the initial values of the state variables, i.e., their values in coal before pyrolysis. These will also serve as initial conditions

for the differential equations. The second part illustrates the use of the state variables in computing the quantities of interest in pyrolysis, e.g., weight loss, amount of tar formed, amount of various gases formed, etc.

This section essentially demonstrates that the choice of state variables satisfies the first of the two criteria mentioned in the last section.

State variables of the second kind are generated during reaction and are assumed to be initially absent in coal. Only the first ten variables (i.e. those of the first kind) along with concentrations of carboxylic and carbonyl groups are used to characterize the reactive portion of coal. The calculations are based on three pieces of information:

(a) Elemental Analysis of Coal: This generally includes percentages of carbon, hydrogen, nitrogen, sulfur, oxygen, and ash (which, for the purpose of these calculations will be taken to equal mineral matter).

(b) Density of Coal Material: True density — excluding the pore volume in the coal particles — is used. Gan et al. (1972a) have indicated that coal density determined by helium displacement will be the true density because helium penetrates most pores. They have plotted helium densities of various American coals against their carbon content. This plot is shown in Fig. 4.4.1 and will be used in this thesis for determining densities of the coals for which simulation runs have been made in the next chapter.

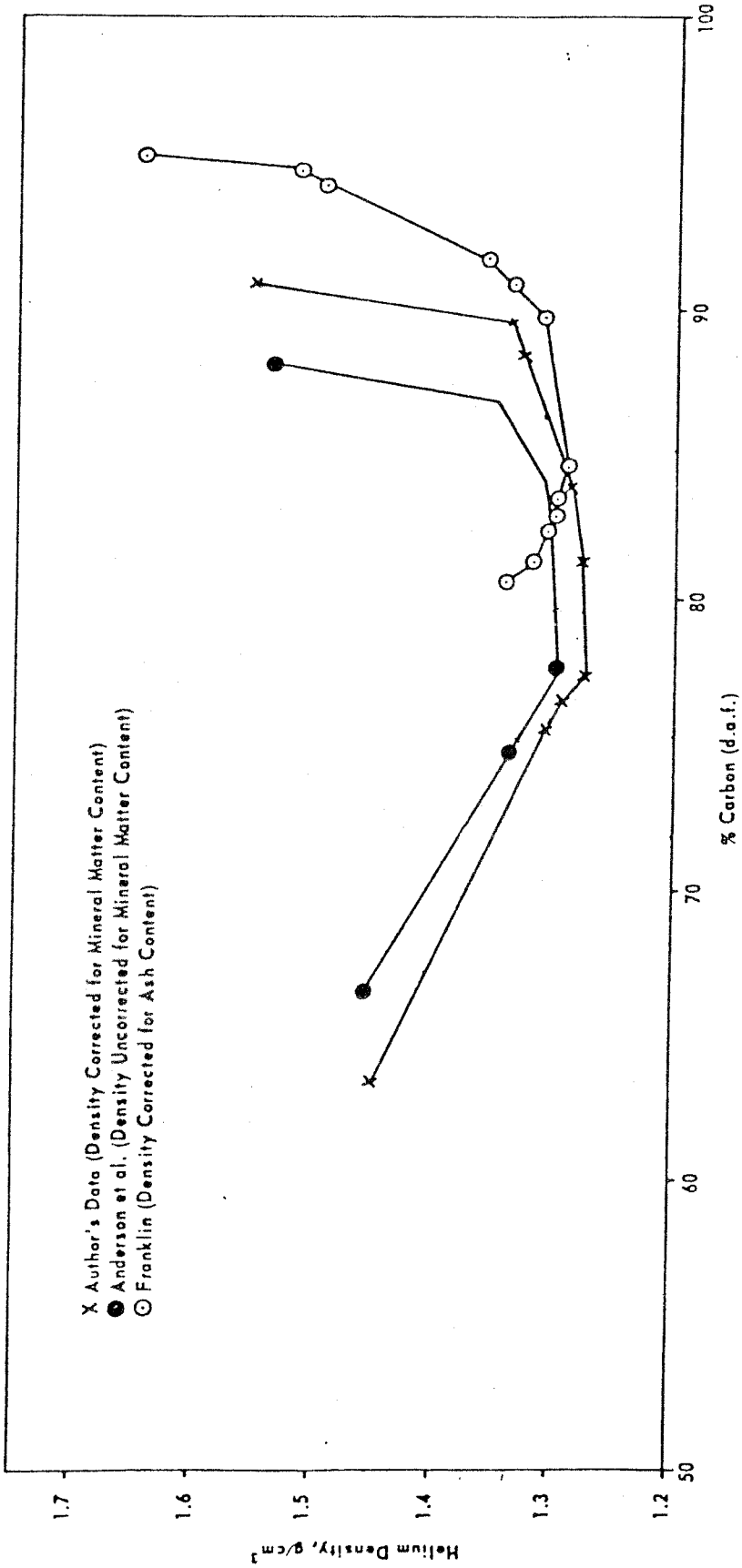

Figure 4.4.1: Variation of True Density with Carbon Content of Coals (from Gan et al., 1972 a).

(c) NMR Results: Both ^{1}H and ^{13}C NMR results are used. The former provides percentages of aromatic, alpha and beta hydrogens, while the latter determines aromaticity, i.e., percentage of carbon that is aromatic. It was mentioned in Chapter 2 that direct NMR on coal has recently been attempted. In this thesis, NMR data on pyrolysates and extracts have been used for calculations, and since they may not be representative of the coals themselves, adjustments in their values have been allowed.

In addition to the above three pieces of information, some pyrolysis results have also been used to deduce relative concentrations of some functional groups. However, these deductions can be replaced with suitable assumptions which do not require pyrolysis results.

Let C, H, N, S and O represent fractions by weight of carbon, hydrogen, nitrogen, sulfur and oxygen in a coal. Further, let the carbon be divided into C_{ar} and C_{al} for aromatic and aliphatic carbons, and the hydrogen into H_{ar}, H_a, H_b for aromatic, alpha and beta hydrogens. Note that:

$$C + H + N + S + O + Ash = 1$$

$$C_{ar} + C_{al} = 1$$

$$H_{ar} + H_a + H_b = 1$$

Let the true density of coal be ρ gas/c.c. Then, Y_1, the concentration of alpha hydrogens can be easily calculated as

$$Y_1 = \frac{H_a \times H \times \rho \times 10^3}{1} \quad \text{moles/liter} \qquad \ldots(4.4.1)$$

The aliphatic portion of carbon has a concentration:

$$C_{aliphatic} = \frac{C_{al} \times C \times \rho \times 10^3}{12} \text{ moles/liter} \qquad \ldots(4.4.2)$$

However, this concentration includes those carbon atoms which are involved in carboxylic and carbonyl groups. Since one mole of CO_2 is produced from one mole of (- COOH) groups and one mole of CO is produced from one mole of (- CO) groups, knowing the amounts of CO_2 and CO formed per unit weight of the coal sample, one can calculate the concentration of carbon involved in these groups. Let this concentration be C_o. Then the concentration of carbon present in aliphatic sidechains and bridges can be calculated as the difference between $C_{aliphatic}$ and C_o.

$$C'_{aliphatic} = C_{aliphatic} - C_o \qquad \ldots(4.4.3)$$

The $C'_{aliphatic}$ further needs to be divided into alpha and beta portions.

The concentration of beta hydrogens is given by:

$$H_{beta} = \frac{H_b \times H \times \rho \times 10^3}{1} \text{ moles/liter} \qquad \ldots(4.4.4)$$

Then, counting the number of beta hydrogen atoms in the functional groups represented by Y_2, Y_3 and Y_5,

$$3Y_2 + 5Y_3 + 2Y_5 = H_{beta} \qquad \ldots(4.4.5)$$

Using relative production of methane, ethane and ethylene as the guideline, we can roughly estimate the following fractions:

$$\frac{Y_2}{Y_3} = a \quad \text{and} \quad \frac{Y_2}{Y_5} = b \qquad \ldots(4.4.6)$$

Substituting (4.4.6) into (4.4.5),

$$3Y_2 + \frac{5}{a} Y_2 + \frac{2}{b} Y_2 = H_{beta}$$

or

$$Y_2 = \frac{H_{beta}}{(3 + 5/a + 2/b)} \text{ moles/liter} \qquad ...(4.4.7)$$

and

$$Y_3 = \frac{H_{beta}}{a(3 + 5/a + 2/b)} \text{ moles/liter} \qquad ...(4.4.8)$$

and

$$Y_5 = \frac{H_{beta}}{b(3 + 5/a + 2/b)} \text{ moles/liter} \qquad ...(4.4.9)$$

But, using a balance on beta carbons (and beta plus carbons) involved in the above three groups:

$$Y_2 + 2Y_3 + Y_5 = C_{beta} \qquad ...(4.4.10)$$

where C_{beta} represents concentration of beta carbons. Equations (4.4.7), (4.4.8) and (4.4.9) can be substituted in (4.4.10) to compute C_{beta}.

$$C_{beta} = \frac{H_{beta}(1 + 2/a + 1/b)}{(3 + 3/a + 2/b)} \qquad ...(4.4.11)$$

Then, since

$$C_{alpha} = C'_{aliphatic} - C_{beta}$$

or

$$Y_{18} = C_{aliphatic} - C_o - C_{beta} \qquad ...(4.4.12)$$

One of the bonds of each alpha carbon is connected to a peripheral aromatic carbon on a cluster, while the other three bonds are taken up by substituent groups consisting of sidechains and bridges. The only exceptions are those alpha carbons which participate in methylene bridges and hence have

two of their bonds connected with aromatic clusters. In such cases, two clusters share the same alpha carbon. This explains why Y_8 and Y_{18} differ if methylene bridges are present in the system.

The total concentration of all substituents on alpha carbons should equal three times the concentration of alpha carbons. Thus,

$$Y_1 + Y_2 + Y_3 + Y_4 + Y_5 + Y_8 - Y_{18} = 3Y_{18} \qquad ...(4.4.14)$$

or

$$Y_4 + Y_8 = 4Y_{18} - (Y_1 + Y_2 + Y_3 + Y_5) \qquad ...(4.4.14)$$

In the above equation, Y_4 and Y_8 are the only unknowns. The former represents concentration of alpha carbons involved in ethylene bridges, while the latter determines the concentration of methylene bridges ($= Y_8 - Y_{18}$). In Chapter 3 it was mentioned that dissociation of ethylene bridges has an activation energy of about 50 kcal/mole while that of methylene bridges requires about 70 kcal/mole. Hence, the ratio Y_4/Y_8 will be an important parameter in predicting the amount of tar formed during pyrolysis. In the absence of any à priori information, this ratio can be treated as an adjustable parameter. Low values of the parameter will result in less tar and vice versa. Then, Eq. (4.4.14), together with the assumed value of Y_4/Y_8, will determine both Y_4 and Y_8.

The volume, Y_{19}, will be simply,

Y_{19} = Weight of the Particles/True Density (liters)

Typically, a 100 gm sample of coal will be considered. Hence,

$$Y_{19} = (100/\rho) \times 10^{-3} \text{ liters}$$

where ρ is in gms/cc.

It was discussed in Chapter 3 that of the three functional groups of

oxygen, only the phenolic need to be considered simultaneously with the carbon-hydrogen structure. Production of carbon monoxide and carbon dioxide was postulated to be separate from the reactions of carbon and hydrogen groups, and is to be modeled as two first-order processes. It is also assumed, due to lack of specific information, that ether linkages are initially absent. The concentration of phenolic groups, Y_{10}, can be calculated by using the amount of water vapor formed per unit weight of sample when coal dried of physically adsorbed water is pyrolyzed. The water produced will be 'chemical' water which can be modeled by phenolic condensation reactions involving two phenolic groups as discussed in Chapter 3. Then, if W_{H_2O} is the amount of water vapor produced per gram of the coal sample,

$$Y_{10} = \frac{2 \times W_{H_2O} \times \rho}{18} \times 10^3 \quad \text{moles/liter} \qquad \ldots(4.4.15)$$

The concentration of aromatic clusters, Y_{24}, remains the only state variable yet to be specified. No method seems to be available for its direct determination. It has, therefore, been treated as an adjustable parameter subject to the following constraints:

(1) Its value should lead to reasonable values for the parameters characterizing an 'average' cluster. These parameters include number of aromatic carbons and number of peripheral sites per cluster.

It was stated in Chapter 3 that although the clusters in a given coal are not all alike in their size, and may contain heteroatoms like nitrogen and sulfur, for modeling purposes

they will be represented by average clusters of uniform characteristics. Thus they will all contain the same number of aromatic carbons and have the same number of peripheral aromatic carbons which can bear alpha carbons and other substituents. The concentration of aromatic carbons in coal is given by

$$C_{aromatic} = \frac{C_{ar} \times C \times \rho}{12} \times 10^3 \text{ moles/liter}$$

Thus,

$$\text{No. of aromatic carbons per cluster} = s_1 = \frac{C_{aromatic}}{Y_{24}} \quad ...(4.4.16)$$

The concentration of peripheral sites should equal the total of all substituents and aromatic hydrogen.

$$H_{aromatic} = \frac{H_{ar} \times H \times \rho}{1} \times 10^3 \text{ moles/liter}$$

$$\text{Sites} = Y_8 + Y_{10} + (- COOH) + (- CO) + H_{aromatic} \text{ moles/liter}$$

where (- COOH) and (- CO) are concentrations of those groups calculated on the basis of CO_2 and CO produced in pyrolysis. Then,

$$\text{No. of peripheral sites per cluster} = s_2 = \frac{\text{Sites}}{Y_{24}} \quad ...(4.4.17)$$

Some typical values of the structural parameters s_1 and s_2 are shown below:

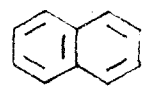

Two Ring Cluster

$s_1 = 10$

$s_2 = 8$

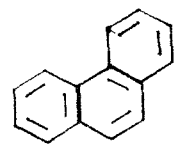

Three Ring Cluster

$s_1 = 14$

$s_2 = 10$

In general:

$$s_1 = 6n - 2(n - 1)$$

$$s_2 = 6_n - 4(n - 1)$$

where n = no. of rings

It is not necessary that the calculated values of s_1 and s_2 correspond exactly to 2, 3, 4, 5 ..., etc. ring clusters. Intermediate values would indicate that the coal has a mix of clusters of different sizes. Higher rank coals will have higher values of s_1 and s_2 indicating more compactification.

The number of alpha carbon connections per cluster (Y_8/Y_{24}) and the number of oxygen bonds per cluster $(Y_{10} + Y_{11})/Y_{24}$ are important parameters from the point of view of the model as will be seen in the next section. The FORTRAN code for the model is valid for (Y_8/Y_{24}) between 3 and 4 and $(Y_{10} + Y_{11})/Y_{24}$ between 0 and 1, or 1 and 2, or 2 and 3. It can, however, be changed for application to other values by changing the relevant FORTRAN statements. These values were considered suitable for the bituminous coals for which simulation runs were made.

(2) Its value determines the degree of 'tightness' of the coal structure and hence should be chosen carefully.

The number of bridges per cluster is a measure of the 'tightness' of the structure. Large values of this number imply low probability of a cluster becoming free by rupture of a bridge. Hence, the amount of tar produced will be reduced while the amount of gases formed will increase. The maximum number of bridges carried by a cluster will be equal to three times the number of alpha

carbons on that cluster. Ether bridges, which are assumed unbreakable, are initially absent but will be formed as phenolic condensation takes place. Their presence will contribute to the 'tightness' of the structure.

$$\text{number of bridges per cluster} = \frac{Y_4/2 + Y_8 - Y_{18}}{Y_{24}} \qquad \ldots(4.4.18)$$

Calculations in the next chapter show that for bituminous coals this ratio is between 1.5 and 3.

The above two constraints together result in an appreciable reduction in the range of values that can be assigned to Y_{24}. Although sometimes it is difficult to satisfy all the constraints while calculating the initial conditions, they are desirable because they imply uniqueness of the calculated values.

As mentioned before, concentrations of carboxylic and carbonyl groups are calculated on the basis of CO_2 and CO produced during pyrolysis experiments. This concludes the discussion on the calculation of initial values of the state variables.

The first criterion mentioned in the last section also required that the state variables be easily amenable to calculations of quantities of interest in pyrolysis, like weight loss, etc. The following calculations fulfill this requirement.

The weight loss can be calculated by computing the difference in the carbon, hydrogen, oxygen, nitrogen and sulfur content of the coal before and after pyrolysis. Recalling that the state variables Y_2, Y_3 and Y_5 were defined to include their corresponding double bond and beta radical

structures:

$$\text{Carbon} = 12(Y_{18} + Y_2 + 2Y_3 + Y_5 + C_{aromatic})Y_{19} \quad \ldots(4.4.19)$$

$$\text{Hydrogen} = 1(Y_1 + 3Y_2 + 5Y_3 + 2Y_5 + Y_{10} - Y_7 - Y_{12} + H_{aromatic})Y_{19} \quad \ldots(4.4.20)$$

$$\text{Oxygen} = 16(Y_{10} + Y_{11}/2)Y_{19} \quad \ldots(4.4.21)$$

and let N and S represent the density of nitrogen and sulfur in coal (assumed to remain constant); then the weight loss is given by

$$\text{Weight Loss} = (\text{Carbon} + \text{Hydorgen} + \text{Oxygen})_i - (\text{Carbon} + \text{Hydrogen} + \text{Oxygen})_f + (Y_{19_i} - Y_{19_f})(N + S) + CO + CO_2 \quad \ldots(4.4.22)$$

where the subscripts i and f stand for "initially" and "finally". The amount of gases formed can be easily calculated from the appropriate state variables.

$$H_2 = 2Y_{13}\,, \quad C_2H_4 = 28Y_{15}\,, \quad C_nH_m = 55Y_{17}$$
$$CH_4 = 16Y_{14}\,, \quad C_2H_6 = 30Y_{16}\,, \quad H_2O = 18Y_{20} \quad \ldots(4.4.23)$$

For the hydrocarbons higher than C_2, an average molecular weight of 55 has been assumed. The amount of tar produced is simply:

$$\text{Tar} = \text{Weight Loss} - H_2 - CH_4 - C_2H_4 - C_2H_6 - C_nH_m - H_2O - CO - CO_2 \quad \ldots(4.4.24)$$

This indirect method for calculating tar is necessitated because the direct method of counting the clusters and their substituent groups leaving the coal is quite cumbersome.

Other quantities of interest, like degree of deactivation of the structure as measured by the increase in the number of bridges per cluster and formation of double bonds, can also be followed during pyrolysis with

the help of appropriate variables.

5. Reacting Configurations in Terms of the State Variables

In this section mathematical strategies are formulated to compute the concentrations of various combinations of functional groups which participate in reactions. The reactions and their rate expressions are listed in the next section. Refer to Table 4.3.2 for a summary of this section.

It was discussed in Chapter 3 that presence of a double bond or a radical on an alpha carbon affects the reactivity of other functional groups on that alpha carbon. Consequently, rates of reactions of a functional group cannot be computed in terms of its total concentration alone. A mathematical scheme is needed to distribute sidechains, bridges, double bonds and radicals to alpha carbons, to compute what fractions of the functional groups are affected by being in the vicinity of the deactivating groups. Successful implementation of such a scheme will justify the choice of the state variables from the viewpoint of the second criterion mentioned in section 3.

Cheong (1976) made à posteriori adjustments in his mathematical model to account for the effects of double bonds and radicals. Considering their importance in the whole scheme of pyrolysis, the model presented in this thesis handles their distribution in a much more comprehensive and rigorous manner. The methodology developed is then applied to distributional problems of other functional groups as well. Briefly, a statistical transformation is used to convert the 'raw' state variables into concentrations

of combinations of functional groups. These combinations are termed reacting configurations.

Consider the sidechains Y_1, Y_2, Y_3, Y_5, bridges Y_4, Y_8 - Y_{18}, double bonds Y_6, Y_7 and alpha radicals Y_9. In the absence of any information regarding a perferential arrangement of sidechains and bridges, they can be considered randomly distributed on the alpha carbons. The process of bond-dissociation is also random, with the exception that a bond next to a radical or a double bond can be considered unbreakable. Hence, the occurrence of radicals and the subsequent formation of double bonds has no definite pattern. This randomness in the initial structure of coal as well as in the processes affecting that structure provides the basis for the statistical transformation.

Each of the state variables Y_7 and Y_{12} consists of three contributions, one each corresponding to the groups Y_2, Y_3 and Y_5. Let these contributions be represented by Y_7', Y_7'', Y_7''' and Y_{12}', Y_{12}'', Y_{12}'''. For example, Y_7' will be the concentration of a (= CH_2) and Y_{12}' of (- $\dot{C}H_2$) and so on. It is assumed for simplicity that

$$\frac{Y_7'}{Y_7} = \frac{Y_2}{Y_2 + Y_3 + Y_5} \qquad \ldots(4.5.1)$$

and

$$\frac{Y_{12}'}{Y_{12}} = \frac{Y_2}{Y_2 + Y_3 + Y_5} \qquad \ldots(4.5.2)$$

and similarly for other components of Y_7 and Y_{12}. This helps in determining each of these components and allows separation of Y_2, Y_3 and Y_5 into three components. For example:

$$Y_3 = Y_3\left[1 - \underbrace{\frac{Y_7}{Y_2 + Y_3 + Y_5}}_{-C_2H_5} - \frac{Y_{12}}{Y_2 + Y_3 + Y_5}\right] + \underbrace{\frac{Y_3}{Y_2 + Y_3 + Y_5}}_{=C_2H_4} Y_7 + \underbrace{\frac{Y_3}{Y_2 + Y_3 + Y_5}}_{-CH_2\dot{C}H_2} Y_{12}$$

Similarly Y_2 and Y_5 can be divided into their components.

Let the functional groups being considered be divided into the following groups:

$$M_R = Y_9 \qquad \ldots(4.5.3)$$

$$M_D = Y_6 + Y_7 \qquad \ldots(4.5.4)$$

$$M_P = Y_8 - Y_{18} \qquad \ldots(4.5.5)$$

$$M_H = Y_5\left[1 - \frac{Y_7}{Y_2 + Y_3 + Y_5} - \frac{Y_{12}}{Y_2 + Y_3 + Y_5}\right] + Y_5 \frac{Y_{12}}{Y_2 + Y_3 + Y_5} \qquad \ldots(4.5.6)$$

$$\begin{aligned} M_G = {} & Y_1 + Y_2\left[1 - \frac{Y_7}{Y_2 + Y_3 + Y_5} - \frac{Y_{12}}{Y_2 + Y_3 + Y_5}\right] \\ & + Y_3\left[1 - \frac{Y_7}{Y_2 + Y_3 + Y_5} - \frac{Y_{12}}{Y_2 + Y_3 + Y_5}\right] + Y_4 \\ & + Y_2 \frac{Y_{12}}{Y_2 + Y_3 + Y_5} + Y_3 \frac{Y_{12}}{Y_2 + Y_3 + Y_5} \end{aligned} \qquad \ldots(4.5.7)$$

The groups can be interpreted as follows: M_R represents alpha radicals, M_D is the total concentration of double bonds, M_P stands for the concentration of methylene bridges, M_H corresponds to the concentration of hydroaromatic structures including the beta radicals but excluding double bonds, and M_G consists of alpha hydrogens, $(-CH_3)$ and $(-\dot{C}H_2)$, $(-C_2H_5)$ and $(-CH_2\dot{C}H_2)$ and ethylene bridges.

The idea behind lumping the variables into groups is to facilitate their distribution among the alpha carbons. The distribution is made

subject to the following constraints:

(i) At most one pair of double bonds per alpha carbon,

(ii) At most one alpha radical per alpha carbon,

(iii) Co-existence of an alpha radical and double bonds on the same alpha carbon not allowed,

(iv) At most one ethylene bridge per alpha carbon,

(v) At most one hydroaromatic structure per alpha carbon.

The motivation for the last two constraints is simplicity in mathematics by reduction of the number of possible combinations of the five groups of variables. Such assumptions are unlikely to affect the results in any significant way. As a consequence of the fourth constraint, an alpha carbon will have at most two bonds connected with aromatic carbons on clusters.

Since an alpha carbon can carry at the most three substituent groups, two in the case of double bonds, the possible combinations of the five groups of variables subject to the five constraints are:

Category I: K_{DH}, K_{DP}, K_{DG}

Category II: K_{RHG}, K_{RHP}, K_{RPG}, K_{RGG}

Category III: K_{HPG}, K_{HGG}

Category IV: K_{PGG}, K_{GGG}

Each K represents a particular type of alpha carbon and includes all combinations of its subscripts. For example, K_{RHG} includes K_{RGH}, K_{GRH}, K_{HRG}, K_{GHR} and K_{HGR}. The summation of all K's should equal the concentration of alpha carbons in the system. Initially, before reaction, only the last two

categories of combinations are present. The M's can now be written in terms of concentration of K's:

$$K_{DH} + K_{DP} + K_{DG} = M_D \qquad \ldots(4.5.8)$$

$$K_{RHG} + K_{RHP} + K_{RPG} + K_{RGG} = M_R \qquad \ldots(4.5.9)$$

$$K_{DH} + K_{RHG} + K_{RHP} + K_{HPG} + K_{HGG} = M_H \qquad \ldots(4.5.10)$$

$$K_{DP} + K_{RHP} + K_{RPG} + K_{HPG} + K_{PGG} = M_P \qquad \ldots(4.5.11)$$

$$K_{DG} + K_{RHG} + K_{RPG} + 2K_{RGG} + K_{HPG} + 2K_{HGG} + 2K_{PGG} + 3K_{GGG} = M_G \qquad \ldots(4.5.12)$$

These are five equations in eleven unknowns.

Let K_i's denote concentrations of the K's (K_{DH}, K_{DP},...), where i ranges from 1 to 11 in the same order as the combinations are listed under the four categories. For example, K_{DH} has a concentration K_1, K_{DP} has a concentration K_2, and so on, up to K_{GGG} which has a concentration K_{11}. Consider the number of ways in which the K_i's can be chosen from their total Y_{18}:

$$\Omega = \binom{Y_{18}}{K_1} 3^{K_1} \binom{Y_{18} - K_1}{K_2} 3^{K_2} \ldots\ldots\ldots \binom{K_{18} - K_1 - K_2 - K_3}{K_4} 6^{K_4} \ldots\ldots$$

$$\ldots\ldots\ldots \binom{Y_{18} - K_1 - K_2 - K_3 - K_4 - K_5 - K_6 - K_7}{K_8} 6^{K_8} \ldots\ldots\ldots\ldots$$

$$\ldots\ldots\ldots \binom{Y_{18} - K_1 - K_2 \ldots\ldots - K_9 - K_{10}}{K_{11}} 1^{K_{11}} \qquad \ldots(4.5.13)$$

The notation used here is the same as in Probability Theory (Feller, 1976). Thus, $\binom{a}{b}$ represents the number of ways b objects can be chosen from a objects without repetition. The factors 3^{K_1}, 6^{K_8}, etc. account for the various possible arrangements of the subscripts of each K. For example,

it was mentioned earlier that the three substituents R, H and G in K_{RHG} can be arranged in five other ways, and hence a total of six arrangments.

The quantity Ω can be simplified to

$$\Omega = (Y_{18}!/K_1!K_2!\ldots K_{11}!)3^{K_1+K_2+\ldots}\ 6^{K_4+K_5+\ldots} \qquad \ldots(4.5.14)$$

In deriving expression (4.5.14), use has been made of the following balance:

$$\sum_{i=1}^{11} K_i = Y_{18} \qquad \ldots(4.5.15)$$

Under random distribution of the five groups of variables among alpha carbons, each of the K_i's becomes a random variable, and has an expected value $E_i(K_i)$. The expected value of a random variable x is generally calculated by,

$$E(x) = \sum_k x_k p(x_k)$$

where the summation is over all the possible values of x, and $p(x_k)$ is the probability that $x = x_k$. To simplify the mathematics, it will be assumed here that the expected values of K_i's will be very close to those calculated by maximizing the quantity Ω given by expression (4.5.14), subject to the five constraints represented by equations (4.5.8) through (4.5.12). This would give the most probable overall distribution.

Further, instead of maximizing Ω, one can maximize $\ln(\Omega)$ which is given by,

$$\ln(\Omega) = \ln(Y_{18}!) + (K_1 + K_2 + K_3 + K_7 + K_9 + K_{10})\ln 3 + (K_4 + K_5 + K_6 + K_8)\ln 6 - \ln(K_1!) - \ln(K_2!)\ldots\ldots\ldots - \ln(K_{11}!) \qquad \ldots(4.5.16)$$

Using the modified Stirling's formula,

$$\ln N! = N \ln N - N$$

expression (4.5.16) can be written as

$$\ln(\Omega) = \ln(Y_{18}!) + (K_1 + K_2 + K_3 + K_7 + K_9 + K_{10}) \ln 3 + (K_4 + K_5 + K_6 + K_8) \ln 6 - K_1 \ln K_1 + K_1 - K_2 \ln K_2 + K_2 - \ldots\ldots\ldots - K_{11} \ln K_{11} + K_{11} \quad \ldots(4.5.17)$$

This problem of finding the values of K_i which maximize the function $\ln(\Omega)$, subject to the five constraints (4.5.8) - (4.5.12), can be tackled using Lagrangae Multipliers. Define:

$$F = \ln(Y_{18}!) + (K_1 + K_2 + K_3 + K_7 + K_9 + K_{10}) \ln 3 + (K_4 + K_5 + K_6 + K_8) \ln 6 - K_1 \ln K_1 + K_1 - K_2 \ln K_2 + K_2 - \ldots\ldots\ldots - K_{11} \ln K_{11} + K_{11} + \lambda_1(K_1 + K_2 + K_3 - M_D) + \lambda_2(K_4 + K_5 + K_6 + K_7 - M_R) + \lambda_3(K_1 + K_4 + K_5 + K_8 + K_9 - M_H) + \lambda_4(K_2 + K_5 + K_6 + K_8 + K_{10} - M_P) + \lambda_5(K_3 + K_4 + K_6 + 2K_7 + K_8 + 2K_9 + 2K_{10} + 3K_{11} - M_G) \quad \ldots(4.5.18)$$

where λ_1, λ_2, λ_3, λ_4 and λ_5 are the five Lagrangae Multipliers for the five constraints. Differentiating F with respect to each of the K_i's and setting $(\partial F/\partial K)_i$ equal to zero, one gets

$$K_1 = 3 \exp(\lambda_1 + \lambda_3),\ K_2 = 3 \exp(\lambda_1 + \lambda_4), \ldots\ldots\ldots$$

$$K_4 = 6 \exp(\lambda_2 + \lambda_3 + \lambda_5), \ldots\ldots\ldots,\ K_{11} = \exp(3\lambda_5)$$

Define

$$\exp(l_1) = x(1), \quad \exp(l_2) = x(2), \quad \exp(l_3) = x(3)$$

$$\exp(l_4) = x(4), \quad \exp(l_5) = x(5)$$

Then, the K_i's can be expressed in terms of the five unknowns x(I) as shown in table 4.5.1. Substituting the K_i's in equations (4.5.8) through (4.5.12), five equations in five unknowns are obtained. These equations are nonlinear and are not amenable to analytical solution. They can be solved numerically. However, convergence of numerical algorithms cannot be taken for granted. This difficulty will be discussed in the next chapter. For now, it will be assumed that x(1), x(2),...x(5) can be determined by solving the five equations. Consequently the K_i's can be determined.

To distinguish between the various components of the group G, define the following probabilities:

$$p_1 = Y_1/M_G \qquad \ldots(4.5.19)$$

$$p_2 = Y_2[1 - A_1 - A_2]/M_G \qquad \ldots(4.5.20)$$

$$p_3 = Y_3[1 - A_1 - A_2]/M_G \qquad \ldots(4.5.21)$$

$$p_4 = Y_4/M_G \qquad \ldots(4.5.22)$$

$$p_5 = Y_2A_2/M_G \qquad \ldots(4.5.23)$$

$$p_6 = Y_3A_2/M_G \qquad \ldots(4.5.24)$$

where

$$A_1 = Y_7/(Y_2 + Y_3 + Y_5), \quad A_2 = Y_{12}/(Y_2 + Y_3 + Y_5)$$

Then, p_1K_{RHG} is the concentration of alpha carbons carrying a radical, a

Table 4.5.1

Reacting Configurations K's in Terms of the Five Unknowns x(1), x(2),...x(5)

	K	K_i	F(x(I))
1.	K_{DH}	K_1	3x(1)x(3)
2.	K_{DP}	K_2	3x(1)x(4)
3.	K_{DG}	K_3	3x(1)x(5)
4.	K_{RHG}	K_4	6x(2)x(3)x(5)
5.	K_{RHP}	K_5	6x(2)x(3)x(4)
6.	K_{RPG}	K_6	6x(2)x(4)x(5)
7.	K_{RGG}	K_7	3x(2)x(5)x(5)
8.	K_{HPG}	K_8	6x(3)x(4)x(5)
9.	K_{HGG}	K_9	3x(3)x(5)x(5)
10.	K_{PGG}	K_{10}	3x(4)x(5)x(5)
11.	K_{GGG}	K_{11}	x(5)x(5)x(5)

hydroaromatic structure, and a hydrogen atom. Similarly, $p_3 p_5 K_{PGG}$ will be the concentration of alpha carbons carrying a methylene bridge, $(-C_2H_5)$ group, and a $(-\dot{C}H_2)$ group. Thus, probabilities p_1 through p_6 will be used to characterize the group G. Similarly, define

$$p_{H1} = Y_5[1 - A_1 - A_2]/M_H$$

and

$$p_{H2} = Y_5 A_2/M_H$$

These two probabilities will help in distinguishing between a hydroaromatic structure and its beta radical.

The mathematics developed so far provides the means of calculating the concentration of any particular combination of functional groups on alpha carbons.

An ethylene bridge, $\Phi\text{-}C_\alpha\text{-}C_\alpha\text{-}\Phi'$, involves two alpha carbons and the bridge will not rupture if either of the alpha carbons carries a radical or a double bond. Hence, not all ethylene bridges are eligible for dissociation, and the concentration of those which are eligible needs to be calculated. This difficulty does not arise with methylene bridges because they each involve only one alpha carbon — a situation which can be handled in terms of the K's calculated earlier.

Similarly, the probability that a cluster becomes 'free' when a bridge ruptures has yet to be calculated. This involves distribution of alpha carbons carrying bridges among the clusters. Then the cluster carrying just one ethylene or methylene bridge will be the precursor to a 'free' clsuter.

Consider first the calculation of 'breakable' ethylene bridges. This

involves calculation of concentration of C_{alpha} - C_{alpha} linkages such that none of the two carbons carries a radical or a double bond. The alpha carbons can be divided into two groups:

(1) Those which have at least one bond occupied by an ethylene bridge but carry neither a double bond nor a radical. Let their concentration be X. They can be further divided into three groups:

(a) Those with only one bond involved in an ethylene bridge:

$$X_1 = p_4K_{HPG} + 2p_4(1 - p_4)K_{HGG} + 2p_4(1 - p_4)\ K_{PGG} + 3p_4(1 - p_4)^2K_{GGG}$$

(b) Those with only two bonds involved in ethylene bridges:

$$X_2 = p_4^2K_{HGG} + p_4^2K_{PGG} + 3p_4^2(1 - p_4)K_{GGG}$$

(c) Those with all three bonds involved in ethylene bridges:

$$X_3 = p_4^3K_{GGG}$$

(2) Those which have at least one bond occupied by an ethylene bridge but also carry a double bond or a radical. Let their concentration be Z. There are two groups among the Z's.

(a) Those with only one bond involved in an ethylene bridge:

$$Z_1 = p_4K_{DG} + p_4K_{RHG} + p_4K_{RPG} + 2p_4(1 - p_4)K_{RGG}$$

(b) Those with two bonds involved in ethylene bridges:

$$Z_2 = p_4^2K_{RGG}$$

It should be noted that the sum of X and Z does not equal Y_{18} because some alpha carbons will not carry bridges at all.

The two groups can lead to three types of combinations: XX, XZ, ZZ.

For example XZ represents concentration of ethylene type linkages between an alpha carbon belonging to the first group and an alpha carbon belonging to the second group. Obviously, the concentration of interest is XX. If the total concentration of linkages is denoted by Y_4', then

$$Y_4' = XX + XZ + ZZ = (X_1 + 2X_2 + 3X_3 + Z_1 + 2Z_2)/2 = Y_4/2$$

There are two constraints on the quantities XX, XZ and ZZ:

$$2XX + XZ = X_1 + 2X_2 + 3X_3 \qquad \ldots(4.5.25)$$

$$2ZZ + XZ = Z_1 + 2Z_2 \qquad \ldots(4.5.26)$$

Under random combination of the two groups X and Z, XX, XZ and ZZ become random variables. As in the case of K's, their expected values can be approximated by those values which maximize a function,

$$\Omega = \binom{Y_4'}{XX}\binom{Y_4' - XX}{XZ}\binom{Y_4' - XX - XZ}{ZZ} \qquad \ldots(4.5.27)$$

Again the approach of Lagrange Multipliers is used to obtain the quantities of interest in terms of two unknowns X(1) and X(2):

$$XX = X(1)^2, \quad XZ = X(1)X(2), \quad ZZ = X(2)^2 \qquad \ldots(4.5.28)$$

Substituting these in the equations (4.5.25) and (4.5.26) and solving the resultant two equations for the two unknowns X(1) and X(2) gives:

$$X(1) = ((X_1 + 2X_2 + 3X_3)/(2 + 1))^{\frac{1}{2}}$$

and $X(2) = 1\,x(1)$

where

$$1 = [(-(m - 1) + ((m - 1)^2 + 16m)^{\frac{1}{2}})/4m]$$

and $m = (X_1 + 2X_2 + 3X_3)/(Z_1 + 2Z_2)$

Thus all the three quantities XX, XZ and ZZ can be determined, where XX is the required concentration of 'breakable' bridges.

Distribution of alpha carbons among clusters can also be carried out in a similar manner. Since carbons involved in methylene type bridges are in the alpha position with respect to two aromatic clusters, it is the distribution of Y_8 among clusters Y_{24} that is of interest. The ratio Y_8/Y_{24} will be typically between 2 and 5 for most coals of interest here, i.e., subbituminous and bituminous. The mathematical expressions developed in this model will be applicable to the case when this ratio is between 3 and 4. The other two cases, when this ratio is between 2 and 3 or 4 and 5, can be treated in a similar manner. Hence, although only a special situation is being modeled, it is not an inherent limitation of the model. The mathematics can be easily extended to the other cases.

Strictly speaking, a coal matrix will consist of a mix of clusters carrying different numbers of alpha carbon connections (i.e., Y_8). Since the ratio Y_8/Y_{24} is assumed to be between 3 and 4, it is further assumed for computational convenience that clusters carry either 3 or 4 alpha carbon connections. In other words, the possibility of a cluster carrying 1, 2, 5 or more alpha carbon connections is being discounted. If this possibility were considered, the mathematics would have been applicable for any value of the ratio Y_8/Y_{24}, but also would have been more complicated. Let N_1 and N_2 represent the concentrations of clusters carrying 3 and 4 alpha carbon connections, respectively. Then,

$$N_1 + N_2 = Y_{24} \qquad \ldots(4.5.29)$$

and $$3N_1 + 4N_2 = Y_8 \qquad \ldots(4.5.30)$$

These two equations lead to

$$N_1 = 4Y_{24} - Y_8$$

and $$N_2 = Y_8 - 3Y_{24}$$

The alpha carbon connections Y_8 can be divided into two groups:

(1) Those which lead to alpha carbons carrying at least one bridge. The bridge may be methylene, ethylene or a double bond linkage between two alpha carbons (i.e. Y_6). The concentration of such alpha carbon connections is given by

$$CAL1 = (Y_6/(Y_6 + Y_7))\left[K_{DH} + (1 - p_4)K_{DG}\right] + p_4K_{DG} + K_{DP} + p_4K_{RHG} + K_{RHP} + K_{RPG} + p_4(2 - p_4)K_{RGG} + K_{HPG} + p_4(2 - p_4)K_{HGG} + K_{PGG} + p_4(3 - 3p_4 + p_4^2)K_{GGG} + Y_8 - Y_{18} \quad ...(4.5.31)$$

(2) Those which lead to alpha carbons carrying no bridges at all. Their concentration is given by

$$CAL2 = (Y_7/(Y_6 + Y_7))\left[K_{DH} + (1 - p_4)K_{DG}\right] + (1 - p_4)K_{RHG} + (1 - p_4)^2K_{RGG} + (1 - p_4)^2K_{HGG} + (1 - p_4)^3K_{GGG} \quad ...(4.5.32)$$

It should be noted that

$$CAL1 + CAL2 = Y_8$$

These two types of alpha carbon connections are to be distributed among the two types of clusters N_1 and N_2. It was mentioned in Chapter 3 that only a negligible concentration of clusters in coal will be free of connections with the coal matrix. Therefore, it is assumed here that each cluster carries at least one alpha carbon which carries at least one bridge. In other words, every cluster is connected to at least one other cluster through a methylene, ethylene or a double bond bridge. This

requirement that each cluster carry at least one hydrocarbon bridge is more restrictive than is necessary, because even an ether linkage will keep a cluster connected to the matrix. The justification for the added restriction is that it allows separate distribution of hydrocarbon and ether bridges, thus simplifying the mathematics.

Subject to the above-mentioned constraint, distribution of CAL1 and CAL2 among N_1 and N_2 leads to the following combinations:

N_1: N_{bnn}, N_{bbn}, N_{bbb} and

N_2: N_{bnnn}, N_{bbnn}, N_{bbbn}, N_{bbbb}

where

b: an alpha carbon connection leading to an alpha carbon carrying at least one bridge.

n: an alpha carbon connection leading to an alpha carbon not carrying bridges at all.

For example, N_{bbn} represents concentration of clusters which bear three alpha carbons, two of which carry at least one bridge each while the third lacks the bridges completely. Similarly, N_{bbbn} stands for the concentration of clusters carrying four alpha carbons, three with bridges and one without. The two balances on N's are:

$$N_{bnn} + 2N_{bbn} + 3N_{bbb} + N_{bnnn} + 2N_{bbnn} + 3N_{bbbn} + 4N_{bbbb} = CAL1 \qquad ...(4.5.33)$$

and

$$2N_{bnn} + N_{bbn} + 3N_{bnnn} + 2N_{bbnn} + N_{bbbn} = CAL2 \qquad ...(4.5.34)$$

Under random distribution of alpha carbons among the clusters, the N's become random variables. Their expected values can be calculated as was

demonstrated in similar situations eariler. However, it is more convenient to handle the distribution on N_1 and N_2 separately.

Since at least one alpha carbon on each cluster should belong to the first group (i.e. it should carry at least one bridge), divide CAL1 into two groups as follows:

$$CAL11 = \frac{2N_1}{2N_1 + 3N_2} (CAL1 - N_1 - N_2) + N_1 \qquad ...(4.5.35)$$

and

$$CAL12 = \frac{3N_2}{2N_1 + 3N_2} (CAL1 - N_1 - N_2) + N_2 \qquad ...(4.5.36)$$

Then, CAL11 is the concentration of alpha carbon connections of the first group available for distribution among N_1 clusters, and CAL12 for distribution among N_2 clusters. Similarly, CAL2 can be divided into CAL21 and CAL22; the former is to be distributed among N_1 clusters and the latter among N_2 clusters.

$$CAL21 = \frac{2N_1}{2N_1 + 3N_2} \; CAL2 \qquad ...(4.5.37)$$

$$CAL22 = \frac{3N_2}{2N_1 + 3N_2} \; CAL2 \qquad ...(4.5.38)$$

Thus, there are two parts to the distribution of Y_8 among Y_{24}:

(1) Calculation of expected values of N_{bnn}, N_{bbn} and N_{bbb} by distributing CAL11 and CAL21 among N_1 clusters. The probability function to be maximized is:

$$\Omega = \binom{N_1}{N_{bnn}} 3^{N_{bnn}} \binom{N_1 - N_{bnn}}{N_{bbn}} 3^{N_{bbn}} \binom{N_1 - N_{bnn} - N_{bbn}}{N_{bbb}}$$

and the three constraints are:

$$N_{bnn} + N_{bbn} + N_{bbb} = N_1$$

$$N_{bnn} + 2N_{bbn} + 3N_{bbb} = CAL11$$

$$2N_{bnn} + N_{bbn} = CAL21$$

Following the procedure demonstrated earlier, the results are:

$$N_{bnn} = 3\, x(1)x(2)^2$$

$$N_{bbn} = 3\, x(1)^2 c(2)$$

$$N_{bbb} = x(1)^3$$

where x(1) and x(2) are given by:

$$x(1) = (CAL21/(61^2 + 31))^{1/3}$$

and

$$x(2) = 1\, x(1)$$

where

$$1 = [-(m - 2) + ((m - 2)^2 + 4(2m - 1))^{\frac{1}{2}}]/[2(2m - 1)]$$

where

$$m = CAL11/CAL21$$

(2) Calculation of expected values of N_{bnnn}, N_{bbnn}, N_{bbbn}, N_{bbbb} by distributing CAL12 and CAL22 among N_2 clusters. In this case the probability function can be written as:

$$\Omega = \binom{N_2}{N_{bnnn}} 4^{N_{bnnn}} \binom{N_2 - N_{bnnn}}{N_{bbnn}} 6^{N_{bbnn}} \binom{N_2 - N_{bnnn} - N_{bbnn}}{N_{bbbn}} 4^{N_{bbbn}}$$

$$\binom{N_2 - N_{bnnn} - N_{bbnn} - N_{bbbn}}{N_{bbbb}}$$

The constraints are:

$$N_{bnnn} + N_{bbnn} + N_{bbbn} + N_{bbbb} = N_2$$

$$N_{bnnn} + 2N_{bbnn} + 3N_{bbbn} + 4N_{bbbb} = CAL12$$

$$3N_{bnnn} + 2N_{bbnn} + N_{bbbn} = CAL22$$

Using the same procedure as before,

$$N_{bnnn} = 4x(1)x(2)^3, \quad N_{bbbn} = 4x(1)^3x(2)$$

$$N_{bbnn} = 6x(1)^2x(2)^2, \quad N_{bbbb} = x(1)^4$$

where

$$x(1) = [CAL22/(12l^3 + 12l^2 + 4l)]^{\frac{1}{4}}$$

and $x(2) = lx(1)$

where l is given by the real root of the cubic equation:

$$l^3(3m - 1) + l^2(3m - 3) + l(m - 3) - 1 = 0$$

where

$$m = CAL12/CAL22$$

The probability of generation of a free cluster following a bridge rupture can now be expressed in terms of the N's. Define:

$$p_7 = \text{Prb}\left\{\begin{array}{l}\text{An alpha carbon carrying bridges has}\\ \text{exactly one ethylene type bridge but}\\ \text{no radical or double bond.}\end{array}\right\}$$

$$= \frac{2p_4(1 - p_4)K_{HGG} + 3p_4(1 - p_4)^2K_{GGG}}{CAL1}$$

and

$$p_8 = \text{Prb}\left\{\begin{array}{l}\text{An alpha carbon carrying bridges has}\\ \text{exactly one methylene type bridge but}\\ \text{no radical or double bond.}\end{array}\right\}$$

$$= \frac{(1 - p_4)K_{HPG} + (1 - p_4)^2K_{PGG}}{CAL1}$$

Then, if p_9 and p_{10} denote the probability that a cluster becomes free following the rupture of a ethylene bridge and a methylene bridge, respectively, they can be calculated as follows:

$$p_9 = \frac{p_7[N_{bnn} + N_{bnnn}]}{Y_{24}} \qquad \ldots(4.5.39)$$

and

$$p_{10} = \frac{p_8[N_{bnn} + N_{bnnn}]}{Y_{24}} \qquad \ldots(4.5.40)$$

These probabilities will allow determination of rate of generation of free clusters in terms of rates of dissociation of bridges.

Finally, distribution of oxygen groups among clusters can be treated in a similar fashion. The aim of distributing oxygen groups — phenolic and etheric — is to calculate the probability that a cluster is free of etheric linkages. Let this probability be denoted by p_{11}.

The ratio $(Y_{10} + Y_{11})/Y_{24}$ will be different for different coals. It will be low for bituminous coals but high for subbituminous coals which contain relatively more oxygen. In this model it is assumed that this ratio lies between 0 and 3. This range will suffice for the coals of interest in this thesis. Then, depending on the value of this ratio, three cases are to be considered:

(1) $0 < (Y_{10} + Y_{11})/Y_{24} \leq 1$

In this case, p_{11} is simply given by:

$$p_{11} = \frac{Y_{24} - Y_{11}}{Y_{24}}$$

It should be noted that initially, before reaction, absence of

etheric linkages make p_{11} unity. As pyrolysis progresses, p_{11} decreases monotonically.

(2) $1 < (Y_{10} + Y_{11})/Y_{24} \leq 2$

Assume that clusters carry either 1 or 2 oxygen bonds (Φ - O$\cdots$, Φ - OH), and let N_1' and N_2' be their respective concentrations.

$$N_1' = 2Y_{24} - Y_{10} - Y_{11}$$

$$N_2' = Y_{10} + Y_{11} - Y_{24}$$

Divide Y_{10} and Y_{11} between N_1' and N_2' as follows:

$$N_1': \quad \frac{N_1'}{N_1' + 2N_2'} Y_{10} , \quad \frac{N_1'}{N_1' + 2N_2'} Y_{11}$$

$$N_2': \quad \frac{2N_2'}{N_1' + 2N_2'} Y_{10} , \quad \frac{2N_2'}{N_1' + 2N_2'} Y_{11}$$

(a) The possible configurations of N_1' clusters are N_O, N_{OH}. Clearly:

$$N_O = \frac{N_1'}{N_1' + 2N_2'} Y_{11}$$

$$N_{OH} = \frac{N_1'}{N_1' + 2N_2'} Y_{10}$$

(b) The possible configurations of N_2' clusters are $N_{O,O}$, $N_{O,OH}$ and $N_{OH,OH}$. Using the random distribution approach and maximizing the relevant probability function subject to appropriate constraints, these N's can be calculated as:

$$N_{O,O} = x(1)^2 , \quad N_{O,OH} = 2x(1)x(2) , \quad N_{OH,OH} = x(2)^2$$

where

$$x(1) = [(2N_2'/(N_1' + 2N_2'))Y_{10}/(21^2 + 21)]^{\frac{1}{2}}$$

and $x(2) = l\, x(1)$

$$l = Y_{10}/Y_{11}$$

Then, the probability that a cluster is free of ether linkages is given by:

$$P_{11} = \frac{N_{OH} + N_{OH,OH}}{Y_{24}}$$

(3) $2 < (Y_{10} + Y_{11})/Y_{24} \leq 3$

The approach is similar to that in case (2) except that clusters carry either 2 or 3 oxygen bands. The possible configurations are given by:

$$N_{O,O} = x(1)^2 , \quad N_{O,OH} = 2x(1)x(2) , \quad N_{OH,OH} = x(2)^2$$

where

$$x(1) = [(2N_1'/(2N_1' + 3N_2'))Y_{10}/(2l^2 + 2l)]^{\frac{1}{2}}$$

and

$$x(2) = lx(1)$$

where

$$N_1' = 3Y_{24} - Y_{10} - Y_{11}$$

$$N_2' = Y_{10} + Y_{11} - 2Y_{24}$$

$$l = Y_{10}/Y_{11}$$

and

$$N_{O,O,O} = x(1)^3, \quad N_{O,O,OH} = 3x(1)^2x(2)$$

$$N_{O,OH,OH} = 3x(1)x(2)^2 , \quad N_{OH,OH,OH} = x(2)^3$$

where

$$x(1) = [(3N_2'/(2N_1' + 3N_2'))Y_{10}/(3l + 6l^2 + 3l^3)]^{1/3}$$

$$x(2) = lx(1)$$

$$1 = 2[(m + 1)^3/27m^3]^{\frac{1}{2}} - (2m - 1)/3m$$

$$m = Y_{11}/Y_{10}$$

Then, the probability p_{11} is given by:

$$p_{11} = \frac{N_{OH,OH} + N_{OH,OH,OH}}{Y_{24}}$$

Thus, the probability p_{11} can be calculated in all the three cases. This completes the distribution of oxygen groups among the clusters.

Summary of Section 5:

The aim of the section was to develop mathematical methodology for converting state variables into (i) concentrations of reacting configurations, (ii) probability functions associated in the generation of free clusters. The approach is summarized in table 4.5.2.

The differential equations governing the rate of change in the chemical system will be written in terms of the state variables. This will necessitate distribution of state variables to calculate the quanties of interest, i.e. the reactive configurations (as shown in this section) at each step of integration of the differential equations. The alternative would have been to treat the reacting configurations as the state variables. In that case the number of differential equations would have been larger. It is believed that the computer time required to calculate the distributions at each step is less than the additional time needed to integrate more equations.

Assumption of randomness in making these distributions avoids the necessity to assume a specific structure. For example, Cheong (1976) had

Table 4.5.2

Summary of Section 5

Operation	Result
1. Distribution of functional groups among alpha carbons.	Concentrations (K's) of the various combinations of the functional groups.
2. Distribution of ethylene linkages between alpha carbons.	Concentration (XX) of 'breakable' ethylene bridges.
3. Distribution of alpha carbon connections among clusters.	Probability of a cluster becoming free of hydrocarbon bridges.
4. Distribution of oxygen bonds among clusters.	Probability that a cluster is free of ether linkages.

assumed a honeycomb arrangement of clusters in which each cluster was connected to three neighboring clusters. There is no à priori basis for such an arrangement. On the other hand, his approach leads to more detailed information about the structure than is obtainable from random distributions. The latter, for example, need additional assumptions to differentiate between free fragments consisting of different number of clusters. However, this ability to differentiate was not deemed necessary in this model. Only single cluster fragments were taken into account and the results were satisfactory.

Except for the K's, calculations of all other quantities are straightforward. The K's can be calculated by solving numerically a set of five nonlinear equations. Considering that distributions are calculated at each step of integration, this method of calculating the K's is not satisfactory. A simplification in this regard will be discussed later in the next chapter.

Many portions of the mathematics implicitly utilize some basic balances like equation (4.4.13). Satisfying these balances requires meticulous accuracy in formulating the differential equations and points to the mathematical consistency of sections 4 and 5.

6. Chemical Reactions and Their Rates

This section treats the stoichiometry and kinetics of the chemical reactions in coal pyrolysis. The rates are expressed in terms of the quantities calculated in section 5. The kinetic parameters are listed in Appendix II.

The chemical reactions of coal pyrolysis were discussed in chapter 3. It was concluded that thermal dissociation of weak bonds in coal's structure leads to formation of free radicals which subsequently take part in several reactions. Dissociation of sidechains and bridges results in production of hydrocarbon gases and tar, respectively. Increasing concentration of radicals and double bonds in the system deactivates the structure, and ultimately volatile production halts completely.

It is generally recognized (Cheong, 1976, and Benson, 1976) that free radical chain reactions such as those considered in this thesis belong to the class of elementary reactions for which rates have a first-order dependence on the concentrations of the reacting species. The rate constant k has an Arrhenius-type dependence on temperature:

$$k = A \exp(-E/R_g T)$$

where A is the pre-exponential factor and E is the activation energy for the reaction.

The reactions and their rates are listed in table 4.6.1. As before, Φ stands for a peripheral aromatic carbon on a cluster. For many reactions, all three substituents on alpha carbons are not specified in the stoichiometry. However, the rate expressions account for all allowable configurations. The only exceptions are rates for reactions 30 through 35.

Some additional probability functions used in the rate expressions of table 4.6.1 are defined as follows:

$$m_1 = \text{prb}\{X \text{ has a } -\dot{C}H_2 \text{ radical}\} = \frac{2p_{H1}p_4p_5K_{HGG} + 2p_4p_5K_{PGG} + 3p_4p_5(2 - p_4 - p_5)K_{GGG}}{X_1 + X_2 + X_3}$$

$$m_2 = \text{prb}\{X \text{ has a } -\dot{\underset{\vdots}{C}}H \text{ radical}\} = \frac{p_{H2}p_4(2 - 2p_5 - 2p_6 - p_4)K_{HGG} + p_4p_{H2}K_{HPG}}{X_1 + X_2 + X_3}$$

$$c_1 = \text{prb}\{X \text{ has an alpha hydrogen}\} = \frac{2p_4p_1K_{HGG} + 2p_4p_1K_{PGG} + 3p_4p_1(2 - p_4)K_{GGG}}{X_1 + X_2 + X_3}$$

$$c_2 = \text{prb}\{Z \text{ has an alpha radical}\} = \frac{p_4K_{RHG} + p_4K_{RPG} + p_4(2 - p_4)K_{RGG}}{Z_1 + Z_2}$$

$$c_3 = \text{prb}\{X \text{ has a } (-CH_3)\} = \frac{2p_4p_2K_{HGG} + 2p_4p_2K_{PGG} + 3p_4p_2(2 - p_4)K_{GGG}}{X_1 + X_2 + X_3}$$

$$c_4 = \text{prb}\{X \text{ has a } (-C_2H_5)\} = \frac{2p_4p_3K_{HGG} + 2p_4p_3K_{PGG} + 3p_4p_3(2 - p_4)K_{GGG}}{X_1 + X_2 + X_3}$$

$$c_5 = \text{prb}\{X \text{ has a } (-\underset{\vdots}{C}H_2)\} = \frac{p_4K_{HPG} + p_4(2 - p_4)K_{HGG}}{X_1 + X_2 + X_3}$$

Table 4.6.1

Pyrolysis Reactions and Their Rates

Bond Dissociation

(1) $\Phi\text{-C-H} \rightarrow \Phi\text{-C}\cdot + \text{H}\cdot$

$$\gamma_1 = k_1[p_1K_{HPG} + 2p_1(1 - p_1)(K_{HGG} + K_{PGG}) + 3p_1(1 - p_1)^2K_{GGG} + 2p_1^2(K_{HGG} + K_{PGG}) + 6p_1^2(1 - p_1)K_{GGG} + 3p_1^3K_{GGG}]$$

(2) $\Phi\text{-C-CH}_3 \rightarrow \Phi\text{-C}\cdot + \text{CH}_3\cdot$

$$\gamma_2 = k_2[p_2K_{HPG} + 2p_2(1 - p_2)(K_{HGG} + K_{PGG}) + 3p_2(1 - p_2)^2K_{GGG} + 2p_2^2(K_{PGG} + K_{HGG}) + 6p_2^2(1 - p_2)K_{GGG} + 3p_2^3K_{GGG}]$$

(3) $\Phi\text{-C-C}_2\text{H}_5 \rightarrow \Phi\text{-C}\cdot + \text{C}_2\text{H}_5\cdot$

$$\gamma_3 = k_3[p_3K_{HPG} + 2p_3(1 - p_3)(K_{HGG} + K_{PGG}) + 3p_3(1 - p_3)^2K_{GGG} + 2p_3^2(K_{HGG} + K_{PGG}) + 6p_3^2(1 - p_3)K_{GGG} + 3p_3^3K_{GGG}]$$

(4) $\Phi\text{-C-C-}\Phi' \rightarrow \Phi\text{-C}\cdot + \cdot\text{C-}\Phi'$

$$\gamma_4 = k_4[XX](1 - m_1 - m_2)^2$$

(Refer to text for m_1 and m_2.)

Table 4.6.1. Pyrolysis Reactions and Their Rates (continued)

(5) 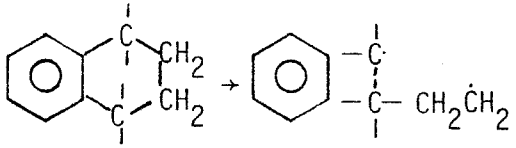

$$\gamma_5 = k_5[K_{HPG} + K_{HGG}]$$

(6) $\Phi\text{-}C\text{-}\Phi' \rightarrow \Phi\text{-}C\cdot + \cdot\Phi'$

$$\gamma_6 = k_6[(1 - p_5)K_{HPG} + (1 - p_5)^2 K_{PGG}]$$

Double Bond Formation

(7) $\Phi\text{-}\dot{C}\text{-}CH_3 \rightarrow \Phi\text{-}C{=}CH_2 + H\cdot$

$$\gamma_7 = k_7[p_2(K_{RHG} + K_{RPG}) + 2p_2(1 - p_2)K_{RGG} + 2p_2^2 K_{RGG}]$$

(8) $\Phi\text{-}\dot{C}\text{-}CH_2CH_3 \rightarrow \Phi\text{-}C{=}CH_2 + CH_3\cdot$

$$\gamma_8 = k_8[p_3(K_{RHG} + K_{RPG}) + 2p_3(1 - p_3)K_{RGG} + 2p_3^2 K_{RGG}]$$

(9) $\Phi\text{-}\dot{C}\text{-}CH_2CH_3 \rightarrow \Phi\text{-}C{=}CHCH_3 + H\cdot$

$$\gamma_9 = k_9[p_3(K_{RHG} + K_{RPG}) + 2p_3(1 - p_3)K_{RGG} + 2p_3^2 K_{RGG}]$$

Table 4.6.1. Pyrolysis Reactions and Their Rates (continued)

(10) 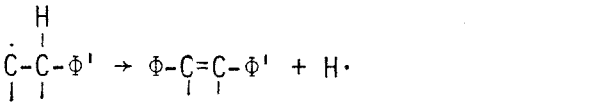

$$\gamma_{10} = k_{10}[XZ^{\cdot}]c_1c_2$$

(Refer to text for c_1 and c_2.)

(11) 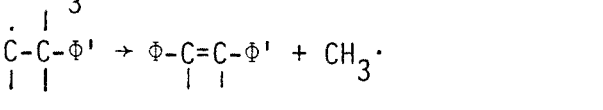

$$\gamma_{11} = k_{11}[XZ]c_3c_2$$

(12) 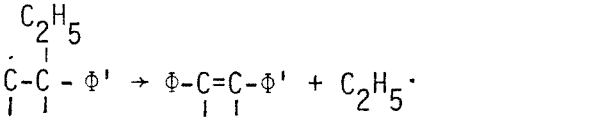

$$\gamma_{12} = k_{12}[XZ]c_4c_2$$

(Refer to text for c_4 and c_2.)

(13) 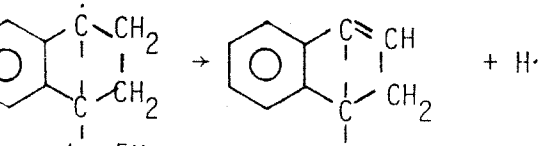

$$\gamma_{13} = k_{13}[K_{RHG} + K_{RHP}]$$

Table 4.6.1. Pyrolysis Reactions and Their Rates (continued)

(14) 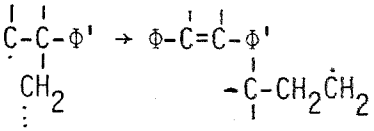

The hydroaromatic structure belongs to the aromatic cluster Φ'.

$$\gamma_{14} = k_{14}[XZ]c_5c_2$$

(Refer to text for c_5 and c_2.)

(15) 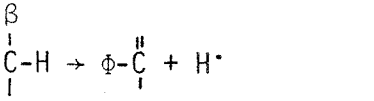

β represents a beta radical corresponding to a hydroaromatic structure, or to ($-\dot{C}H_2$).

$$\gamma_{15} = k_{15}[2p_{H1}p_5p_1K_{HGG} + 2p_5p_1K_{PGG} + 3p_5p_1(2 - p_5)K_{GGG}] + k_{15}[2p_{H2}(1 - p_5)p_1K_{HGG} + p_{H2}p_1K_{HPG}]$$

(16) 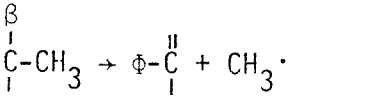

$$\gamma_{16} = k_{16}[2p_{H1}p_5p_2K_{HGG} + 2p_5p_2K_{PGG} + 3p_5p_2(2 - p_5)K_{GGG}] + k_{16}[2p_{H2}(1 - p_5)p_2K_{HGG} + p_{H2}p_2K_{HPG}]$$

(17) 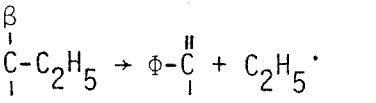

$$\gamma_{17} = k_{17}[2p_{H1}p_5p_3K_{HGG} + 2p_5p_3K_{PGG} + 3p_5p_3(2 - p_5)K_{GGG}] + k_{17}[2p_{H2}(1 - p_5)p_3K_{HGG} + p_{H2}p_3K_{HPG}]$$

Table 4.5.1. Pyrolysis Reactions and Their Rates (continued)

(18) 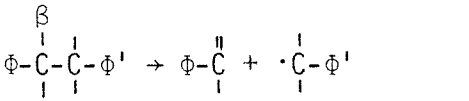

$$\gamma_{18} = k_{18}[XX]m_1(1 - m_1 - m_2) + k_{18}[XX]m_2(1 - m_1 - m_2)$$

(Refer to text for m_1 and m_2.)

(19) 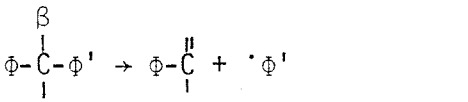

$$\gamma_{19} = k_{19}[p_{H1}p_5K_{HPG} + p_5(2 - p_5)K_{PGG}] + k_{19}[p_{H2}(1 - p_5)K_{HPG}]$$

(20) 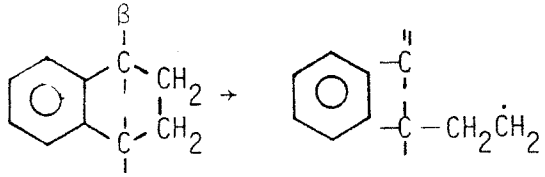

$$\gamma_{20} = k_{20}[p_{H1}p_5K_{HPG} + p_{H1}p_5(2 - p_5)K_{HGG}]$$

(21) 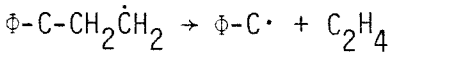

$$\gamma_{21} = k_{21}[p_6K_{HPG} + p_6(2 - p_6)K_{HGG} + p_6(2 - p_6)K_{PGG} + p_6(3 - 3p_6 + p_6^2)K_{GGG}]$$

Table 4.6.1. Pyrolysis Reactions and Their Rates (continued)

Recombination

(22) $\Phi\text{-}\overset{|}{\underset{|}{C}}\cdot + \cdot\overset{|}{\underset{|}{C}}\text{-}\Phi' \rightarrow \Phi\text{-}\overset{|}{\underset{|}{C}}\text{-}\overset{|}{\underset{|}{C}}\text{-}\Phi'$

$$\gamma_{22} = k_{22}[K_{RHG} + K_{RHP} + K_{RPG} + K_{RGG}]^2$$

Hydrogen Abstraction

(23) $H\cdot + H_\alpha \rightarrow H_2 + \text{Alpha Radical}$

$$\gamma_{23} = k_{23}[p_1 K_{HPG} + 2p_1(1 - p_1)(K_{HGG} + K_{PGG}) + 3p_1(1 - p_1)^2 K_{GGG} + 2p_1^2(K_{HGG} + K_{PGG}) + 6p_1^2(1 - p_1)K_{GGG} + 3p_1^3 K_{GGG}]\gamma_{21}$$

(24) $H\cdot + H_\beta \rightarrow H_2 + \text{Beta Radical}$

$$\gamma_{24} = k_{24}[H_{beta}]\gamma_{21}$$

(a) $\Phi\text{-}\overset{|}{\underset{|}{C}}\text{-}CH_3 + H\cdot \rightarrow \Phi\text{-}\overset{|}{\underset{|}{C}}\text{-}\dot{C}H_2 + H_2$

$$\gamma_{24_{(a)}} = k_{24}[p_2 K_{HPG} + 2p_2(1 - p_2)(K_{HGG} + K_{PGG}) + 3p_2(1 - p_2)^2 K_{GGG} + 2p_2^2 K_{HGG} + 2p_2^2 K_{PGG} + 6p_2^2(1 - p_2)K_{GGG} + 3p_2^3 K_{GGG}]\gamma_{21}$$

Table 4.6.1. Pyrolysis Reactions and Their Rates (continued)

(b) $\Phi\text{-}\dot{C}\text{-}C_2H_5 + H\cdot \rightarrow \Phi\text{-}\dot{C}\text{-}CH_2\dot{C}H_2 + H_2$

$$\gamma_{24_{(b)}} = k_{24}[p_3K_{HPG} + 2p_3(1 - p_3)(K_{HGG} + K_{PGG}) + 3p_3(1 - p_3)^2K_{GGG} + 2p_3^2(K_{HGG} + K_{PGG}) + 6p_3^2(1 - p_3)K_{GGG} + 3p_3^3K_{GGG}]\gamma_{21}$$

(c) 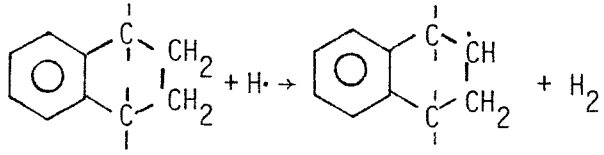

$$\gamma_{24_{(c)}} = k_{24}[p_{H1}K_{HPG} + p_{H1}K_{HGG}]\gamma_{21}$$

$$\gamma_{24} = \gamma_{24_{(a)}} + \gamma_{24_{(b)}} + \gamma_{24_{(c)}}$$

(25) $CH_3\cdot + H_{alpha} \rightarrow CH_4 + \text{Alpha Radical}$

$$\gamma_{25} = k_{25}[\text{same as in } \gamma_{23}]\gamma_{22}$$

Table 4.6.1. Pyrolysis Reactions and Their Rates (continued)

(26) $CH_3\cdot + H_{beta} \rightarrow CH_4$ + Beta Radical

$$\gamma_{26_{(a)}} = k_{26}[\text{same as in } \gamma_{24_{(a)}}]Y_{22}$$

$$\gamma_{26_{(b)}} = k_{26}[\text{same as in } \gamma_{24_{(b)}}]Y_{22}$$

$$\gamma_{26_{(c)}} = k_{26}[\text{same as in } \gamma_{24_{(c)}}]Y_{22}$$

$$\gamma_{26} = \gamma_{26_{(a)}} + \gamma_{26_{(b)}} + \gamma_{26_{(c)}}$$

(27) $C_2H_5\cdot + H_{alpha} \rightarrow C_2H_6$ + Alpha Radical

$$\gamma_{27} = k_{27}[\text{same as in } \gamma_{23}]Y_{23}$$

(28) $C_2H_5\cdot + H_{beta} \rightarrow C_2H_6$ + Beta Radical

$$\gamma_{28_{(a)}} = k_{28}[\text{same as in } \gamma_{24_{(a)}}]\, Y_{23}$$

$$\gamma_{28_{(b)}} = [k_{28} \text{ same as in } \gamma_{24_{(b)}}]\, Y_{23}$$

$$\gamma_{28_{(c)}} = k_{28}[\text{same as in } \gamma_{24_{(c)}}]\, Y_{23}$$

Table 4.6.1. Pyrolysis Reactions and Their Rates (continued)

$$\gamma_{28} = \gamma_{28(a)} + \gamma_{28(b)} + \gamma_{28(c)}$$

(29) Beta Radical + H_{alpha} → Alpha Radical + $(-CH_3)$ or $(-C_2H_5)$ or $(-\overset{\vdots}{C}H_2)$

(a) $\Phi-\overset{|}{C}-\dot{C}H_2 + H_{alpha} \rightarrow \Phi-\overset{|}{C}-CH_3$ + Alpha Radical

$$\gamma_{29(a)} = k_{29}[\text{same as in } \gamma_{23}][p_5K_{DG} + p_5(K_{HPG} + (2 - p_5)K_{HGG} + (2 - p_5)K_{PGG} + (3 - 3p_5 + p_5^2)K_{GGG})]$$

(b) $\Phi-\overset{|}{C}-CH_2\dot{C}H_2 + H_{alpha} \rightarrow \Phi-\overset{|}{C}-CH_2CH_3$ + Alpha Radical

$$\gamma_{29(b)} = k_{29}[\text{same as in } \gamma_{23}][p_6K_{DG} + p_6(K_{HPG} + (2 - p_6)K_{HGG} + (2 - p_6)K_{PGG} + (3 - 3p_6 + p_6^2)K_{GGG})]$$

(c) $\Phi-\overset{|}{C}-\overset{\vdots}{\dot{C}}H + H_{alpha} \rightarrow \Phi-\overset{|}{C}-\overset{\vdots}{C}H_2$ + Alpha Radical

$$\gamma_{29(c)} = k_{29}[\text{same as in } \gamma_{23}][p_{H2}K_{DH} + P_{H2}K_{HPG} + P_{H2}K_{HGG}]$$

$$\gamma_{29} = \gamma_{29(a)} + \gamma_{29(b)} + \gamma_{29(c)}$$

Table 4.6.1. Pyrolysis Reactions and Their Rates (continued)

Addition-Displacement

(30) $\Phi\text{-}\dot{C}\text{-} + H\cdot \rightarrow \Phi H + \cdot\dot{C}\text{-}$

Substituents on alpha carbon can be (-H), ($-CH_3$), ($-C_2H_5$).

$\gamma_{30} = k_{30}[K_{GGG}]Y_{21}$

G's will be specified in the differential equations.

(31) $\Phi\text{-}\dot{C}\text{-} + CH_3\cdot \rightarrow \Phi\text{-}CH_3 + \cdot\dot{C}\text{-}$

$\gamma_{31} = k_{31}[\text{same as } \gamma_{30}]Y_{22}$

(32) $\Phi\text{-}\dot{C}\text{-} + C_2H_5\cdot \rightarrow \Phi\text{-}C_2H_5 + \cdot\dot{C}\text{-}$

$\gamma_{32} = k_{32}[\text{same as } \gamma_{30}]Y_{23}$

(33) 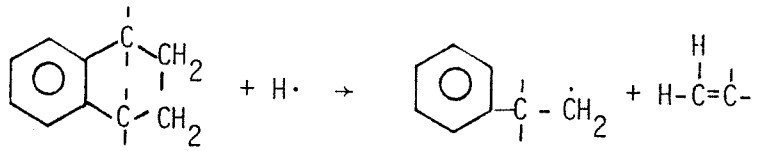 + $H\cdot \rightarrow$

Substituents on alpha carbons can be (-H), ($-CH_3$), ($-C_2H_5$).

$\gamma_{33} = k_{33}[K_{HGG}]Y_{21}$

G's will be specified in the differential equations.

Table 4.6.1. Pyrolysis Reactions and Their Rates (continued)

(34) 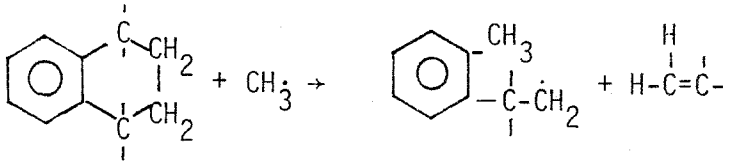

$$\gamma_{34} = k_{34}[\text{same as in } \gamma_{33}]Y_{22}$$

(35) 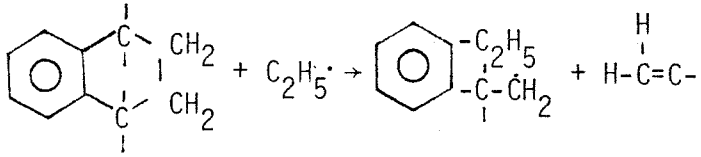

$$\gamma_{35} = k_{35}[\text{same as in } \gamma_{33}]Y_{23}$$

(36) $\Phi\text{-}\dot{C}\text{-}\Phi' + H\cdot \rightarrow \Phi H + \cdot\dot{C}\text{-}\Phi'$

$$\gamma_{36} = k_{36}[(1 - p_4)^2 K_{PGG}]Y_{21}$$

(37) $\Phi\text{-}\dot{C}\text{-}\Phi' + CH_3\cdot \rightarrow \Phi\text{-}CH_3 + \cdot\dot{C}\text{-}\Phi'$

$$\gamma_{37} = k_{37}[\text{same as in } \gamma_{36}]Y_{22}$$

(38) $\Phi\text{-}\dot{C}\text{-}\Phi' + C_2H_5\cdot \rightarrow \Phi\text{-}C_2H_5 + \cdot\dot{C}\text{-}\Phi'$

$$\gamma_{38} = k_{38}[\text{same as in } \gamma_{36}]Y_{23}$$

Table 6.4.1. Pyrolysis Reactions and Their Rates (continued)

Phenolic Condensation

(39) $\Phi\text{-OH} + \text{HO-}\Phi' \rightarrow \Phi\text{-O-}\Phi' + H_2O$

$$\gamma_{39} = k_{39}[Y_{10}]^2$$

Production of Oxides of Carbon

(40) $\Phi\text{-COOH} \rightarrow \Phi H + CO_2$

$$\gamma_{40} = k_{40}[\text{-COOH}]$$

(41) $\Phi\text{-}\overset{\overset{O}{\|}}{C}\text{-}CH_3 \rightarrow \Phi\text{-}CH_2 + CO$

$$\gamma_{41} = k_{41}[\text{-CO}]$$

In a system of competing chemical reactions, the values assigned to the kinetic parameters, A and E, may have an important effect on product distribution. For example, in coal pyrolysis the relative rates of chain and bridge dissociation will determine the relative amounts of hydrocarbon gases and tar formed. Thus it is important to obtain reliable values of the rate parameters for the reactions postulated in table 4.6.1. Although these values are not available in the literature, reasonably good estimates of their magnitudes can be obtained through a knowledge of the relevant bond strengths, the theory of thermochemical kinetics (Benson, 1976), and certain gas phase experimental data. There are two difficulties in applying the available information to the reactions under consideration. Firstly, the reacting configurations in coal are much more complex than those considered theoretically or experimentally in the literature. Secondly, reactions in coal are in condensed phase while the literature focuses on gas phase reactions.

The first difficulty arises because in the case of reactions of coal, the reacting species are not independent molecules but functional groups distributed throughout the coal matrix. Reactivity of a functional group is likely to be affected by its environment, i.e., by its surrounding groups. Although it will be difficult to account for all such effects, some approximate modifications can be made in the rate parameters. For example, the literature generally discusses dissociation of substituents on alpha carbons attached to a single benzene ring. Since clusters in coal consist of two or three rings, the bond strength of substituents can be reduced by approximately 3 kcal/mole from the values for benzene systems. Similarly, resonance stabilization will make activation

energies of some aromatic reactions higher than that of their aliphatic analogues. Take as an example:

(a) $\Phi\text{-}CH_2\text{-}\dot{C}H_2 \rightarrow \Phi\text{-}CH{=}CH_2 + H\cdot$

(b) $CH_3\text{-}CH_2\text{-}\dot{C}H_2 \rightarrow CH_3CH{=}CH_2 + H\cdot$

Activation energy for (a) will be about 8.5 kcal/mole lower than that of (b). On the other hand, there are effects which can be neglected because they are unlikely to have a major impact. Thus, the rate parameters for dissociation of alpha hydrogen from the following three configurations will be considered the same:

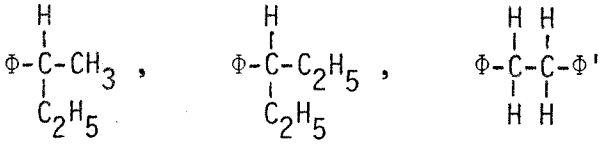

Some justification for the assumed values of the kinetic parameters is presented in Appendix II.

There does not exist any quantitative theory that adequately relates gas phase kinetics to reactions in condensed phase. Two phenomena in the condensed phase, the cage effect (Walling and Lepley, 1971; Herkes et al., 1969) and the gel effect (Cardenas and O'Driscoll, 1976), are generally considered responsible for the differences in kinetics. When reactive species are produced in pairs in close proximity in a condensed phase, an appreciable probability exists that they will react before diffusing apart. This phenomenon, the cage effect, will be most pronounced in the dissociation of bridges in the coal matrix:

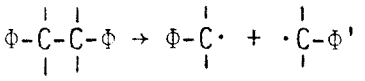

Low mobility of the alpha radicals produced will result in recombination — almost a negligible probability in gas phase because the radicals rapidly diffuse apart. Thus the rate of dissociation in the coal phase will be lower than in the gas phase. Since the decrease is due to a diffusive limitation, modification should be made in the frequency factor A for the reaction. Cheong (1976) used a 'cage parameter' to account for the reduction in the frequency factor.

The gel effect refers to the reduced probability of a bimolecular reaction in condensed phase due to limitations of proximity, orientation, alignment, etc. Thus, in the case of combination of two alpha radicals on the coal matrix to form an ethylene-type bridge, the two groups should be in close proximity and should have proper orientation. These requirements amount to substantial restrictions on the reaction, considering that both the groups are attached to the matrix. Similar restrictions will apply to such reactions as hydrogen abstraction when both groups are in solid phase (e.g., reaction (29) in table 4.6.1). However, the limitation will be less severe because the two groups do not have to combine with each other to form a stable bond as in the case of recombination of alpha radicals. Cheong (1976) postulated an increase in the activation energies of the reactions subject to gel effect.

7. The Differential Equations

This section formulates the differential equations governing the rate of change of the state variables with time during pyrolysis.

The state variables characterizing the reactants and the products in coal pyrolysis were defined in section 3. Their initial values were

calculated in section 4. Their use in calculating the quantities of interest in pyrolysis was also demonstrated. This section discusses their variation with time as pyrolysis progresses.

The differential equations derived here are essentially mass balances on species of interest. The concentration of a specie or a functional group can either increase or decrease due to chemical reactions. Rates of reactions to be considered were formulated in the last section. In addition to the change due to reactions, a functional group can be lost with the departing free clusters which leave the coal matrix and constitute tar, as discussed in section 3.3. To account for this loss, two quantities need to be calculated: the rate of generation of free clusters from each bridge dissociation reaction and the concentration of a functional group on a free cluster. However, differential equations for state variables Y_{13} through Y_{17} and Y_{20} representing the gaseous products will be straightforward because it is assumed (as explained in section 3.3) that they do not participate in secondary reactions. Similarly, equations for the small radicals Y_{21} through Y_{23} will be less complicated because their concentration changes only due to chemical reactions. A further simplification will be introduced in the next chapter by assuming pseudo steady state for these small radicals.

The state variables affected by departure of free clusters are: Y_1, Y_2, Y_3, Y_5, Y_7, Y_8, Y_9, Y_{10}, Y_{12}, Y_{18}, Y_{19} and Y_{24}. The aliphatic and ether bridges are not affected because only loss of single free clusters is considered and a single cluster cannot carry bridges. It was mentioned in section 3.3 that fragments containing one or two clusters can become volatile if they are free of connections with the coal matrix following

the dissociation of a bridge (refer to figure 3.3.2). However, if one assumes a specific arrangement of clusters and bridges, for example the honeycomb arrangement proposed by Cheong (1976), it is found that the probability of generation of a two-cluster fragment is about 6 to 8 times less than the probability of generation of a single-cluster fragment. In addition, in a bituminous coal in which each cluster is believed to consist of at least two or three rings along with all their aliphatic and oxygen substituents, a two-cluster fragment will be quite bulky (molecular weight about 400 - 600 for two three-ring clusters each carrying four alpha carbons). Such fragments will not have appreciable vapor pressure at temperatures of interest in this work (up to about 700^{o}C). Even if these fragments do vaporize, they will face severe transport limitations due to their size, and it is unlikely that they will be able to escape out of the coal particles. In subbituminous coals, large concentrations of ether linkages produced by phenolic condensation reduce the probability of generation of free fragments, especially two-cluster fragments. In light of all these limitations on two-cluster fragments, only single-cluster free fragments are considered in this model. Two-cluster fragments will be treated as part of the coal matrix.

Rate of Escape of Free Clusters

A cluster is free if it lacks methylene-type bridges, ethylene-type bridges, double bond bridges and ether linkages. Precursors to such free clusters consist of clusters carrying single 'breakable' bridges. Hence, the rate of generation of free clusters can be calculated by modifying the rate of dissociation of breakable bridges by the fraction of clusters

carrying a single breakable bridge at any given time. Such overall modifications in place of detailed accounting are justified because of the assumption of randomness in the system.

The rate of generation of free clusters has to be further modified to obtain the rate of escape of free clusters from coal. These two rates are different because free clusters can reattach to the radical sites on the coal matrix while diffusing out of a particle. It was discussed in section 3.4 that the extent of reattachment of free clusters depends on the concentration of radical sites (Y_g) and the residence time of diffusing clusters within the particle (say, τ). Thus:

$$\left\{\begin{matrix}\text{Rate of Escape} \\ \text{of Free Clusters}\end{matrix}\right\} = f(Y_g,\tau) \left\{\begin{matrix}\text{Rate of Generation} \\ \text{of Free Clusters}\end{matrix}\right\}$$

where $f(Y_g,\tau)$ will be a fraction. A simple mathematical analysis to determine the function 'f' can be carried out as follows. Consider the subunits in a coal particle (refer to figure 3.4.1). It was discussed in section 3.4 that transport limitations within a subunit are more severe than in the pore phase. Cluster reattachment to the coal matrix has its maximum probability within the subunits. Consider the situation of simultaneous diffusion and reattachment of free clusters in a subunit. The free clusters tend to diffuse towards the pore phase while being simultaneously produced and depleted by chemical reactions. Let R be the rate of generation of free clusters per unit volume. The rate (per unit volume) of reattachment is taken to be kY_gA, where k is a rate constant and A is the concentration of free clusters within the subunit. Although a spherical geometry is more suitable for a subunit, considering that

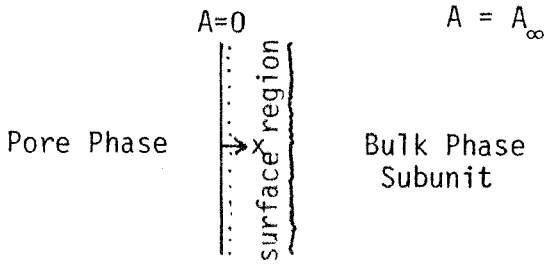

gradients in A will be limited to a small region near the pore and bulk interface, a rectangular geometry will be considered as shown above. Equating the diffusion and production terms:

$$D \frac{d^2A}{dx^2} = - R + kY_9A$$

where D is the effective diffusivity of free clusters within the micropores of the subunit. This equation has to be solved subject to the boundary conditions:

at $x = 0$, $A = 0$

as $x \to \infty$, $\frac{dA}{dx} = 0$, $A = A_\infty$

The direction in which x increases leads to the interior of the subunit. The solution is given by:

$$\frac{dA}{dx} = \left(\frac{2}{D}\right)^{\frac{1}{2}} \left[R(A_\infty - A) - \frac{kY_9}{2} (A_\infty^2 - A^2)\right]^{\frac{1}{2}}$$

Thus:

$$\left.\frac{dA}{dx}\right|_{x=0} = \left(\frac{2}{D}\right)^{\frac{1}{2}} \left[RA_\infty - \frac{kY_9}{2} A_\infty^2\right]^{\frac{1}{2}}$$

But in the interior of the subunit, the rate of production of free clusters equals the rate of reattachment:

$$R = kY_g A_\infty$$

or

$$A_\infty = \frac{R}{kY_g}$$

Thus,

$$\left.\frac{dA}{dx}\right|_{x=0} = \frac{R}{(DkY_g)^{\frac{1}{2}}}$$

Then

$$\text{Flux}\Big|_{x=0} = R\left(\frac{D}{kY_g}\right)^{\frac{1}{2}}$$

The flux at x=0 gives the rate of escape of free clusters per unit surface area of the subunits. This surface area can be taken to be approximately equal to the surface area of pores greater than about 20 $\overset{o}{A}$ in diameter (transitional pores and macropores). Let s represent the area of these pores per unit volume of the coal particle. Then:

$$\left\{\begin{matrix}\text{Rate of Escape of}\\ \text{Free Clusters/Volume}\end{matrix}\right\} = \left(\frac{D}{kY_g}\right)^{\frac{1}{2}} s \left\{\begin{matrix}\text{Rate of Generation of}\\ \text{Free Clusters/Volume}\end{matrix}\right\}$$

Thus,

$$f(Y_g,\tau) = \left(\frac{D}{kY_g}\right)^{\frac{1}{2}} s$$

Uncertainties in the values of D, k and s, especially D, limit the reliability of this expression.

We will use a simpler approach to account for reattachment. Since repeated distribution of the functional groups produces a mixing effect, it is not important to determine the precise sites of reattachment. In fact for the purposes of this model, the effects of reattachment can be simulated by reducing the rates of dissociation of bridges. Such a reduction in rate can be interpreted to be a reduction in volume, i.e., only

a small region near the surface of a subunit is considered active in production of free clusters. Once formed, free clusters in this region will instantaneously leave the coal matrix and will not be subject to reattachment. No free clusters will be formed in the interior region. Hence, dissociation of bridges in the interior region will be subject to cage effect as discussed in the last section. It will lead to instantaneous recombination of the radicals produced by dissociation. The effect will be present in the surface region also, but to a much lesser degree.

A fraction x is used in this model to reduce the rates of bridge dissociation reactions. It can be interpreted as a combination of cage effect and the function f. Its effect on the predicted results will be discussed in the next chapter.

Consider the dissociation of an ethylene-type bridge represented by reaction (4) in table 4.6.1.

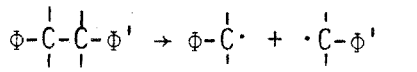

Following the dissociation, either one or both of the clusters could be free. Hence:

$$\begin{aligned}\text{Rate of Escape of Free Clusters Produced by Reaction (4)} &= xr_4 \{p_9 p_{11}(1 - p_9) + p_9 p_{11} p_9 (1 - p_{11}) \\ &\quad + p_9 p_{11}(1 - p_9) + p_9 p_{11} p_9 (1 - p_{11}) \\ &\quad + 2p_9^2 p_{11}^2\} \\ &= 2p_9 p_{11}\, xr_4\end{aligned}$$

The first four terms on the right-hand side account for the cases when one of the clusters is free but the other is not; while the last term represents the probability that both clusters are free. Similarly:

Rate of Escape of Free Clusters Produced by Reaction (6) $= 2p_{10}p_{11}\, xr_6$

Rate of Escape of Free Clusters Produced by Reaction (18) $= 2p_9p_{11}\, xr_{18}$

Rate of Escape of Free Clusters Produced by Reaction (19) $= 2p_{10}p_{11}\, xr_{19}$

Rate of Escape of Free Clusters Produced by Reactions (36), (37) and (38) $= 2p_{10}p_{11}\, x(r_{36} + r_{37} + r_{38})$

Thus,

Overall Rate of Escape of Free Clusters Due to Bridge Dissociation

$$= x\{2p_9p_{11}(r_4 + r_{18}) + 2p_{10}p_{11}(r_6 + r_{19} + r_{36} + r_{37} + r_{38})\} \quad \ldots(4.7.1)$$

Rate of Loss of Functional Groups

The escaping free clusters carry all the substituent functional groups on their peripheral aromatic carbons. The rate of loss of a functional group can be calculated by considering each bridge-dissociation reaction separately. For each of these reactions, the rate of escape of free clusters is multiplied by a probability function representing the concentration of a functional group on the free clusters generated by the reaction.

The model requires that before dissociation of bridges, each cluster in the system carry either 3 or 4 alpha carbons. Free clusters generated by reactions 4, 18, 37 and 38 will also carry either 3 or 4 alpha carbons. However, half of the free clusters produced by reaction 6, 19 and 36 will

have only two or three alpha carbons. The concentrations of functional groups represented by the state variables Y_1, Y_2, Y_3, Y_5, Y_7, Y_8, Y_9, Y_{12} and Y_{18} on the alpha carbons carried by free clusters can be calculated by using the distribution of K's on the precursors to the free clusters. Loss of phenolic groups can be calculated directly in terms of the state variable Y_{10}.

While computing concentrations of Y_2, Y_3 and Y_5 on the free clusters, special care is taken to account for the fact that these state variables include the corresponding double bond and beta radical structures of their functional groups. This leads to complicated expressions for the rate of change of these state variables. Some functional groups like Y_1, Y_2' and Y_3' can occupy one, two or all three substituent positions on an alpha carbon, while some others like Y_5, Y_7 and Y_9 cannot be present in two's or three's on the same alpha carbon.

The overall rates of loss of alpha hydrogens (Y_1), methyl groups (Y_2), and alpha radicals (Y_9) are shown in figures 4.7.1, 4.7.2, 4.7.3, respectively, for purposes of illustration. These expressions and others that can be obtained in a similar fashion for other state variables are fairly complicated. Although simpler approaches can be adopted (for example, it can be assumed that rate of loss of a functional group is directly proportional to its concentration), they may result in an inability to satisfy consistency requirements like equation (4.4.13), at each step of integration of differential equations. If this happens, the statistical distributions in section 5 will no longer be valid and the entire mathematical scheme will fail. Hence, accuracy is indispensable and simplicity has to be sacrificed.

Rate of Loss of Alpha Hydrogens (Y_1) with Escaping Free Clusters =

$$\left\{\frac{2p_4p_1K_{HGG} + 6p_4p_1(p_1 + p_2 + p_3 + p_6)K_{GGG}}{2p_4(p_1 + p_2 + p_3 + p_6)K_{HGG} + 3p_4(p_1 + p_2 + p_3 + p_6)^2K_{GGG}}\right\}(2r_4 + r_{18})xp_9p_{11} +$$

$$\left\{\frac{p_1[Y_7/(Y_6 + Y_7)]K_{DG} + p_1K_{RHG} + 2p_1(1 - p_4 - p_5)K_{RGG} + 2p_1(1 - p_4)K_{HGG} + 3p_1(1 + p_4^2 - 2p_4)K_{GGG}}{[Y_7/(Y_6 + Y_7)](K_{DH} + (1 - p_4)K_{DG}) + p_{H1}(1 - p_4 - p_5)K_{RHG} + (1 - p_4 - p_5)^2K_{RGG} + (1 - p_4)^2K_{HGG} + (1 - p_4)^3K_{GGG}}\right\}$$

$$(r_4p_9 + r_6p_{10} + r_{18}p_9 + r_{19}p_{10} + (r_{36} + r_{37} + r_{38})p_{10})(2 + (N_{bnnn}/(N_{bnn} + N_{bnnn}))$$

$$2xp_{11} + \left\{\frac{p_1K_{HPG} + 2p_1(p_1 + p_2 + p_3 + p_6)K_{PGG}}{p_{H1}(p_1 + p_2 + p_3 + p_6)K_{HPG} + (p_1 + p_2 + p_3 + p_6)K_{PGG}}\right\}(r_6 + r_{36} + r_{37} + r_{38})xp_{10}p_{11} +$$

$$\left\{\frac{2p_4p_1p_{H2}K_{HGG} + 6p_4p_1p_5K_{GGG}}{2p_4(p_{H2}(p_1 + p_2 + p_3 + p_6) + p_{H1}p_5)K_{HGG} + 6p_4p_5(p_1 + p_2 + p_3 + p_6)K_{GGG}}\right\}(r_{18})xp_9p_{11} +$$

$$\left\{\frac{2p_5p_1K_{PGG} + p_{H2}p_1K_{HPG}}{2p_5(p_1 + p_2 + p_3 + p_6)K_{PGG} + p_{H2}(p_1 + p_2 + p_3 + p_6)K_{HPG}}\right\}(r_{19})xp_{10}p_{11} + 5(r_{36} + r_{37} + r_{38})xp_{10}p_{11}$$

Figure 4.7.1: Rate of Loss of Alpha Hydrogens (Y_1) with Escaping Free Clusters.

Rate of Loss of Methyl Groups with Escaping Free Clusters =

$$\left\{\frac{2p_{H1}p_4p_2K_{HGG} + 6p_4p_2(1 - p_2 - p_4 - p_5)K_{GGG} + 6p_4p_2^2K_{GGG}}{2p_{H1}p_4(1 - p_4 - p_5)K_{HGG} + 3p_4(1 - p_4 - p_5)^2K_{GGG}}\right\} (2r_4 + r_{18})xp_9p_{11} +$$

$$\left[\left\{\frac{p_2(Y_7/(Y_6 + Y_7))(1 + Y_2/(Y_2 + Y_3 + Y_5)) + (1 - p_2 - p_4 - p_5)(Y_7/(Y_6 + Y_7))(Y_2/(Y_2 + Y_3 + Y_5)) + p_5(Y_7/(Y_6 + Y_7))(1 + (Y_2/(Y_2 + Y_3 + Y_5))}{(Y_7/(Y_6 + Y_7))(K_{DH} + (1 - p_4)K_{DG}) + p_{H1}(1 - p_4 - p_5)K_{RHG} + (1 - p_4 - p_5)^2K_{RGG} + (1 - p_4)^2K_{HGG} + (1 - p_4)^3K_{GGG}}\right\} +\right.$$

$$\left\{\frac{p_2p_{H1}K_{RHG} + 2p_2(1 - p_5 - p_4)K_{RGG} + 2(p_2 + p_5)(1 - p_2 - p_4 - p_5)K_{HGG} + 2(p_2^2 + 2p_2p_5)K_{HGG} + (Y_7/(Y_6 + Y_7))(Y_2/(Y_2 + Y_3 + Y_5))K_{DH}}{(Y_7/(Y_6 + Y_7))(K_{DH} + (1 - p_4)K_{DG}) + p_{H1}(1 - p_4 - p_5)K_{RHG} + (1 - p_4 - p_5)^2K_{RGG} + (1 - p_4)^2K_{HGG} + (1 - p_4)^3K_{GGG}}\right\} +$$

$$\left.\left\{\frac{3(p_2 + p_5)(1 - p_2 - p_4 - p_5)^2K_{GGG} + 2(3p_2^2 + 6p_2p_5)(1 - p_2 - p_4 - p_5)K_{GGG} + 3(p_2^3 + 3p_2^2p_5)K_{GGG}}{(Y_7/(Y_6 + Y_7))(K_{DH} + (1 - p_4)K_{DG}) + p_{H1}(1 - p_4 - p_5)K_{RHG} + (1 - p_4 - p_5)^2K_{RGG} + (1 - p_4)^2K_{HGG} + (1 - p_4)^2K_{GGG}}\right\}\right]$$

$$(2r_4p_9 + 2r_6p_{10} + 2r_{18}p_9 + 2r_{19}p_{10} + 2(r_{36} + r_{37} + r_{38})p_{10})(2 + (N_{bnnn}/(N_{bnn} + N_{bnnn}))xp_{11} +$$

$$\left\{\frac{p_{H1}p_2K_{HPG} + 2p_2(1 - p_2 - p_5 - p_4)K_{PGG} + 2p_2^2K_{PGG}}{p_{H1}(1 - p_4 - p_5)K_{HPG} + (1 - p_4 - p_5)^2K_{PGG}}\right\} (r_6 + r_{36} + r_{37} + r_{38})p_{10}xp_{11} +$$

$$\left\{\frac{2p_4p_2p_{H2}K_{HGG} + 6p_4p_5(1 - p_2 - p_5 - p_4)K_{GGG} + 12p_2p_4p_5K_{GGG}}{2p_4p_5p_{H1}K_{HGG} + 2p_4p_{H2}(1 - p_4 - p_5)K_{HGG} + 6p_4p_5(1 - p_4 - p_5)K_{GGG}}\right\} (r_{18})xp_9p_{11} +$$

$$\left\{\frac{2p_5(1 - p_2 - p_4 - p_5)K_{PGG} + 4p_2p_5K_{PGG} + p_{H2}p_2K_{HPG}}{2p_5(1 - p_4 - p_5)K_{PGG} + p_{H2}(1 - p_4 - p_5)K_{HPG}}\right\} (r_{19})xp_{10}p_{11} + r_{38}xp_{10}p_{11}$$

Figure 4.7.2: Rate of Loss of Methyl Groups (Y_2) with Escaping Free Clusters.

Rate of Loss of Alpha Radicals (Y_9) with Escaping Free Clusters =

$$\left\{2r_4p_9 + r_6p_{10} + r_{18}p_9 + (r_{36} + r_{37} + r_{38})p_{10}\right\} xp_{11} \quad +$$

$$\left\{\frac{(1 - p_4 - p_5)p_{H1}K_{RHG} + (1 - p_4 - p_5)^2K_{RGG}}{(Y_7/(Y_6 + Y_7))(K_{DH} + (1 - p_4)K_{DG}) + p_{H1}(1 - p_4 - p_5)K_{RHG} + (1 - p_4 - p_5)^2K_{RGG} + (1 - p_4)^2K_{HGG} + (1 - p_4)^3K_{GGG}}\right\}$$

$$(2r_4p_9 + 2r_6p_{10} + 2r_{18}p_9 + 2r_{19}p_{10} + 2(r_{36} + r_{37} + r_{38})p_{10})xp_{11}(2 + (N_{bnnn}/(N_{bnn} + N_{bnnn}))$$

Figure 4.7.3: Rate of Loss of Alpha Radicals (Y_9) with Escaping Free Clusters.

The differential equations can now be formulated as shown below.

(I) For the hydrocarbon gases, Y_{13} through Y_{17} and water vapor Y_{20}, the differential equations are simply:

Rate of Change of Moles = Rate of Production by Reaction

For example:

$$\frac{d[Y_{13}]}{dt} = [r_{23} + r_{24}]Y_{19}$$

$$\frac{d[Y_{16}]}{dt} = [r_{27} + r_{28}]Y_{19}$$

and

$$\frac{d[Y_{20}]}{dt} = [r_{39}]Y_{19}$$

(II) For the small radicals, Y_{21} through Y_{23}:

Rate of Change of Moles = Rate of Production by Reactions − Rate of Consumption by Reactions

For example:

$$\frac{d[Y_{21}\ Y_{19}]}{dt} = [\{r_1 + r_7 + r_9 + r_{10} + r_{13} + r_{15}\} - \{r_{23} + r_{24} + (1 - p_4 - p_5 - p_6)^3\ r_{30} + (1 - p_4 - p_5 - p_6)^2\ r_{33} + r_{36}\}]Y_{19}$$

(III) For the concentration of clusters, Y_{24}:

Rate of Change of Moles = − [Overall Rate of Escape of Free Clusters] (From equation (4.7.1)

or

$$\frac{d[Y_{24}Y_{19}]}{dt} = -[p_9(r_4 + r_{18}) + p_{10}(r_6 + r_{19} + r_{36} + r_{37} + r_{38})]2xp_{11}Y_{19}$$

(IV) For the ethylene-type bridges, Y_4:

Rate of Change of Moles = Rate of Production by Reaction − Rate of Depletion by Reaction

$$\frac{d[Y_4Y_{19}]}{dt} = [2r_{22} - 2xr_4 - 2r_{10} - 2r_{11} - 2r_{12} - 2r_{14} - 2xr_{18}]Y_{19}$$

For the double bond bridges, Y_6 and ether bridges, Y_{11}:

Rate of Change of Moles = Rate of Production by Reaction

$$\frac{d[Y_6Y_{19}]}{dt} = 2[r_{10} + r_{11} + r_{12} + r_{14}]Y_{19}$$

and

$$\frac{d[Y_{11}Y_{19}]}{dt} = 2[r_{39}]Y_{19}$$

For the phenolic groups, Y_{10}:

Rate of Change of Moles = − Rate of Depletion by Reaction − Rate of Depletion with Free Clusters

$$\frac{d[Y_{10}Y_{19}]}{dt} = -2[r_{39}]Y_{19} - \frac{Y_{10}}{Y_{24}}[\text{rate of loss of clusters from equation (4.7.1)}]\,Y_{19}$$

(V) For the state variables, Y_1, Y_2, Y_3, Y_5, Y_7, Y_8, Y_9, Y_{12}:

Rate of Change of Moles = Rate of Production by Reaction − Rate of Depletion by Reaction − Rate of Depletion with Free Clusters

For example:

$$\frac{d[Y_1 Y_{19}]}{dt} = [\{a(3r_{31} + 2r_{32}) + b(3r_{34} + 2r_{35}) + 3r_{37} + 2r_{38}\}$$
$$- \{r_1 + r_{10} + r_{15} + r_{23} + r_{25} + r_{27} + r_{29}$$
$$+ (c + 2d + 3p_1^3)(r_{30} + r_{31} + r_{32}) + (e + 2p_1^2)(r_{33} + r_{34} + r_{35})\}$$
$$- \{\text{expression in figure 4.7.1}\}] Y_{19}$$

where

$$a = (1 - p_4 - p_5 - p_6)^3$$
$$b = (1 - p_3 - p_5 - p_6)^2$$
$$c = 3p_1(1 - p_1 - p_4 - p_5 - p_6)^2$$
$$d = 3p_1^2(1 - p_1 - p_4 - p_5 - p_6)$$
$$e = 2p_1(1 - p_1 - p_4 - p_5 - p_6)$$

The differential of volume (dY_{19}/dt) appears on the left-hand side of all differential equations except those for gases. An additional assumption is required to evaluate this differential. Since very little consideration has been given so far to physical changes in coal brought about by chemical reactions, it will be assumed here that coal's volume changes solely due to the loss of free clusters. In other words, the concentration of clusters in coal remains constant during pyrolysis. Such an assumption will also help maintain the validity of the various constraints (for example, either 3 or 4 alpha carbons per cluster) on the statistical distributions. Thus:

$$\frac{dY_{24}}{dt} = 0$$

hence,

$$\frac{d[Y_{24}Y_{19}]}{dt} \equiv Y_{24}\frac{dY_{19}}{dt} + Y_{19}\frac{dY_{24}}{dt}$$

$$\equiv Y_{24}\frac{dY_{19}}{dt}$$

Then, using the differential equation for the rate of change of moles of clusters:

$$\frac{dY_{19}}{dt} = -\frac{1}{Y_{24}}[p_9(r_4 + r_{18}) + p_{10}(r_6 + r_{19} + r_{36} + r_{37} + r_{38})]2xp_{11}Y_{19}$$

With the help of this expression, the left-hand sides of all differential equations can be put in the form of rate of change of concentration rather than moles. For example, for the phenolic groups:

$$\text{Left-Hand Side} = Y_{10}\frac{dY_{19}}{dt} + Y_{19}\frac{dY_{10}}{dt}$$

Thus,

$$\frac{dY_{10}}{dt} = -2[r_{39}]$$

and for the double bond bridges, Y_6:

$$\frac{dY_6}{dt} = 2[r_{10} + r_{11} + r_{12} + r_{14}] + \frac{Y_6}{Y_{24}}[p_9(r_4 + r_{18} + p_{10}(r_6 + r_{19} + r_{36} + r_{37} + r_{38})]\,2xp_{11}$$

Similarly for other variables.

Overall, there is a set of 23 simultaneous differential equations which govern the rate of change in the chemical structure of coal and the rate of production of volatiles during pyrolysis. Although basically these equations are similar to equations obtained for any multiple-specie-

multiple-reaction system, there are two additional complications: first, rates are expressed in terms of quantities obtained by applying statistical transformations to the state variables; second, expressions for loss of functional groups with escaping clusters make the equations very complex.

Chapter V

COMPUTER SIMULATIONS

1. General

This chapter discusses computer calculations based on the mathematical scheme developed in the last chapter. The strategy for implementation of the above scheme on computer is presented in the next section. It is followed by a discussion of two simplifications introduced in mathematics in order to facilitate computation. Finally, results for specific coals are presented and discussed. Limitations of the model are discussed under Conclusions after Chapter 6.

As in any computer simulation scheme, the aim here is to substitute an experiment in laboratory by an "experiment" on the computer. A code is developed, which when fed with information on the coal and the experimental conditions predicts results of pyrolyzing the coal for a specified time. Basically, the code determines variation with time of the state variables characterizing the coal. A set of 23 simultaneous differential equations governing the rates of such variations was developed in the last chapter. Integration of this set will determine the state variables as functions of time; these functions can then be used to determine all quantities of interest, e.g., weight loss, amount of tar formed, amount of gases formed, etc.

We use a special package of FORTRAN IV codes, called EPISODE, for numerical integration of the differential equations. This package is described in the next section. In using this package the user has three responsibilities: to set up a subroutine containing the differential equations; to provide the relevant data, e.g. the rate parameters and the initial conditions on the state variables; to select suitable values for the 'tuning-parameters' which determine the effectiveness of the integration

scheme. The mathematics involved in carrying out the first two responsibilities was discussed in the last chapter. The tuning-parameters are selected after some trial and error.

The computer used was the IBM 370/3032 batch processor at the California Institute of Technology. All coding was done in FORTRAN IV, and the computations were carried out in single precision.

2. Integration Scheme and Code

Integration of the differential equations of pyrolysis basically amounts to the general problem of finding a solution vector Y(t) for a set of simultaneous differential equations:

$$\frac{dY(t)}{dt} = f(Y(t),t) \qquad \ldots(5.2.1)$$

subject to the initial conditions:

$$Y(t_o = 0) = Y_o \qquad \ldots(5.2.2)$$

Although, usually, the right-hand side of (5.2.1) consists of a function of Y and t, in our case it consists of a function of the quantities obtained by applying statistical transformations to the variables Y. Hence:

$$\frac{dY(t)}{dt} = f(ST(Y(t)) \qquad \ldots(5.2.3)$$

where ST stands for Statistical Tranformation. However, this difference does not affect the method of solution.

In a system of differential equations, some variables change faster than others. If the difference between the time constants of fastest changing and slowest changing variables is too large, the system requires special techniques for numerical integration because the usual techniques

either become unstable or take inordinate number of steps. Such a system is called 'stiff' in Applied Mathematics. Differential equations representing multi-specie, multi-reaction systems are often stiff, and this was found to be the case with the set of equations under consideration. Large differences in the rates of the various reactions are responsible for the stiffness of the system.

A package of FORTRAN subroutines called EPISODE, which was developed at the Lawrence-Livermore Laboratory (Hindmarsh and Byrne, 1975) for integration of stiff and non-stiff systems, has been used in this work. The package is available from the Argonne Code Center, Argonne National Laboratory.

This package is an improved version of a similar package called GEAR (Hindmarsh, 1974), which was based on Gear's method (Gear, 1971). It uses a Variable-Step Variable-Order Backward Differentiation Formula (BDF) method of orders 1 through 5 for integration. This method is considered to have the property of stiff stability. It is an implicit method and requires solution of a system of nonlinear algebraic equations at each step. Variants of Newton's method, called Chord methods, are used for purposes of iteration. For a detailed explanation of the terms and the features, refer to (Gear, 1971, Chapter 11).

The package provides 8 subroutines — DRIVE, INTERP, TSTEP, COSET, ADJUST, PSET, DEC and SOL — and calls for 3 routines — MAIN, DIFFUN and PEDERV — to be supplied by the user. The overall structure of the package is shown in the figure 5.2.1, where a downward sloping line from one box to another indicates that the lower routine is called by the upper one. DRIVE is the driver subroutine for the package and is called by the MAIN calling

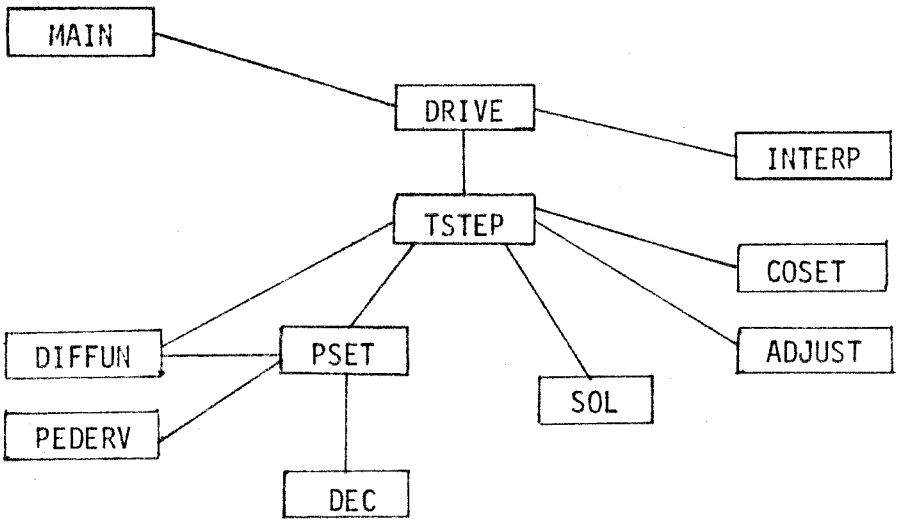

Figure. 5.2.1: Structure of the EPISODE Package
(from Hindmarsh and Byrne, 1975).

program. It also serves as the main means of communication with the package. TSTEP and PSET are the other important routines from our point of view (a detailed understanding of the rest of the routines did not become necessary). TSTEP performs a single step of integration, and controls the local error for that step. PSET sets up a matrix P involving the Jacobian matrix J, where

$$J = \frac{\partial f}{\partial Y}$$

and f is given by the right-hand side of the equations (5.2.3). It then processes P for subsequent solution of algebraic systems as part of the Chord Corrector-Iteration Method. In our case, the functions f are not amenable to analytical differentiation with respect to Y (which, if possible, would have been supplied in the subroutine PEDERV) and hence numerical differentiation had to be used to calculate the matrix J. This was found to be very time consuming, and sometimes failed due to improper choice of the increments in Y for calculating the difference quotients.

The differential equations were set up in the subroutine DIFFUN which essentially contained the entire mathematical model presented in the last chapter. The subroutine first calculated all the distributions and the probability functions; then rates of reactions and rates of loss of clusters and functional groups were computed; finally, the differential equations were formulated.

It is interesting to note that every call to DIFFUN results in a redistribution of functional groups in the structure — as if at each step of integration the structure is disassembled and then put together again. This is a direct consequence of choosing the total concentrations of functional

groups as the state variables. From the point of view of rates of reactions, such repeated distributions will not make any difference because the significant quantity is the total concentration of a bond or a functional group.

3. Simplifications in the Mathematical Scheme

Two simplifications in the mathematics involved in computer calculations are discussed in this section. One involves use of a simpler method to calculate the K's (refer to Chapter IV, section 5), while the other reduces the number of differential equations by assuming pseudo steady-state for the small radicals — $(H\cdot)$, $(CH_3\cdot)$, and $(C_2H_5\cdot)$. Such simplifications facilitate computer calculations in two ways: they eliminate the need for iterative numerical algorithms which often pose convergence problems; and they reduce computation time, thereby allowing more frequent runs.

A scheme was devised in section 5 of the last chapter for calculation of K's — the concentrations of various combinations of functional groups, e.g., K_{DH}, K_{RHG}, K_{GGG}, etc. They were expressed in terms of five unknowns, x(1), x(2), ... x(5), which were to be calculated by solving a set of five nonlinear algebraic equations. Numerical algorithms based on Newton's method or other methods (for better convergence) are available for solution of nonlinear equations. However, in order to ensure their convergence, these algorithms invariably require a good initial guess of the values to be determined. Even then they often fail to converge within a reasonable number of steps. Such convergence difficulties were repeatedly

encountered by the author in using these algorithms in the subroutine DIFFUN. Considering that DIFFUN is called by the integration package EPISODE several times at each step of integration, a simulated run for 30-second pyrolysis uses the nonlinear equations solver literally hundreds of times. It was found that frequently the entire computation was halted because of the failure of the algorithms to calculate the x(i)'s.

To avoid these failures, an alternative scheme to calculate the K's was formulated. It eliminates the need for solving nonlinear equations, although yields very close results.

The alpha carbons (concentration Y_{18}) can be divided into three groups:

(i) Those which carry radicals — since only one radical is allowed per alpha carbon, the concentration of such alpha carbons will be Y_9.

(ii) Those which carry double bonds — only one pair per alpha carbon is allowed — hence their concentration will be $(Y_6 + Y_7)$.

(iii) Those which do not carry radicals or double bonds; their concentration is simply $(Y_{18} - Y_6 - Y_7 - Y_9)$.

Substituents in the groups M_G, M_H and M_P are distributed among these alpha carbons. Each alpha carbon in the first category (Y_9) can take two additional substituents, in the second category $(Y_6 + Y_7)$ one substituent, while three substituents can be allotted to each in the third category. It will now be assumed that distribution of each of the groups M_G, M_H and M_P among the three categories will be proportional to their relative need for additional substituents. For example:

$$\frac{M_G^1}{2N_1} = \frac{M_G^2}{N_2} = \frac{M_G^3}{3N_3} = \frac{M_G}{2N_1 + N_2 + 3N_3}$$

where N_1, N_2 and N_3 are concentrations of the three categories (thus, $N_1 = Y_g$, and so on), and M_G^1, M_G^2 and M_G^3 are the three components of the group M_G. Similarly for M_H and M_P. Then:

$$M_G^1 = \frac{2N_1}{2N_1 + N_2 + 3N_2} M_G$$

$$M_H^1 = \frac{2N_1}{2N_1 + N_2 + 3N_2} M_H$$

and

$$M_P^1 = \frac{2N_1}{2N_1 + N_2 + 3N_2} M_P$$

Hence the original distributional problem can be divided into three parts: distribution of M_G^1, M_H^1 and M_P^1 among N_1, of M_G^2, M_H^2, M_P^2 among N_2, and of M_G^3, M_H^3 and M_P^3 among N_3. These distributions can be accomplished by using the same approach as demonstrated in the last chapter. Calculations are straightforward and do not involve nonlinear equations. The K's calculated are found to be very close to those obtained by solving nonlinear equations. Besides eliminating convergence difficulties, the alternative scheme also results in substantial savings in computation time.

The second simplification introduced reduces the number of differential equations to be integrated. Since the Jacobian matrix $J(= \frac{\partial f_i}{\partial y_j})$ has to be calculated numerically — a procedure that is responsible for a large portion of the computation time — a reduction in the number of equations is very desirable. To this end, psuedo steady-state is assumed for the small radicals ($H\cdot$), ($CH_3\cdot$) and ($C_2H_5\cdot$).

The pseudo steady-state assumption is frequently used in chemical kinetics to express concentrations of highly reactive intermediate species in a chemical system, in terms of concentrations of stable species. It postulates that the intermediate species are at steady-state with respect to the stable species. In other words:

Rate of production of intermediate species by reaction	=	Rate of depletion of intermediate species by reaction

This principle when applied to the small radicals Y_{21}, Y_{22}, Y_{23}, implies:

$$\frac{dY_{21}}{dt} = 0$$

$$\frac{dY_{22}}{dt} = 0$$

$$\frac{dY_{23}}{dt} = 0$$

and they can be calculated in terms of the K's, i.e., indirectly as a function of the other state variables. These steady-state concentrations are used in all rate expressions involving the small radicals. Then we are left with only 20 differential equations.

Similar simplification was attempted for the beta radicals, Y_{12}. However, it could not be implemented due to complexity of the expressions involved, and the fact that the variables Y_2, Y_3 and Y_5 contain concentrations of their respective beta radical structures. The variable Y_{12} was found to exhibit cyclic behavior during integration. This means that it remained low for several steps of integration, then suddenly shot up in the next step, and came down back to its original level in the step after next. Similar behavior of variables in other chemical systems has been reported in the

literature (Field and Noyes, 1974). The numerical integration scheme could not cope with such a behavior and sometimes during the course of integration calculated negative values for Y_{12}. If this occurred, computation came to a halt. After several trials, the difficulty was overcome by assigning a typical value to Y_{12} in case it was calculated to be negative. Considering that beta radical concentrations are generally very small ($\leq 10^{-5}$ moles/liter), their exact values are not very important from the point of view of the final results of integration.

4. Simulation Results and Discussion

Results of computer calculations for pyrolysis of two high volatile C (HVC) bituminous coals are presented and discussed in this section.

There were two reasons for choosing HVC coals for simulation. First, the literature contains a lot of information about coals of this rank. A substantial number of concepts about coal's chemical structure have been formulated on the basis of the results obtained by analyzing bituminous coals and their derivatives. Several structural features included in the chemical model in this work are based on investigations of such coals. In addition, pyrolytic behavior of HVC coals has been reported extensively in the literature. The qualitative trends of such behavior are very well established. Based on these trends, several general inferences can be drawn about the chemical reactions in pyrolysis — a feature that justifies our aim of developing a general model. For example, the competition between tar and gas formation and the effect of temperature on their relative yields can be very easily seen in the pyrolysis results for HVC coals. These coals

are also of interest for use in commercial processes because compared to lower rank coals their carbon content is higher and more hydrocarbons can be recovered from them (lower rank coals have a higher oxygen content and produce large amounts of carbon dioxide which is of little value), while compared to higher rank coals their C/H ratio is lower (which makes them relatively more self-sufficient in hydrogen) and they are more reactive due to a less tight structure.

Secondly, reliable structural data and pyrolysis results were available for the two HVC coals. Extensive experimental work was done by the author with one of the coals (Hamilton, Kentucky #9), while results for the other coal (PSOC-212) were reported in the literature. The author's experiments gave time-resolved results for the Hamilton coal, while the literature reported temperature dependence of the volatile yield for the coal PSOC-212. Such results are very appropriate for comparison with the predictions of the model because it is based primarily on the kinetics of the chemical reactions.

Although not presented here, trial runs were also made for another HVC coal (PSOC-190). The preliminary results indicated that the model will be successful in simulating the experimental data obtained by the author.

Runs with a subbituminous coal (PSOC-241) were also tried. While the predicted qualitative trends agreed closely with experiments performed by the author with this coal, the quantitative agreement was unsatisfactory. Further improvement was limited by the constraint adopted in the model that each cluster carries either 3 or 4 alpha carbon connections. In subbituminous coals, clusters would carry either 2 or 3. It should be noted that this is not a fundamental limitation of the model, which can be modified to deal

with the situation.

Case I: HVC Bituminous Hamilton (Kentucky #9) Coal

We will follow the methodology formulated in section 4 of the last chapter for calculating the initial concentrations of the functional gorups.

Elemental analysis of a dry sample of 60 - 80 mesh particles of this coal gave the following results:

	% Sample
Ash	7.9
Carbon	73.5
Hydrogen	5.1
Nitrogen	1.5
Sulfur	3.3
Oxygen (diff.)	8.7

For the purpose of calculations in this thesis, ash in a coal will be taken to equal its mineral matter content. Then, on a dry mineral matter free (dmmf) basis, the carbon content in this coal is 79.8%.

Referring to figure 4.4.1, the true density (helium density) of this coal will be approximately 1.30 gms/cm^3.

^1H NMR and ^{13}C NMR analyses on extract and pyrolyzate derived from this coal were performed by the author's research group and reported earlier (Gavalas and Oka, 1978). Since yield of extracts was very low (8%), data on pyrolyzates (yield about 20%) are more relevant to the parent coal. In addition, elemental composition of the pyrolzates was

found to be very similar to that of the coal. This is consistent with our concept that low temperature pyrolyzate is very close to the parent coal in chemical structure.

The ^{1}H NMR analysis of the pyrolyzates gave the following distribution of hydrogen:

	% Hydrogen in Pyrolyzates
H_{alpha}	34
H_{beta}	33
$H_{arom. + phenolic}$	33

The hydrogen content of tar is generally found to be slightly higher than that of coal (Solomon, 1977) because clusters in tar carry more sidechains and also the free clusters which constitute tar pick up hydrogen atoms to satisfy their radical sites. Since most radical sites are on alpha carbons, the H_{alpha} content in tar will be higher than in coal. Similarly, H_{beta} in tar will be lower than in coal because sidechains in tar may involve double bonds, while double bonds are absent in coal. On the basis of these two arguments, we make an adjustment and assume the following hydrogen distribution for this coal.

	% Hydrogen in Coal
H_{alpha}	32
H_{beta}	35
$H_{arom. + phenolic}$	33

Although results for ^{13}C NMR analysis on extracts were also reported, they are unreliable. Hence, we have to make an assumption about the

aromaticity (f_a = Aromatic Carbon/Total Carbon) of this coal. In the literature, aromaticity is generally reported as a function of carbon content. However, there is controversy about the values reported, and different techniques yield different results (for example, Vander Hart and Retcotsky, 1976). After examining various sources that discussed aromaticity in coals, it was decided that the appropriate range of f_a for this coal is between 0.65 and 0.70.

$f_a = 0.65 - 0.70$

Figure 5.4.1 presents step by step the method for calculating the initial values for the state variables. A computer code was developed for calculating the initial conditions for different values of the assumed parameters. The structural parameters whose values may have to be assumed are listed in the Table 5.4.1, and their effect on volatile generation indicated. Although aromaticity (f_a) and hydrogen distribution (H_{alpha}, H_{beta}, $H_{arom.}$) have been included in this table, their values may be approximately known. For example, for the Hamilton coal we know the hydrogen distribution (as given earlier), while for the coal PSOC-212 we have an approximate idea about aromaticity. Due to the increasing use of modern spectroscopic techniques in coal research, it is likely that more precise information on these parameters will be available in the future.

Of the remaining three parameters, the last two have a more significant effect on volatile yield (sensitivity of the results to the various parameters of the model will be discussed in detail in section 5). There does not appear to be any à priori guideline for selecting the ratio of methylene to ethylene bridges. If every other parameter is held constant,

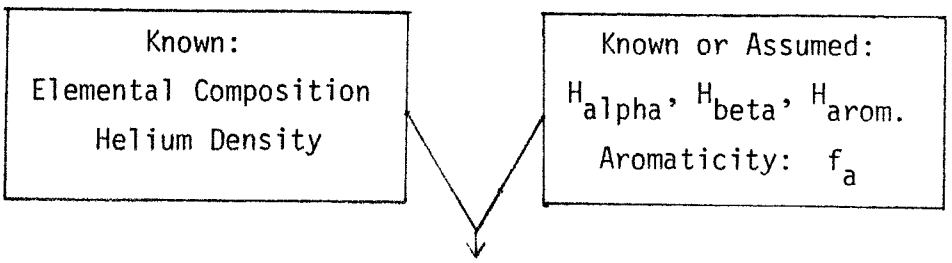

1. Calculate the total concentration of aliphatic carbon.
2. Subtract carbon in carboxyl and carbonyl groups to get concentration of carbon in sidechains and bridges.
3. Calculate concentration of alpha hydrogen Y_1 and beta hydrogen H_b.
4. Using H_b and an assumption about the relative concentrations of methyl, ethyl and hydroaromatic groups, calculate Y_2, Y_3 and Y_5; then calculate C_{beta}.
5. Subtract C_{beta} from the carbon concentration obtained in step 2 to get the concentration of alpha carbons Y_{18}.
6. From Equation (4.4.14) get $(Y_4 + Y_8)$.
7. Assuming the ratio of concentration of methylene to ethylene bridges, calculate Y_4 and Y_8.
8. Assume concentration of clusters Y_{24}.
9. Calculate number of aromatic carbons per cluster, number of peripheral sites per cluster, number of bridges per cluster, number of alpha carbon connections per cluster.

Figure 5.4.1: Calculation of Initial Conditions

Table 5.4.1

Choice of Structural Parameters

PARAMETER	GUIDELINE FOR SELECTION OF A VALUE	EFFECT ON VOLATILE PRODUCTION
fa	1. Graph of fa vs. Carbon Content. 2. ^{13}C NMR analysis of pyrolyzates	Change in amount of tar due to change in Bridge/ Cluster ratio.
H_{alpha}, H_{beta}, $H_{arom.}$	^{1}H NMR, IR Analyses	Change in amount of hydrogen and hydrocarbon gases formed.
Y_2/Y_3, Y_2/Y_5	Pyrolysis Results	Change in relative amounts of CH_4, C_2H_4, and C_2H_6.
$(Y_8 - Y_{18})/(Y_4/2)$ Ratio of Methylene to Ethylene Bridges	—	Change in amount of tar formed; more pronounced effect of temperature on tar formation.
Cluster Concentration Y_{24}	Value should lead to a reasonable size for an average cluster (refer to section 4.4 for the parameters s_1 and s_2).	Change in amount of tar formed.

the sum ($Y_4 + Y_8$) will be fixed, and higher values of this ratio will imply :

(a) More bridges per cluster.

(b) More bridges of higher dissociation energy (methylene bridges have a dissociation energy of 70 kcal/mole, while ethylene bridges have about 50 kcal/mole).

These two changes are responsible for the effect on the volatile production indicated in Table 5.4.1. Although the size of an average cluster limits the values that can be assigned to the cluster concentration Y_{24} (section 4.4), it is chosen after several trials because pyrolysis results are very sensitive to its value.

The computer program for calculating the initial concentrations was fed with the following information on Hamilton coal:

1. Elemental Composition as listed before.
2. Density as listed before.
3. Concentration of carbon in carboxyl and carbonyl groups:
   Pyrolysis experiments at $510^{o}C$ with this coal yielded about 0.5 gms of CO_2 and 0.24 gm of CO per 100 gm sample of dry coal. This corresponds to a carboxylic concentration of 0.15 moles/liter and a carbonyl concentration of 0.12 moles/liter. Hence, the concentration of carbon in these two groups equals 0.27 moles/liter.
4. Distribution of hydrogen as listed before.
5. Ratios Y_3/Y_2 and Y_5/Y_2:
   Y_3/Y_2 is assumed to be 0.3846 on the basis of the molar ratio

of C_2H_6 to CH_4 produced in the experiment. Similarly, Y_5/Y_2 is assumed to be 0.1111 on the basis of the molar ratio of C_2H_4 to CH_4.

The program calculated the various concentrations as a function of aromaticity fa ranging from 0.65 to 0.71 at intervals of 0.01. The results are presented in the Table 5.4.2. Obviously, Y_1, Y_2, Y_3 and Y_5 remain unchanged because their values depend on the hydrogen distribution (which was maintained constant) rather than on aromaticity. The last three columns need further discussion.

Let us consider three cases: fa = 0.67, 0.68 and 0.69. We will assume the methylene to ethylene bridge ratio to be 0.25 for each case.

<u>fa = 0.67</u>

Since $(Y_8 - Y_{18})/(Y_4/2) = 0.25$

$\therefore \quad Y_8 - Y_{18} = 0.125\ Y_4$

But, $Y_4 + Y_8 - Y_{18} = 24.616$

Thus, $Y_4 = 24.616/1.125 = 21.881$ moles/liter

and $Y_8 - Y_{18} = 2.733$

Since $Y_{18} = 17.526$ moles/liter

we get $Y_8 = 20.261$ moles/liter

and Total Concentration of Bridges $= Y_4/2 + Y_8 - Y_{18}$

$= 10.9405 + 2.735 = 13.6755$ moles/liter

Now let us compute the concentration of peripheral sites using the equation given in section 4.4. We first need to calculate the concentration of phenolic groups Y_{10}. Unfortunately, in ^1H NMR analysis one cannot differentiate between aromatic and phenolic hydrogen. Hence we use the

Table 5.4.2

Initial Concentrations* as a Function of Aromaticity

(Hamilton Coal)

fa	Y_1	Y_2	Y_3	Y_5	Y_{18}	$Y_4 + Y_8 - Y_{18}$	Aromatic Carbon
0.65	21.216	4.510	1.735	0.501	19.118	29.394	51.756
0.66	21.216	4.510	1.735	0.501	18.322	27.005	52.552
0.67	21.216	4.510	1.735	0.501	17.526	24.616	53.349
0.68	21.216	4.510	1.735	0.501	16.730	22.228	54.145
0.69	21.216	4.510	1.735	0.501	15.934	19.839	54.941
0.70	21.216	4.510	1.735	0.501	15.137	17.450	55.737
0.71	21.216	4.510	1.735	0.501	14.341	15.061	56.534

*All concentrations in moles/liter.

amount of water formed experimentally for calculating the phenolic concentration. Again, pyrolysis of a dry sample at 510°C produced 2 gms of water per 100 gm sample. Assuming that all of it was formed by phenolic condensation, and noting that 1 mole of water is produced from 2 moles of phenolic groups, we get the (-OH) concentration to be 2.888 moles/liter. Since some phenolic groups will be lost with the free clusters, we assume

Y_{10} = 3.0 moles/liter

Then we get

Sites = 42.41 moles/liter.

In brief then,

Y_4 = 21.881 moles/liter

Y_8 = 20.261 moles/liter

Bridges = 13.67555 moles/liter

$C_{aromatic}$ = 53.349 moles/liter

Sites = 42.410 moles/liter

We can assume a maximum cluster concentration of 5.3349 moles/liter. This is because an average cluster in HVC coals is expected to consist of more than 2 rings, i.e., it will have at the minimum 10 aromatic carbons and 8 peripheral sites. Lower cluster concentrations would satisfy this criterion but will increase the bridge to cluster ratio which will make the structure tight. The minimum concentration that can be assumed for the present model is 5.06525 moles/liter because the number of alpha carbon connections per cluster cannot exceed 4. If we assume a value of 5.33 moles/liter,

Bridges/Clusters = 2.5657

Y_8/Clusters = 3.80

Aromatic Carbon/Clusters = 10.009

Sites/Clusters = 7.9568

The number of sites per cluster is less than 8. We cannot expect to satisfy this constraint very well because we have not accounted for the functional groups of nitrogen and sulfur and for the entire oxygen content of this coal (phenolic, carboxyl and carbonyl groups put together account for only 3.42 moles/liter of oxygen while the total oxygen concentration is 7.068 moles/liter). Hence we will try to meet the criterion whenever possible, but will accept values of sites/cluster less than but close to 8, especially when trying to match the experimental results for tar production.

fa = 0.68

Following the method presented in the previous case,

Y_4 = 19.758 moles/liter

Y_8 = 19.2 moles/liter

Bridges = 12.349 moles/liter

$C_{arom.}$ = 54.145 moles/liter

Sites = 41.349 moles/liter

Assuming a cluster concentration of 5.2 moles/liter,

Bridges/Clusters = 2.3748

Y_8/Clusters = 3.69

Aromatic Carbon/Clusters = 10.4125

Sites/Clusters = 7.9517

fa = 0.69

In this case we get

Y_4 = 17.635 moles/liter

Y_8 = 18.138 moles/liter

Bridges = 11.022 moles/liter

$C_{arom.}$ = 54.941 moles/liter

Sites = 40.286 moles/liter

We assume a cluster concentration of 5.1 moles/liter,

Bridges/Clusters = 2.161

Y_8/Clusters = 3.556

Aromatic Carbon/Clusters = 10.772

Sites/Clusters = 7.9

Computer runs were made with all three sets and the last set (fa = 0.69) gave results which were in the best agreement with the experimental results. Hence, it was adopted as the base case for simulation. For quick reference, values for all 20 state variables are listed in the Table 5.4.3.

Double bonds (Y_6 and Y_7) are assumed initially absent in coal. Ether bonds (Y_{11}) are also assumed absent. They will be formed during reaction by phenolic condensation. The literature on coal structure supports the assumption of negligible concentration of purely etheric linkages in medium rank coals. Blom et al. (1957) have reported small concentrations of methoxy linkages.

Simulation Results: Using the initial conditions listed in the Table 5.4.3 and the kinetic parameters listed in Appendix II, simulation runs at 510 ^{o}and 600^{o}C were made. The value used for the parameter x was 0.15. As discussed in the last two chapters, this value can be considered as the

Table 5.4.3

Initial Values of the State Variables in the Hamilton Coal

Y_1 =	21.216 moles/liter	Y_{11} =	0.000 moles/liter
Y_2 =	4.510 moles/liter	Y_{12} =	0.000 moles/liter
Y_3 =	1.735 moles/liter	Y_{13} =	0.000 moles
Y_4 =	17.635 moles/liter	Y_{14} =	0.000 moles
Y_5 =	0.501 moles/liter	Y_{15} =	0.000 moles
Y_6 =	0.000 moles/liter	Y_{16} =	0.000 moles
Y_7 =	0.000 moles/liter	Y_{17} =	0.000 moles
Y_8 =	18.138 moles/liter	Y_{18} =	15.934 moles/liter
Y_9 =	0.000 moles/liter	Y_{19} =	0.077 liters
Y_{10} =	3.000 moles/liter	Y_{20} =	0.000 moles

fraction of the subunit volume in the surface region, i.e., near the pores (refer to figure 3.4.1). It is in this region only that dissociation of bridges can lead to production of free clusters. In the interior region (85% of the subunit volume) transport limitations (and consequently higher probability of recombination) do not allow release of free clusters. Hence, x is used to reduce the rate of free cluster formation. This is a simple way of simulating the real situation of random recombination of free clusters with the coal matrix. The value used for x (0.15) is based on a similar concept employed by Cheong (1976) in his model. However, he had considered the two regions as separate chemical systems each with its own state variables. The asymptotic weight loss (or tar) is not affected significantly by a moderate change in the value of x (refer to section 5). It is affected more by the structural parameters. However, the rate of weight loss in the first few seconds of pyrolysis depends more significantly on the value of x.

The predictions of the simulations are presented in the figures 5.4.2, 5.4.3, 5.4.4, 5.4.5 and 5.4.6. Figures 5.4.7, 5.4.8, 5.4.9, 5.4.10 and 5.4.11 show variation of some functional groups in the chemical system; they will help in understanding the model predictions. The shape and the smoothness of the curves in these figures is characteristic of kinetic models.

We will discuss the curves in terms of the time and temperature dependence of the yield of the volatiles.

Consider the time variation at $510^{o}C$ of weight loss and tar (figure 5.4.2), hydrocarbon gases CH_4, C_2H_4 and C_2H_6 (figure 5.4.3), and hydrogen and water vapor (figure 5.4.4). They are typical of experimental results

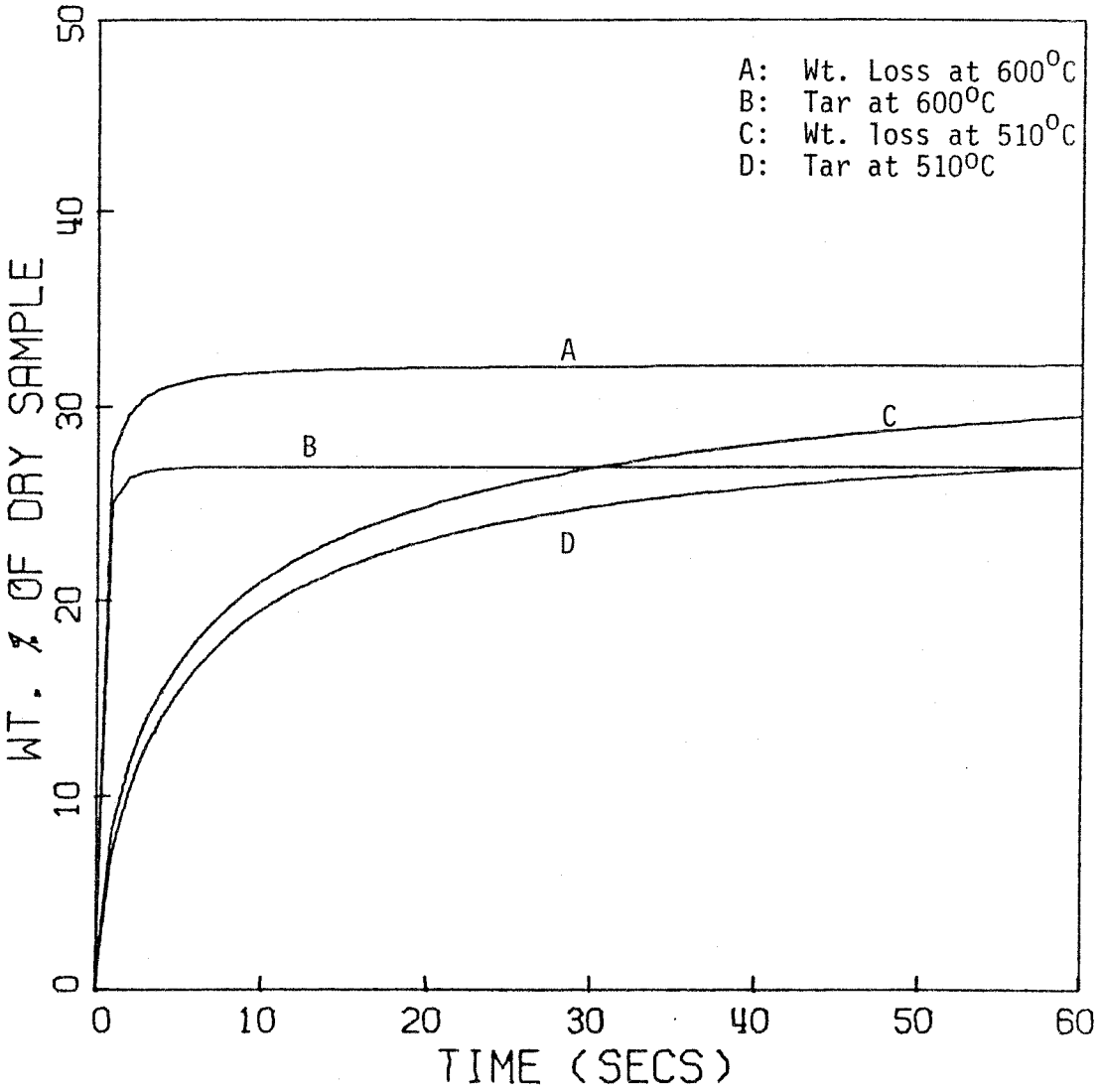

Figure 5.4.2: Variation of Weight Loss and Tar with Pyrolysis Time.

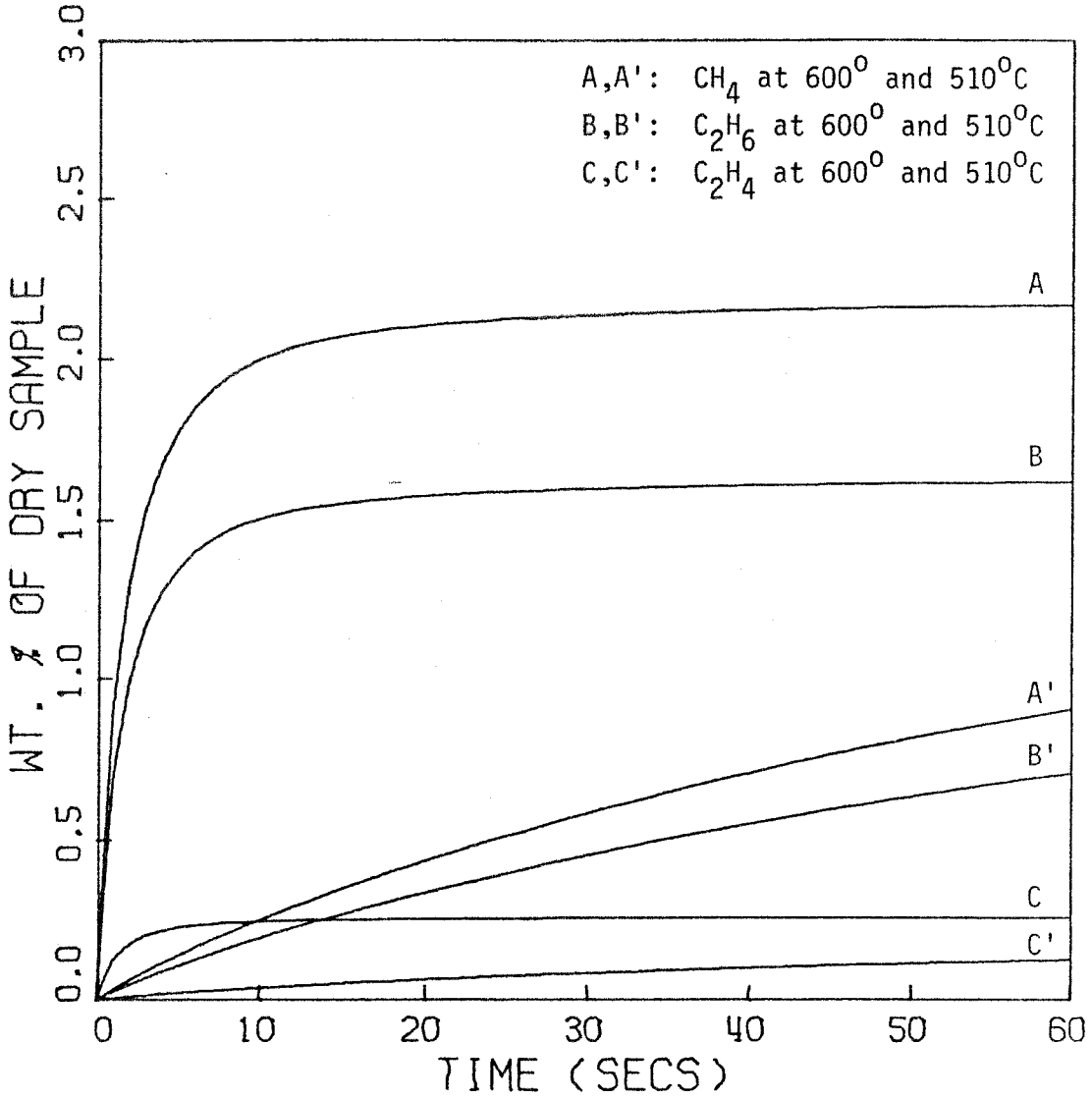

Figure 5.4.3: Variation of Hydrocarbon Gases with Time.

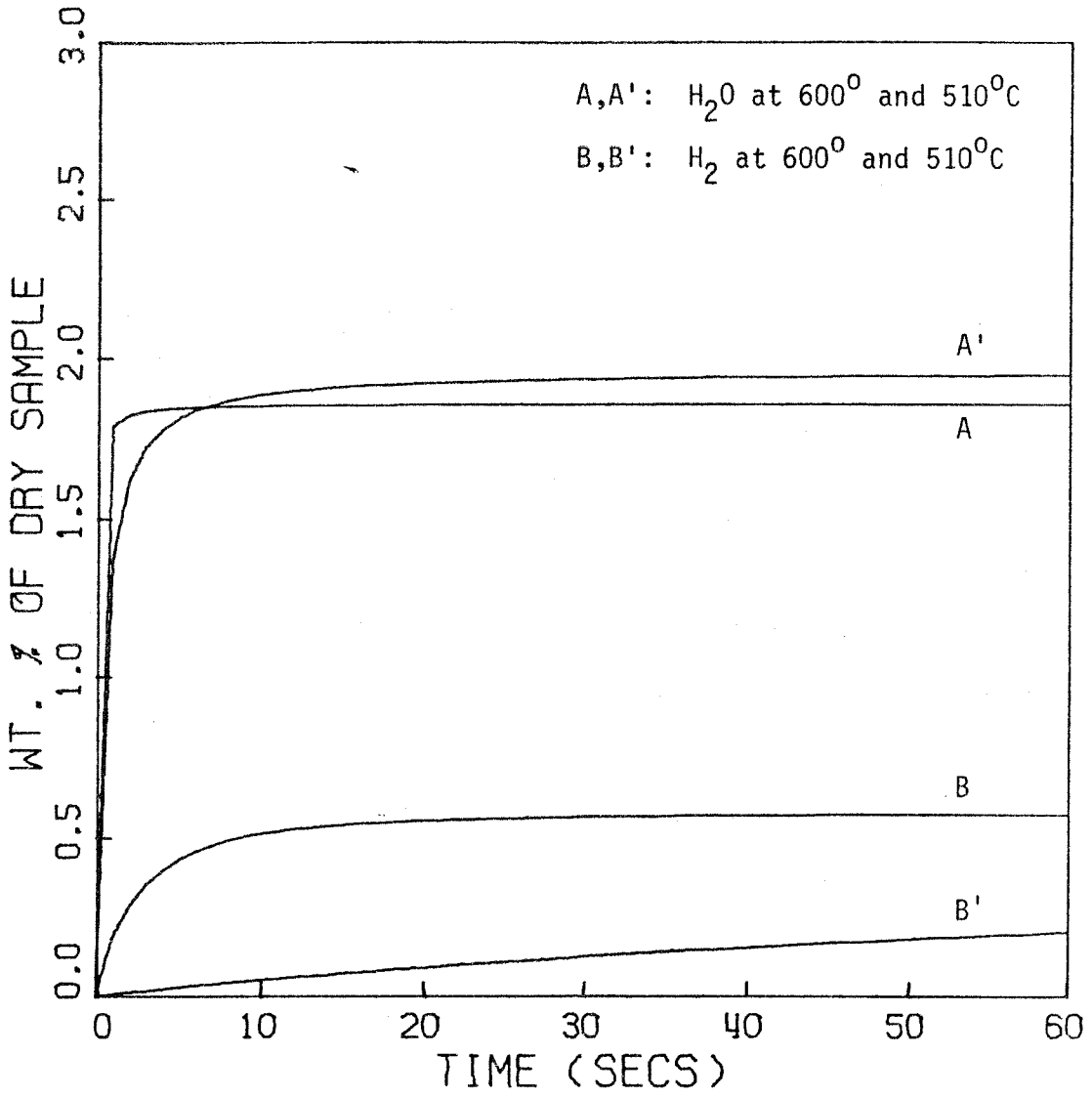

Figure 5.4.4: Variation of Water Vapor and Hydrogen with Time.

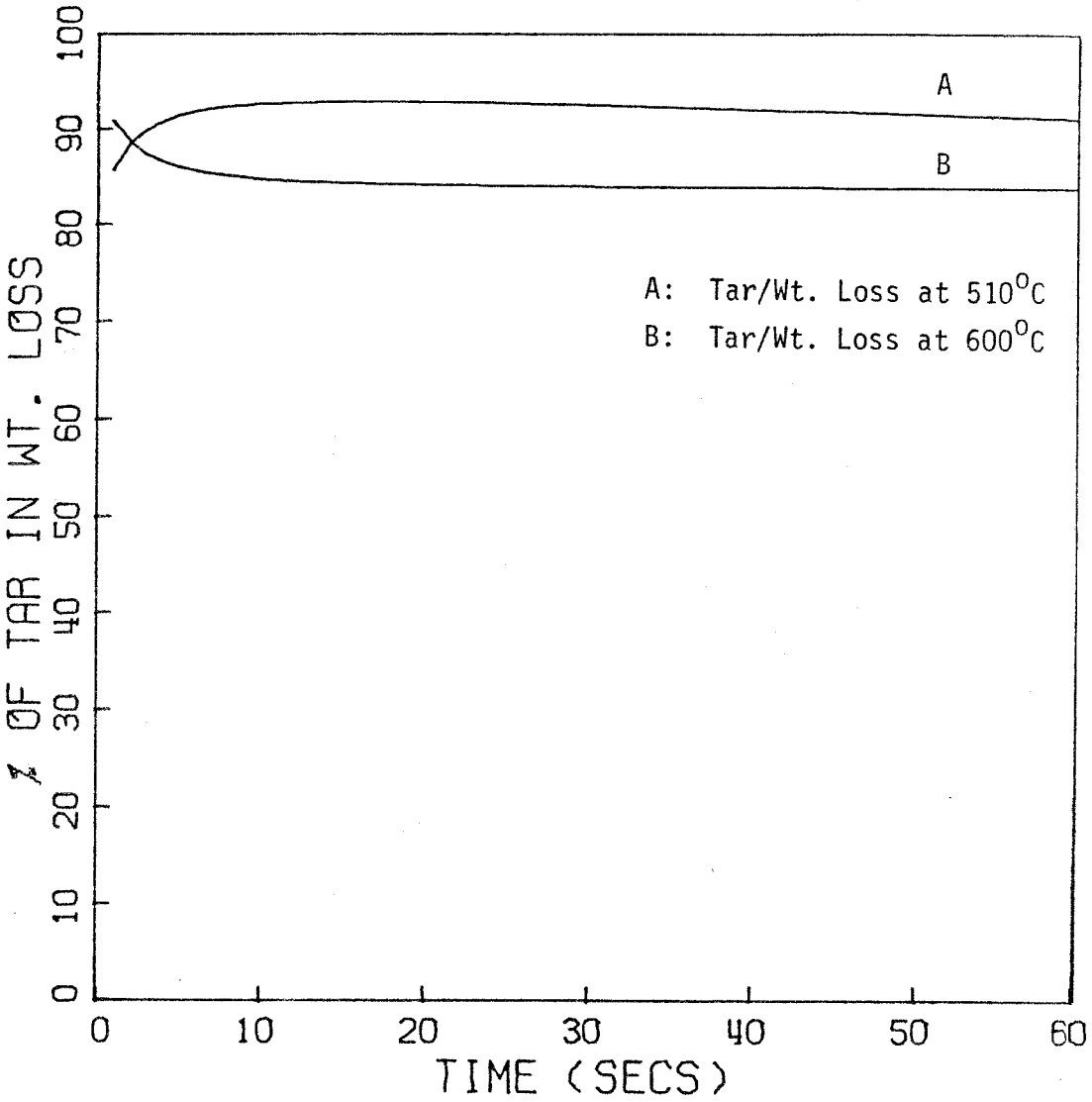

Figure 5.4.5: Variation of Tar/Wt. Loss (Tar Selectivity) with Time.

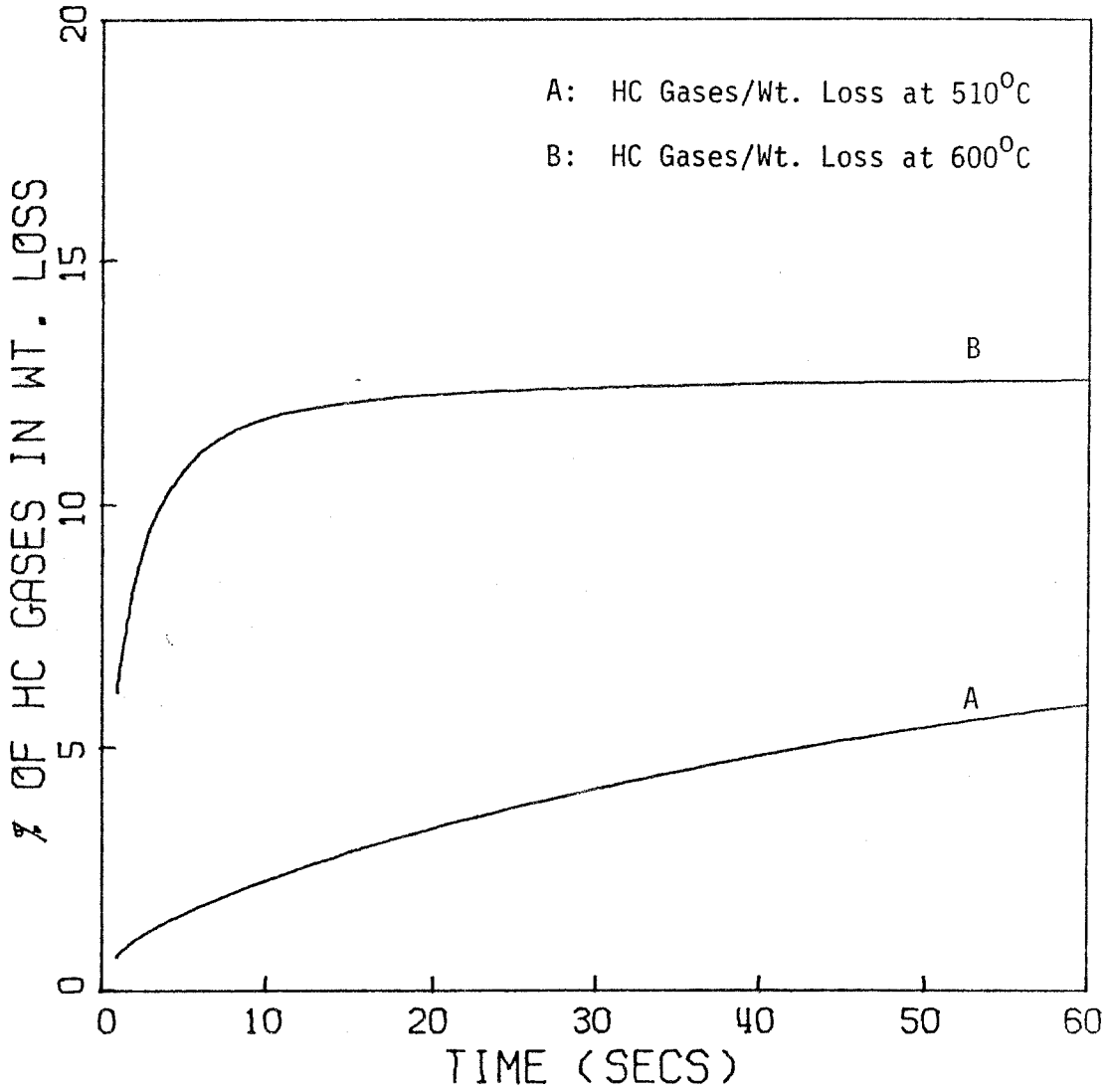

Figure 5.4.6: Variation of (CH_4 + C_2H_4 + C_2H_6)/Wt. Loss (Gas Selectivity) with Time.

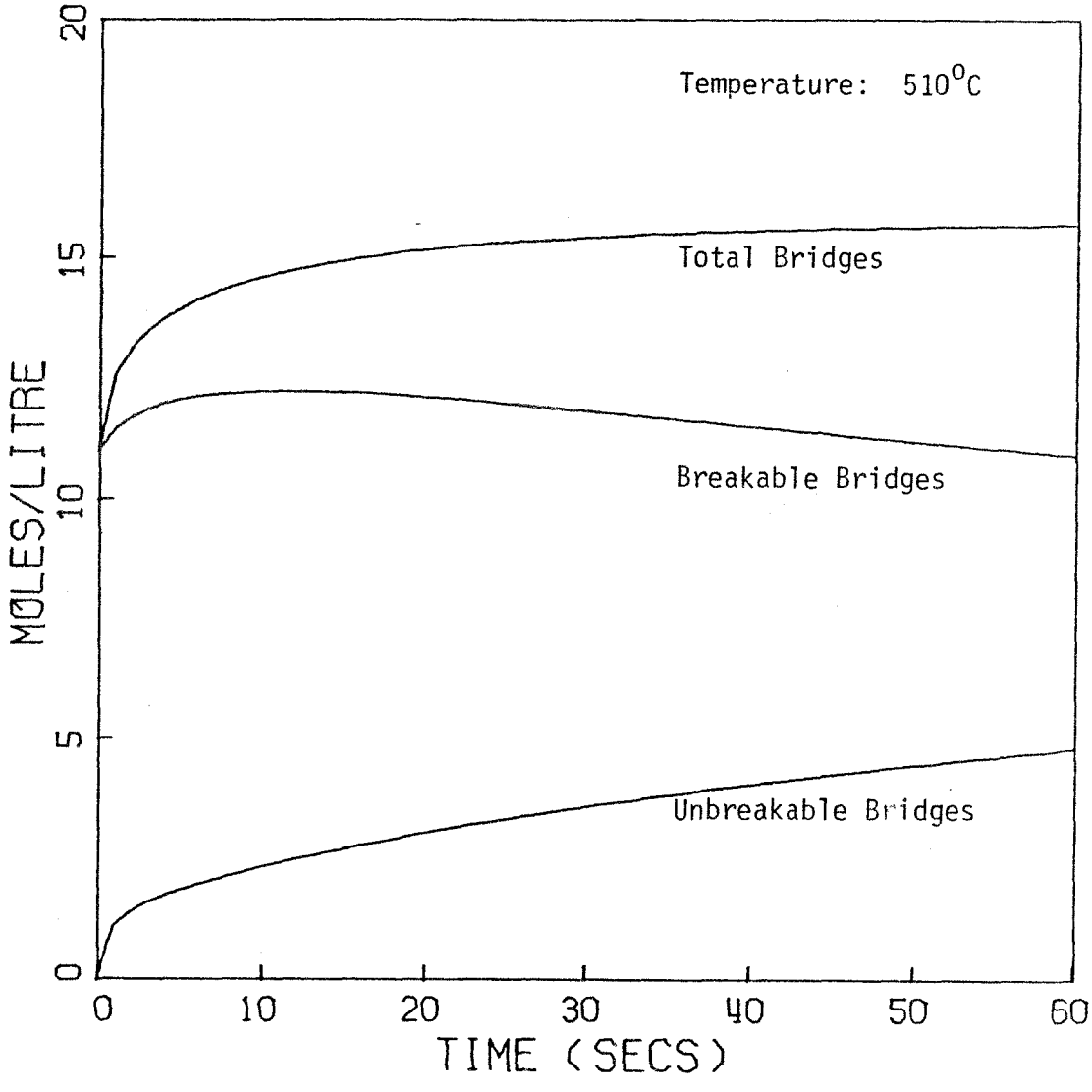

Figure 5.4.7: Variation of Bridges with Time at 510°C.

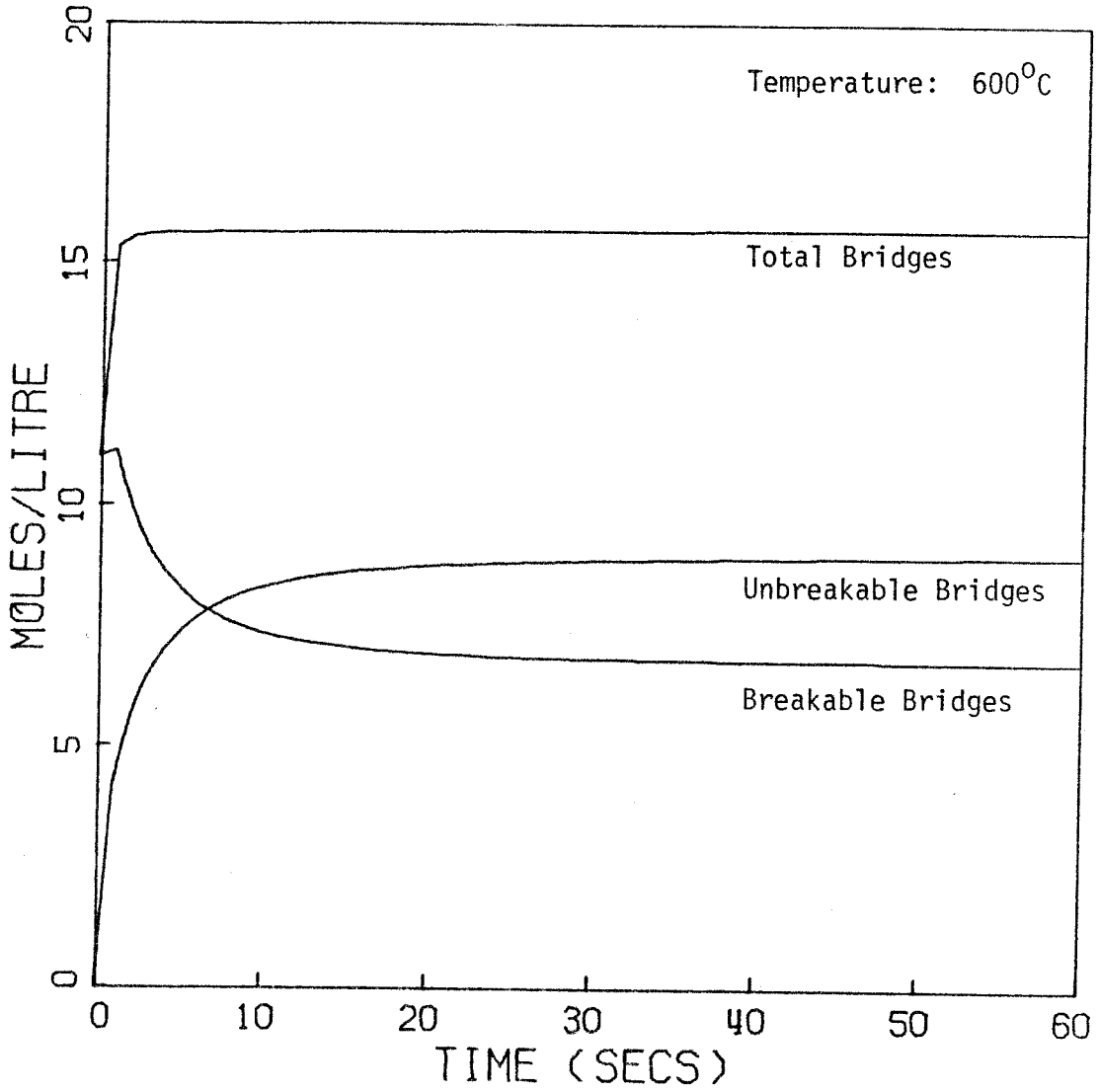

Figure 5.4.8: Variation of Bridges with Time at 600°C.

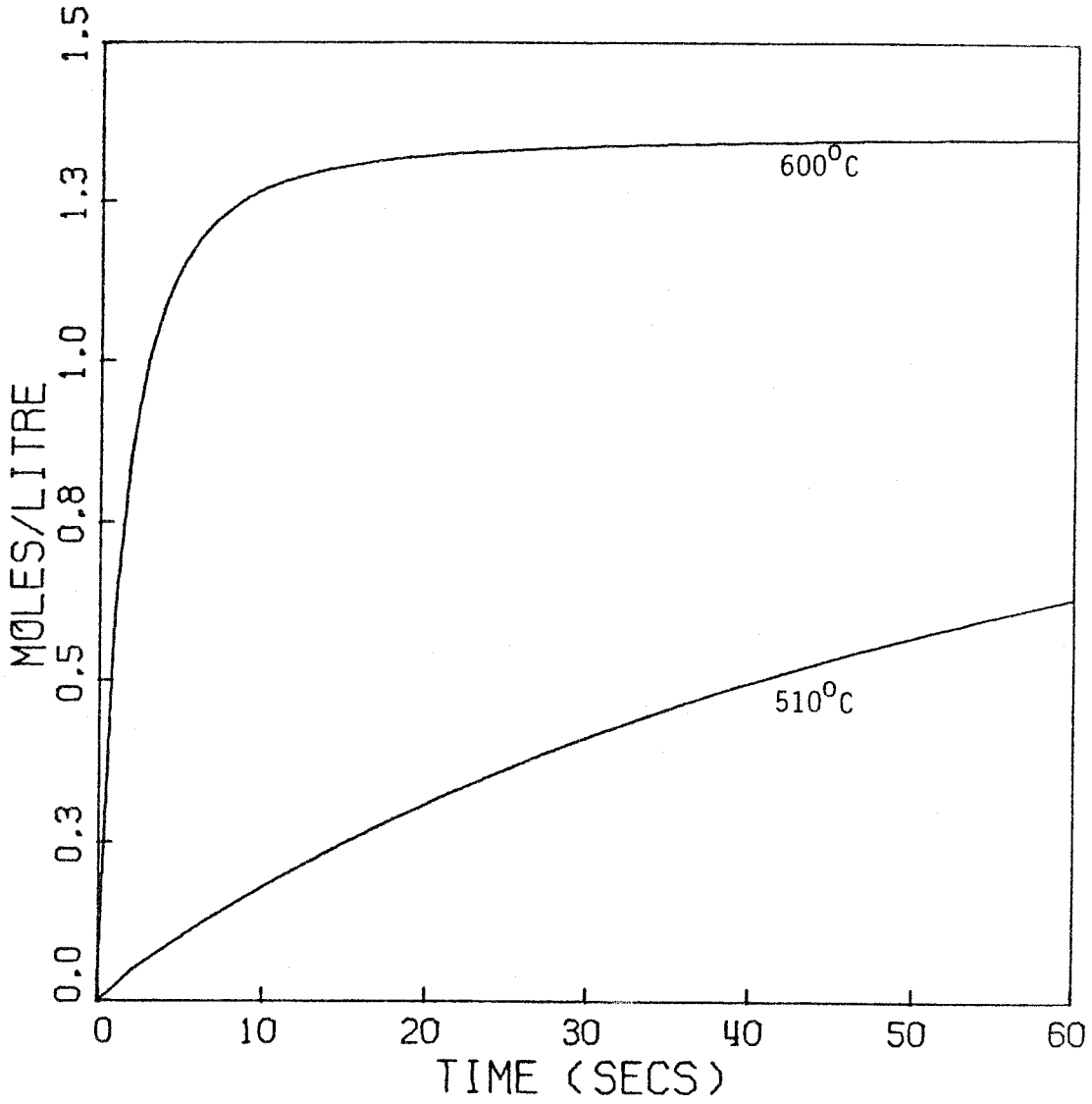

Figure 5.4.9: Variation of Sidechain Double Bonds with Time.

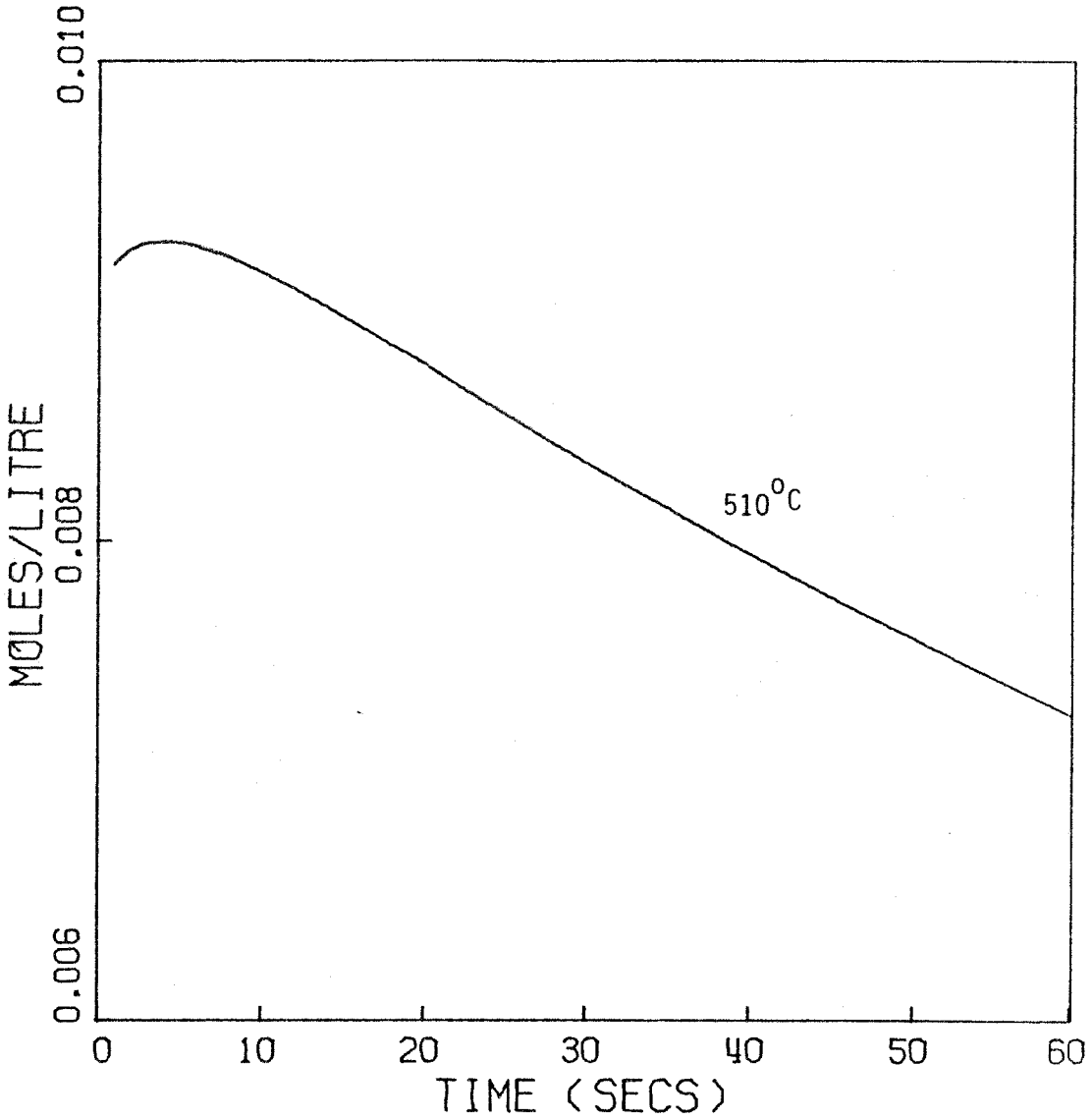

Figure 5.4.10: Variation of Alpha Radicals with Time at 510°C.

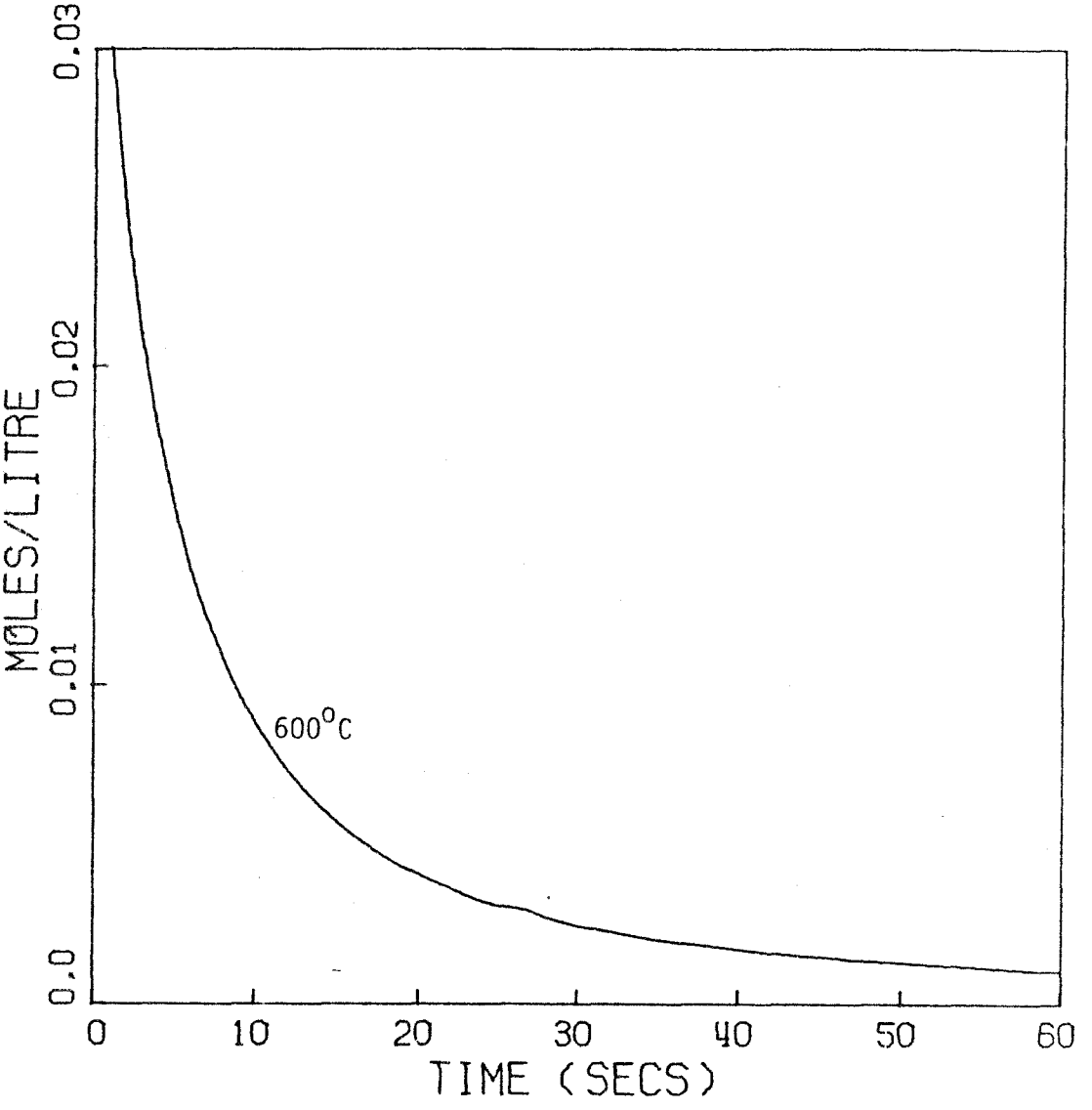

Figure 5.4.11: Variation of Alpha Radicals with Time at 600°C.

of pyrolysis of coal. The rate of increase in the total weight loss and the amount of tar is highest at the beginning and slows down as pyrolysis progresses. Eventually they both attain different asymptotic values, although weight loss does so later than tar does. On the other hand, the rate of production of hydrocarbon gases and hydrogen shows little change with time. The amounts of these gases keep increasing almost linearly and do not show an asymptotic behavior even after one minute of reaction. This difference between the behavior of tar production and gas production is responsible for the increasing gap between the tar and the weight loss curves in the figure 5.4.2. Most of the water vapor is produced during the first few seconds of reaction, and thereafter it quickly reaches an asymptotic value. Tar is the major component of the volatiles, followed by water vapor, methane, ethane, hydrogen and ethylene.

The above results can be explained from a mechanistic viewpoint as follows. The rate of production of free clusters which constitute tar depends on two factors: rate of dissociation of bridges, and the probability of a cluster becoming free following the dissociation of a bridge. As is seen in figure 5.4.7, the concentration of breakable bridges (methylene + ethylene) quickly reaches a maximum and thereafter decreases steadily, while the concentration of unbreakable bridges (double bond and ether) increases almost linearly after an initial rapid rise. In fact, the concentration of 'breakable' bridges will be less than that shown because some bridges will co-exist with double bonds and radicals on the same alpha carbon and hence will not break. Thus, the rate of bridge dissociation will go down with increasing time due to lower concentrations of breakable bridges, and the probability of a cluster becoming free will be reduced

because more and more clusters will be tied to the coal matrix by permanent bridges. This explains the reduction in formation of tar.

The small radicals which lead to formation of hydrogen and hydrocarbon gases are formed by two mechanisms: either by direct dissociation of sidechains as in reactions 1, 2, 3 and 5 (in Table 4.6.1), or by indirect elimination during double bond formation as in reactions 10, 11, 12 and 14. The overall activation energy for gas formation is higher than for tar formation. Hence, initially production of gases lags behind that of tar. Sidechains are lost with the departing free clusters. As reaction progresses, production of tar slows down due to the earlier mentioned reasons. Production of gases also is reduced due to the presence of double bonds (which hinder both direct and indirect formation of small radicals) but only slightly. The presence of alpha radicals in the system has only negative effects on tar formation. They, however, have both negative and positive effects on gas formation; the former on direct dissociation and the latter on indirect elimination. Thus, formation of gases continues for a longer time than formation of tar, although eventually all volatile formation would halt due to very high concentrations of double bonds in the structure.

The behavior of tar to weight loss ratio and hydrocarbon gases to weight loss ratio (figures 5.4.5 and 5.4.6) more clearly shows the shift of selectivity in favor of the gases with increasing time. The tar-to-weight loss ratio initially appears to rise because we include water vapor in the gases. If water vapor is excluded from weight loss, the tar-to-weight loss ratio will be highest at the beginning and will decrease monotonically. The gas-to-weight loss ratio increases monotonically.

These trends are consistent with experimental results.

At 600°C, most of the volatile production takes place in the first few seconds. Tar attains a constant value in just two seconds, while at 510°C it begins to level only after about 58 seconds. The asymptotic value of tar at 600°C is slightly higher than at 510°C. Experimental results on pyrolysis reported in the literature (e.g., Solomon and Colket, 1978) show that tar evolution becomes appreciable at 450°C and attains a maximum around 650°C. It does not increase with temperature beyond 650°C. In fact, if pyrolysis is carried out for a long time — about 60 seconds or more — tar does not increase with temperature beyond 500°C. This behavior is very clearly seen in 80 seconds pyrolysis of PSOC-212 (figure 5.4.12) reported by Solomon (1977). The model predictions seem to be in excellent agreement with this behavior.

The leveling in the temperature dependence of tar implies an inherent structural limitation on production of free clusters. The model provides an explanation for this limitation in terms of the concentrations of the bridges, as seen in figure 5.4.8. The unbreakable bridges rise rapidly, the breakable bridges fall rapidly, and the total bridges quickly attain a high value and thereafter rise very slowly. After just one second, the bridge-to-cluster ratio is approximately 3, compared to its initial value of 2.161. Compared to the rate at 510°C, at 600°C the structure becomes 'tight' very rapidly. Hence, temperature affects the rate of tar formation rather than its ultimate amount. The ultimate amount depends solely on the structural tightness.

The change in the behavior of the hydrocarbon gases is also very interesting. Unlike at 510°C, at 600°C these gases show approximately

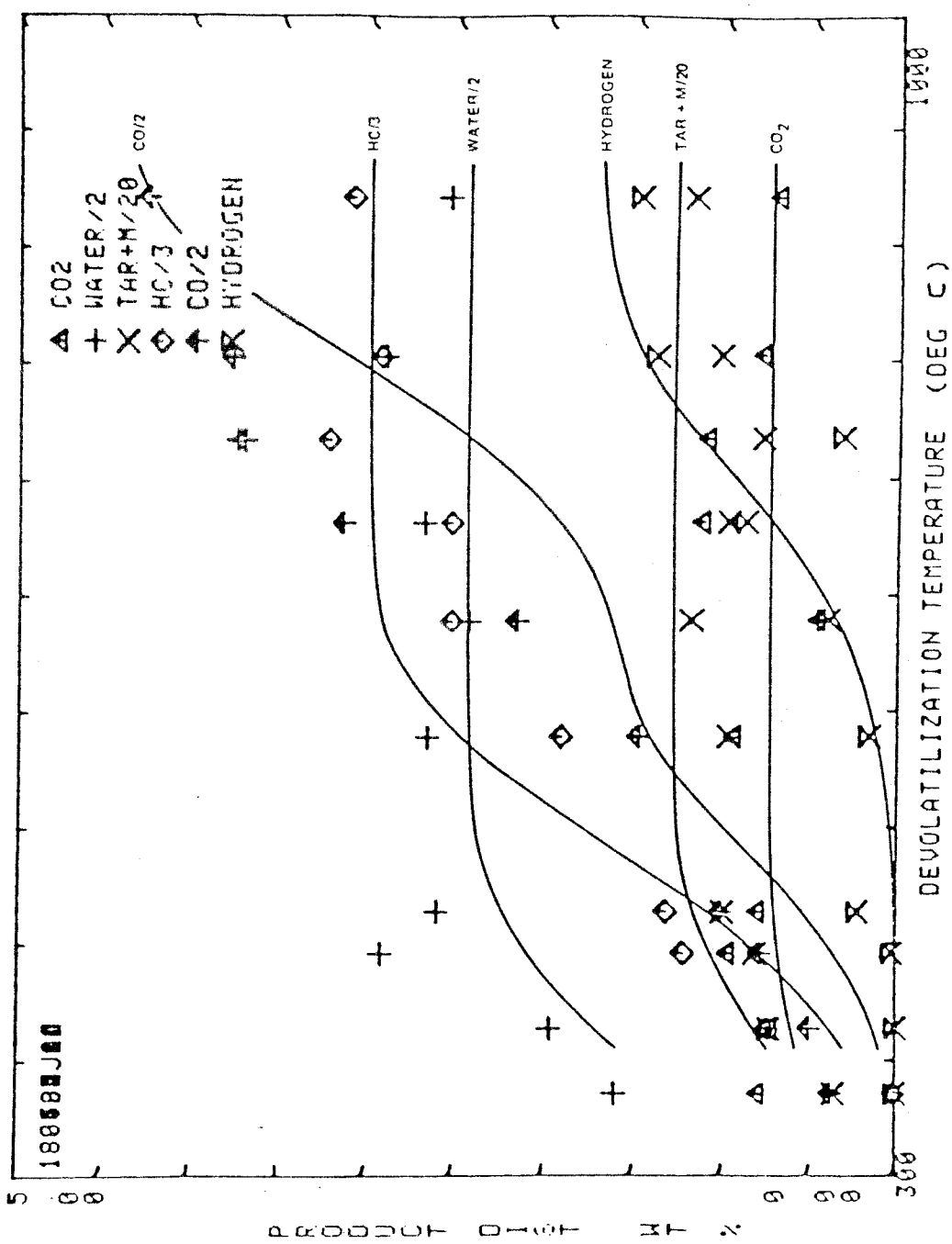

Figure 5.4.12: Temperature Dependence of Pyrolysis Results for Coal PSOC-212 (from Solomon, 1977).

asymptotic behavior. However, they begin to level 10 seconds after tar levels — in fact, the alkanes keep rising slowly but steadily. The behavior of hydrogen is also very similar. The rapid rise in the double bonds in the sidechains (figure 5.4.9), together with the fast increase in double bond bridges, makes any sidechain dissociation or elimination very unlikely. At 10 seconds ($600^{o}C$) the total double bond concentration in the system is 14.23 moles/liter, while the alpha carbon concentration is 15.73 moles/liter. Hence, only 9.5% of the alpha carbons can be expected to be free of double bonds. In addition, the rapid decline in the concentration of alpha radicals at 600^{o} (figure 5.4.11) will reduce the rates of formation of small radicals by elimination reactions 10, 11 and 12. All these factors will result in a gradual decline of gas production.

Although the temperature dependence of the ultimate amount of gases produced is not very clear from the curves presented (simulation runs at higher temperatures were found to pose numerical difficulties in integration), it can be deduced by analogy with tar. At higher temperatures the gases will attain the asymptotic values faster but the ultimate value will not change beyond some temperature (except for CO and H_2 which may rise after $700^{o}C$). This is because, just like in tar, the ultimate amount produced depends critically only on the structural limitations, like the concentration of double bonds. The temperature beyond which the asymptotic value of gases will not increase will be higher than the temperature beyond which the asymptotic value of tar does not increase ($500 - 550^{o}C$). This is also the case for the experimental results with other coals (e.g. PSOC-212 in the figure 5.4.12).

It is interesting to note that the amount of water formed at $600^{o}C$

is slightly less than at 510°C. This is due to an increased rate of loss of phenolic groups due to an increase in the formation of free clusters. The corresponding decrease in the concentration of ether linkages may be responsible for the slight increase in the asymptotic value of tar at 600°C.

Figures 5.4.5 and 5.4.6 show that selecivity of tar production goes down with temperature while that of gases increases. This shift in selectivity is a direct result of the difference in activation energies of gas and tar forming reactions — the former being higher than the latter. As discussed in Chapter 3, the chemical system in the model consists of several series-parallel reactions. There is competition between sets of reactions leading to different products. If we assign E_1 and E_2 to be the

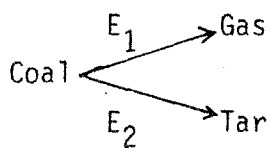

overall activation energies of gas and tar formation, respectively, then as E_1 is higher than E_2, at lower temperatures tar will be the preferred product. At higher temperatures the selectivity will shift in favor of the gases because the increase in temperature has a more significant effect on the reaction with the higher activation energy.

Predictions vs. Experimental Results: Comparison of model predictions with experimental results for vacuum pyrolysis of this coal at 510°C is presented in the figures 5.4.13, 5.4.14, 5.4.15, 5.4.16 and 5.4.17. The experimental data were obtained by repeating the experiments for different durations using the setup described in Chapter 6. Results

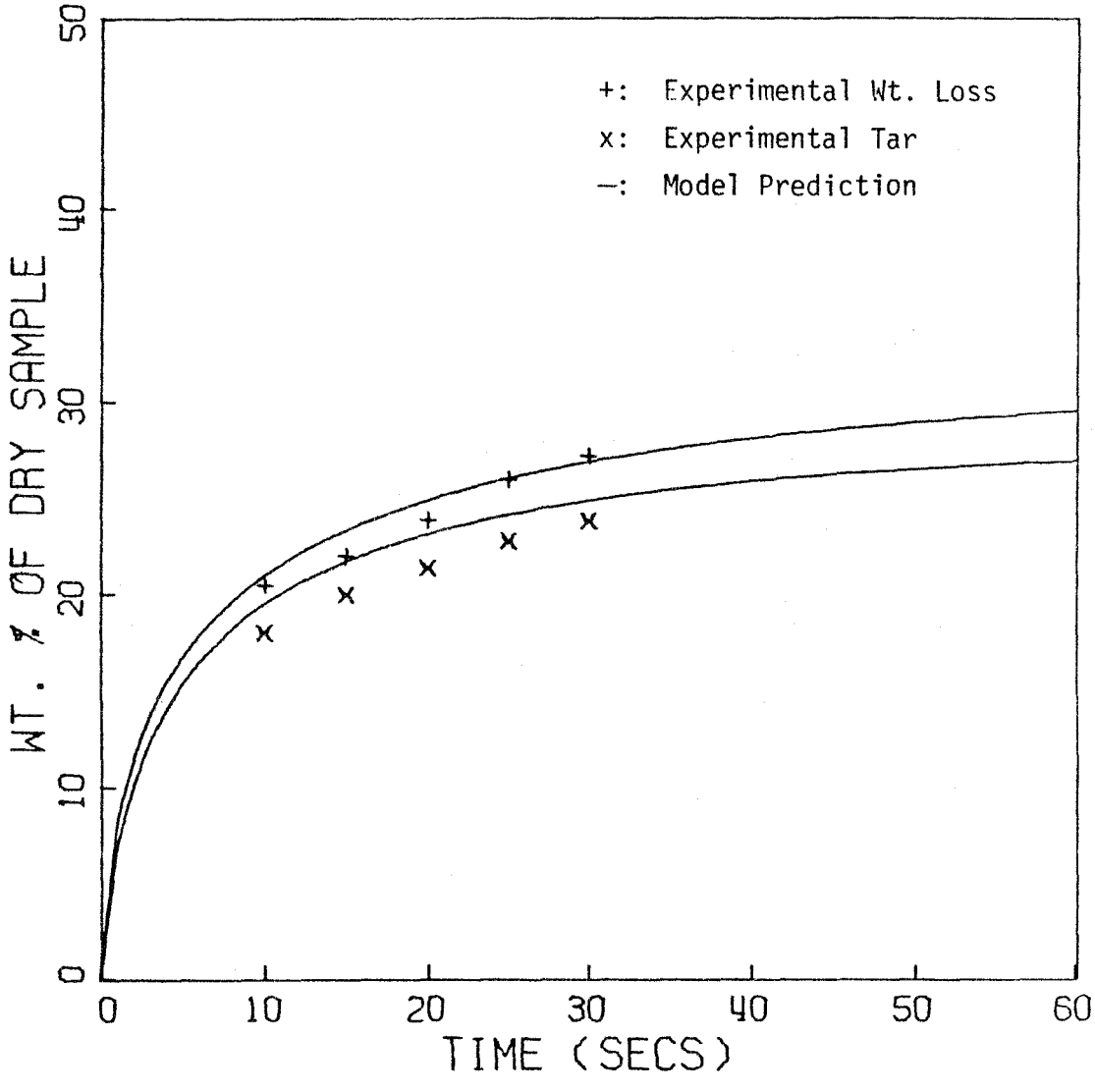

Figure 5.4.13: Comparison of Predicted Wt. Loss and Tar with Experimental Results at 510^{o}C.

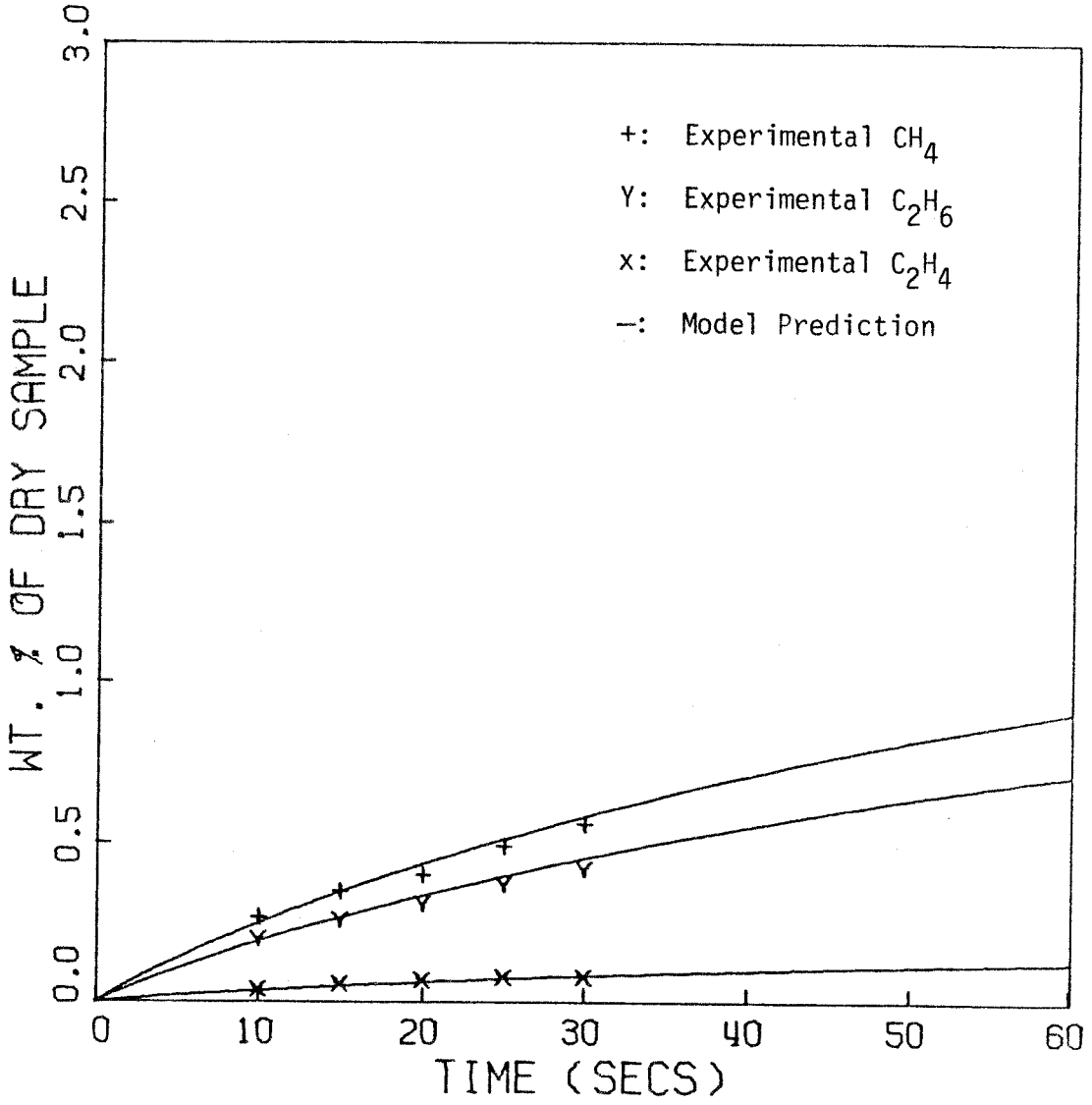

Figure 5.4.14: Comparison of Predicted HC Gases with Experimental Results at 510°C.

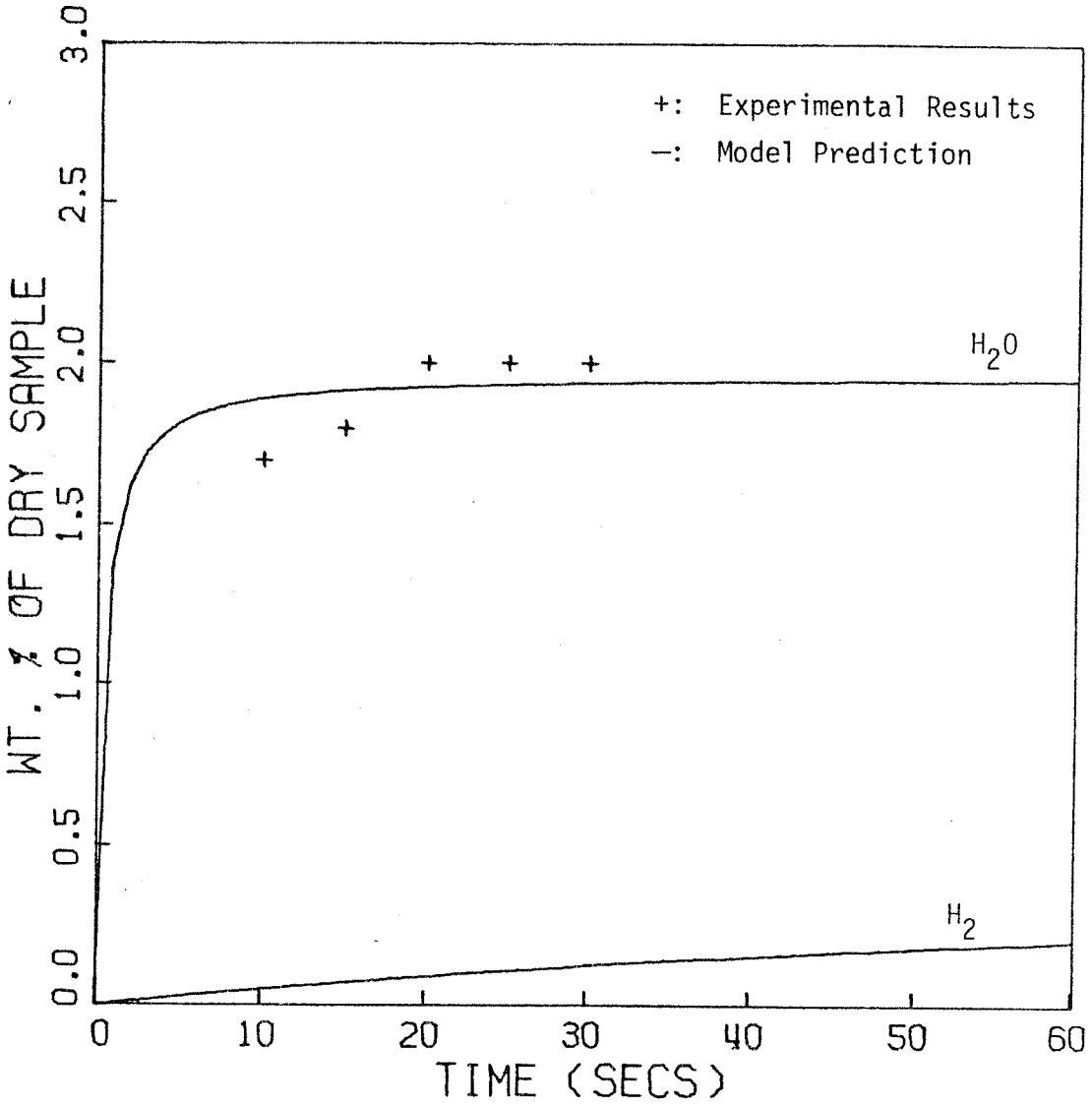

Figure 5.4.15: Comparison of Predicted Water Vapor with Experimental Results at 510°C.

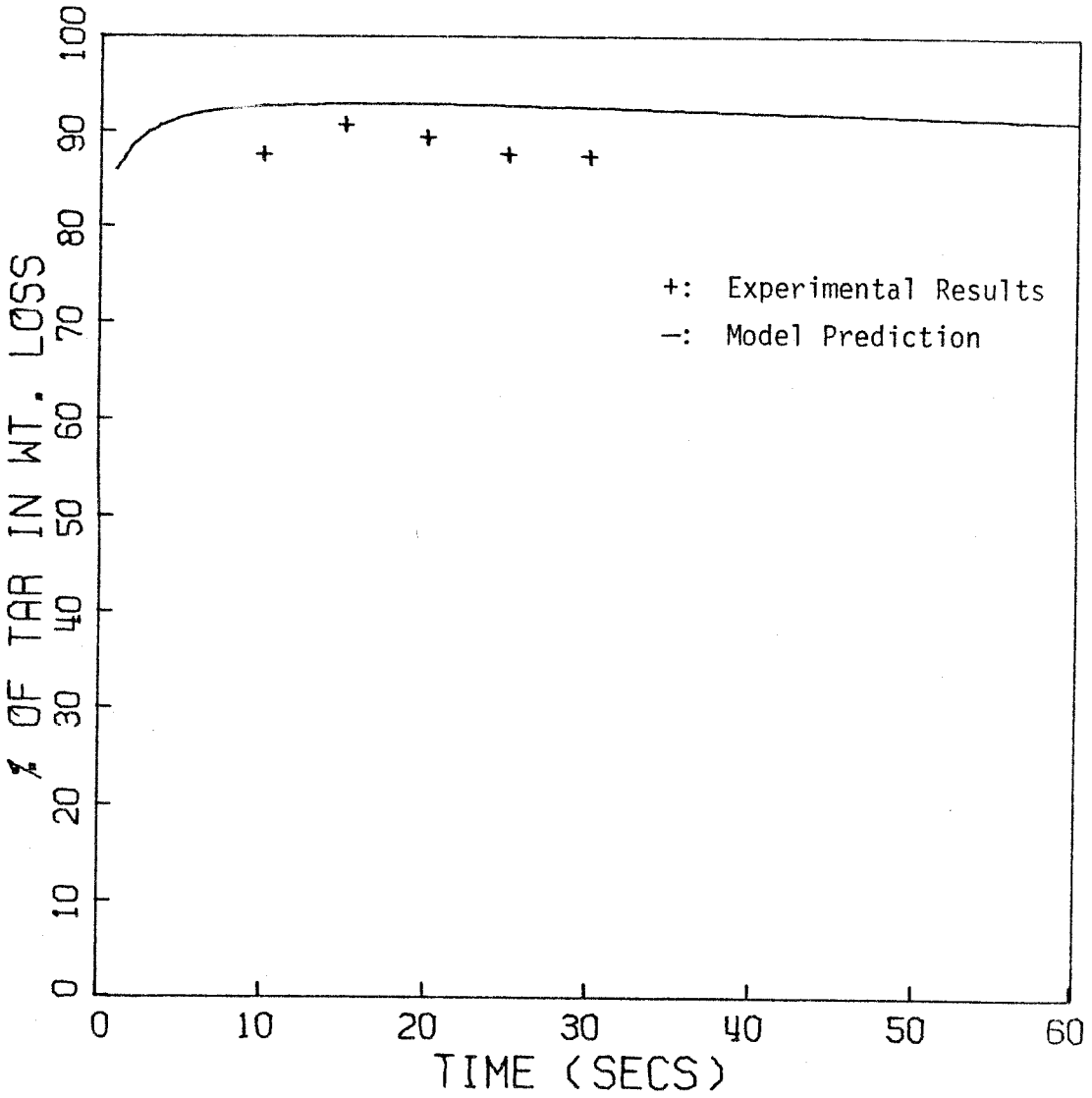

Figure 5.4.16: Comparison of Predicted Tar Selectivity with Experimental Results at 510^{o}C.

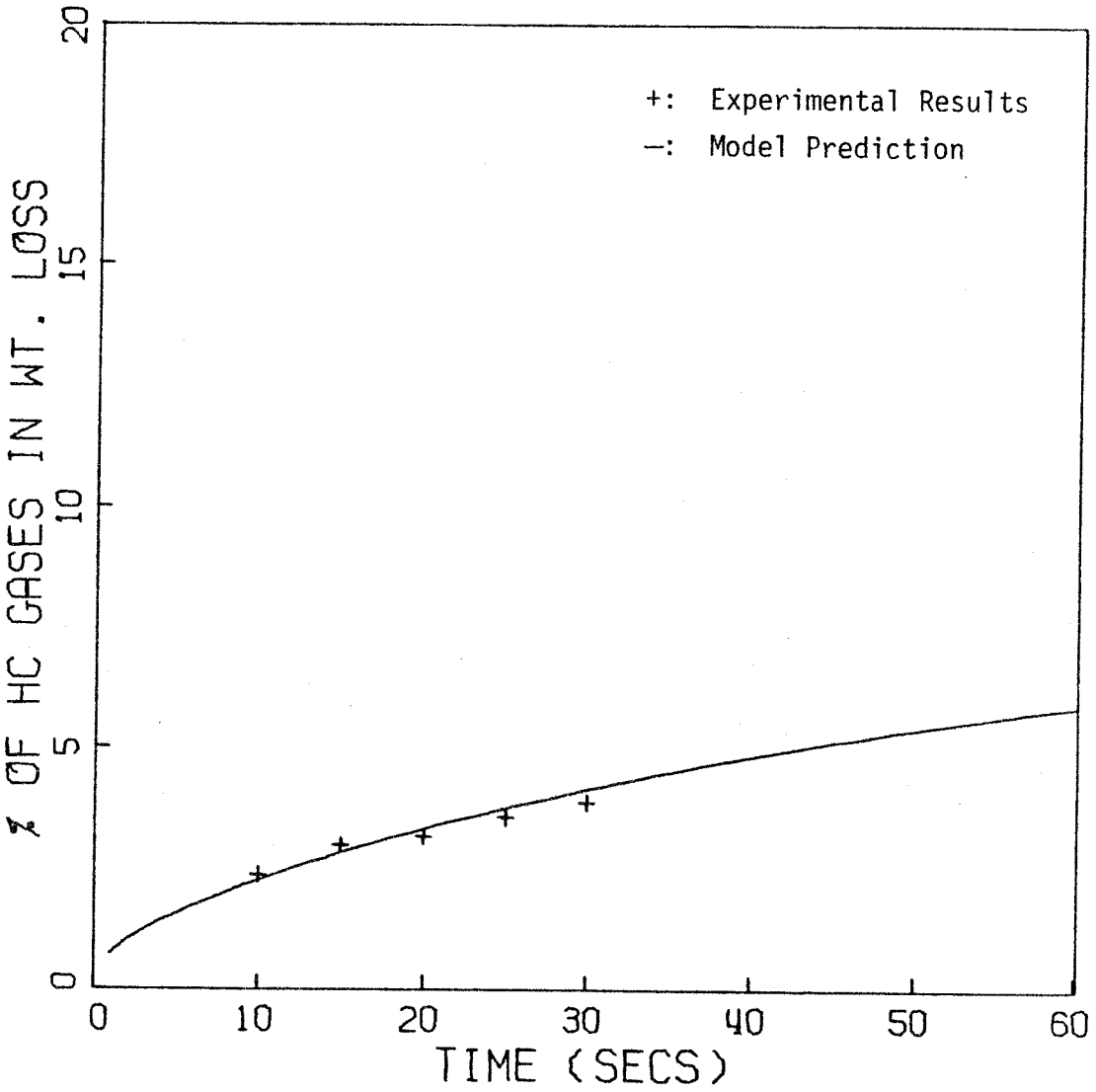

Figure 5.4.17: Comparison of Predicted HC Gas Selectivity with Experimental Results at 510^{o}C.

for experiments under 10 seconds were considered unreliable due to uncertainity in the heat-up time (refer to Chapter 6 for discussion). Measurement of tar produced was unsatisfactory due to its deposition on inaccessible surfaces inside the reactor. Similarly, reliable determination of amounts of water vapor by gas chromatographic methods was difficult due to inaccurate integration of its broad, skewed peak by the integrator. Considering these difficulties, the agreement between the simulation and the experiments is very good.

Effect of Temperature-Time History: Most of the simulation results presented in this thesis are based on the assumption of isothermal kinetics. Since in an actual experiment some finite time would be required to attain the highest temperature, pyrolysis investigators have been interested in identifying the effect of heating rate (or, more generally, of the temperature-time history) on the volatile production. To study this effect, a simulation run was made assuming the following profile: temperature increases linearly from 400^{o} to $600^{o}C$ in 2 seconds and remains constant thereafter. The results were compared with those obtained for isothermal kinetics at $600^{o}C$. The comparison is shown in the table 5.4.4 and the figures 5.4.18 and 5.4.19.

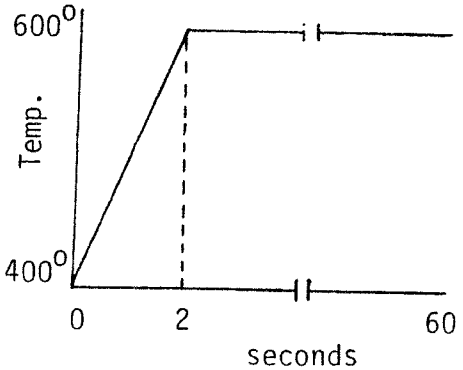

Temperature Profile

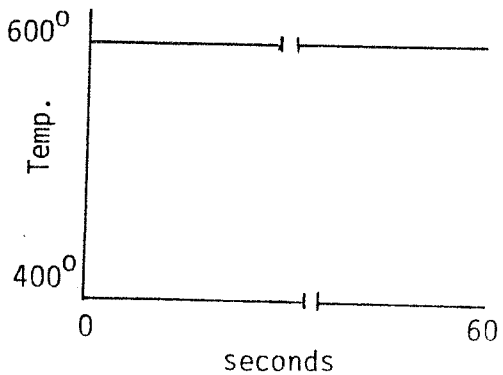

Isothermal

Table 5.4.4

Effect of Temperature-Time History
on Volatile Production

Pyrolysis Time in Seconds	Isothermal at 600°C		400° to 600°C in 2 seconds	
	Tar*	Water*	Tar*	Water*
1	25.20	1.795	2.29	0.668
2	26.42	1.829	18.75	1.780
5	26.93	1.850	25.99	1.930
10	26.99	1.857	26.18	1.942
20	27.00	1.860	26.20	1.946
30	27.00	1.861	26.21	1.948
60	27.00	1.863	26.22	1.949

*Weight percent of dry coal sample.

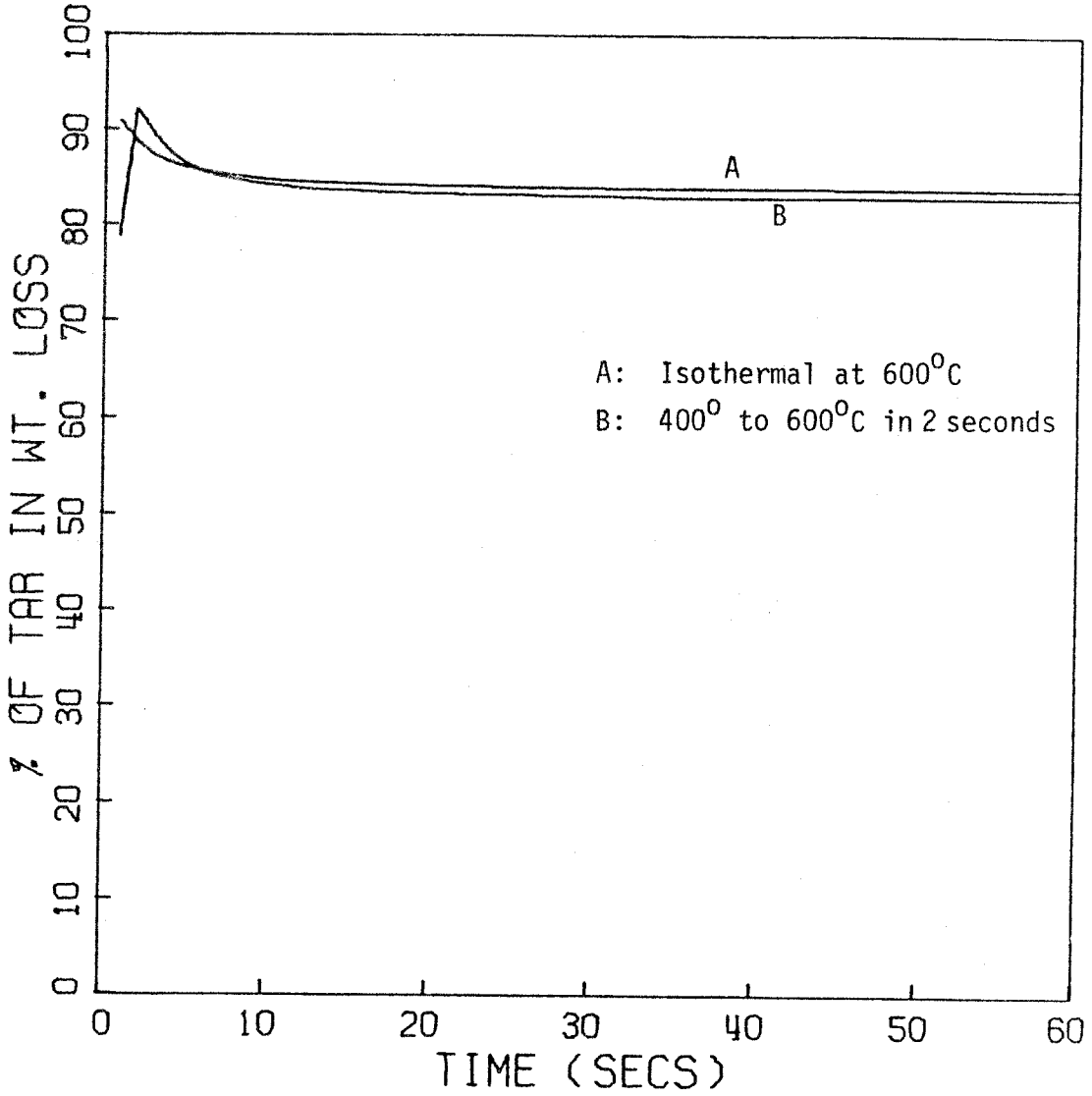

Figure 5.4.18: Effect of Temperature-Time History on Tar Selectivity.

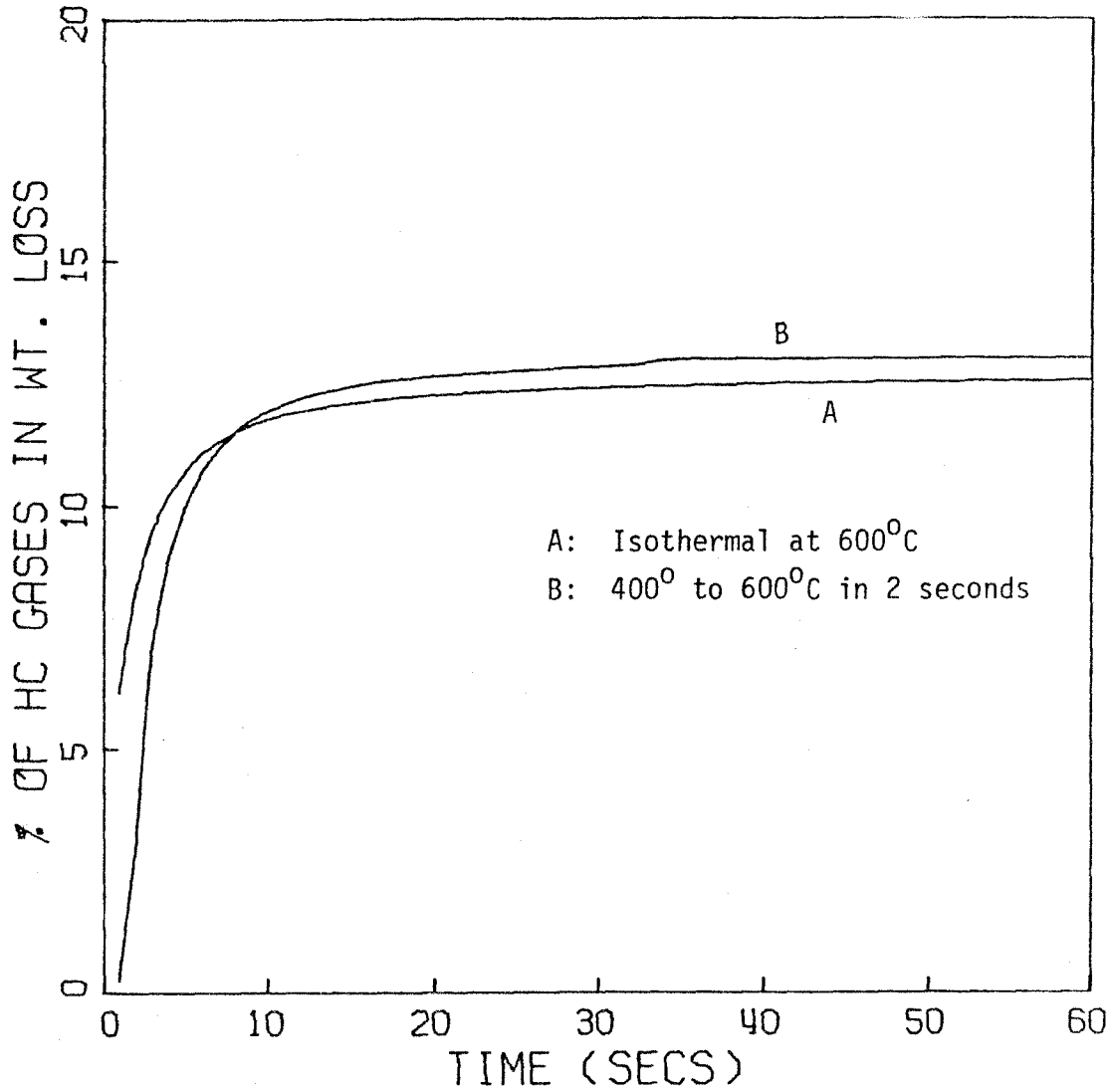

Figure 5.4.19: Effect of Temperature-Time History on HC Gas Selectivity.

The ultimate yield is slightly higher under isothermal conditions due to higher amount of tar. However, the gases are less. Tar is reduced in the heating rate simulation due to higher concentration of ether linkages as evidenced by higher amount of water formed. The reduction in tar helps in increasing formation of small radicals, and hence gases, because fewer sidechains are lost with free clusters. Accordingly, the ultimate tar selectivity is slightly higher and gas selectivity lower for the isothermal case. At the end of 1 second, the tar selectivity and the HC gas selectivity in the heating rate simulation are lower because the proportion of water in the volatiles is higher. Between 1 and 2 seconds, both selectivities increase rapidly at the expense of water. After 2 seconds the structure has already become very tight, reducing the rate of tar formation. Consequently, tar selectivity goes down while gas selectivity continues to rise. Overall, the difference in yield or distribution between the two cases is only slight. Anthony and Howard (1976) and Anthony et al. (1976) have also indicated that at high heating rates (higher compared to the rates employed in a standard Fischer retort procedure) changes in heating rate have a negligible effect on volatiles yield.

Case II: HVC Bituminous PSOC-212 Coal

Experimental results for this coal have been reported by Solomon (1977). We will compare the results for 20 seconds of pyrolysis with the model predictions.

Elemental composition on a dry mineral matter free basis was reported to be:

	% Sample
Carbon	79.37
Hydrogen	5.11
Oxygen	13.04
Nitrogen	1.65
Organic Sulfur	0.83

The mineral matter content was 3.05%. Therefore, on a mineral matter inclusive basis the composition can be approximated as:

	% Sample
Mineral Matter	3
Carbon	77
Hydrogen	5
Oxygen	12.55
Nitrogen	1.55
Sulfur (Total)	0.90

As before, referring to figure 4.4.1, the true density of the coal would be 1.3 gms/cm^3.

Solomon (1979) also reports the hydrogen distribution in this coal based on IR analysis. Since the sample used for IR work was from coal oxidized by atomospheric oxygen (private communication with Solomon) and the distribution does not add up to the total hydrogen content, we will make adjustments in the numbers. We will retain the percentage of aromatic hydrogen reported by him (in a private communication he expressed confidence in numbers related to aromatic hydrogen, but not aliphatic), but increase the aliphatic and reduce the hydroxyl contents:

	% Hydrogen
Aromatic	32
Aliphatic	62
Hydroxyl (Phenolic)	6

The choice of 6% for phenolic groups is supported by the amount of water vapor formed experimentally. It corresponds to a concentration of 3.9 moles/liter which is slightly higher than 3.75 moles/liter required on the basis of water vapor formed (some phenolic groups will be lost with the departing free clusters).

After some trials the aliphatic hydrogen was divided as 30% and 32% for alpha hydrogen and beta hydrogen, respectively. The choice was based on the production of hydrogen and hydrocarbon gases.

Solomon and Colket (1978) report the aromaticity of this coal determined by ^{13}C-^{1}H cross-polarization NMR to be approximately 0.72. Simulation runs were made using aromaticity of 0.7, 0.71 and 0.72. Based on the results and the need to obtain a reasonable size for an average cluster, fa = 0.7 was chosen for comparison with the experimental results.

Similarly, trials were made with methylene-to-ethylene bridge ratio between 0.25 and 0.30. The results corresponding to the value 0.27 were found to be in best agreement with the experimental results.

In the tables 5.4.5, 5.4.6 and 5.4.7 all the relevant information on this coal and the calculated initial values of the state variables are listed and compared with the values for Hamilton coal. The mineral matter free basis carbon content of the two coals is almost the same, and hence the density is the same. Aromaticities of the two are very close. Lower values

Table 5.4.5

Comparison of Elemental Composition, Aromaticity and Hydrogen Distribution of PSOC-212 and Hamilton Coals

	PSOC-212	Hamilton
Mineral Matter/Ash	3.0	7.9
Carbon	77.0	73.5
Hydrogen	5.0	5.1
Oxygen	12.55	8.7
Nitrogen	1.55	1.5
Sulfur	0.90	3.3
Density	1.3	1.3
Aromaticity	0.70	0.69
$H_{aromatic}$	32%	28.5%
H_{alpha}	30%	32%
H_{beta}	32%	35%
$H_{phenolic}$	6%	4.5%

Table 5.4.6

Comparison of the Initial Values of the State Variables* for PSOC-212 and Hamilton Coals

	PSOC-212	Hamilton
Y_1	19.500 moles/liter	21.216 moles/liter
Y_2	4.043 moles/liter	4.510 moles/liter
Y_3	1.555 moles/liter	1.735 moles/liter
Y_4	21.404 moles/liter	17.635 moles/liter
Y_5	0.449 moles/liter	0.501 moles/liter
Y_8	19.504 moles/liter	18.138 moles/liter
Y_{10}	3.900 moles/liter	3.000 moles/liter
Y_{18}	16.614 moles/liter	15.934 moles/liter
Y_{19}	0.077 liters	0.077 liters

*Unlisted state variables are zero for both the coals.

Table 5.4.7

Comparison of Structural Parameters for PSOC-212 and Hamilton Coals

	PSOC-212	Hamilton
Cluster Concentration	5.83 moles/liter	5.1 moles/liter
Methylene/Ethylene Bridges	0.27	0.25
Bridges/Clusters	2.331	2.161
Alpha Carbon Connections/Clusters	3.345	3.556
Aromatic Carbon/Clusters	10.015	10.772
Sites/Clusters	7.72	7.9

of H_{alpha} and H_{beta} for PSOC-212 lead to lower concentrations of the sidechains, while higher oxygen content results in higher phenolic concentration. In addition, the bridge/cluster ratio is slightly higher for PSOC-212. Average clusters in the two coals have very similar characteristics.

Predictions: Simulation results for PSOC-212 at 510°C and 565°C are presented in the figures 5.4.20, 5.4.21, 5.4.22, 5.4.23 and 5.4.24. They are qualitatively similar to the results for the Hamilton coal. The mechanistic explanations given earlier apply here also. Differences in phenolic concentrations and bridge/cluster ratios are responsible for the quantitative differences. Both these factors reduce the amount of tar formed by making the structure more tight (higher phenolic concentrations lead to higher concentrations of ether linkages). A reduction in the loss of free clusters (tar) also implies a reduction in the loss of sidechains. Consequently, although sidechain concentrations in PSOC-212 are lower, more gases are produced. Compared to the Hamilton coal the tar selectivity is lower and the gas selectivity is higher. This inverse relationship between tar and gas formation has been observed experimentally also (for example, more severe transport limitations within coal particles — due to pressure or particle size — shifts the selectivity in favor of the gases). It points to the competitive nature of product formation in pyrolysis.

Predictions vs. Experimental: In tables 5.4.8 and 5.4.9 the model predictions for PSOC-212 are compared with the experimental results for vacuum pyrolysis at 510°C and 565°C reported by Solomon (1977). The agreement is generally very good. Experimental results for individual

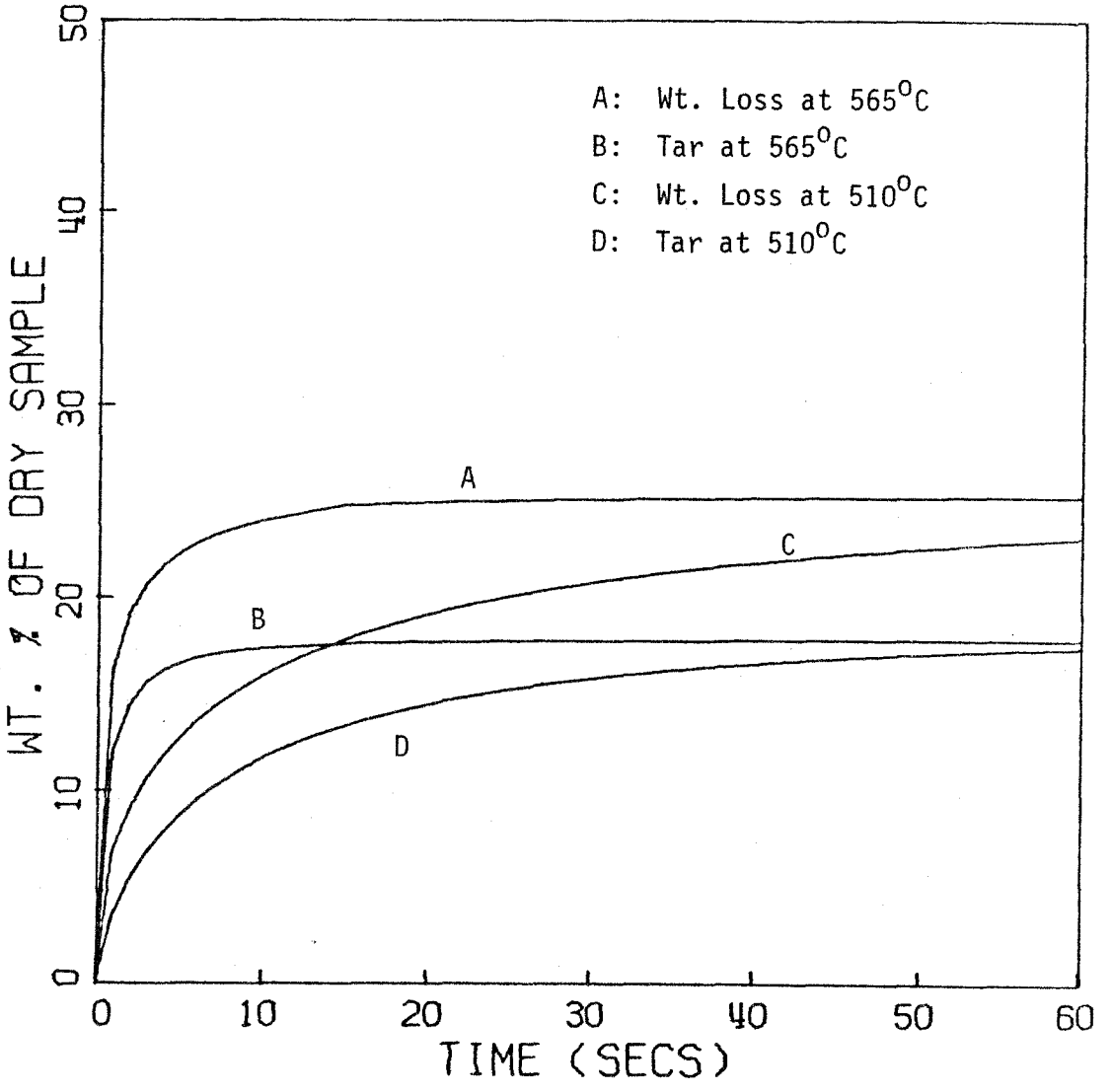

Figure 5.4.20: Variation of Weight Loss and Tar with Pyrolysis Time.

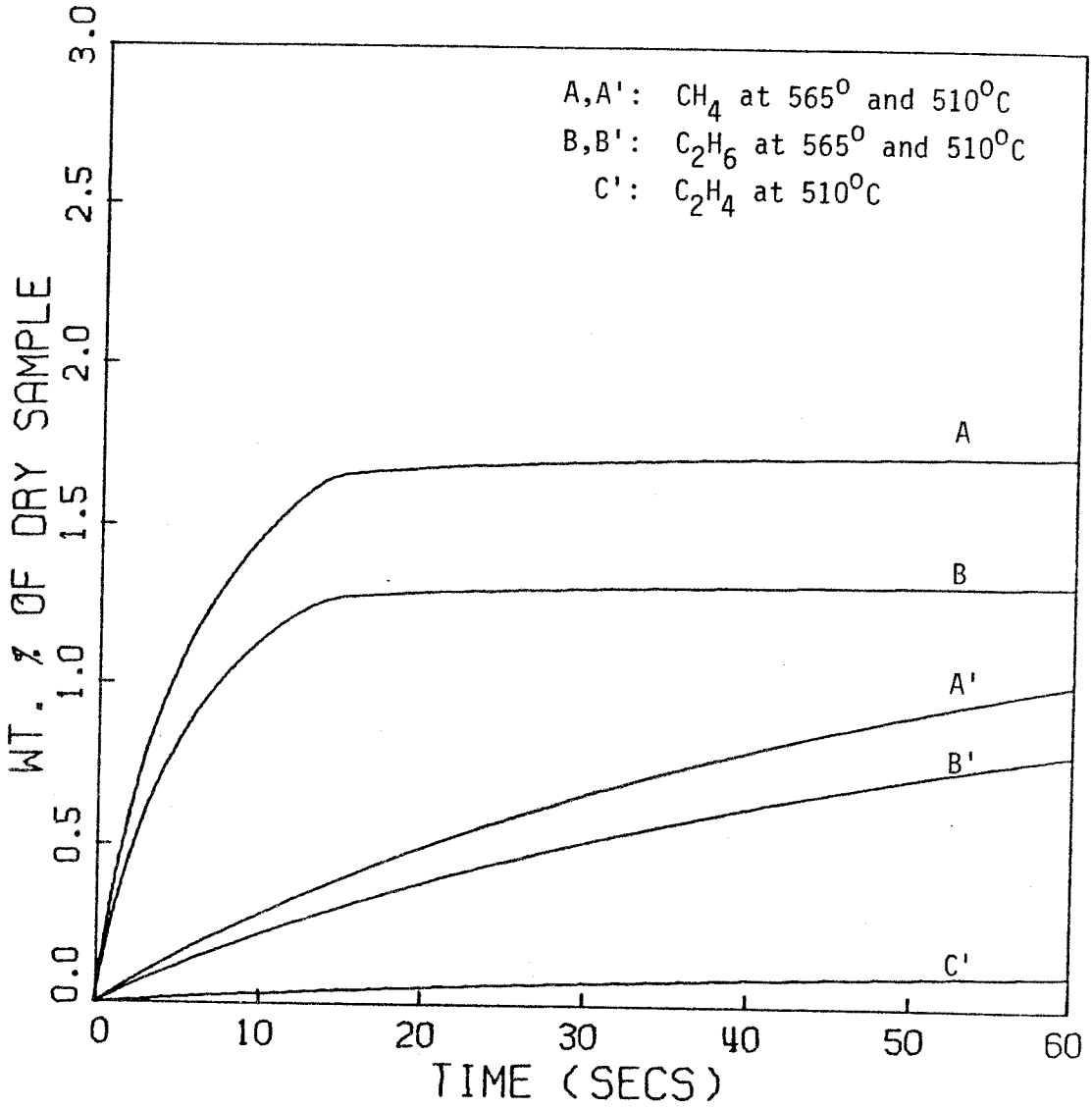

Figure 5.4.21: Variation of Hydrocarbon Gases with Time.

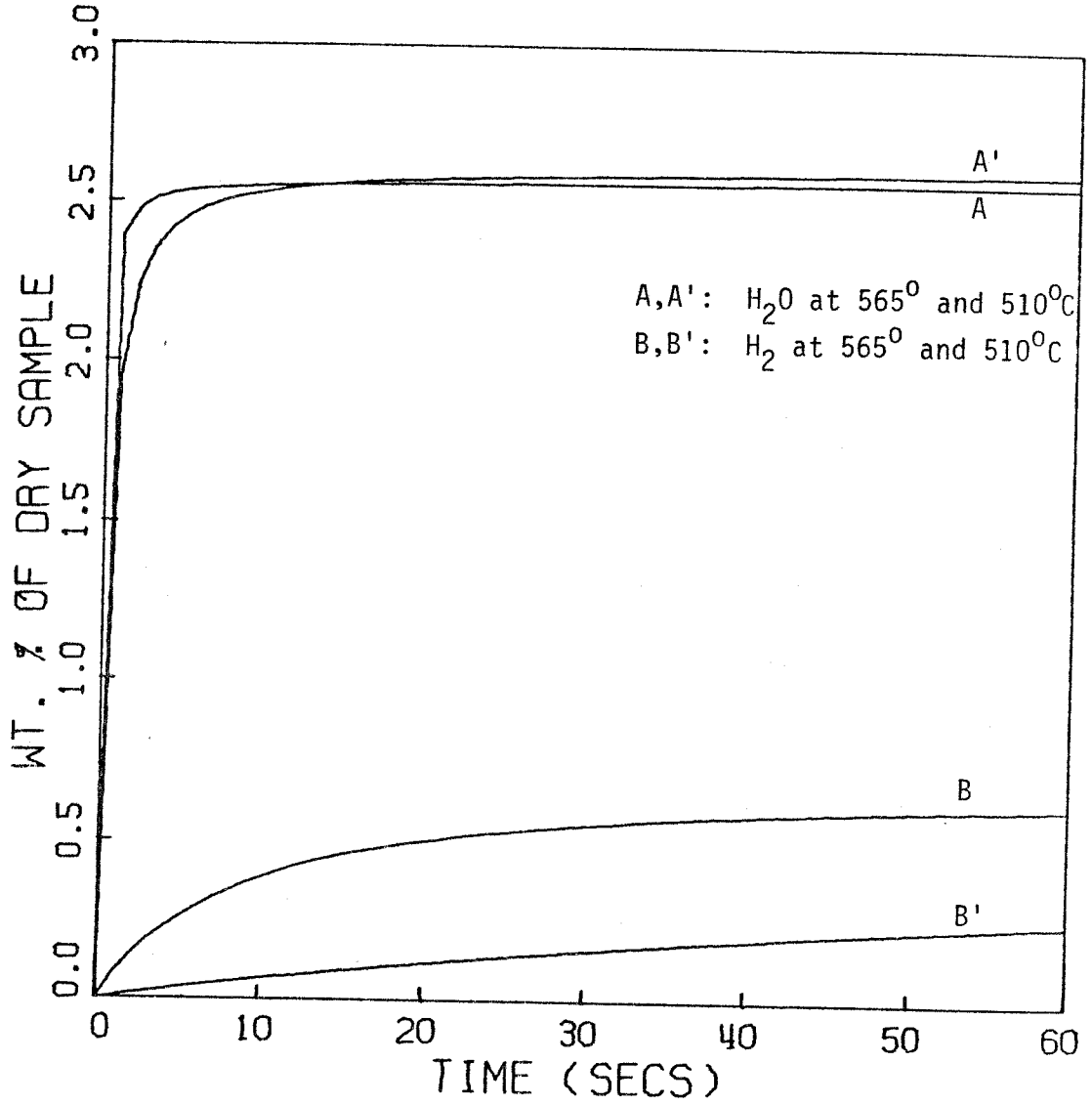

Figure 5.4.22: Variation of Water Vapor and Hydrogen with Time.

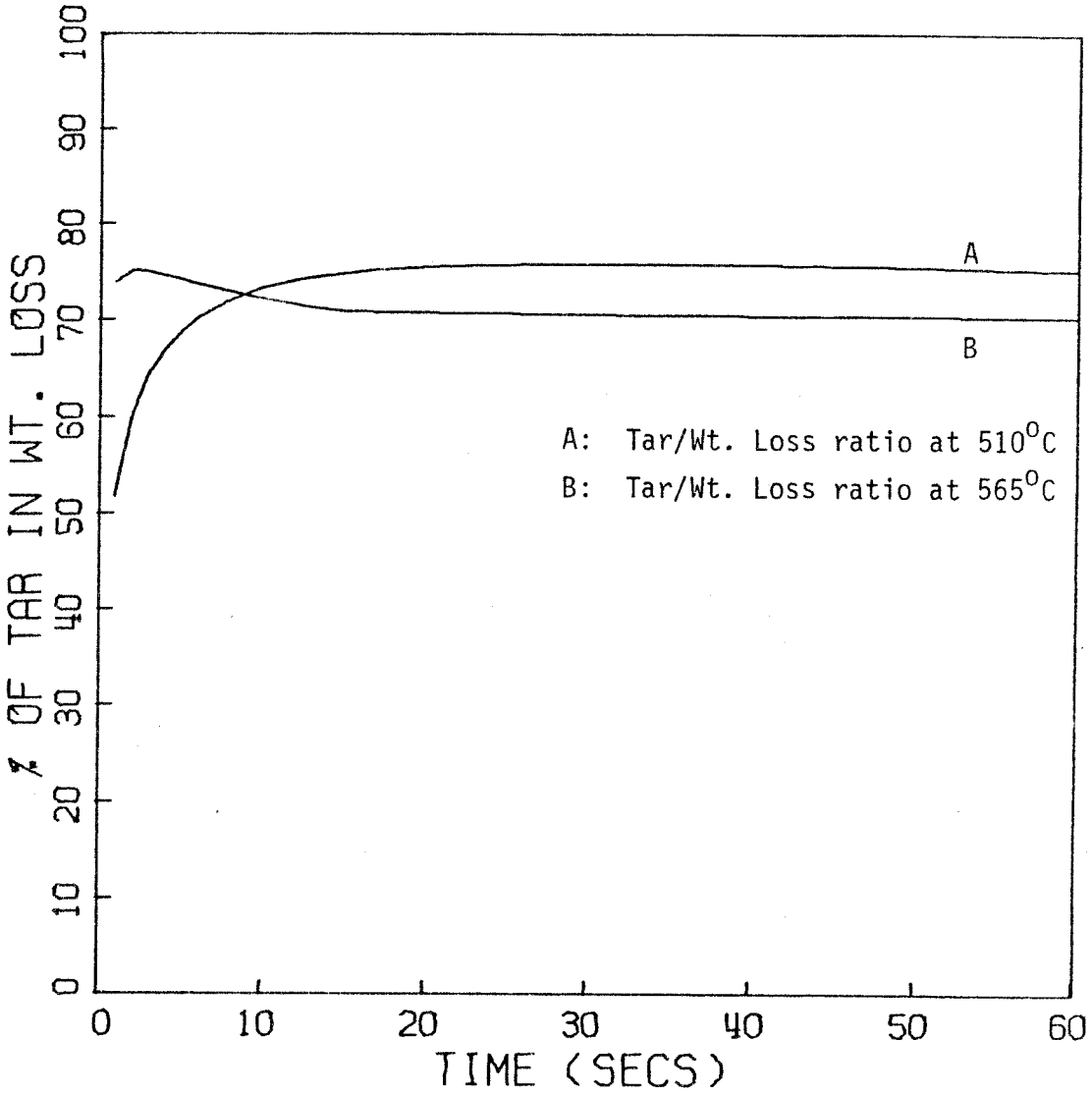

Figure 5.4.23: Variation of Tar/Wt. Loss (Tar Selectivity) with Time.

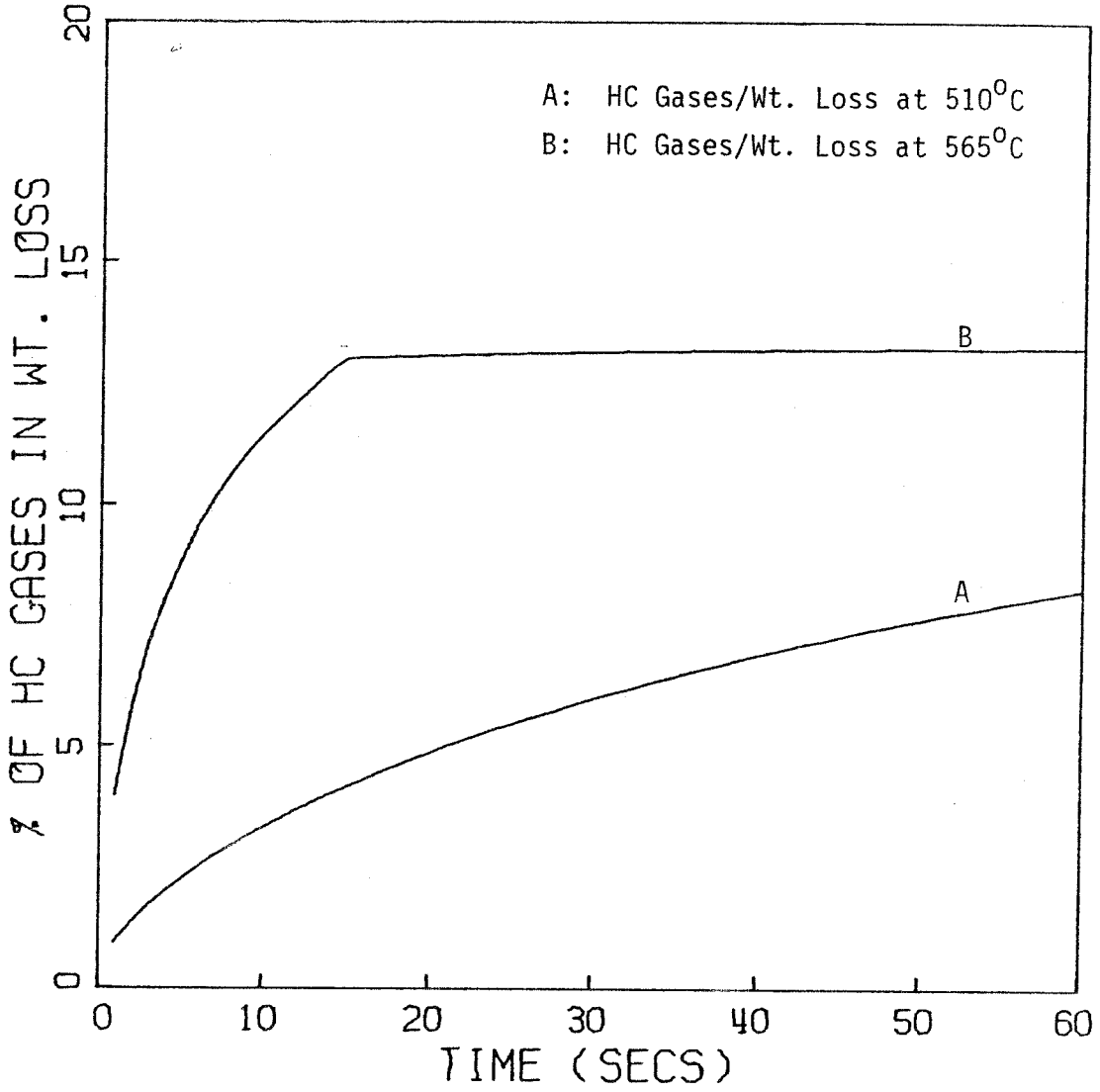

Figure 5.4.24: Variation of (CH_4 + C_2H_4 + C_2H_6)/Wt. Loss (Gas Selectivity) with Time.

Table 5.4.8

Comparison of Model Predictions with Experimental Results* for Pyrolysis of PSOC-212 Coal at 510°C

	Model Predictions**	Experimental Results**
Weight Loss	19.75	19.0
Tar	14.93	14.0
CH_4	0.509	-
C_2H_4	0.057	-
C_2H_6	0.394	-
HC Gases	0.96†	1.65†
H_2O	2.66	2.6
H_2	0.12	0.05

*From Solomon (1977).

**Both predictions and experimental results are weight percentages of dry mineral matter free sample.

†HC gases in predictions include only CH_4, C_2H_4 and C_2H_6; in experimental results higher hydrocarbon gases are also included.

Table 5.4.9

Comparison of Model Predictions with Experimental Results* for Pyrolysis of PSOC-212 Coal at 565°C

	Model Predictions**	Experimental Results**
Weight Loss	25.8	24.5
Tar	18.27	19.0
CH_4	1.73	-
C_2H_4	0.309	-
C_2H_6	1.33	-
HC Gases	3.37†	1.65†
H_2O	2.64	2.55
H_2	0.51	0.08

*From Solomon (1977).

**Weight percentages of dry mineral matter free sample.

†Number under predictions includes CH_4, C_2H_4 and C_2H_6; experimental result includes higher gases also.

hydrocarbon gases were not reported. At 510°C, the sum of the C_1 and C_2's predicted by the model appear reasonable in comparison to the total of HC gases detected experientally. At 565°C, the experimental value for HC gases is most likely in error — it is the same as the value at 510°C while it is a well-established observation that HC gases increase with temperature in this range (e.g., Anthony and Howard, 1976). Disagreements in hydrogen are probably due to high concentration of alpha hydrogen used in the model.

5. Model Sensitivity to the Parameters

This section presents results and discussion of model sensitivity testing in which structural and kinetic parameters were perturbed to determine their effect on the simulation results.

Although values used for the structural and kinetic parameters in simulation are based on theoretical concepts, they are not well established and are subject to uncertainty. For example, while calculating the initial values of the state variables we started with just the elemental analysis and some NMR data, and made several adjustments and assumptions. Similarly, values used for the kinetic parameters (Appendix II) do not take into account all the complex effects of neighboring functional groups on the reaction, and the fact that the chemical interaction occurs in a condensed phase. For some reactions, e.g., phenolic condensation, even the gas phase kinetics are not well established.

The uncertainty in the values of these parameters provide the incentive to determine how critically they affect the simulation results.

The sensitivity testing is carried out for isothermal pyrolysis of the

Hamilton coal at 510^{o}C. We choose seven paramters, three structural and four kinetic, for perturbation:

(1) x: this parameter defines the fraction of the subunit volume active in tar formation; the base value was 0.15.

(2) Bridge-to-Cluster Ratio: it is a measure of the 'tightness' of the coal structure; the base value used was 2.161.

(3) Methylene-to-Ethylene Bridge Ratio: higher values of this ratio will reduce the rate of free cluster formation; base value was 0.25.

(4) E_4: the activation energy of ethylene bridge dissociation, reaction 4 in table 4.6.1; base value = 52 kcals/mole.

(5) E_{39}: the activation energy of phenolic condensation, reaction 39 in table 4.6.1; base value = 35 kcals/mole.

(6) E_{10}, E_{11}, E_{12}: the activation energies of elimination of small radicals to form double bond bridges, reactions 10, 11 and 12 in table 4.6.1; base values were 38, 37 and 37 kcals/mole, respectively.

(7) E_2, E_3, E_5: the activation energies of sidechain dissociations, reactions 2, 3 and 5 in table 4.6.1; base values were 65, 63 and 63 kcals/mole, respectively.

Tables 5.5.1, 5.5.2 and 5.5.3 show the effect of the parameters on the results obtained for 30-second pyrolysis. Sensitivity S, is defined as:

S = (% Change in a Quantity/% Perturbation) x 100

We will now discuss the effect of each parameter.

A 33% change in x reduces tar by almost 12% and alkanes by 3%, but

Table 5.5.1

Sensitivity of Weight Loss to Structural and Kinetic Parameters

Parameter	Base Value	Perturbed Value	% Perturbation	% Change in Wt. Loss*	$S_{\text{Wt. Loss}}$**
x	0.15	0.10	33.3	-10.2	30.6
Bridge-to-Cluster Ratio	2.16	2.249	4.07	- 8.5	209.0
Ratio of Methylene to Ethylene Bridges	0.25	0.30	20.0	- 7.1	35.5
E_4	52.00	51.00	1.9	+14.6	766.3
E_{39}	35.00	36.00	2.9	+ 4.3	148.3
E_{10}, E_{11}, E_{12}	38, 37, 37	39, 38, 38	2.7	+ 3.2	118.5
E_2, E_3, E_5	65, 63, 63	66, 64, 64	1.6	+ 0.15	9.4

*Positive sign indicates increase and negative sign decrease.

**S = (% Change in a Quantity/% Perturbation) x 100.

Table 5.5.2

Sensitivity of Tar to Structural and Kinetic Parameters

Parameter	% Perturbation	% Change in Tar	% Change in Tar Selectivity	S_{Tar}	$S_{Tar\ Selectivity}$
x	33.3	-11.6	-1.53	34.8	4.6
Bridge-to-Cluster Ratio	4.07	- 9.9	-1.6	243.0	39.3
Ratio of Methylene to Ethylene Bridges	20.0	- 8.1	-1.19	40.5	6.0
E_4	1.9	+16.2	+1.44	852.6	75.8
E_{39}	2.9	+ 5.2	+0.81	179.3	27.9
E_{10}, E_{11}, E_{12}	2.7	+ 5.2	+1.9	192.6	70.4
E_2, E_3, E_5	1.6	+ 0.72	+0.6	45.0	37.5

Table 5.5.3

Sensitivity of Gases to Structural and Kinetic Parameters

Parameter	% Perturbation	% Change in Alkanes	% Change in Alkenes	$S_{alkanes}$	$S_{alkenes}$
x	33.3	- 3.27	+20.6	9.8	61.9
Bridge-to-Cluster Ratio	4.07	+ 3.5	+19.8	86.0	486.0
Ratio of Methylene to Ethylene Bridge	20.0	+ 0.7	+ 5.4	3.5	27.0
E_4	1.9	+ 9.7	+10.3	510.0	542.0
E_{39}	2.9	- 1.9	+39.4	65.5	1358.0
E_{10}, E_{11}, E_{12}	2.7	-27.6	-22.6	1022.0	837.0
E_2, E_3, E_5	1.6	-12.6	- 4.0	787.5	250.0

increases C_2H_4 by 21%. Reduction in tar would be expected because of a reduction in the rate of bridge dissociation and hence of free cluster formation. It was found that the change in x has a greater effect on the tar-time profile than on the ultimate amount of tar produced. After 1 second the difference in tar was 25%, after 10 seconds 17%, while after 60 seconds it was only 9%. Therefore, it appears that the ultimate amount is determined by other structural and kinetic parameters, and that x affects only the initial rate of tar production. As mentioned in section 4, amounts of hydrogen and alkanes depend on production of small radicals, which can take place by at least two mechanisms: direct dissociation of sidechains, or indirect elmination during double bond formation. For example:

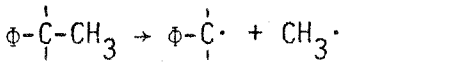

Reaction 2 in table 4.6.1

and

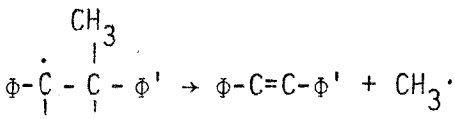

Reaction 11 in table 4.6.1

Since low values of rates of bridge dissociation will reduce the concentration of alpha radicals, production of hydrogen and alkanes by the second mechanism will go down. However, this loss will be compensated to some extent by an increase in direct dissociation due to increased availability of the sidechains. The overall effect is a slight reduction in the amount of these gases. Since mechanism of ethylene production is quite complex and depends on several factors, it is difficult to explain its behavior. As would be expected, water produced for x = 0.1 is slightly more due to the reduced loss of phenolic groups. Tar selectivity is reduced due to a more severe effect of the change on tar than on the

total volatile yield.

The bridge-to-cluster ratio is increased from 2.161 to 2.249 (4.07%) by reducing the cluster concentration from 5.1 moles/liter to 4.9 moles/liter. This implies more cross-linking among the clusters, making the structure more tight. Therefore, probability of formation of free clusters following the dissociation of a bridge is reduced and consequently amount of tar formed is reduced. This ratio does not affect formation of gases by the indirect mechanism because rate of bridge dissociation is not affected and hence concentration of alpha radicals remains the same. The gases formed by the direct mechanism, however, are increased due to the reduction in the loss of sidechains with tar. Therefore, the overall amount of gases increases. All the results are very sensitive to this ratio.

Increase in methylene to ethylene bridge ratio increases the average activation energy of bridge dissociation — E for methylene bridge dissociation is 68 kcal/mole while for ethylene bridge is 52 kcal/mole. Therefore, activation energy for tar formation moves closer to that for gas formation. At constant temperature, such relative change in activation energies of competing reactions improves the selectivity of the product with the higher activation energy. We see this trend in the results shown. It should be noted that by changing the relative concentrations of the two types of bridges we are automatically changing the total concentration of bridges and hence bridge-to-cluster ratio (if every other quantity is constant). For example, the bridge-to-cluster ratio becomes 2.199 while the base value was 2.161. Hence, tar value is affected more severely than one would expect. Consequently, increase in gas production

by the direct mechanism exceeds the slight decrease by the indirect mechanism, and the overall amount of gases is increased.

Activation energy for ethylene bridge dissociationis the most important parameter in the system. The value we use (52 kcal/mole) is very close to that suggested by O'Neal and Benson (1973). A reduction of 1 kcal/mole increases both tar and gases, the former somewhat more than the latter.

Since in the first few seconds of pyrolysis there is a competition between formation of free clusters and formation of ether linkages (which make the structure tight), reduction in the rate of phenolic condensation improves tar production by increasing the probability that a cluster will be free of ether bridges. More tar implies more loss of sidechains and hence less gases. In effect, phenolic condensation in pyrolysis serves to shift the selectivity in favor of the gases by restricting tar production through ether bridges. This effect is clearly seen in the pyrolysis of coals containing high amounts of oxygen, like subbituminous coals.

The inverse relationship between tar and gas formation is very clearly demonstrated by the effect of increasing the activation energies for formation of double bond bridges. While the amount of tar formed is increased due to a reduction in the concentration of unbreakable bridges, the amount of gases formed is reduced due to a reduction in the rates of both direct and indirect mechanisms. Gases are more sensitive to these parameters than tar.

Similarly, reduction in the rates of sidechain dissociations increases tar by reducing the concentration of alpha radicals, but decreases gases as would be expected. By comparing the sensitivity with that for

double bond bridge formation, we see that more gases are formed by indirect than by direct mechanism. This implies an inseparability of gas and tar formation mechanisms which is contrary to the assumptions of most models presented in the literature.

Chapter VI

PYROLYSIS EXPERIMENTS AND RESULTS

1. General

Pyrolysis experiments for various coals are discussed in this chapter. First, the techniques and the apparatus used are described in detail, and then the experimental strategy and the data obtained are discussed.

This section consists of general comments on the scope of the experimental work.

The mechanism of volatiles production during coal pyrolysis was discussed in Chapter III. It is obvious from that discussion that both the yield and the product distribution depend on the structure of the coal and the experimental conditions employed. The model predictions presented in the last chapter clearly show such dependence. The experimental program followed was also designed to study the effects of various coal-related and experiment-related parameters on volatiles production. The stress was on the variety of the experiments performed rather than on extensive data acquisition with one coal or one set of experimental conditions. The objective was to determine the qualitative trends in the pyrolytic behavior of a wide spectrum of coals under a variety of conditions. (However, not all coals and experiments are reported here.) The experimental results, in conjunction with the findings reported in the literature, were meant to provide the basis for formulating the theoretical concepts regarding coal's structure and reactivity.

To study the effects of coal composition, bituminous and subbituminous coals were used for the experiments. Coals in these two ranks most closely conform to the general theoretical concepts, and there is a lot of commercial as well as academic interest in their behavior. While high ash

and low hydrocarbon content in lignites makes them unattractive for use in industrial processes, anthracites are less interesting because of their low reactivity resulting from a highly carbonized structure.

The effects of the experimental parameters were studied by varying one parameter at a time. The parameters included: temperature, time-temperature history, pressure, particle-size and nature of the surrounding environment (chemical nature as well as flow patterns). The range of the parameters is presented in later sections. Effects of the techniques and the apparatus used were not investigated, although under some conditions they may affect specific products (e.g., effects of the reactor geometry on cracking of tar). Therefore, the results are interpreted solely in terms of the dependence of the physico-chemical processes within coal particles, on these variables.

The results monitored included: weight loss, amount of tar formed and amount of various gases formed. In many experiments the tar was collected for analysis with Gel Permeation Chromatography and ^{1}H and ^{13}C NMR. Some tar fractions were also analyzed for their elemental composition. Gases were quantified using Gas Chromatography. Some concurrent experiments were performed by the author's research group to study the effect of pyrolysis on pore structures of a bituminous and a subbituminous coal.

2. The Experimental Set-Up

The set-up used for the experiments is described under two parts:

(1) The reactor and the associated accessory system.

(2) The apparatus for product analysis.

Wherever in context, the merits and demerits of the experimental techniques are discussed.

The Reactor System: Pyrolysis of pulverized coal can be carried out in one of the two ways: in a batch process in which a captive, stationary sample is subjected to high temperatures; or in a continuous flow system in which coal is continuously fed to and removed from a hot reactor. Anthony and Howard (1976) have categorized and tabulated the various experimental techniques and conditions used in relatively recent investigations reported in the literature. The techniques range from the simple, standard method of proximate analysis in a crucible, to heating in a fluidized bed of hot sand particles. The pyrolysis literature also contains reports on use of novel methods, e.g., use of microwaves or lasers for heating.

In this work, a batch process (also called captive sample technique) using an electrical grid carrying the coal sample and being heated by a current pulse, was chosen for experiments. Such an arrangement provides better monitoring and control of the temperature and the heating rate, compared to the continuous flow techniques. Being a batch process, it also allows better product collection and hence better mass balances. Its greatest drawback is its limitation on the sample size: in order to ensure rapid heating and uniform temperatures, the sample has to be limited to 100 - 200 mgs. Consequently, the amount of products is small and their accurate analysis becomes difficult. In addition, considering that different chunks of a coal from the same seam often differ in composition, such a small sample may not be representative. Questions have

also been raised (Suuberg, 1977 ; Anthony and Howard, 1976) about the possible catalytic effect of the metal in the wire mesh. However, no effects have been reported in literature (except for the interaction between stainless steel screens and hydrogen sulfide which is not a product of interest here) and none were detected by the author.

The reactor system can be divided into three parts:

(1) The reactor and the associated flow system.

(2) The power supply and its controller.

(3) The time-temperature monitoring system.

A schematic diagram of the apparatus is shown in the figure 6.2.1. Photographs 6.2.2a and 6.2.2b show the top and side view of the bottom portion of the reactor. The entire system is shown in the photographs 6.2.3a and 6.2.3b.

The reactor consisted of a top and a bottom part, sealed together by ten bolts and nuts. A fine gasket between the two helped in reducing leaks. The bottom part was mounted on two elevated arms as shown in the photographs. Its inner surface was flat. A folded stainless-steel wire screen was stretched between two copper electrodes (one of the electrodes was pulled by a spring so as to keep the screen stretched) mounted on two rods projecting from the bottom part. The rods passed through the bottom part and their other ends were connected to the power supply. Similarly, a gas inlet tube with an opening at the top (at the same level as the screen) passed through the bottom part towards the front. After coming out of the opening, the gas jet swept the volatile products away from the hot screen. A small, thin ceramic tube carrying a chromel-alumel thermocouple (3 mil diameter) entered between the two folds of the wire screen

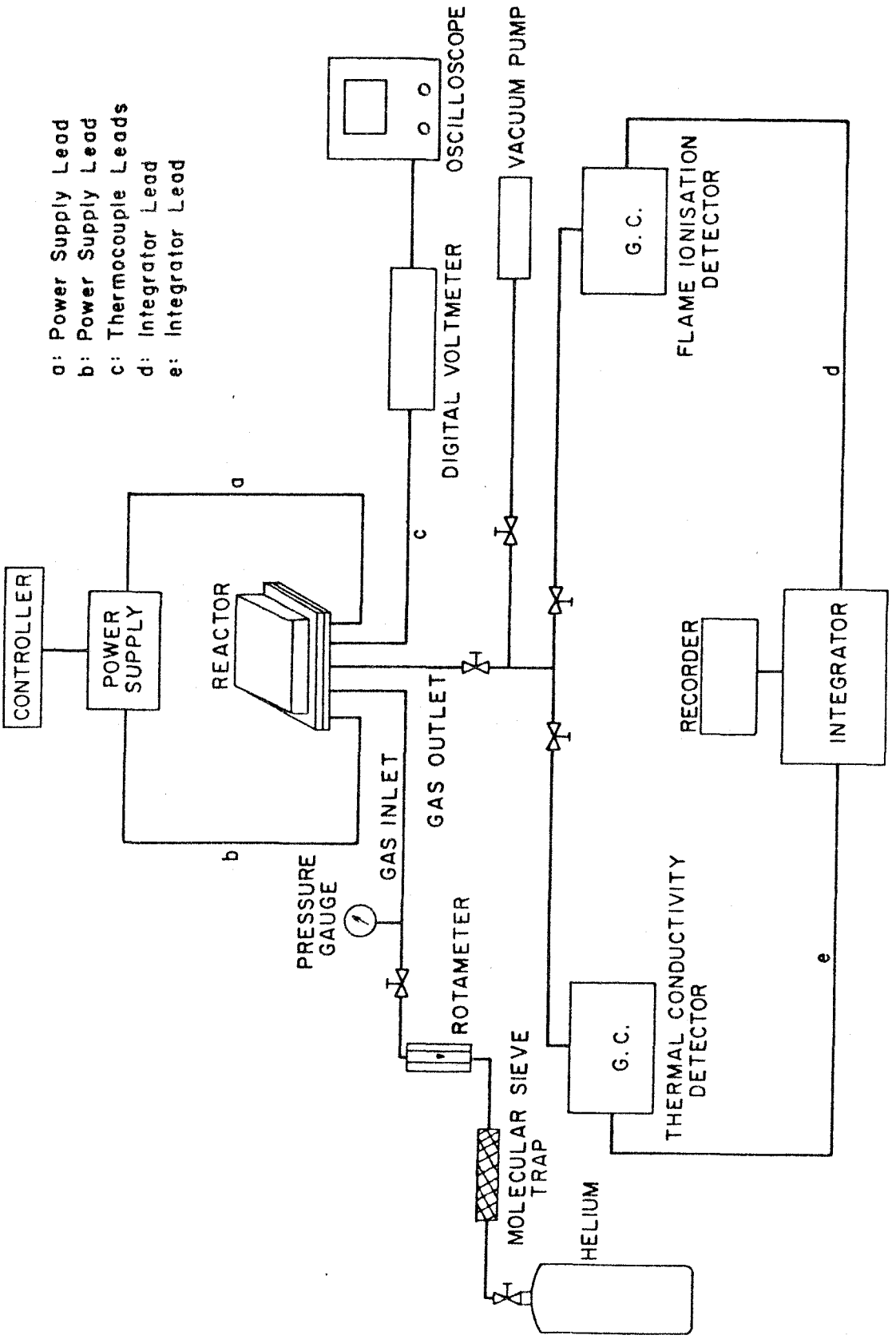

Figure 6.2.1: Schematic Diagram of the Experimental System.

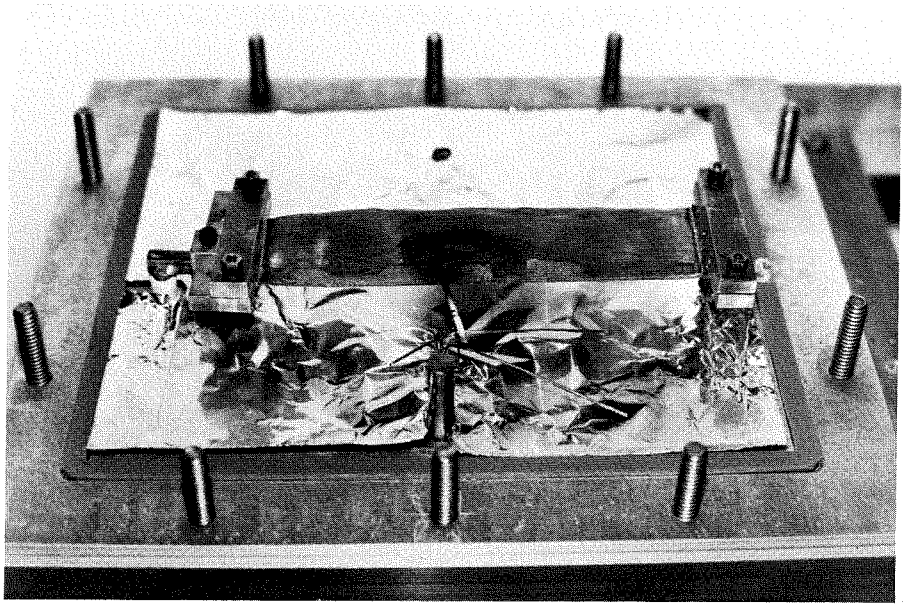

Figure 6.2.2a: Top View of the Bottom Portion of the Reactor.

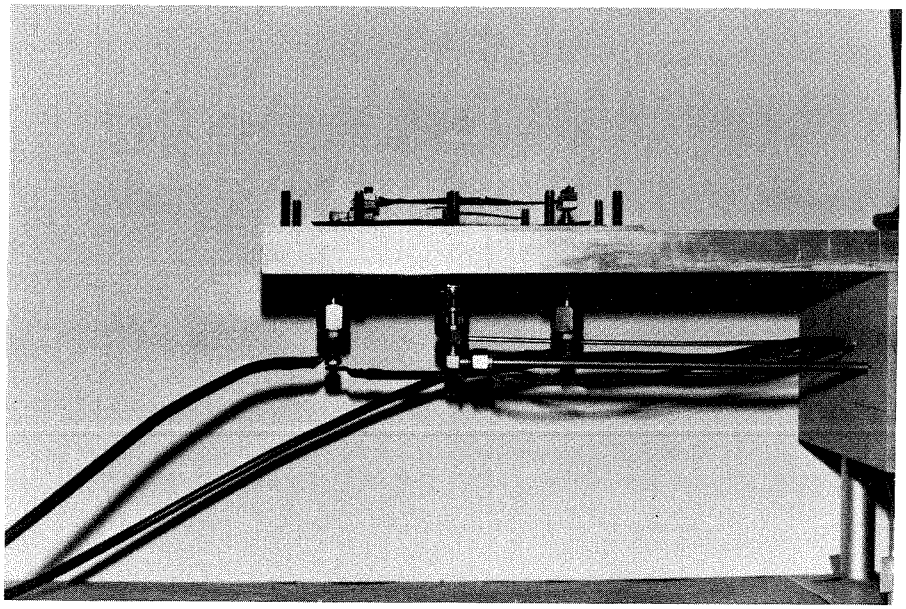

Figure 6.2.2b: Side View of the Bottom Portion of the Reactor.

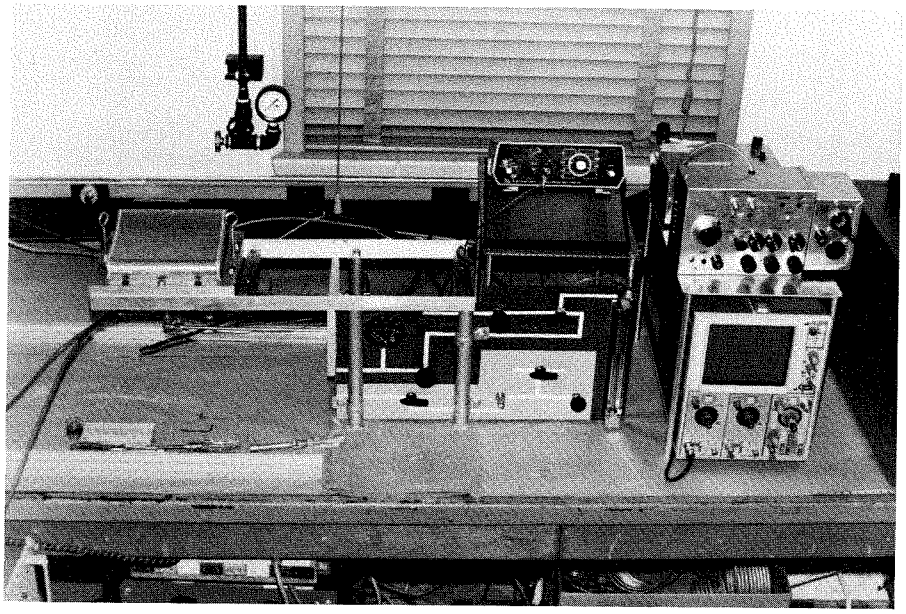

Figure 6.2.3a: The Reactor, the Flow Controls and the Temperature Monitoring System.

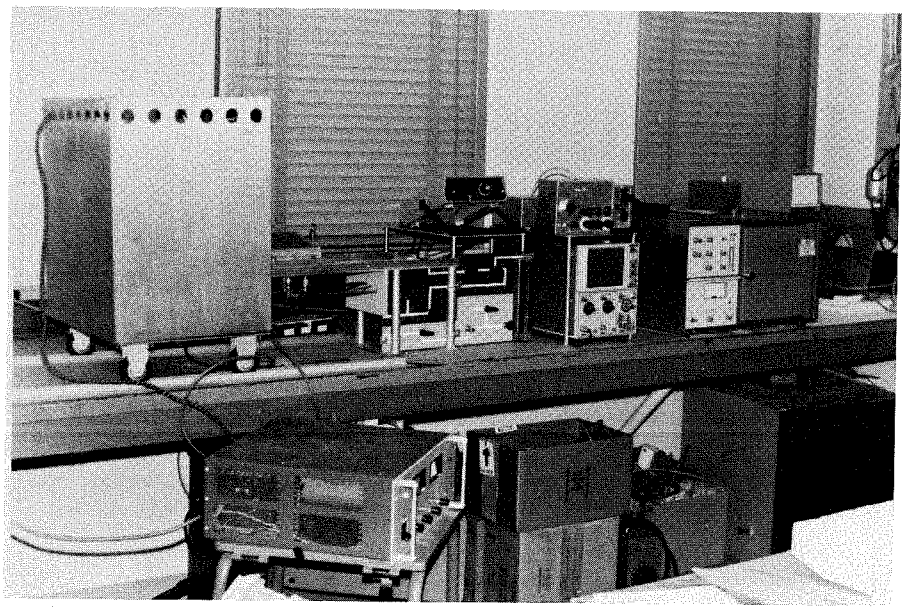

Figure 6.2.3b: The Complete Experimental System.

perpendicularly. The last 1 cm of each thermocouple lead and its junction was bare, so as to be in direct contact with the sample of coal particles spread in a thin layer between the two folds. The other ends of the leads were connected to permanent leads coming through the bottom part. The thermocouple was held in place with a small wire stand. Towards the back of the bottom part, there was an opening for gas exit. The opening was fitted with a micropore filter assembly. The top part of the reactor had an increasing cross-sectional area towards the back to provide larger surface area for tar deposition.

The inlet gas line was connected to a helium tank through a pressure gauge, valves, a rotameter, and a molecular sieve trap for removal of impurities from the helium. The pressure gauge indicated the pressure inside the reactor. The outlet line from the reactor had a metering valve, and then it divided into two lines: one connected to a vacuum pump through a valve; the other to the gas chromatographs. The gas chromatograph line was further divided into two sections, one leading to a chromatograph fitted with a thermal conductivity detector, and the other to a chromatograph fitted with a flame ionization detector.

A custom-built power supply was used to heat the screen with two successive constant current pulses with independently adjustable amplitudes. A controller regulated the duration of each pulse. The first pulse was set at a very high amperage to rapidly elevate the screen and the coal sample to the final temperature of pyrolysis, when the other pulse took over and maintained the temperature for the desired duration. Heating rates as high as $1000^{o}C$/sec could be achieved by properly choosing the amperage and the duration of the first pulse. However, smooth

transition to the second pulse became increasingly difficult after $500^{o}C$/sec. Limitation on the controller ruled out rates higher than $1000^{o}C$/sec.

The temperature of the coal particles was monitored as a function of time with the help of the thermocouple inserted between the folds of the wire screen. The leads of the thermocouple were fed to a digital voltmeter for temperature read-out in terms of millivolts. An analog output from the voltmeter was connected to an oscilloscope for continuous recording of time-temperature history. This history was monitored in every experiment.

The reactor was mounted on extended metallic arms so that if desired it could be completely surrounded with an oven mobile on rails. By maintaining the oven at 100^{o}- $200^{o}C$, the medium range molecular weight organic compounds deposited on the inside reactor walls could be vaporized for chromatographic analysis after a pyrolysis experiment.

Product Collection and Analysis: Characterization of the pyrolysis products is indispensable in formulating theoretical concepts about coal's structure and mechanism of reaction. Volatile products of low temperature pyrolysis have a one-to-one correspondence with components of coal's structure. Accordingly, product collection (avoidng loss on surfaces and by secondary reactions) and analysis (accuracy) were important aspects of the experiments performed.

Gas analysis was done using chromatography. Before heating the coal sample, the reactor was evacuated and flushed with helium several times to remove the air. During heating, the reactor was isolated by

closing the inlet and the outlet valves. The gases produced remained in the reactor for a few minutes before their analysis began. To check the possibility of secondary interactions (e.g., chemical reaction or physical adsorption) due to the continued contact between the gases, the char, and the hot screen, several experiments were done in which the gases were collected in a separate container or in a Porapak Q trap in liquid nitrogen, and then analyzed. It was determined that storage of gases inside the reactor did not have any adverse effects. Internal collection is preferred over external collection because it results in better mass balances.

Two gas chromatographs were used. One was a Varian Aerograph (series 1400) fitted with two thermal conductivity detectors for analyzing the inorganic gases: hydrogen, carbon monoxide, carbon dioxide and water vapor. Porapak, Carbosieve and Molecular Sieve columns were used. Lower hydrocarbons (CH_4, C_2H_4, C_2H_6) were also detected using this chromatograph. The other was an HP 5710A installed with a flame ionization detector. Porapak and SE-30 columns were used for analyzing lower and middle range organic compounds (up to C_6). Temperature programming was extensively used with both instruments.

The signals from the chromatographs were fed to an integrator (Spectra-Physics, Autolab System I) for digital integration of the peaks and for subsequent data reduction. A recorder (Linear Instruments Corp., Model 251) connected to the integrator generated chromatograms for each analysis.

The chromatographs were calibrated by taking samples from the reactor containing a known mixture of gases. For this purpose the

reactor was assembled as for an experiment except that there was no coal sample in the screen. This method of calibration cancelled any errors introduced in subsequent analysis by background effects.

In general, identification and quantification of gaseous products by chromatography was good. The only major difficulty was with integration of water-vapor peaks. Because of its polar properties, the separation of water vapor by the earlier-mentioned stationary phases resulted in a skewed peak with a long tail. For low concentrations, a substantial portion of the peak area was under the tail which was generally ignored by the integrator. At higher concentrations, the accuracy of integration improved.

The tar produced during the reaction was found deposited on all available surfaces inside the reactor. Most of it was recovered by lining the inside walls (of both top and bottom parts) with aluminum foils. The foils were weighed before and after the experiment and the tar was dissolved in tetrahydrofuran (THF). Glass wool soaked in THF was used to collect the tar from other surfaces in the reactor (e.g., electrodes). The micropore filter at the gas exit retained the suspended aerosols of tar. The tar samples from the three sources were combined and filtered. Subsequently THF was removed by evaporation and the sample left was sealed in a flask under argon. Samples from several replicate experiments were combined for Gel Permeation Chromatography (GPC).

The details of GPC and NMR analysis of tar have been previously reported by Gavalas and Oka (1978). In brief, a 52 cm long column containing 200 - 400 mesh particles of crosslinked polystyrene (Bio Beads SV-8) with molecular exclusion limit of 1000 was used for GPC. Three fractions were

collected from the column with molecular weights in the ranges 300 - 700, 700 - 1000, and greater than 1000. The column was calibrated with model compounds. The ^{1}H and ^{13}C NMR were done using Varian spectrometers. Again, THF was used as the solvent and the solvent signals were subtracted from the main signals. Model compounds were used to test the accuracy of the results. Elemental compositions of tar fractions were also determined.

A Typical Experiment: Samples were prepared for experiments by grinding large chunks of coal in a ball mill and subsequent overnight drying in vacuum at 100°C. To avoid atmospheric oxidation or moisturization, the samples were stored in a dessicator in brown bottles flushed with argon.

A 200 mg sample was weighed and spread between the folds of the screen. Care was taken to spread the sample uniformly near the center (longitudinal) of the screen. It was found that temperature was not uniform near the ends, possibly due to heat loss to the electrodes. The ends of the screen were mounted on the electrodes and stretched. Aluminum foils, appropriately cut for the shape and size of the reactor, were weighed and placed on the inside reactor walls. The thermocouple was positioned such that its junction was surrounded by coal particles in the screen.

Next, the two parts of the reactor were bolted together. The reactor was alternately evacuated and flushed with helium several times. The settings on the power supply and the controller were preset for the desired temperature and duration after repeated trials with first the screen only, and then with the screen and a sample. After shutting off the inlet and outlet valves, the power supply was switched on. The

temperature was monitored with the voltmeter and the oscilloscope.

After heating was completed, the reactor was pressurized with helium to a specific pressure to allow reasonable flow rates between the reactor and the sampling valves of the gas chromatographs. Occasionally gas samples were taken from the reactor with precision syringes. After the gas analysis was completed (with both the GC's) the reactor was disassembled and the char on the screen, and the aluminum foils were weighed. The tar was collected as described earlier.

3. The Experimental Program

The coals and the range of experimental conditions employed are summarized in the table 6.3.1. As mentioned before, subbituminous and bituminous coals are of interest both from the industrial and the academic viewpoints. The temperature range used was that of "primary" pyrolysis. Beyond about 700^{o}C, the pyrolytic change may be rather drastic, making it difficult to obtain information on coal's structure by analyzing the products. The heating rate was generally about 500^{o}C/sec. The controller allowed a maximum heating rate of 1000^{o}C/sec. The pressure in the reactor varied from about 70 mm of mercury to 2 atmospheres. The reactor developed leaks at higher pressures. While most experiments were performed in an environment of helium, some experiments were conducted in an atmosphere of isobutane (as a hydrogen donor). Coal particles ranged from 100 to 450 microns in size (their largest dimension).

Basically, three types of experiments were performed:

Table 6.3.1

Experimental Program

Coal Type	:	Bituminous, Subbituminous
Temperature	:	450^{o} - 650^{o}C
Heating Rate	:	50 - 1000^{o}C/sec
Pressure	:	Vacuum - 2 atm.
Carrier Gas	:	Helium, Isobutane
Particle Size	:	80 - 450 μm

(1) Tar Collection Experiments

(2) Transport Experiments

(3) Kinetic Experiments

The tar collection experiments yielded large samples of tar for analysis with GPC and NMR. The results gave valuable information on distribution of carbon and hydrogen among aliphatic and aromatic structures, and on the mechanism of tar formation. The transport experiments helped in elucidation of mass transfer limitations within coal particles. The dependence of yield and selectivity on pressure and particle size was measured. The effects of temperature, time and time-temperature history were studied under the kinetic experiments.

4. Results and Discussion

We will discuss the results for each type of experiment separately.

Table 6.4.1 shows the elemental composition of the four coals for which results will be presented here. Although some other coals were also studied, the results obtained were mostly qualitative. The carbon content varies from 67.8% to 81.3%, while the atomic C/H ratio is between 0.75 and 0.85. The oxygen contents of the subbituminous and the PSOC-190 coals are high compared to the other two coals. Nitrogen and sulfur contents are low in all the coals. Thus, the emphasis on the carbon, hydrogen and oxygen structures in this research is justified.

The table shows that the ash content of a coal sample depends on the size of the coal particles. This is due to differences in the resistance to mechanical breakage of the different petrographic components

Table 6.4.1

Elemental Composition of Coals (dry)

Coal	Particle Size Mesh	Ash %	C %	H %	N %	S %	O (diff.)
Subbituminous B, Wyoming Monarch Seam, PSOC-241	35 - 45	6.0	67.8	4.7	1.2	0.8	19.5
	120 - 170	8.8	65.6	4.5	1.2	1.2	18.7
HVC Bituminous, Illinois #6 Seam, PSOC-190	34 - 45	8.1	68.6	4.8	1.1	3.0	14.4
	120 - 170	11.1	65.0	4.6	1.1	3.3	14.9
HVC Bituminous, Hamilton Kentucky #9 Seam	35 - 45	6.9	73.8	5.2	1.5	3.0	9.6
	60 - 80	7.9	73.5	5.1	1.5	3.3	8.7
	120 - 170	8.1	72.9	5.0	1.4	3.3	9.3
HVB Bituminous, West Virginia	35 - 45	5.5	81.3	5.4	1.4	0.7	5.7
	60 - 80	5.7	81.0	5.4	1.4	0.7	5.8
	120 - 170	6.0	81.0	5.3	1.4	0.8	5.5

(macerals) in coal. As a result, the grinding and sieving operations involved in preparation of coal samples affect the relative concentrations of different macerals. Consequently, the composition of a sample depends on its particle-size. To prevent the effects of such differences from masking the particle-size dependence of physical processes, most of the results reported here are on an ash-free basis. The relative enrichment of ash in smaller particles has also been discussed by Suuberg (1977).

Tar Analysis Results: Tables 6.4.2 and 6.4.3 show the results of tar analysis for three coals.

In the table 6.4.2, GPC analysis of THF-soluble tar obtained from the HVC bituminous (Hamilton) coal under different experimental conditions is shown. The last three columns give the weight % of tar in three molecular weight ranges: 300 - 700, 700 - 1000, and greater than 1000. The first, quick observation that can be made about these results is that the numbers in the same column are very close to each other (with a few exceptions). Since the experiments were performed under different conditions of time, temperature, particle size and surrounding environment, the closeness of the numbers implies that the tar composition is not a very strong function of these variables. This is a significant observation because it ties up with the mechanism of tar production discussed in Chapter 3. It was concluded that tar is a random sample of coal, consisting of aromatic clusters which are disconnected from the coal matrix due to bridge dissociation. Since a random process is not affected very significantly by moderate variations in the experimental conditions, we do not observe wide variations in the molecular weight

Table 6.4.2

Molecular Weight Fractionation (by GPC) of Tar Obtained from Pyrolysis of a HVC Bituminous Coal (Hamilton)

S.N.	Temperature °C	Duration, Minutes	Particle Size Mesh	Reactor* Environment	Weight %		
					Molecular Weight Range 300 - 700	Molecular Weight Range 700 - 1000	Molecular Weight Range >1000
1	500	2.5	45/60	Helium	36	47	17
2	600	2.5	45/60	Helium	37	51	12
3	450	2.5	60/80	Helium	34	49	17
4	500	0.5	60/80	Helium	38	44	18
5	500	2.5	60/80	Helium	30	52	17
6	500	2.5	60/80	Vacuum	32	49	19
7	500	2.5	60/80	Isobutane	31	54	15
8	500	2.5	60/80	Isobutane	37	49	15
9	600	2.5	60/80	Helium	37	50	13
10	500	1.0	120/170	Vacuum	21	48	31
11	500	2.5	120/170	Isobutane	34	51	14
12	600	2.5	120/170	Helium	37	46	17

*Gas pressure in the reactor was 1 atmosphere.

distribution of tar. Thus, these results substantiate the mechanism of tar production used in the model.

The three fractions can be interpreted (for this coal) as percentages of tar fragments consisting of two clusters, three clusters and more than three clusters, respectively. Approximately 50% of the fragments consist of three clusters. Larger fragments face more severe transport limitations compared to smaller fragments, and it is unlikely that they are a direct product of bridge dissociation. Most probably, the majority were formed by combination of single cluster fragments in the pore phase (transition and macropores). However, we cannot be sure of this mechanism because of the various attendant complications, e.g., possibility of dissociation of bridges between the clusters of a multicluster fragment. But it is interesting to note that the distribution shifts in favor of the bulkier fragments in the tar obtained from the smallest particles (120/170 mesh) under vacuum (S.N. 10). Thus, clearly tar molecules face mass transfer limitations within coal particles.

Results for ^{1}H and ^{13}C NMR for extracts and pyrolysates of three coals are shown in the table 6.4.3. Because of the lack of adequate samples, the ^{13}C NMR results could not be obtained for the pyrolysates. Although, as mentioned earlier in this thesis, the characteristics of a coal may be somewhat different from those of its derivatives, such results as shown in the table can give us very valuable information. Pyrolysate results will be more relevant considering the low yields of extracts. They were used in the last chapter to calculate the concentrations of the functional groups in coal.

Table 6.4.3

Elemental Analysis, Molecular Weights and NMR Data for Extracts and Pyrolysates

Coal	Sample	Yield Wt. %	GPC* (%)			^{1}H NMR (%)			^{13}C NMR (%)		Elemental Analysis					
											L		M		S	
			L	M	S	H_α	$H_{\beta+}$	H_{ar+Ph}	C_{ar}	C_{al}	C	H	C	H	C	H
Subbituminous	Ext.	4.5	32	54	14	20	68	12	42	58	76.1	8.9	77.5	8.7	82.6	8.5
	Pyr.	6.0	26	48	26	23	58	19	-	-	75.6	8.1	73.7	8.3	76.1	7.3
HVC Bituminous (Hamilton)	Ext.	8.0	36	48	16	32	40	28	58	42	81.3	7.8	81.5	7.1	85.5	7.4
	Pyr.	19.1	20	49	31	34	33	33	-	-	75.1	7.1	76.5	7.1	-	-
HVB Bituminous	Ext.	1.6	32	44	24	32	37	31	-	-	85.7	6.9	87.6	7.6	89.5	7.2
	Pyr.	10.5	27	42	31	37	31	32	-	-	85.8	6.7	85.9	8.0	85.9	6.7

*L, M, S: Fractions with molecular weights > 1000, 700 - 1000 and 300 - 700.

^1H NMR results show that more than 60% of the hydrogen occurs in aliphatic structures. The hydrogen distribution was used in the last chapter to calculate the initial concentrations of the sidechains on alpha carbons. The fraction of α to $\beta+$ hydrogen increases with coal rank in both the extracts and the pyrolysates. The same fraction is larger in the pyrolysates than the extracts. Under the conditions employed for these results, the extracts consist mostly of unconnected clusters in the coal. The carbon distribution shows higher aromaticity for higher rank coal.

Results of Transport Experiments: The effect of transport limitations (within coal particles) on the yield and composition of the products was investigated by varying the particle size in the range 100 to 450 μm, and the pressure between one atmosphere of helium and vacuum ($\sim$ 70 mm of Hg).

Tables 6.4.4 - 6.4.7 show particle size dependence of results for each pressure for the Hamilton coal. Tables 6.4.4 and 6.4.6 show the overall results, while composition of hydrocarbon gases is shown in the tables 6.4.5 and 6.4.7. The missing material was computed as the difference between the weight loss and the weight of identified volatiles. It is believed that the missing material must have been tar because not all of the tar formed was recoverable. Tar is deposited on all exposed surfaces inside the reactor and is difficult to collect. Hence, while computing the tar selectivity (the last column in the tables 6.4.4 and 6.4.6), the missing material was added to the "observed" tar. Solomon (1977) adopted a similar approach to account for incomplete mass balances. The detailed analyses of hydrocarbon gases is presented primarily to

Table 6.4.4

Particle Size Dependence of Pyrolysis Results for a HVC Bituminous Coal (Hamilton, Kentucky # 9 Seam)

$T = 500^{o}C$, $dT/dt = 500^{o}C/sec$, $P = 1$ atm. He, Duration = 30 sec.

Particle Size	Wt. % of Dry, Ash-Free Coal								(Tar + Missing)/ Wt. Loss
	Weight Loss	Tar	CO	CO_2	H_2O	CH_4	C_{2+}*	Missing	
35/45 Mesh (~ 450 μm)	24.8	18.64	0.213	0.531	2.857	0.433	1.530	0.596	77.6%
60/80 Mesh (~ 200)	28.1	20.30	0.277	0.530	2.176	0.544	1.762	2.511	81.2%
120/170 Mesh (~ 110)	28.2	20.10	0.243	0.538	2.930	0.495	1.598	2.296	79.4%

*Composition of the hydrocarbon gases is given in Table 6.4.5.

Table 6.4.5

Particle Size Dependence of Hydrocarbon Gases from Pyrolysis of a HVC Bituminous Coal (Hamilton, Kentucky # 9)

$T = 500^{o}C$, $dT/dt \approx 500^{o}C/sec$, P = 1 atm. He, Duration = 30 sec.

Particle Size	Wt. % of Dry, Ash-Free Coal											
	C_2H_4	C_2H_6	C_3H_6	C_3H_8	unidentified	C_4H_8	C_4H_{10}	iso-C_5H_{12}	C_5H_{12}	iso-C_6H_{14}	C_6H_{14}	C_6H_6
35/45 Mesh (∿450 μm)	0.085	0.328	0.204	0.204	0.058	0.114	0.205	0.092	0.092	0.059	0.045	0.044
60/80 Mesh (∿200 μm)	0.104	0.396	0.235	0.236	0.059	0.134	0.226	0.085	0.085	0.067	0.098	0.037
120/170 Mesh (∿ 110 μm)	0.099	0.362	0.181	0.233	0.053	0.128	0.205	0.081	0.082	0.063	0.055	0.056

Table 6.4.6

Particle Size Dependence of Pyrolysis Results for a HVC Bituminous Coal (Hamilton, Kentucky # 9)

$T = 500^{o}C$, $dT/dt \approx 500^{o}C/sec$, P = Vacuum ($\sim$ 70 mm of Hg), Duration = 30 sec.

Particle Size	Wt. % of Dry, Ash-Free Coal								(Tar + Missing)/ Wt. Loss
	Weight Loss	Tar	CO	CO_2	H_2O	CH_4	C_{2+} *	Missing	
35/45 Mesh ($\sim$ 450 μm)	27.7	21.94	0.171	0.493	1.611	0.344	1.126	2.015	86.5%
60/80 Mesh ($\sim$ 200 μm)	30.3	23.83	0.195	0.495	2.172	0.419	1.179	2.010	85.3%
120/170 Mesh ($\sim$ 110 μm)	28.6	22.69	0.128	0.467	1.632	0.290	0.987	2.406	87.7%

*Composition of the hydrocarbon gases is given in Table 6.4.7.

Table 6.4.7

Particle Size Dependence of Hydrocarbon Gases from Pyrolysis of a HVC Bituminous Coal (Hamilton, Kentucky # 9)

$T = 500^{o}C$, $dT/dt \approx 500^{o}C/sec$, P = Vacuum ($\sim$ 70 mm of Hg), Duration = 30 sec.

Particle Size	Wt. % of Dry, Ash-Free Coal											
	C_2H_4	C_2H_6	C_3H_6	C_3H_8	unidentified	C_4H_8	C_4H_{10}	iso-C_5H_{12}	C_6H_{12}	iso-C_6H_{14}	C_6H_{14}	C_6H_6
35/45 Mesh ($\sim$ 450 μm)	0.073	0.240	0.146	0.147	0.043	0.083	0.137	0.069	0.081	0.043	0.032	0.032
60/80 Mesh ($\sim$ 200 μm)	0.085	0.280	0.142	0.173	0.039	0.086	0.135	0.065	0.083	0.042	0.025	0.024
120/170 Mesh ($\sim$ 110 μm)	0.061	0.194	0.102	0.127	0.040	0.066	0.094	0.100	0.077	0.045	0.062	0.019

indicate their range: C_1 - C_6. Higher hydrocarbons probably condensed as tar. It is interesting to note that alkanes are higher than alkenes. This is in agreement with their mechanisms of formation as shown in the table 4.6.1.

The weight loss at vacuum is higher than at atmospheric pressure for each of the three particle sizes. Reduction in the particle size has a more significant effect at atmospheric pressure than at vacuum. Similarly, the amount of tar is higher and the gases are less at vacuum for each of the three cases. This trend is more clearly shown by the increase in tar selectivity in going from atmospheric pressure to vacuum. The higher mass transfer limitations on tar molecules and the inverse relationship between tar and gas formation were discussed in the earlier chapters in detail. These experimental results justify the concept of competitive reactions as opposed to independent parallel reactions. In the latter case, reduction in mass transfer limitations on one of the products should not affect the absolute amounts of the others, which is clearly not the case.

Results for PSOC-190 coal (tables 6.4.8 and 6.4.9) show similar trends, although mass balances here may be considered slightly worse than in the previous coal. Both weight loss and tar are higher under vacuum, except for the smallest particle size (120/170) for which differences are negligible. This coal gives more oxygen containing gases (CO, CO_2, H_2O) compared to the Hamilton coal as would be expected considering its higher oxygen content (table 6.4.1). Higher amounts of water vapor explain the difference in the yield of tar: higher concentrations of phenolic groups lead to higher concentrations of ether linkages, which increases cross-linking among clusters, making the structure more tight. Therefore, oxygen

Table 6.4.8

Particle Size Dependence of Pyrolysis Results
HVC Bituminous Coal (PSOC-190)

$T = 500^{o}C$, $dT/dt \approx 500^{o}C/sec$, $P = 1$ atm. He, Duration = 30 sec.

Particle Size	Wt. % of Dry, Ash-Free Coal								(Tar + Missing)/ Wt. Loss
	Weight Loss	Tar	CO	CO_2	H_2O	CH_4	C_{2+}	Missing	
35/45 Mesh (∿ 450 μm)	20.57	7.83	0.98	2.61	5.98	0.46	0.76	1.95	47.5%
45/60 Mesh (∿ 280 μm)	20.78	8.27	0.97	2.45	5.98	0.37	0.76	1.98	49.3%
60/80 Mesh (∿ 200 μm)	22.10	8.24	0.77	2.42	6.04	0.29	0.77	3.57	53.4%
120/170 Mesh (∿ 110 μm)	25.00	8.66	1.01	4.95*	6.19	0.33	0.79	3.07	47.0%

*Most likely incorrect.

Table 6.4.9

Particle Size Dependence of Pyrolysis Results for a HVC Bituminous Coal (PSOC-190)

$T = 500^{o}C$, $dT/dt \approx 500^{o}C/sec$, $P \approx 70$ mm of Hg, Duration = 30 sec.

Particle Size	Wt. % of Dry, Ash-Free Coal								(Tar + Missing/ Wt. Loss
	Weight Loss	Tar	CO	CO_2	H_2O	CH_4	C_{2+}	Missing	
35/45 Mesh (~ 450 μm)	22.74	9.36	0.96	2.35	5.98	0.24	1.09	2.76	53.3%
45/60 Mesh (~ 280 μm)	22.36	9.03	0.55	2.52	5.98	0.16	1.09	3.03	53.9%
60/80 Mesh (~ 200 μm)	23.10	8.80	1.10	2.48	6.04	0.34	1.10	3.24	52.1%
120/170 Mesh (~ 110 μm)	25.00	9.00	1.69	5.42*	6.19	0.36	1.12	1.22	41.0%

*Most likely incorrect.

has a detrimental effect on tar yield.

Pressure and particle size dependence is also seen in the results for the subbituminous coal (tables 6.4.10 and 6.4.11). The amounts of tar are lower than in the previous coals. Again, the reason is higher etheric cross-linking as evidenced by higher amounts of water produced. Oxides of carbon are also produced in larger amounts.

The overall conclusion of transport experiments can be stated as follows: although smaller particles and lower pressures result in slightly higher yields of tar, the increase does not justify inclusion of an elaborate transport model in an already complicated kinetic model. It should be noted that this conclusion does not apply to the transport limitations within micropore systems (but only to macropore systems). Secondary reactions like recombination of free tar clusters with the coal matrix occur mostly within a subunit (figure 3.4.1), and transport analysis within that region is a desirable feature.

Results of Kinetic Experiments: Effects of time, temperature and time-temperature history were studied under these experiments.

Time-resolved data for Hamilton coal at 510^{o}C were presented in the last chapter. They were obtained by repeating the experiment for different time durations. Difficulty was encountered in getting reliable results for durations of less than 10 seconds. In all experiments with this coal, it was observed that the final, steady temperature could not be attained in less than five seconds. Even at high settings of the power supply, the temperature rose rapidly up to 450^{o}C, but after that took about 3 to 4 seconds to reach the final, steady value. This resulted in low yield of

Table 6.4.10

Particle Size Dependence of Pyrolysis Results
for a Subbituminous Coal (PSOC-241)

$T = 520^{o}C$, $dT/dt \approx 500^{o}C/sec$, $P = 1$ atm. He, Duration = 30 sec.

Particle Size	Wt. % of Dry, Ash-Free Coal								(Tar + Missing)/ Wt. Loss
	Weight Loss	Tar	CO	CO_2	H_2O	CH_4	C_{2+}	Missing	
35/45 Mesh (~ 450 μm)	22.34	6.28	1.63	6.54	6.00	0.277	1.0	0.613	30.85%
45/60 Mesh (~ 280 μm)	23.30	6.28	2.40	7.60	5.57	0.340	1.0	0.100	29.70%
60/80 Mesh (~ 200 μm)	25.00	6.56	2.42	7.53	6.00	0.344	1.0	1.146	30.82%
120/170 Mesh (~ 110 μm)	25.90	6.58	1.60	6.41	6.00	0.274	1.0	4.036	41.00%

Table 6.4.11

Pressure Dependence of Pyrolysis Results
for a Subbituminous Coal (PSOC-241)

$T = 520^{o}C$, $dT/dt \approx 500^{o}C/sec$, Duration = 30 sec.

Particle Size	Pressure	Wt. % of Dry, Ash-Free Coal			(Tar + Missing)/ Wt. Loss
		Weight Loss	Tar	Missing	
35/45 Mesh (∿ 450 μm)	70 mm of Hg	23.40	6.38	0.800	30.70%
	1 atm of He	22.34	6.28	0.613	30.85%
120/170 Mesh (∿ 110 μm)	70 mm of Hg	25.20	7.35	3.500	43.00%
	1 atm of He	25.90	6.58	4.036	41.00%

products. The rate of weight loss computed on the basis of the results for 3, 5 and 8 second durations was appreciably less than for the longer durations. In other words, there was an initial lag in volatile product formation. It is believed that this lag can be attributed to the initial melting of the coal when it attains a plastic state. Anthony and Howard (1976) have pointed out that the temperature of transition to the plastic state in coals is very similar to that of pyrolysis. It generally starts around 420^{o}C. The volatile products cannot escape because the entire structure begins to collapse and the pores are filled with liquid. Consequently, regions of highpressure gas are formed within the particle, and they expand until they eventually burst through the particle surface. Because some time will pass before the gas in the bubbles escapes (after it has been chemically produced), there is a delay in volatile production.

However, the data for longer durations (refer to figures 5.4.13 - 5.4.18) clearly show the characteristic time profiles of pyrolysis products. The rate of tar production remains higher compared to the rate of gas production for a long time. However, after about 20 seconds tar production slows down slightly while gas production picks up. Most of the water is formed in the first ten seconds. After about 70 to 80 seconds, the products reach an asymptotic value.

Dependence of ultimate weight loss on temperature for the Hamilton coal is shown in the figure 6.4.1. It appears that the weight loss will stabilize after about 650^{o}C. Solomon 's results (1977) for a variety of other coals show similar behavior. However, beyond about 900^{o} or 1000^{o}C, the weight loss may increase again due to more drastic transformations leading to graphitization.

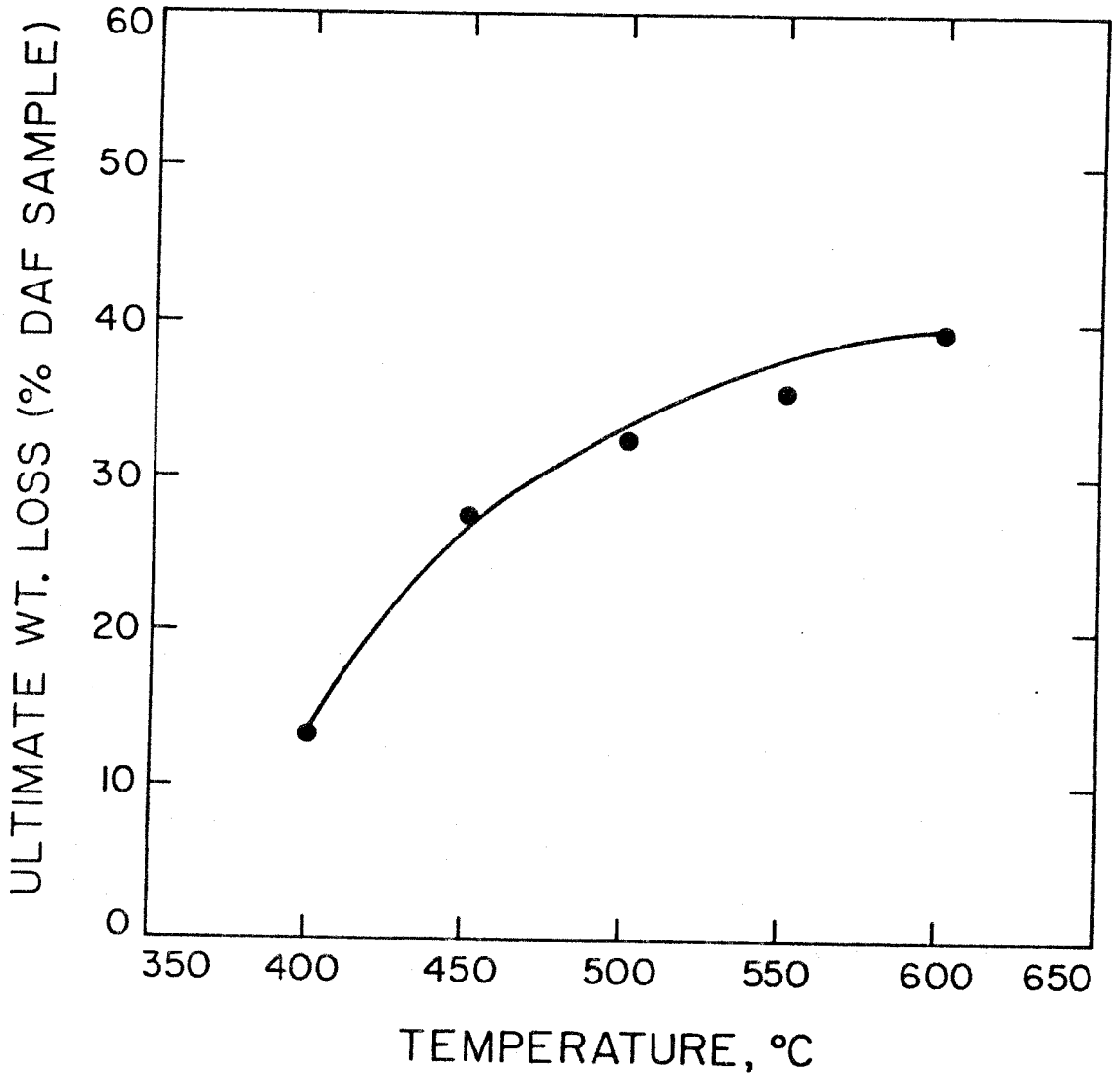

Figure 6.4.1: Variation of Ultimate Weight Loss with Temperature for the Hamilton Coal.

The almost asymptotic behavior between 600^{o} and 900^{o}C is very interesting because it points to the pivotal importance of structural constraints on volatile production. As shown in the model predictions in the last chapter, the tar attains an asymptotic value at some temperature between 550^{o} and 600^{o}C, while the gases stabilize at slightly higher temperatures (around 650^{o}C). Increasing the temperature further does not significantly increase the yield predicted bythe model. The double bonds present in the structure make further dissociation impossible.

The importance of time-temperature history in pyrolysis has been discussed earlier in Chapters 3 and 5. Results of different heating profiles for the subbituminous coal are shown in the figures 6.4.2 and 6.4.3. In the four cases shown in the figure 6.4.2, the final temperature (600^{o}C) is attained in 20, 15, 10 and 5 seconds, respectively. The weight loss increases with increasing heating rate. The last two cases in the figure 6.4.3 show a similar trend for a smaller particle size. The weight loss of 24.5% for a heating rate of 100^{o}C/sec in case (a) compares with 25.9% obtained for a heating rate of 500^{o}C/sec (table 6.4.10).

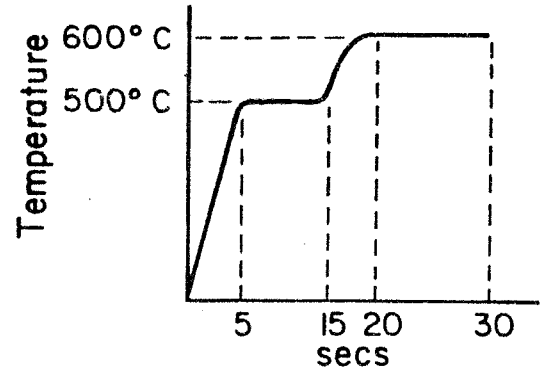

(a) Wt. Loss (% of Dry Sample) = 32.8%

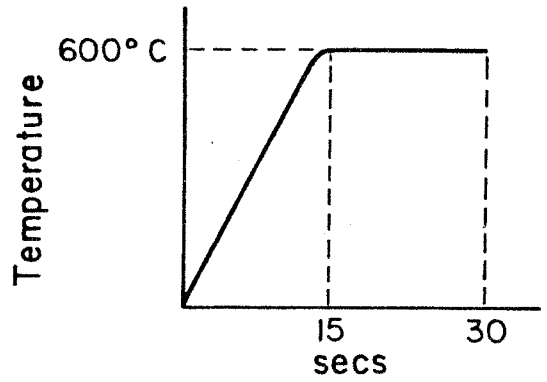

(b) Wt. Loss = 32.4%

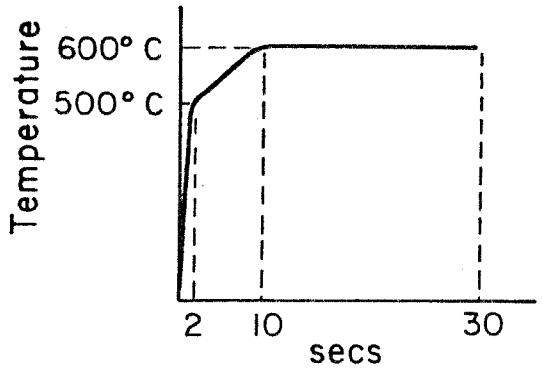

(c) Wt. Loss = 33.9%

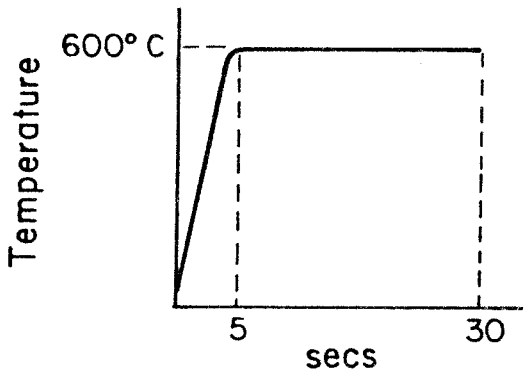

(d) Wt. Loss = 34.8%

Figure 6.4.2: Effect of Time-Temperature History on Wt. Loss Subbituminous Coal (PSOC-241). Particles: 60/80 Mesh, P = 1 atm. He.

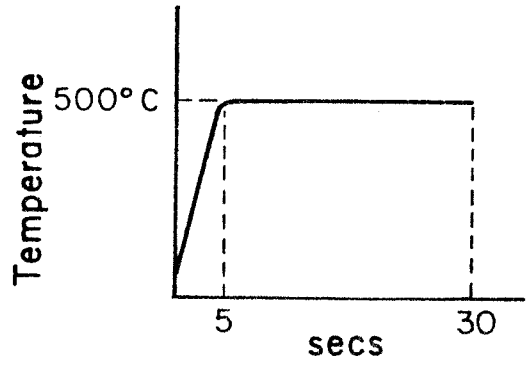

(a) Wt. Loss (% of Dry Sample) = 24.5%

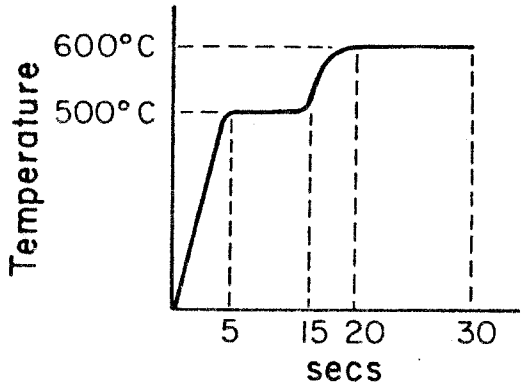

(b) Wt. Loss = 35.3%

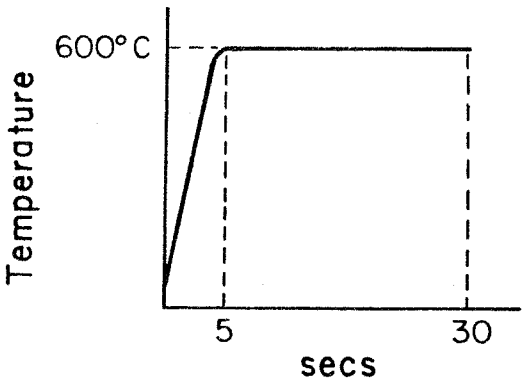

(c) Wt. Loss = 37.6%

Figure 6.4.3: Effect of Time-Temperature History on Wt. Loss Subbituminous Coal (PSOC-241). Particles: 120/170 Mesh, P = 1 atm. He.

Chapter VII

CONCLUSIONS AND RECOMMENDATIONS FOR FUTURE WORK

We will first discuss the model and the experiments separately, identifying the avenues open for further investigation. Then, the overall conclusions will be presented.

The Model

The objective in modeling was to devise a mathematical scheme for simulation of the structure and pyrolytic behavior of coal, based on the chemical and physical mechanisms involved. Almost half of the effort consisted of identifying these mechanisms, the other half being devoted to their mathematical simulation. The following paragraphs discuss the various aspects of the model point by point.

Consider first the chemical system consisting of the various functional groups and their reactions. Coal was modeled as a population of average aromatic clusters, connected together by bridges, and carrying sidechains. The bridges consisted of the methylene and the ethylene type, while the sidechains consisted of ($-H_\alpha$), ($-CH_3$), ($-C_2H_5$), and hydroaromatic structures. The oxygen functional groups considered were carboxylic, carbonyl, phenolic and etheric. The model neglected structures involving nitrogen and sulfur. Reactions were considered unlikely in the aromatic portion in the temperature range of interest. In the aliphatic portion, series-parallel reactions were initiated by dissociation of sidechains and bridges forming alpha radicals. Sidechain dissociation leads to gas formation, and bridge dissociation leads to tar formation. Carbon dioxide and carbon monoxide were produced from carboxylic and carbonyl groups, respectively, while phenolic condensation leads to formation of water vapor and ether linkages.

Representation of coal structure as a collection of randomly distributed functional groups (whose total concentrations are specified)

à priori assumptions about the maximum yield, and do not explain its dependence on temperature. Two revisions in the oxygen-group reactions may be considered for a future model: production of carbon monoxide from groups other than carbonyl, e.g., quinones; dissociation of ether bridges. The origin of carbon monoxide in coal pyrolysis is not well established and it is best to include more than one source. Consideration of ether bridge dissociation may be necessary in order to simulate temperature dependence of tar more accurately. As the temperature increases, the increased rate of phenolic condensation rapidly increases the cross-linking among clusters, reducing the probability of free cluster formation. If ether bridges are considered unbreakable, tar production at higher temperatures is adversely affected. Therefore it is desirable to account for their rupture. Lack of specific kinetic information on the rupture was the reason for its exclusion from this model.

Recombination of free clusters with the coal matrix was simulated in the model by reducing the rates of bridge dissociation reactions. The parameter x was interpreted as the fraction of the subunit volume — the surface region — active in tar production. This was a simple way of modeling a complicated situation which if treated rigorously involves consideration of tar residence time and spatial distribution of radicals in the coal matrix. Rigorous treatment is necessary if the pressure and the particle size dependence of the results is to be predicted. However, the complexity of the phenomena involved and the lack of data on relevant parameters makes it difficult to devise a simple but theoretically sound approach to account for the recombination reactions. More investigations are needed in this area in the future.

Another modification that may be considered regarding tar production is to include two-cluster fragments in the volatiles. Restricting the tar to only single-cluster fragments, as was done in this model, may not be justified at high temperatures (at which two-cluster fragments may possess sufficient vapor pressure), especially for coals in which an average cluster consists of less than two rings. However, to include the two-cluster fragments, a more elaborate model of distribution of bridges among clusters will be needed. Probabilities of generation of one-cluster fragments and two-cluster fragments will have to be considered separately.

The mathematics involved in the model was simple in concept but complicated in details. It was mentioned in Chapter 4 that the K's — the concentrations of different combinations of functional groups — are an alternative set of state variables. In retrospect, their selection as state variables might have resulted in some simplifications. The redistribution of functional groups at each step of integration would not have been necessary, and the computation of the rate of loss of functional groups with departing free clusters would have been somewhat simpler. The latter simplification can also be attempted independently by avoiding detailed accounting of each and every substitutent on the departing alpha carbons, e.g., by assuming that the rate of loss of a functional group is proportional to its instantaneous concentration.

Although the differential equations formulated were valid only for those cases for which each cluster carried either 3 or 4 alpha carbons, extension of the model to other cases is quite straightforward. The rates of loss of functional groups will have to be revised. In a future model it would be desirable to remove this restriction altogether by taking into

account all situations between 1 and 5 alpha carbons per cluster. However, this will necessitate a revision in the scheme for distributing alpha carbons amongst clusters.

Lack of reliable kinetic data on the reactions considered in the model makes it necessary to estimate and adjust the kinetic parameters. As discussed in Appendix II, base values for the parameters of some of the reactions can be obtained from the literature. Approximate modifications are made in these values to account for the effect of the surrounding groups on the reactions of a functional group. For some reactions for which no information was available, the kinetic parameters were estimated to lie in a certain range and the calculations used values within this range. With the continuing research on the kinetics of free radical reactions, it is likely that this area of uncertainty will diminish.

The Experiments

The experimental work was primarily aimed at obtaining information that could be used as a guideline in theoretical formulation. For example, the results of the tar collection and analysis experiments substantiated the view that low temperature tar is a random sample of the parent coal, and the two have very similar characteristics. This justifies the mechanism proposed in the model that tar is produced by dissociation of bridges. Similarly, use of NMR data in calculating the initial concentrations of various functional groups was demonstrated in Chapter 5.

The transport experiments determined the pressure and particle-size dependence of the yield and distribution of pyrolysis products. It was

concluded that the dependence was not very significant in the range of parameters investigated. Therefore, no provision was made in the model to simulate this dependence.

The effects of time and temperature on pyrolytic behavior were identified by the kinetic experiments. The trends determined guided all aspects of modeling. For example, leveling of volatile yield after some time indicated the occurrence of deactivating reactions which resulted in the formation of char. Similarly, leveling with temperature established the critical dependence of the ultimate yield on structural constraints. Higher initial rate of tar formation compared to gas formation, and increased gas formation at higher temperatures, indicated higher activation energy for gas-producing reactions as compared to tar-producing reactions. Several similar conclusions provided insight into the mechanism of product formation.

It would be desirable to obtain more time-resolved data in the future. Specifically, the effect of melting on short-time pyrolysis should be investigated in detail. It was mentioned in Chapter 6 that melting of coal delays volatile production by a few seconds, possibly due to the blockage caused by the collapse of the pore structure. It will be interesting to compare this behavior with that of other coals, like subbituminous, which largely retain their pore structure.

Overall Conclusions

The objective of this research was to formulate a general theory about the structure and reactivity of coals. Broadly speaking, such a theory points to the similarity of various different types of coals by

sorting out the common features. Specifically, it identifies the important components of a coal's chemical structure and their reactions, points out the dominant mechanisms involved, and helps in isolating the areas requiring further investigation. The work presented in this thesis meets these broad and specific goals.

In the opinion of the author, continued basic research on coal is needed to initiate and support coal's large scale industrial utilization. Efforts being made towards development of chemical and physical techniques for direct elucidation of coal's structure should be promoted. An experimental program to study free-radical reactions of the type of organic structures found in coal is also needed. Such a program can identify the important product formation mechanisms, and can also establish bounds on the kinetic parameters. Further investigation into coal's physical structure will also be very helpful.

In addition to the laboratory research on coal, work should be done continuously on meshing together the various findings of coal researchers, as was done in this thesis, to synthesize a general, overall picture about coal's chemical behavior. This sort of effort will go a long way in providing guidelines for further research.

APPENDIX I

In this appendix, the state variables used to characterize coal are listed for quick reference.

(1) Alpha Hydrogens: Y_1 (moles/liter)

(2) Methyl Sidechains: Y_2 (moles/liter)

This variable includes the corresponding double bond and beta radical structures.

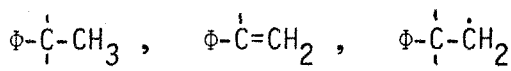

(3) Ethyl Sidechains: Y_3 (moles/liter)

As in Y_2, this variable also includes the corresponding double bond and beta radical structures.

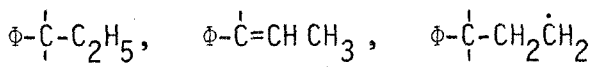

(4) Ethylene Type Bridges: Y_4 (moles/liter)

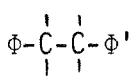

Y_4 corresponds to the number of alpha carbons involved in such bridges.

(5) Hydroaromatic Structures: Y_5 (moles/liter)

As in the case of Y_2 and Y_3, Y_5 includes the corresponding double bond and beta radical structures.

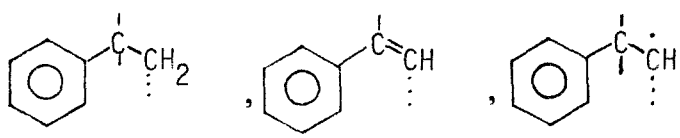

A hydroaromatic structure is visualized to be divided into half, and

Y_5 corresponds to the concentration of such imaginary half structures.

(6) Double Bond Bridges: Y_6 (moles/liter)

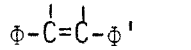

Y_6 corresponds to the number of alpha carbons involved in such bridges.

(7) Double Bond Sidechains: Y_7 (moles/liter)

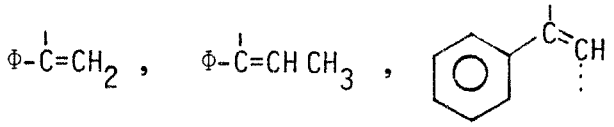

(8) Alpha Carbon Bonds: Y_8 (moles/liter)

(9) Alpha Radicals: Y_9 (moles/liter)

(10) Phenolic Groups: Y_{10} (moles/liter)

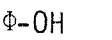

(11) Ether Linkages: Y_{11} (moles/liter)

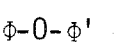

Y_{11} corresponds to the number of clusters involved in such linkages.

(12) Beta Radicals: Y_{12} (moles/liter)

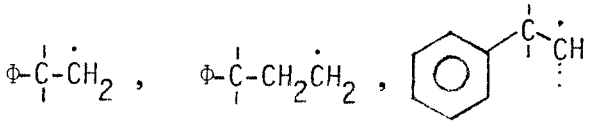

(13) Hydrogen Gas: Y_{13} (moles)

(14) Methane Gas: Y_{14} (moles)

(15) Ethylene Gas: Y_{15} (moles)

(16) Ethane Gas: Y_{16} (moles)

(17) Higher (C_2+) Hydrocarbon Gases: Y_{17} (moles)

(18) Alpha Carbons: Y_{18} (moles/liter)

$\Phi\text{-}\overset{|}{\underset{|\alpha}{C}}\text{-}$

(19) Volume of the coal particles in the sample: Y_{19} (liter)

(20) Water Vapor: Y_{20} (moles)

APPENDIX II

In this appendix, values for the kinetic parameters, A and E, for the reactions listed in table 4.6.1 are presented and discussed.

Bond Dissociation Reactions

Reaction	$\log_{10} A^*$	E(kcal/mole)
1	15.50	84.0
2	15.30	65.0
3	14.90	63.0
4	14.40	52.0
5	14.90	63.0
6	14.40	68.5

*A in sec^{-1}.

Rate parameters for dissociation reactions are based on the characteristics of the bonds involved. O'Neal and Benson (1973) give $\log_{10} A = 15.5$ sec^{-1} and E = 88.3 kcal/mole for the first reaction. We should subtract approximately 3 kcals to account for the fact that the substituent is on a two or three ring system rather than benzene. Similarly, 2 to 5 kcals should be subtracted to take into account the proximity of phenolic or ether groups. Hence, we adjust E_1 to 84 kcal/mole. For the dissociation of methyl groups (reaction 2), O'Neal and Benson (1973) calculated $\log_{10} A = 15.3$ and E = 73.0 kcal/mole. Following the arguments given under reaction 1, activation energy is reduced by 8 kcals. Hence, E_2 = 65 kcal/mole. For the third reaction, O'Neal and Benson (1973) list $\log_{10} A = 14.9$ and E = 68.6 kcal/mole. As before, E is adjusted to

E_3 = 63.0 kcal/mole. Parameters for reaction 5 are taken to be the same as those for reaction 3.

O'Neal and Benson list $\log_{10} A = 14.4$ and $E = 56.8$ for dissociation of ethylene type bridges (reaction 4). We adjust E to 52 kcal/mole. The A factor for reaction 6 is taken to be the same as for reaction 4. Bond-dissociation energy of phenyl-benzyl linkage is listed by Benson (1976) to be 77 kcal/mole. Hence, after adjustment for the surrounding groups, E_6 is taken as E_6 = 68.5 kcal/mole.

Double Bond Formation Reactions

Reaction	$\log_{10} A^*$	E(kcal/mole)
7	12.80	50.0
8	12.80	48.0
9	12.80	50.0
10	12.00	38.0
11	12.00	37.0
12	12.00	37.0
13	12.80	50.0
14	12.00	38.0
15	12.35	38.0
16	12.60	35.0
17	12.45	35.0
18	13.65	35.0
19	13.65	35.0
20	12.45	35.0
21	12.45	36.0

*A in sec^{-1}.

The A factors for reactions 7, 8, 9 and 13 were taken from Cheong (1977). The activation energies for these reactions were obtained by adding the difference between the resonance stabilization energy of the reactant and the product, to the activation energy for an analogous aliphatic reaction. The parameters for reactions 10, 11, 12 and 14 are same as those used by Cheong (1977), except for slight adjustments in the frequency factors. No information on these reactions is available in the literature. For the reactions involving β-radicals, 15 through 21, the values are based on the following reaction:

$$\Phi\text{-}CH_2\text{-}\dot{C}H\text{-}CH_3 \rightarrow \Phi\text{-}CH{=}CH\text{-}CH_3 + H\cdot$$

for which Benson (1976) gives $\log_{10} A = 12.8$ and $E = 38$ kcal/mole.

Recombination Reaction

Reaction	$\log_{10} A^*$	E (kcal/mole)
22	8.00	10.0

*A in sec^{-1} (liter/mole)

The frequency factor A is taken from Cheong (1977). In the gas phase, such a recombination reaction will have zero activation energy. However, in the condensed phase, recombination is hindered by gel effect (discussed in Chapter 4). Hence, following Cheong's approach, an activation energy of 10 kcal/mole is assigned to the reaction.

Hydrogen Abstraction Reactions

Reaction	Log_{10} A*	E (kcal/mole)
23	11.10	10.0
24	11.10	10.0
25	8.00	10.0
26	8.00	10.0
27	8.00	10.0
28	8.00	10.0
29	8.00	20.0

*A is in sec^{-1} (liter/mole)

The frequency factor for hydrogen abstraction by hydrogen atom is $10^{11\pm0.5}$ liter/(mole-sec), and by alkyl radicals is $10^{8.5\pm0.5}$ liter/(mole-sec). The activation energy of a metathesis reaction involving hydrogen transfer is of the order of 10 kcal/mole (both A and E factors for the methathesis reactions are discussed by Benson (1976)). The activation energy for reaction 29 has been increased by 10 kcals to account for reduction in rate due to gel effect.

Addition-Displacement Reactions

Reaction	Log_{10} A*	E (kcal/mole)
30	11.00	15.0
31	7.00	15.0
32	7.00	15.0
33	11.00	10.0
34	7.00	10.0
35	7.00	10.0
36	11.00	10.0
37	7.00	10.0
38	7.00	10.0

*A in sec^{-1} (liter/mole)

There is very little information available on displacement reactions in the literature. Benson (1976) has listed them as one of the three categories of bimolecular reactions, but has given no quantitative information. The values used here are based on the assumption that rates of hydrogen abstraction and displacement reactions are very similar. Cheong (1977) has pointed out that this assumption is justified on the basis of pyrolysis data for toluene. Szwarc (1948) observed that the ratio of hydrogen to methane in the products of toluene was 60% to 40%. It is believed that methane is formed primarily due to the displacement of methyl groups by hydrogen atoms. Therefore, a 60-to-40 ratio indicates comparable rates of hydrogen abstraction and displacment reactions.

Phenolic Condensation Reaction

Reaction	$Log_{10} A^*$	E (kcal/mole
39	8.50	35.0

*A in sec^{-1} (liter/mole)

The author was unable to find any reliable kinetic data on phenolic condensation. From coal pyrolysis data it is obvious that its activation energy is less than that of the dissociation reaction. We use values typical of kinetic parameters of bimolecular reactions.

Literature Cited

Allara, D. L., and D. Edelson, "A Computational Modeling Study of the Low-Temperature Pyrolysis of n-Alkanes; Mechanisms of Propane, n-Butane, and n-Pentane Pyrolyses," International Journal of Chemical Kinetics, 7, 479 (1975).

Anthony, D. B., and J. B. Howard, "Coal Devolatilization and Hydrogasification," AIChE Journal, 22, 4, 625 (1976).

Anthony, D. B., J. B. Howard, H. C. Hottel, and H. P. Meissner, "Rapid Devolatilization and Hydrogasification of Bituminous Coals," Fuel, 55, 121 (1975).

Attar, A., "Chemistry, Thermodyanmics, and Kinetics of Reactions of Sulfur in Coal-Gas Reactions: A Review," Fuel, 57, 201 (1978).

Attar, A., and W. H. Corcoran, "Sulfur Compounds in Coal," Ind. Eng. Chem., Prod. Res. Dev., 16, 168 (1977).

Benson, S. W., Thermochemical Kinetics, Second Edition, John Wiley and Sons, Inc. (1976).

Blom, L., Thesis, University of Delft, The Netherlands (1960).

Blom, L., L. Edelhausen, and D. W. Van Krevelen, "Chemical Structure and Properties of Coal XVIII - Oxygen Groups in Coal and Related Products," Fuel, 36, 135 (1957).

Brown, J. K., "The Infrared Spectra of Coals," J. Chem. Soc. (London), 744 (1955).

Brown, J. K., I. G. C. Dryden, D. H. Dunevein, W. K. Joy, and K. D. Parkhurst, J. Inst. Fuels, 31, 259 (1958).

Cardenas, J. N., and K. F. O'driscoll, "High Conversion Polymerization. I. Theory and Application to Methyl Methacrylate," J. Polymer Sci., 14, 883 (1976).

Chakrabartty, S. K., and H. O. Kretschmer, "Studies on the Structures of Coals:

Part 1: The Nature of Aliphatic Groups," Fuel, 51, 160 (1972).

Part 2: The Valence State of Carbon in Coal," Fuel, 53, 132 (1974).

Part 3: Some Inferences about Skeletal Structures," Fuel, 53, 240 (1974).

Cheong, P. H., "A Modeling Study of Coal Pyrolysis," PhD Thesis, Calif. Inst. of Tech., (1976).

Cheong, P. H., M. Oka, and G. R. Gavalas, "Modeling and Experimental Studies of Coal Pyrolysis," paper presented at the NSF workshop on the Fundamental Organic Chemistry of Coal, Knoxville, Tennessee, (1975).

Chermin, H. A. G., and D. W. van Krevelen, "Chemical Structure and Properties of Coal, XVII," Fuel, 36, 85 (1957).

Depp, E. A., C. M. Stevens, and M. B. Neuworth, "Pyrolysis of Bituminous Coal Models," Fuel, 35, 437 (1956).

Dryden, I. G. C., "Chemical Constitution and Reactions of Coal," in Chemistry of Coal Utilization, supplementary volume, H. H. Lowry, ed., John Wiley and Sons, Inc. (1963).

Factor, A., "The High-Temperature Degradation of Poly (2,6-dimethyl-1,4-phenylene ether)," J. Polym. Sci., 7, 363 (1969).

Feller, William, An Introduction to Probability Theory and its Applications, second edition, Vol. 1, John Wiley and Sons, Inc. (1976).

Field, R. J., and R. M. Noyes, "Oscillations in Chemical Systems. IV. Limit Cycle Behavior in a Model of a Real Chemical Reaction," J. Chem. Phys., 60, 5 (1974).

Gaines, A. F., "The Distribution of Aliphatic Groups in Coals," Fuel, 41, 112 (1962).

Gan, H., S. P. Nandi, and P. L. Walker, Jr., "Nature of the Porosity in American Coals," Fuel, 51, 272 (1972).

Gan, H., S. P. Nandi, and P. L. Walker, Jr., "Porosity in American Coals," Penn. State report submitted to the Office of Coal Research (1972 a).

Gavalas, G. R., and M. Oka, "Characterization of the Heavy Products of Coal Pyrolysis," Fuel, 57, 285 (1978).

Gavalas, G. R., and K. A. Wilks, "Intra Particle Mass Transfer in Coal Pyrolysis," submitted to the AIChE Journal (1978).

Gear, C. W., Numerical Initial Value Problems in Ordinary Differential Equations, Prentice-Hall, N.J. (1971).

Given, P. H., Third International Conference on Coal Science, Valkenburg (1959).

Given, P. H., "The Distribution of Hydrogen in Coals and its Relation to Coal Structure," Fuel, 39, 147 (1960).

Hayatsu, R., R. E. Winans, R. G. Scott, L. P. Moore, and M. H. Studier, "Oxidative Degradation Studies of Coal and Solvent-Refined Coal," in Organic Chemistry of Coal, John W. Larsen, ed., ACS Symposium Series 71 (1978).

Herkes, F. E., J. Friedman, and P. D. Bartlett, "Peresters XIII. Solvent Effects in the Decomposition of t-Butylperoxy α-Phenylisobutyrate with Special Reference to the Cage Effect," Int. J. Chem. Kinet., 1, 193 (1969).

Hindmarsh, A. C., "GEAR: Ordinary Differential Equation System Solver," Lawrence-Livermore Laboratory, Report UCID - 30001, Rev. 3 (1974).

Hindmarsh, A. C., and G. D. Byrne, "EPISODE: An Experimental Package for the Integration of Systems of Ordinary Differential Equations," Lawrence-Livermore Laboratory, Report UCID - 30112 (1975).

Howard, H. C., "Pyrolytic Reactions of Coal," in Chemistry of Coal Utilization, supplementary volume, H. H. Lowry, ed., John Wiley & Sons, Inc. (1963).

Kobayashi, H., "Rapid Decomposition Mechanism of Pulverized Coal Particle," M.S. Thesis, M.I.T. (1972).

Levy, M., M. Steinberg, and M. Szwarc, "The Addition of Methyl Radicals to Benzene," J. Chem. Phys., 76, 3439 (1954).

Lewellen, P. C., "Product Decomposition Effects in Coal Pyrolysis," M.S. Thesis, M.I.T. (1975).

Lowry, H. H., in Chemistry of Coal Utilization, John Wiley & Sons, Inc. (1963).

McCartney, J. T., H. J. O'Donnell, and S. Ergun, Advances in Chemistry, 55, 261 (1966).

Morrison, R. T., and R. N. Boyd, Organic Chemistry, second edition, Allyn and Bacon, Inc. (1966).

Nandi, S. P., and P. L. Walker, Jr., "Activated Diffusion of Methane in Coal," Fuel, 49, 309 (1970).

O'Neal, H. E., and S. W. Benson, Free Radicals, Vol. 2, John Wiley & Sons, Inc., 275 (1973).

Orning, A. A., and B. Greifer, "Infrared Spectrum of the Solid Distillate from High Vacuum Pyrolysis of a Bituminous Coal," Fuel, 35, 381 (1956).

Pitt, G. J., "The Kinetics of the Evolution of Volatile Products from Coal," Fuel, 41, 267 (1962).

Reidelbach, H., and M. Summerfield, "Kinetic Model for Coal Pyrolysis Optimization," American Chemical Society, Div. Fuel Chemistry Reprints, 20, 161 (1975).

Shapatina, E. A., V. A. Kalyuzhnyi, and Z. F. Chukhanov, "Technological Utilization of Fuel for Energy, 1, Thermal Treatment of Fuels," (1960). Reviewed by S. Badzoich, BCURA Monthly Bulletin, 25, 285 (1961).)

Sharkey, A. G., Jr., J. L. Schultz, and R. A. Friedel, "Mass Spectra of Pyrolysates of Several Aromatic Structures Identified in Coal Extracts," Carbon, 4, 365 (1966).

Skylar, M. G., V. I. Shustikov, and I. V. Virozub, "Investigation of the Kinetics of Thermal Decomposition of Coals," Int. Chem. Eng., 9, 595 (1969).

Solomon, P. R., "The Evolution of Pollutants during the Rapid Devolatilization of Coal," Report submitted to NSF, Unit. Tech. Res. Cent., East Hartford, Connecticut (1977).

Solomon, P. R., and A. V. Manzione, "New Method for Sulfur Concentration Measurements in Coal and Char," Fuel, 56, 393 (1977).

Solomon, P. R., and M. B. Colket, "Coal Devolatilization," paper presented at the 17th Conference of the Combustion Institute, Leeds, England (1978).

Solomon, P. R., "Relation between Coal Structure and Thermal Decomposition Products," ACS, Div. of Fuel Chemistry Reprints, 24, 2, 184 (1979).

Stein, S., D. Golden, S. Benson, and R. Shaw, "Thermochemistry and Kinetics of Coal Conversion," (paper available to the author, source not known).

Stone, H. N., J. D. Batchelor, and H. F. Johnstone, "Low Temperature Carbonization Rates in a Fluidized Bed," Ind. Eng. Chem., 46, 247 (1954).

Suuberg, E. M., "Rapid Pyrolysis and Hydropyrolysis of Coal," SC.D. Thesis, M.I.T. (1977).

Szwarc, M., "The C-H Bond Energy in Toluene and Xylenes," J. Chem. Phys., 16, 128 (1948).

Tingey, G. L., J. R. Morrey, "Coal Structure and Reactivity," Battelle Energy Program Report, Battelle, Pacific Northwest Laboratories (1972).

Van Krevelen, D. W., Coal, Elsevier Publishing Company, Amsterdam (1961).

Vander Hart, D. L., H. L. Retcotsky, "Estimation of Coal Aromaticities by Proton-Decoupled Carbon-13 Magnetic Resonance Spectra of Whole Coals," Fuel, 55, 202 (1976).

Walker, P. L., L. G. Austin, and S. P. Nandi, "Chemistry and Physics of Carbon," Marcel Dekker, 2, 239 (1966).

Walling, C., and A. R. Lepley, "Computer Simulation of Cage Processes and Some Difficulties with Present Models," Int. J. Chem. Kinet., 3, 97 (1971).

Wiser, W. H., Proceedings of the EPRI Conference on Coal Catalysis, Santa Monica (1973).

Wiser, W. H., "A Kinetic Comparison of Coal Pyrolysis and Coal Dissolution," Fuel, 47, 475 (1968).

Additional Literature for Section 3.2

Depp, E. A., C. M. Stevens, and M. B. Neuworth, "Pyrolysis of Bituminous Coal Models," Fuel, 35, 437 (1956).

Depp, E. A., M. B. Neuworth, "Pyrolysis of Bituminous Coal Models. II. Nature of Oxygen Linkages," Brennstoff-Chemie (1958).

Factor, A., H. Finkbeiner, R. A. Jerussi, and D. M. White, "Thermal Rearrangement of o-Methyldiaryl Ethers," The Journal of Organic Chemistry, 35, 57 (1970).

Heredy, L. A., A. E. Kostyo, M. B. Neuworth, "Chemical Identification of Methylene Bridges in Bituminous Coal," Fuel, 43, 414 (1964).

Horrex, C., S. E. Miles, "The Pyrolysis of Dibenzyl," Fuel, 187 (1952).

Jones, B. W., M. B. Neuworth, "Thermal Cracking of Alkyl Phenols," Industrial and Engineering Chemistry, 44, 2872 (1952).

Larsen, J. W., E. W. Kuemmerele,"Alkylation and Depolymerization Reactions of Coal: a Selective Review with Supplementary Experiments," Fuel, 55, 163 (1976).

Ouchi, K., "Infra-red Study of Structural Changes during the Pyrolysis of a Phenol-Formaldehyde Resin," Carbon, 4, 59 (1966).

Stein, S. E., D. M. Golden, "Resonance Stabilization Energies in Polycyclic Aromatic Hydrocarbon Radicals," (paper available to the author, source not known).

Wilen, S. H., E. L. Eliel, "Reactions of Free Radicals with Aromatics. II. Involvement of Ring Hydrogen in the Reactions of Methyl Radicals with Alkylbenzenes," J. Am. Chem. Soc., 80, 3309 (1958).